

**The Sedimentology, Morphology and Evolution of
Two Gravel Barachoix, Placentia Bay,
Newfoundland**

by

© Rebecca A. Boger, B.Sc.

A thesis submitted to the School of Graduate Studies
in partial fulfillment of the requirements for the
degree of Master of Science

Department of Geography
Memorial University of Newfoundland

August 1994

St. John's

Newfoundland



National Library
of Canada

Acquisitions and
Bibliographic Services

395 Wellington Street
Ottawa ON K1A 0N4
Canada

Bibliothèque nationale
du Canada

Acquisitions et
services bibliographiques

395, rue Wellington
Ottawa ON K1A 0N4
Canada

Your file Votre référence

Our file Notre référence

The author has granted a non-exclusive licence allowing the National Library of Canada to reproduce, loan, distribute or sell copies of this thesis in microform, paper or electronic formats.

The author retains ownership of the copyright in this thesis. Neither the thesis nor substantial extracts from it may be printed or otherwise reproduced without the author's permission.

L'auteur a accordé une licence non exclusive permettant à la Bibliothèque nationale du Canada de reproduire, prêter, distribuer ou vendre des copies de cette thèse sous la forme de microfiche/film, de reproduction sur papier ou sur format électronique.

L'auteur conserve la propriété du droit d'auteur qui protège cette thèse. Ni la thèse ni des extraits substantiels de celle-ci ne doivent être imprimés ou autrement reproduits sans son autorisation.

0-612-36099-7

Abstract

A detailed study of gravel barrier beaches at Ship Cove and Big Barasway has shown significant differences in morphology, sediment texture and structures, as well as lateral variability within each system. The individual shoreline assemblages reflect differences in the amount and seasonal variability of sediment supply, in the hydrodynamic settings of the barachoix and, in the orientation with respect to the prevailing southwesterly waves. At Ship Cove, the bayhead barrier has a high elevation, steep beachface, and extensive cusp development; the morphology is a result of its swash alignment, its fixed sediment supply and high wave energy reaching the barrier. The sediment shows a strong cross-shore sorting by shape and size, and cusps largely influence the orientation of clast fabrics.

The presence of a gently-sloping subtidal and intertidal platform in the central 800 m and a 200 m-long vegetated island within the bayhead barrier system at Big Barasway, result in the development of separate and distinctive flow cells, each with differing dynamics and sedimentation. The swash alignment, the high wave energy, and the fixed sediment supply of the southern section result in a similar morphology and sediment texture to that at Ship Cove.

The moderate wave energy reaching the northern section results in a gentler beachfront slope and lower elevation. In addition, the drift alignment and sediment removal along the northern section is causing a thinning of the barrier in areas and progradation in other places. Cross-shore sorting of sediment by shape and size is weaker than that at the southern end of Big Barasway and at Ship Cove. Clast fabrics are generally weaker, although strong orientations can occur.

Overwashing and ice foot development act to modify both shorelines. Landward movement of the barriers is estimated at 0.3 - 0.9 m/year. The outlet at Big Barasway is stable, whereas that at Ship Cove opens and closes on a daily basis in mid- to late summer. Anthropogenic modification at Ship Cove has caused instability, as a result of aggregate removal and a forced northerly relocation of the outlet. Radiocarbon dates, sedimentological and archaeological data indicate that transgression is currently occurring along the southeast Placentia Bay shore, and further modification of the coastline is anticipated in the subsequent century.

Acknowledgements

Many people assisted and advised me during my studies. I wish to acknowledge Mandy Munro, Catriona McKenzie, Glenda Moss, Nikki Prentice, Sharon Scott, Ralph House and Debbie Butler for their advice and help in data collection. A special thanks to Stan and Deloris Tobin at Ship Cove for the many cups of tea on cold days, their local knowledge, and the use of their boat for collecting the echo sounding measurements. Also, I am grateful to Dr. Jacobs, Head of the Geography Department, for constructing a device to suspend the transducer along the side of Stan's boat and to Max Batten for the loan of the theodolite from the Cabot Institute. I thank Colin Banfield for his help and Geoff Farmer for his careful editing. I would like to acknowledge Don Forbes at The Bedford Institute of Oceanography in Nova Scotia and Dave Liverman at the Newfoundland Department of Mines and Energy for discussion and use of data. Furthermore, I would like to thank Dave for introducing me to the wonderful world of Macintosh graphic software and the firm of Pratt, Henley, Blackwood for the use of computers and office facilities.

I extend a special thanks to my supervisor, Norm Catto. His knowledge, patience and guidance helped me to conduct the field work and complete the thesis. Partial funding was provided by the School of Graduate Studies and through an NSERC Grant to Norm Catto.

Re-entering the academic realm in a discipline different from my undergraduate background was challenging and at times, overwhelming. I would like to particularly thank Kitty Drake, Philip Pratt and Eric Facey for their emotional and financial support, without which this thesis would not have been

possible. Lastly, I would like to thank my four-legged field assistant, Rusty, who, during the summer field season in 1991, assured me that I was studying beaches and that I was walking on rocks. To Rusty, I dedicate this thesis.

Table of Contents

Abstract	ii
Acknowledgments	iv
Table of Contents	vi
List of Tables	ix
List of Figures	x
List of Plates	xiii
1 BACKGROUND INFORMATION	1
1.1 Introduction	1
1.2 Present Study	3
1.3 Previous Work	5
1.4 Terminology	8
1.5 Objectives	10
1.6 Outline	10
2 STUDY AREA	12
2.1 Location and Physical Setting of Study Area	12
2.2 Climate	12
2.2.1 General Climatic Setting	12
2.2.2 Wave Climate	13
2.2.3 Tides	16
2.2.4 Sea Ice	16
2.2.5 Climate and Hydrology	16
2.3 Soils and Vegetation	21
2.4 Bedrock Geology	23
2.5 Glacial History	25
2.6 Holocene Sea-Level Changes	27
2.7 Human Activity	30
3 METHODS	32
3.1 Characteristics of the Barrier Sediment	32
3.1.1 Clast Shape	32
3.1.2 Sediment Texture	34
3.1.3 Clast Fabrics	34
3.2 Tracer Clasts	37

3.3	Profile Measurements.....	38
3.4	Echo Sounding Measurements	40
3.5	Cores	43
3.6	Exposures	43
3.7	Cliff Erosion	43
3.8	Aerial Photos.....	44
4	¹⁴C AGE DETERMINATION AND HOLOCENE SEA-LEVEL	45
4.1	Description.....	45
4.2	Discussion	46
5	DESCRIPTION OF THE BARRIER AT SHIP COVE	54
5.1	Morphology	54
5.2	Clast Lithology	87
5.3	Sediment Texture	89
5.4	Clast Shape.....	98
5.5	Fabric Analysis	100
6	DISCUSSION OF THE BARRIER AT SHIP COVE	115
6.1	Morphology	115
6.1.1	Cusp Formation.....	115
6.1.2	Outlet Stability	119
6.1.3	Seasonal Change, Storm Response, and Recent Evolution...124	
6.2	Sedimentology	125
6.2.1	Cross-shore Shape and Size Sorting.....	125
6.2.2	Lateral Textural Variation.....	130
6.2.3	Fabric Analysis	131
6.2.4	Exposures	135
6.2.5	Summary of Sediment Distribution	137
7	DESCRIPTION OF THE BARRIER SYSTEM AT BIG BARASWAY.....	140
7.1	Introduction	140
7.2	Zone A	141
7.2.1	Morphology	141
7.2.2	Morphological Variation.....	152
7.2.3	Clast Lithology	161
7.2.4	Sediment Texture	161
7.2.5	Clast Shape.....	164
7.2.6	Fabric Analysis	168
7.3	Zone B.....	174
7.4	Zone C.....	176
7.4.1	Morphology	176
7.4.2	Clast Lithology	182

7.4.3 Sediment Texture	183
7.4.4 Clast Shape.....	184
7.4.5 Fabric Analysis.....	188
7.5 Zone D	190
7.5.1 Morphology	190
7.5.2 Clast Lithology	211
7.5.3 Sediment Texture	213
7.5.4 Clast Shape.....	215
7.5.5 Fabric Analysis.....	217
8 DISCUSSION OF THE BARRIER SYSTEM AT BIG BARASWAY	223
8.1 Introduction	223
8.2 Zone A	225
8.2.1 Morphology	225
8.2.2 Cross-shore Clast Shape and Size Sorting.....	228
8.2.3 Fabric Analysis	234
8.2.4 Summary of Sedimentary Assemblages.....	236
8.3 Zones C and D.....	240
8.3.1 Morphology	240
8.3.2 Sedimentology.....	246
8.3.3 Fabric Analysis	249
8.3.4 Summary of Sedimentary Assemblages.....	251
9 SEDIMENT CORES	253
9.1 Descriptions	253
9.2 Interpretation.....	257
10 CONCLUSIONS.....	268
References.....	278

List of Tables

Table 1	Extreme wave heights for Placentia Bay.....	15
Table 2	Monthly mean temperature and precipitation data for Argentina, 1951-1980	17
Table 3	Monthly mean temperature and precipitation values for Big Barasway, June 1991-June 1993	19
Table 4	Monthly and annual mean discharges in cubic metres per second for 1983-1992; Little Barasway Brook near Placentia-Station no. 02ZK003.....	20
Table 5	Dimensions of the barrier beach at Ship Cove.....	56
Table 6	Dimensions of the cusps at Ship Cove, July 1991	69
Table 7	Status of outlet at Ship Cove on selected dates.....	85
Table 8	Compositions of the clast lithologies for the samples taken from the barrier crest and the swash bar, and for the samples combined, Ship Cove	87
Table 9	Clast fabric data for Ship Cove.....	102
Table 10	Summary of the sedimentary characteristics along zone C, Ship Cove	139
Table 11	Dimensions of the barrier along zone A, Big Barasway	142
Table 12	Clast fabric data for zone A, Big Barasway	168
Table 13	Dimensions of the barrier along zone C, Big Barasway	177
Table 14	Clast fabric data for zone C, Big Barasway.....	188
Table 15	Dimensions of the barrier along zone D, Big Barasway	191
Table 16	Clast fabric data for zone D, Big Barasway	219
Table 17	Summary of sedimentary characteristics along zone A, Big Barasway.....	239
Table 18	Summary of sedimentary characteristics along zones C and D, Big Barasway	252

List of Figures

Figure 1	Location of study area.....	4
Figure 2	Terminology of barrier features.....	9
Figure 3	Map of Placentia Bay showing region of locally-generated seas affecting study area and direction of waves from offshore regions	14
Figure 4a	Schematic diagram of a peripheral bulge at two points in time, 18,000 BP and now	29
Figure 4b	Schematic diagram showing the RSL history at four sites	29
Figure 5	Sketch showing the calculation of maximum error associated with the location of offshore positions	42
Figure 6	Map of the barrier at Ship Cove	insert
Figure 7	Map of the barrier at Big Barasway	insert
Figure 8	Stratigraphic sequence at Ship Cove.....	47
Figure 9	Stratigraphic sequence at Big Barasway.....	48
Figure 10	Profiles of transects SC-1 - SC-3, Ship Cove.....	57
Figure 11	Profiles of transects SC-4 - SC-6, Ship Cove.....	58
Figure 12	Profiles of transects SC-7 - SC-9, Ship Cove.....	59
Figure 13	Profiles of transects SC-10 and SC-11, Ship Cove.....	60
Figure 14	Profiles of transects SC-12 and SC-13, Ship Cove.....	61
Figure 15	Profiles of transects SC-14 and SC-15, Ship Cove.....	62
Figure 16	Profiles of transects SC-16 and SC-17, Ship Cove.....	63
Figure 17	Profiles of transects SC-18 and SC-19, Ship Cove.....	64
Figure 18	Profile of transect SC-20, Ship Cove.....	65
Figure 19a	Schematic planar view of beach cusp morphology	70
Figure 19b	Schematic cross-section of a beach cusp	70
Figure 20	Comparison of profiles of transects SC-8 and SC-11 measured July, August and September 1991.....	74
Figure 21	Comparison of profiles of transect SC-17 measured July, August and September 1991.....	75
Figure 22	Comparison of profiles of transects SC-2 and SC-11 measured July 1991, May 1992 and December 1992.....	78
Figure 23	Comparison of profiles of transects SC-14 and SC-17 measured July 1991, May 1992 and December 1992.....	79
Figure 24	Profiles of GSC-394 measured July, September and December 1993 and February 1994	80
Figure 25	Comparison of 1948, 1967 and 1980 aerial photos of Ship Cove.....	86
Figure 26	Lithologies for Ship Cove	88
Figure 27	Sediment textures for Ship Cove.....	90
Figure 28	Sedimentary sequence along zone A, Ship Cove.....	95
Figure 29	Exposure A, Ship Cove	96

Figure 30	Exposure C, Ship Cove	97
Figure 31	Clast shape analysis for Ship Cove	99
Figures 32-39	Clast fabrics, Ship Cove	103-110
Figure 40	Schematic diagram showing pattern of water flowing through cusp centre.....	114
Figure 41	Profiles of transects BB-1 - BB-4; zone A, Big Barasway	143
Figure 42	Profiles of transects BB-5 and BB-6; zone A, Big Barasway.....	144
Figure 43	Profiles of transects BB-7 and BB-8; zone A, Big Barasway.....	145
Figure 44	Profiles of transects BB-9 and BB-10; zone A, Big Barasway.....	146
Figure 45	Profiles of transects BB-11 and BB-12; zone A, Big Barasway.....	147
Figure 46	Profiles of transects BB-13 and BB-14; zone A, Big Barasway.....	148
Figure 47	Profiles of Boulder Site and GSC-393 measured July, September and December 1993 and February 1994.....	154
Figure 48	Comparison of profiles of transects BB-3 and BB-8 measured July and October 1991.....	155
Figure 49	Comparison of profiles of transects BB-3 and BB-6 measured in July 1991, December 1992 and June 1993.....	158
Figure 50	Comparison of profiles of transect BB-10 measured July 1991, December 1992 and June 1993.....	159
Figure 51	Comparison of 1948, 1967 and 1980 aerial photos of Big Barasway	160
Figure 52	Lithologies for zone A, Big Barasway.....	162
Figure 53	Sediment textures for zone A, Big Barasway.....	165
Figure 54	Clast shape analysis for zone A, Big Barasway.....	166
Figure 55	Sphericity and roundness analyses for zone A, Big Barasway	167
Figures 56-58	Clast fabrics, zone A, Big Barasway.....	171-173
Figure 59	Profile of transect along zone B, Big Barasway	175
Figure 60	Profiles of transects BB-15 - BB-18, zone C, Big Barasway	178
Figure 61	Profiles of transects BB-18 - BB-20, zone C, Big Barasway	179
Figure 62	Lithology for zone C, Big Barasway	182
Figure 63	Sediment texture for zone C, Big Barasway	185
Figure 64	Exposure, zone C, Big Barasway	186
Figure 65	Clast shape analysis for zone C, Big Barasway	187
Figure 66	Clast fabrics, zone C, Big Barasway	189
Figure 67	Profiles of transects BB-21 - BB-24, zone D, Big Barasway	192
Figure 68	Profiles of transects BB-25 and BB-26, zone D, Big Barasway.....	193
Figure 69	Profiles of transects BB-27 and BB-28, zone D, Big Barasway.....	194
Figure 70	Profiles of transects BB-29 and BB-30, zone D, Big Barasway.....	195
Figure 71	Profiles of transects BB-31 and BB-32, zone D, Big Barasway.....	196
Figure 72	Profiles of transects BB-33 and BB-34, zone D, Big Barasway.....	197
Figure 73	Profiles of transects BB-35 - BB-37, zone D, Big Barasway	198
Figure 74	Profiles of transects BB-38 - BB-40, zone D, Big Barasway	199

Figure 75	Comparison of profiles of transects BB-26 and BB-31 measured July 1991, December 1992 and June 1993.....	202
Figure 76	Comparison of profiles of transects BB-34 and BB-40 measured July 1991, December 1992 and June 1993.....	203
Figure 77	Profiles of GSC-392 measured July, September and December 1993	210
Figure 78	Lithology for zone D, Big Barasway	212
Figure 79	Sediment texture for zone D, Big Barasway	214
Figure 80	Clast shape analysis for zone D, Big Barasway.....	216
Figures 81-83	Clast fabrics, zone D, Big Barasway.....	220-222
Figure 84	Stratigraphic sequence of cores, Big Barasway	256
Figure 85	Map showing the approximate locations of tidal creeks and flood tidal deltas at Big Barasway	260
Figure 86	Diagram showing the correlation of the sedimentary units of the cores	267
Figure 87	Outline of the critical factors differentiating the sedimentology and morphology of the barriers at Ship Cove and Big Barasway	273

List of Plates

Plate 1	Overview of the barrier at Ship Cove, looking south. May 1992	55
Plate 2	Backbarrier and lagoon at Ship Cove, July 1991.....	55
Plate 3	Overview of Ship Cove, looking north. July 1991	66
Plate 4	The eroding bluff bounding zone B and sediment along the upper-beachface. July 1991.....	67
Plate 5	Lower-beachface cusps along zone C and eroding bluff bounding the northern end of the barrier. July 1991.....	68
Plate 6	Cusps along zone C. August 1991.....	71
Plate 7	Circular mound of pebbles amongst the cobble-dominated beach crest after spring thaw. April 1992.....	73
Plate 8	Convex beachface profile after winter storms along zone C, December 1991	77
Plate 9	Overwash channel. March 1992	83
Plate 10	Outlet forming. August 1991	84
Plate 11	Swash bars along outlet. October 1992.....	84
Plate 12	Imbricated cobbles along the beach crest. July 1991	91
Plate 13	Exposure A, Ship Cove.....	94
Plate 14	Exposure B, Ship Cove.....	94
Plate 15	Overview of the beach at Ship Cove taken in August 1954.....	123
Plate 16	Overview of the barrier at Big Barasway. July 1991.....	141
Plate 17	Northward transport of sediment along the northern end of zone A. July 1991.....	151
Plate 18	Gravel cones and depressions on the backbarrier along zone A. June 1993	152
Plate 19	Overview of the southern end of zone A. July 1992.....	153
Plate 20	Ice foot development along zone A. February 1992.....	157
Plate 21	Overview of zone B. GSC-5319 taken from the peat bounding the beach. August 1992.	174
Plate 22	Overview of zone C. July 1991	176
Plate 23	Lateral bar along the southern side (zone C) of outlet exposed during low tide. July 1992.....	180
Plate 24	Erosion of the barrier near the outlet, zone C. The lateral bar is in the background. July 1992.....	181
Plate 25	Elongated cusps becoming backwash channels along zone D. July 1992	201
Plate 26	Backwash channels farther to the north of Plate 26, zone D. July 1992	205

Plate 27	Overview of the beachfront along sections 3 and 4, zone D. December 1991	205
Plate 28	Exposure of wooden frame along zone D. June 1993.....	206
Plate 29	Overview of the barrier taken August 1954.....	206
Plate 30	Southward transport of sediment along section 4, zone D.....	208
Plate 31	Large accumulation of seaweed after storm. November 1992.....	209
Plate 32	Overwashed sediment along the northern end of zone D. June 1993.	211
Plate 33	Cobble with seaweed attached along the barrier crest, zone A. January 1992.	231
Plate 34	Lagoon at low tide, Big Barasway. August 1991	258

Chapter 1

Background Information

1.1 Introduction

Gravel barriers formed by marine processes display wide varieties of morphology, sedimentology, and behaviour. They are generally associated with embayed coasts where wave processes dominate over tidal influences. These features may be located at the head, mouth or within an embayment and are called bayhead, baymouth, and midbay barriers, respectively. They frequently enclose freshwater or brackish lagoons.

In eastern Canada, gravel barriers are commonly called barachoix, barasways, barrisways, or barachois. The first known version of the word, 'barrachoa', was in a Basque document written in 1609 referring to an event in 1602 (Barkham, 1987). In this citation 'barrachoa' is explicitly applied to the bar, not the lagoon. Versions of the word later became associated with the enclosed lagoon. (Barkham, 1985; Glossary of Generic Terms in Canada's Geographical Names, 1987). The names of communities often include a version of 'barrachoa'. This occasionally causes discrepancies between local spellings of communities and the official or unofficial versions printed on topographic and road maps.

These features are common in Newfoundland as well as in other mid-to high-latitude areas (Carter and Orford, 1984; Forbes, 1984). Glacial processes brought high volumes of gravel-sized clasts to the coastal environment. These sediments have either been reworked from offshore deposits by marine

transgression or are actively being eroded from headlands or adjacent cliffs. The glacial sources vary greatly, depending on the local glacial history, and include drumlin fields, glaciomarine and glaciofluvial deposits, thin veneers of glacial diamicton and thick deposits of ice-contact sediments (Forbes and Taylor, 1987).

The types and amounts of the glacial sediment sources greatly influence the morphology and stratigraphy of gravel barriers. Since gravel barriers are conditioned by glaciation, it is important when studying the modern forms to distinguish between relict glacial sediments and morphology and the effects of modern processes on these glacial deposits. This is particularly important when analyzing the temporal and spatial variation of sediment supply and how these variations affect the morphodynamics of beach systems.

In spite of their widespread occurrence, the morphodynamics and sedimentary assemblages of gravel beaches are poorly understood. Until recently, research has emphasized sand-dominated coastal environments (Williams and Caldwell, 1988). Beaches composed of sand behave differently from those of gravel, which may in turn behave differently from beaches composed of mixtures of sand and gravel (Kirk, 1975; Kirk, 1980).

With the increasing interest in global and regional climatic change in addition to regional glacio-isostatic rebound, questions have arisen concerning the responses of these features to rises and to differing rates of rises in sea-level (Carter *et al.*, 1989; Forbes *et al.* 1989). The response of gravel barriers to sea-level change has direct socio-economic consequences, for these landforms commonly protect communities and agricultural areas. For

instance, a large section of the town of Placentia, Newfoundland is built directly on a gravel barrier. At present the town is subject to periodic, extensive flooding (Flood Information Map: Placentia; 1985) and will be extremely sensitive to any rise in sea-level or increase in storm activity. Remedial measures are costly. In 1992, the Federal and Provincial governments and the town of Placentia allocated more than \$3 million for the 'Sea Wall Project', an attempt to solve the flooding problems (Liverman *et al.*, 1994). With a better understanding of coastal processes, problems such as the potential flooding of the town of Placentia may be handled effectively.

In addition to the modern applications of the morphodynamics of this study, detailed sedimentological analysis will aid in the interpretation of pre-Holocene deposits. The lack of understanding of the complexity and variability of modern processes frequently hinders interpretation of ancient deposits (Hart and Flint, 1989; Bourgeois and Leithold, 1984).

1.2 Present Study

This research deals with a comparative analysis of two gravel barriers, Ship Cove and Big Barasway, Placentia Bay, Newfoundland (Figure 1). The geomorphology and sedimentology will be described in detail. Lateral, vertical and seasonal variations, and storm responses in the geomorphology and sedimentology are documented. Differences within and between the two beach systems are explained by the differences in the dynamics and sediment supplies of the barriers. In addition, the stability of the outlets and the landward movement of the barriers through overwashing are explored. The

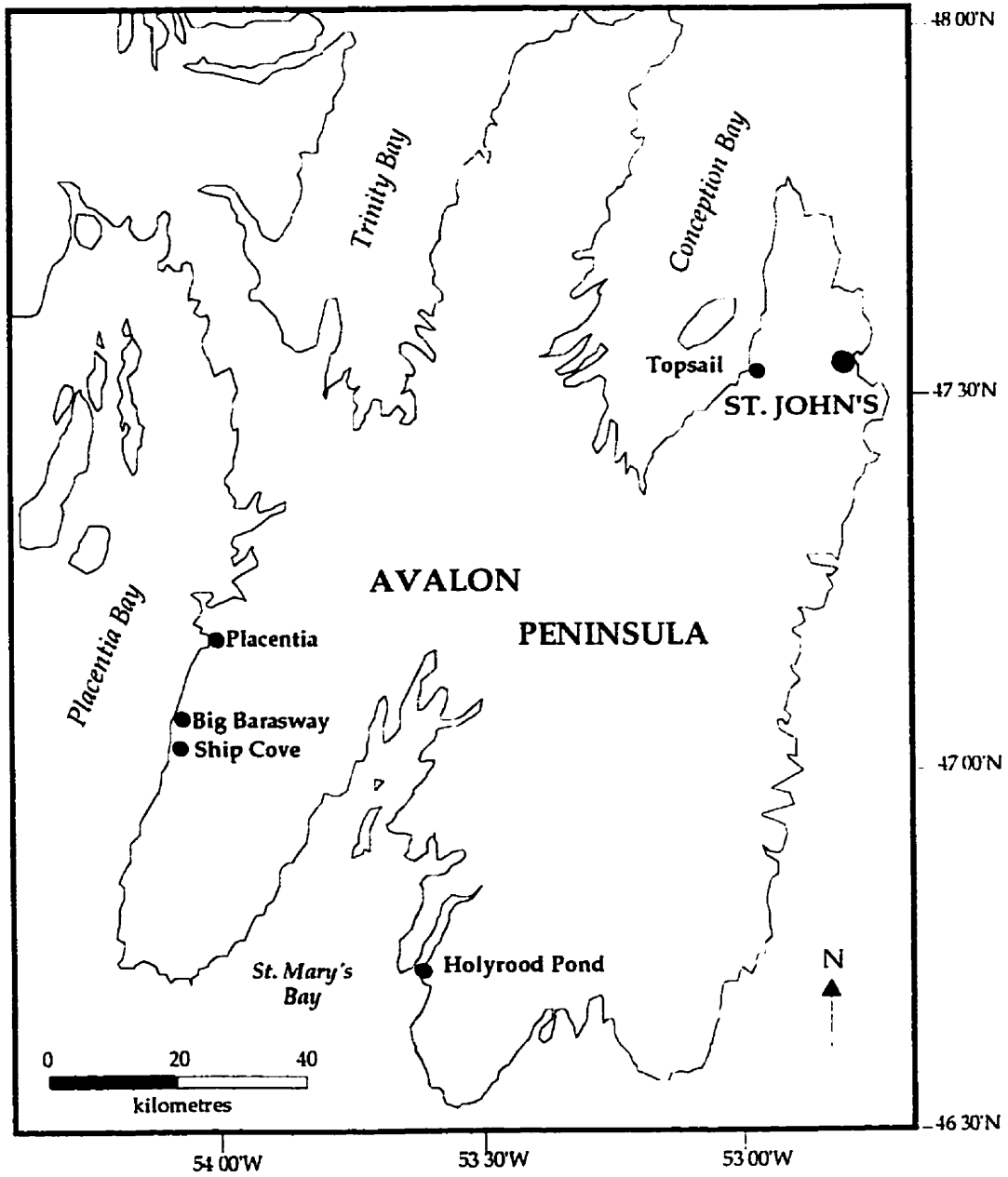


Figure 1: Location of study area

results are compared with models created by Carter *et al.* (1989), Forbes *et al.* (1990) and Orford *et al.* (1991).

1.3 Previous Work

Analysis of beach profiles and the variation of profile configuration over time leads to a better understanding of process-form relationships (Caldwell and Williams, 1986). Beach profiles reflect the interplay of the characteristics of beach sediments, the local wave-energy regime, and nearshore geometry. Thus, they dynamically respond to and mirror changes in nearshore processes (Sherman, 1991). Profile variability is considered less for gravel-dominated beaches than sand-dominated ones (Carter and Orford, 1984).

Beach models for sand-dominated systems often show a seasonal change from 'winter' to 'summer' profiles (for example, Shepard, 1950). A 'winter' profile is comparatively low in elevation, concave upward, and has an offshore bar. A 'summer' beach profile has a high berm and is convex upward. The convex versus concave geometries reflect differing beach volumes. The winter profile reflects sediment removal to the offshore by steep storm waves while the summer profile indicates sediment accretion by low-amplitude, long-period summer swell waves (Sherman, 1991). On a shorter time scale than a seasonal one is the cycle of storm erosion and fair weather, swell wave beach recovery (Zenkovitch, 1967). The beach profiles for storm and recovered states are similar to the 'winter' and 'summer' states.

The concept of cyclic profile variation often evident in sand-dominated beaches has been applied to gravel-dominated systems with varying results.

For example, Sherman (1991) showed erosion and accretion cycles similar to sand-dominated systems. Seasonal variations were seen at two beaches in Wales (Caldwell and Williams, 1986). In a study by Carr *et al.* (1982), no seasonal accretion or erosion periods were observed. During 'winter' (storm) season beach variability was greatest.

Important differences exist in the behaviour and morphology of sand- and gravel-dominated beach systems. Gravel-dominated beaches have steep slopes which are, in part, a response to high percolation rates and high angles of repose. As a consequence, these beaches mainly show characteristics of a reflective state (Wright and Short, 1984) and rarely change into a dissipative state, as sand beaches frequently do. Waves breaking close to shore along gravel beaches allow the generation of strong longshore currents close to the shoreline and high shear stresses which allow the powerful ejection of clasts landward (Orford *et al.*, 1991).

Because gravel is generally transported as bedload (except during extreme storm events), size, shape and its relationship to the background sediment mass greatly influence the capacity of gravel to move. Rejection of large-grained clasts leads to better sorted and graded beaches (Orford *et al.*, 1991). Bluck (1967) formulated a model for gravel-beach particle zonation based on clast size and shape. This model has been used in the interpretations of ancient deposits (Bourgeois and Leithold, 1984; Massari and Parea, 1988). Orford (1975) and Williams and Caldwell (1988) have shown that Bluck's model is not universally applicable. Bluck's model also excludes secondary sorting caused by cusps (Sherman *et al.*, 1990; Sherman *et al.*, 1993).

A body of literature on gravel barriers has grown over the past fifteen years. The majority of the work has been undertaken in Ireland and Nova Scotia by Carter, Orford, Forbes, and their colleagues and students (for example, Caldwell and Williams, 1986; Carr *et al.*, 1982; Carter, 1983; Carter and Orford, 1988; Carter *et al.*, 1990; Duffy *et al.*, 1989; Forbes and Taylor, 1987; Forbes *et al.*, 1990; Jennings and Smyth, 1990; Kirk, 1980; Orford and Carter, 1982a; Orford *et al.*, Sherman, 1991). Because of the relatively few people involved in this field, new researchers are needed.

Carter *et al.* (1989) recognized a hierarchy of mechanisms which control barrier development: sea-level change, basement characteristics (which include the geologic setting and the requirement of maintaining cross-shore drainage), sediment-supply, wave and tide regimes, and sediment texture of the barrier. In Ireland where sea-level has been rising slowly <1 mm/yr over the past 3000 - 4000 years (Carter *et al.*, 1989), many barriers are in compartmented, headland-controlled embayments where sediment supply is limited and little exchange of sediment occurs between embayments. Carter *et al.* (1989) classified the barriers in Ireland by the type of lagoon they enclosed (freshwater, brackish, or saltwater) and the type of cross-shore drainage.

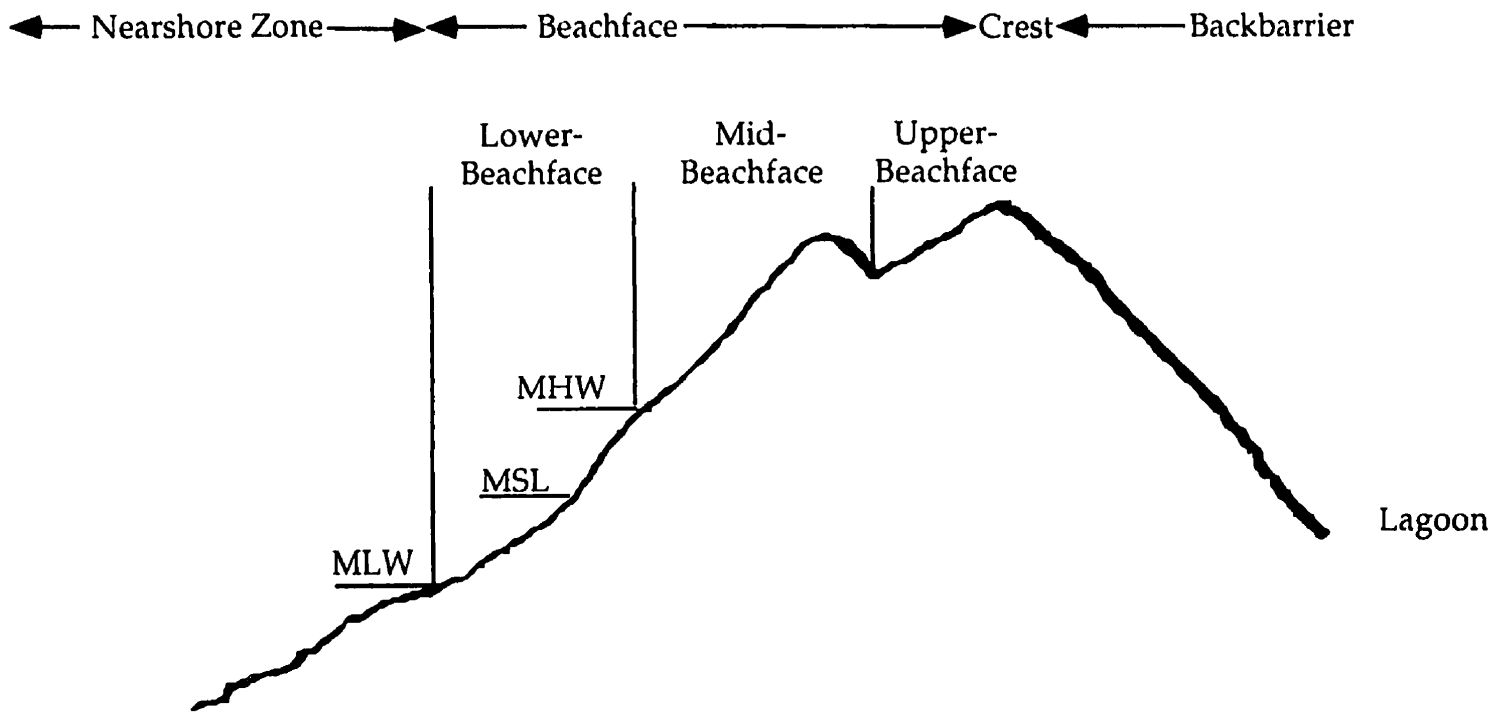
In contrast, the coast of Nova Scotia has undergone a rapid rate of sea-level rise. Between 5000 BP and the last century sea-level rise averaged 2 mm/yr, after which the rate of rise increased to 3.5 mm/yr (Shaw *et al.*, 1993). Classification of barriers along Nova Scotia was based on depositional setting and sediment composition (Forbes *et al.*, 1990). Five categories were developed and included prograded beach-ridge complexes, high gravel storm-

ridges, gravel barriers subject to high rates of washover, trailing and fringing gravel spits and ridges, and sandy barrier complexes with low dunes.

Orford *et al.* (1991) have synthesized the majority of work on gravel barriers and have proposed a model for the evolution of gravel barriers. The first stage begins as a drift-aligned barrier along an eroding transgressive front that, after a period of consolidation and stabilization, may become swash-aligned. This stage is followed by a breakdown stage which is a response to depleting sediment supplies and/or rising sea-levels.

1.4 Terminology

In this paper the following terms will be used (Figure 2). The backbarrier refers to that part of the barrier landward of the crest. The highest point of the barrier, the crest, marks the transition between landward-dipping barrier slopes and seaward-dipping barrier slopes. The beachface includes the region above mean low tide and below the beach crest. The upper-beachface refers to the steeper-dipping slopes above the area of active sediment accumulation and the crest, which at Ship Cove and Big Barasway, begins at 2 - 3 m above mean sea-level. The mid-beachface refers to the area between mean high tide and the upper-beachface whereas the lower-beachface indicates the area between the mean low tide and mean high tide. The nearshore zone is the region between mean low tide and the point where the waves first break.



6

Figure 2: Terminology of barrier features used in this paper.

1.5 Objectives

This project was designed to include the following objectives: 1) To describe in detail the geomorphology of the beach systems,

2) To document the dynamics of the beaches under varying weather regimes. This involved observing:

- the changes in beach profiles
- the movement of sediment
- the stability of stream outlets
- the amount of seepage
- the extent of overwashing during storm events
- the amount of sediment available to the systems.

3) To create sedimentary assemblages describing the sedimentary environments.

4) To outline the critical factors that control the morphology and the sedimentary organization of the individual barriers.

5) To suggest the course of evolution of the barriers throughout the Holocene.

6) To predict the behaviour of the barriers in the near future.

1.6 Outline

Following discussion of the study area (chapter 2) and the methods used for data collection (chapter 3), ^{14}C ages and interpretations of Holocene sea-level change along Placentia Bay, Newfoundland are presented in chapter 4. Chapters 5 and 6 describe and discuss the barrier at Ship Cove. Similarly, chapters 7 and 8 describe and discuss the barrier complex at Big Barasway. The

stratigraphy of the four sediment cores taken from the lagoon at Big Barasway are presented and interpreted in chapter 9; followed by a discussion (chapter 10) of the critical factors controlling the barrier systems at the two sites.

Chapter 2

Study Area

2.1 Location and Physical Setting of Study Area

The study area is located along the eastern coast of Placentia Bay on the Avalon Peninsula of Newfoundland (Figure 1). The coast south of Placentia town is characterized by a series of small valleys with braided streams and gravel beaches in the littoral zone. The surrounding hills are high and slope steeply into the valleys and coast. The two beaches chosen, Big Barasway (47°08'N 54°04'W) and Ship Cove (47°06'N 54°05'W), have developed in adjacent coves located approximately 12 km and 15 km south of Placentia respectively. The 1.3 km long beach at Big Barasway is dominated by a 1.1 km long baymouth barrier. In contrast the 0.5 km long beach at Ship Cove consists of a bayhead barrier along the northern half. These two sites were chosen for analysis because, despite their proximity, the morphology and sedimentology of the barrier systems differ considerably.

2.2 Climate

2.2.1 General Climatic Setting

The climate of Newfoundland is shaped by the interaction of the northern hemisphere mid-latitude atmospheric circulation forming the prevailing Westerly winds, the island's location relative to the Canadian mainland, and the proximity to a cold ocean surface. The Labrador Current strongly influences the climate by bringing southerly flowing Arctic waters to

the coastline. Placentia Bay falls into the Dfb Köppen classification: a cold Boreal Forest climate characterized by adequate precipitation throughout the year. Because of the island's shape, its extensive and indented coastline, and the presence of mountains in the west, complex regional and local variations can be significant (Banfield, 1983). Severe storms can occur in any season; however, most storm waves are generated in late autumn and winter by 'extra-tropical cyclonic disturbances'. Tropical storms in late summer generally dissipate by the time they reach Newfoundland (Forbes, 1984).

2.2.2 *Wave Climate*

The long axis of Placentia Bay is aligned NNE-SSW. Placentia Bay is protected by the central mass of Newfoundland to the north, by the Avalon Peninsula to the east and by the Burin Peninsula to the west of Placentia Bay. This distribution of land masses reduces the possibility of locally-generated waves. Southwesterly storms have the most pronounced impact on this area. Figure 3 shows the region of locally-generated seas affecting the study area and the direction of waves from offshore regions (modified from Shawmont Martec, 1984).

Detailed climatic data for this region is limited. For Placentia, the prevailing winds for November to February are Westerlies, with a mean monthly speed ranging between 28.5 to 30.6 km/hr. For the rest of the year, the prevailing winds are south-southwesterlies with monthly means ranging from 22.0 to 29.1 km/hr (Canadian Climate Normals, 1982). Off the open Atlantic coast to the southwest of Newfoundland, annual deep-water

significant wave heights are in the 7 - 8 m range, whereas the 10-year significant wave heights range from 10 to 13 m (Forbes and Taylor, 1987).

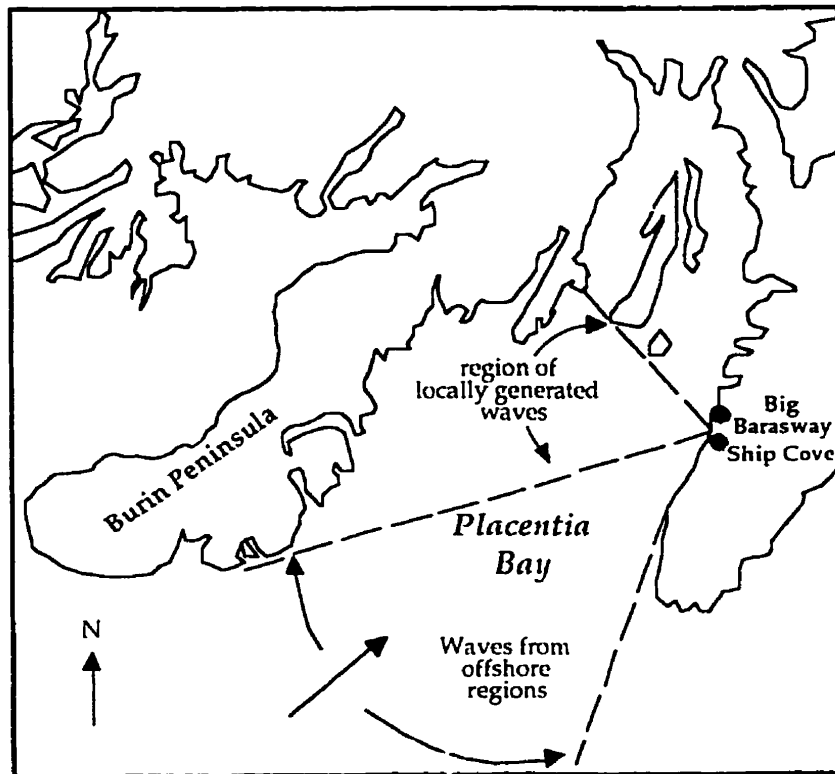


Figure 3: Map of Placentia Bay showing the region of locally generated seas affecting the study area and the direction of waves from the offshore regions, (modified from Shawmont Martec, 1984).

A study conducted to determine the extent of flooding in the area of the town of Placentia (Shawmont Martec, 1984) used wind data tapes for the years between 1971 and 1982 (from the Atmospheric Environment Service) to determine hindcast wave data for Placentia Bay. The Shawmont Martec study revealed a mean wave period of 4 - 5 seconds and 81% of the wave heights less than 1.8 m. However, the limited fetch of Placentia Bay rarely allows waves to fully develop, so there could be a wide range of heights and periods at any given time. This influences the shoaling process and wave run-up on the beaches.

Table 1 shows the deep-water wave height distributions for extreme events in Placentia Bay (Shawmont Martec, 1984). It is estimated that for a fifty-year event, extreme heights would range between 5.9 and 7.8 m. For the hundred-year event, extreme heights would range between 6.3 and 8.6 m.

Return Period (years)	Wave Height Estimate (metres)	Lower Limit (metres)	Upper Limit (metres)
1.0	1.7		
1.1	2.2		
1.3	2.8		
2.0	3.6		
5.0	4.6	4.1	5.1
10.0	5.3	4.7	5.9
20.0	6.0	5.2	6.7
50.0	6.8	5.9	7.8
100.0	7.5	6.3	8.6
200.0	8.1	6.8	9.4
500.0	8.9	7.5	10.4

Table 1: Extreme wave heights for Placentia Bay (Shawmont Martec, 1984; 4-26)

2.2.3 Tides

Based on tidal information at Argentia, St. Brides, and Placentia, the mean tidal range is 1.6 m and the large tidal range is 2.5 m for the study area (Canadian Tide and Current Tables, 1993; Shawmont Martec, 1984). Although technically the area can be classified as a mesotidal environment (Davies, 1964), the tidal range is primarily below 2 m. Because of the relative steepness of the nearshore slope at Ship Cove and Big Barasway, wave energies are high and thus, the coast is classified as wave-dominated (Davis and Hayes, 1984).

2.2.4 Sea Ice

Placentia Bay is generally free of sea ice during the winter months (Markham, 1980), although ice foot development along shorelines affects the wave dynamics. Ice feet are ridges of ice that may form between the beach crest and intertidal area. In recent years, ice foot development has increased along Placentia Bay (Catto and Hooper, 1994; Catto *et al.*, 1994).

2.2.5 Climate and Hydrology

The monthly mean temperatures and mean precipitations for Argentia for the period between 1951 and 1980 are given in Table 2 (Canadian Climate Normals, 1982). The winters are mild, and the mean temperature for January is -1.5°C . The summers are cool with a mean temperature of 14.0°C for July. Precipitation is heaviest between November and February and lowest between March and July. The mean total is 1067.9 mm.

Argentina	Jan	Feb	Mar	Apr	May	Jun	Jul	Aug	Sep	Oct	Nov	Dec	Year
Daily Temperature (°C)	-1.5	-1.9	-0.5	2.3	5.6	9.7	14.0	15.3	12.5	8.4	5.0	0.3	5.8
Rainfall (mm)	167.6	120.1	66.0	120.1	42.6	46.5	83.8	143.5	74.2	M	M	M	M
Snowfall (mm)	53.4	40.7	30.9	9.2	2.2	1.0	0.0	0.0	0.0	1.0	3.2	29.4	171.0
Total Precipitation (mm)	113.9	106.2	70.6	77.3	67.4	74.7	72.7	96.2	83.5	89.6	105.4	110.4	1067.9

Table 2: Mean monthly and annual temperature and precipitation data for Argentina.

The values are adjusted since data are missing in the period of 1951-1980;

(Canadian Climate Normals, 1951-1980: Temperature and Precipitation, 1982).

The mean annual precipitation for Argentia is noticeably lower than for other parts of the Avalon Peninsula; for example, Colinet has a mean of 1391 mm and St. John's west, 1579 mm (C.E. Banfield, Memorial University of Newfoundland, unpublished). The lower precipitation figure is likely due to a rainshadow effect caused by higher ground to the south and east, and to the coastal location of the weather station at Argentia.

The monthly mean temperatures and monthly precipitation values for the weather station at Big Barasway for the duration of the study (June 1991-June 1993) are given in Table 3 (AES). The total precipitation at Big Barasway for 1992 was 1051 mm, a value close to that of the mean annual at Argentia.

The area of the drainage basin of the unnamed stream exiting at Big Barasway is 65.3 km², as estimated from 1:50,000 topographic maps (1 M/1 and 1 N/4). The highest elevation in the drainage basin is 285 m, along Castle Ridge toward the centre of Placentia Peninsula. The main channel length is 13.1 km, and the slope, defined as the percentage of the vertical displacement divided by the horizontal distance, is 4.6%. The stream drains peatland and wooded areas.

The drainage basin for the unnamed stream at Ship Cove covers an area of 33 km². The highest point in the basin is 255 m. The main channel length is 9.4 km, and the slope is 1.1%. The stream drains peatland and wooded areas.

The mean annual runoff for the drainage basins is between 800 - 1800 mm (Department of Environment and Lands, unpublished). Throughout most of Newfoundland, including the Avalon Peninsula, runoff is approximately 80% of precipitation. Stream discharge varies throughout the

Month	Mean Temp. (°C)	Rain (mm)	Snow (mm)	Total Precip. (mm)
Jun-91	7.1	62.2	0.0	62.2
Jul-91	11.9	72.4	0.0	72.4
Aug-91	13.3	50.8	0.0	50.8
Sep-91	12.0	110.6	0.0	110.6
Oct-91	8.0	166.0	10.0	176.0
Nov-91	4.7	126.0	0.0	126.0
Dec-91	-2.5	71.0	45.0	116.0
Jan-92	-4.6	60.0	6.0	66.0
Feb-92	-4.3	46.0	30.0	76.0
Mar-92	-1.9	109.0	8.0	117.0
Apr-92	-0.4	45.0	15.0	60.0
May-92	5.5	109.6	0.0	109.6
Jun-92	9.6	51.0	0.0	51.0
Jul-92	11.4	124.0	0.0	124.0
Aug-92	14.4	81.0	0.0	81.0
Sep-92	12.6	76.6	0.0	76.6
Oct-92	7.6	171.0	0.0	171.0
Nov-92	1.0	49.0	6.0	55.0
Dec-92	-0.8	47.4	16.0	63.4
Jan-93	-5.4	67.8	11.8	79.6
Feb-93	-4.6	119.8	17.6	137.4
Mar-93	-1.5	88.0	17.0	105.0
Apr-93	2.8	77.0	5.0	82.0
May-93	6.0	101.4	0.0	101.4
Jun-93	8.7	114.2	0.0	114.2

Table 3: Monthly mean temperature and precipitation values for Big Barasway, June 1991-June 1993, (AES, unpublished).

Year	Jan	Feb	Mar	Apr	May	Jun	Jul	Aug	Sep	Oct	Nov	Dec	Mean
1983	2.45	0.865	2.51	1.35	0.846	1.95	0.692	1.07	1.26	2.08	1.91	1.69	1.56
1984	2.01	3.49	0.990	3.06	1.84	0.687	0.354	1.27	2.52	0.580	0.783	1.32	1.56
1985	0.896	0.950	1.61	2.21	3.14	0.853	2.11	0.568	0.873	0.747	1.45	1.41	1.41
1986	2.75	2.40	3.85	3.56	0.524	1.90	0.932	0.539	0.714	1.35	3.50	0.685	1.88
1987	1.62	1.73	2.48	3.67	1.25	0.539	0.381	0.289	0.429	1.64	1.56	1.58	1.43
1988	0.698	4.48	2.78	1.83	1.03	2.94	1.35	0.479	0.601	0.899	2.06	1.05	1.67
1989	2.42	2.22	1.01	2.78	0.589	0.790	0.581	0.776	1.05	1.41	1.94	1.53	1.42
1990	2.49	2.53	2.20	2.47	1.24	2.35	0.454	0.550	1.05	2.73	1.38	2.73	1.84
1991	0.420	3.62	2.94	1.02	0.893	0.474	0.283	0.277	0.874	2.16	2.02	1.62	1.37
1992	1.91	0.656	5.52	1.60	3.43	0.471	1.26	0.559	1.07	2.35	0.928	1.63	1.80
Mean	1.766	2.294	2.589	2.355	1.478	1.295	0.840	0.638	1.044	1.595	1.753	1.525	1.594

Table 4: Monthly and annual mean discharges in cubic metres per second for 1983-1992;
 Little Barasway Brook near Placentia - Station no. 02ZK003;
 (Department of Environment and Lands, unpublished).

year. Increased flows on the Avalon Peninsula generally occur between March and June and between October and December. Increased flow may also occur between January and February, triggered by mild temperatures and combined rainfall and winter snowmelt (Water Resources Atlas, 1992).

Table 4 shows the monthly and annual mean discharges for Little Barasway Brook in the drainage basin north of Big Barasway (Department of the Environment, Water Resource Branch, unpublished). For the period 1983 - 1990 the highest discharge occurs between January and April and the lowest between July and September. The annual mean drainage is 50,400,000 m³ (1.6 cumecs). The drainage basin covers an area of 37.2 km². Assuming that the discharges of the streams at Big Barasway and Ship Cove are proportional to that at Little Barasway Brook, the annual discharge is estimated at 88,471,000 m³ which is an average of 2.8 cubic metres per second (cumecs) for the stream at Big Barasway and 44,710,000 m³ (an average of 1.4 cumecs) for the stream at Ship Cove.

2.3 Soils and Vegetation

The study area falls within the Atlantic pedoclimatic zone of Newfoundland (Woodrow and Heringa, 1987). The mineral soils are very acidic and generally developed from till. Thicknesses range between a few centimetres and about 1 metre.

The coastal areas principally contain Orthic and Placic Ferro-Humic Podzols (Heringa, 1981b). The valleys are composed mainly of the Angel's Cove series (Heringa, 1981b) which has a sandy loam texture, is moderately to exceedingly stony, and moderately well drained. The hills adjacent to the

valleys along the coast (Patrick's Cove series) are poorly drained and have similar surface textures and stone content to that of the valleys (Heringa, 1981b).

Areas adjacent to the coastline near sea-level are composed of the Bauline series (Heringa, 1981b) which consists of a sandy loam, is exceedingly stony and rapidly to well drained. The base of the valley at Ship Cove differs from most of the valleys along this coast, as it contains soils of the Waterford series of the Orthic Gleysol sub-group, characterized by a sandy loam, moderate to high gravel content and poor drainage (Heringa, 1981b).

Poorly drained Organic soils, Placic Humo-Ferric Podzols, and Placic Ferro-Humic Podzols cover the higher elevated terrain toward the centre of Placentia Peninsula. Bedrock is commonly exposed along the interior of the Peninsula, on the high grounds between the valleys, and along the coast (Heringa, 1981b).

The coastal areas are dominated by balsam fir and spruce forest. Interspersed are small barrens having a heath-shrub cover, with plants such as sheep-laurel, blueberry, bunchberry, raspberry, partridgeberry, crowberry, tall meadow rue, and reindeer moss (Heringa, 1981a). Two main types of bog, dry dwarf shrub-sphagnum and wet sedge-sphagnum, occur. Dry dwarf shrub-sphagnum is associated with forested areas whereas the sedge-sphagnum lies adjacent to heathland, barrens, and shrub forest (Pollet, 1981). Fens in the area are dominated by *Picea mariana* (black spruce) and *Larix laricina* (tamarack) (Catto, 1992a).

2.4 Bedrock Geology

The island of Newfoundland represents the northeasternmost extension of the Appalachian Orogen system in North America. The orogen is divided into four tectono-stratigraphic zones, each recording a different pre-Silurian evolutionary history. The western Humber and Dunnage Zones represent the ancient margin of North America whereas the Gander Zone includes remnants of the Palaeozoic Iapetus Ocean (Williams, 1979). The Precambrian elements of the Avalon Zone, the easternmost zone, predate the Iapetus Ocean and were originally attached to North Africa (O'Brien and King, 1982). This zone is approximately twice the width of the remainder of the Appalachian Orogen, extending roughly 250 km offshore to the present continental margin (Haworth and Lefort, 1979; O'Brien and King, 1982).

The Avalon Peninsula of the Avalon Zone is primarily composed of unmetamorphosed Hadrynian volcanic and clastic sedimentary rocks (McCartney, 1967; King, 1988). Small exposures of post-Cambrian granite, the Iona Islands Intrusive Suite, lie offshore to the north of Argentia in Placentia Bay. A more extensive irregular stock of Hadrynian granite, the Holyrood Intrusive Suite, lies east and northeast of the study area. Palaeozoic rocks crop out along the eastern and western sides of the Placentia Peninsula and along the heads of Trinity and Conception Bays (King, 1988). These outcrops consist of slate, shale, and minor limestone beds which are transitional upward into more clastic Lower Ordovician beds (McCartney, 1967). Sills of gabbro, diabase and diorite crop out on the southwestern tip of Placentia Peninsula (King, 1988).

The Musgravetown Group forms the majority of Placentia Peninsula. The Big Head Formation of the Musgravetown Group is directly adjacent to Big Barasway and Ship Cove, but is thin and poorly defined at the latter (McCartney, 1967). This formation consists mostly of fine grained, wavy bedded, grey to green sedimentary rocks that overlie the predominantly volcanic Bull Arm Formation and underlie the purplish red sandstone and siltstone beds of the Maturin Ponds Formation (McCartney, 1967; King, 1988). At Ship Cove, grey to black shale of the Heart's Content Formation crops out (King, 1988).

The structural geology of the area was shaped by the two periods of mountain building on the Avalon Peninsula. The first, the Avalonian Orogeny, occurred about 570-650 million years ago. The second occurred during the Cambrian and Ordovician, about 570 to 450 million years ago (King, 1989). On the Placentia Peninsula, orogenic activity has produced a series of northeast-southwest trending gently-dipping synclines and anticlines. At Big Barasway and Ship Cove the beds dip gently to the southeast. A minor fault with a west southwesterly-east northeasterly trend lies between Ship Cove and Big Barasway, separating the rocks of the Big Head Formation from the Heart's Content Formation to the south.

The cliffs along this expanse of coastline are steep. The lithology and steeply-dipping structure of the exposed bedrock along western Placentia Peninsula make the coast moderately to highly resistant to wave attack.

2.5 Glacial History

MacClintock and Twenhofel (1940) and Summers (1949) proposed that the Avalon ice cap was a residual of ice that had invaded the peninsula from the northwest, perhaps originally from Labrador. This remnant ice cap radiated from the central Avalon Peninsula during the later phases of the Wisconsinan. Henderson (1972) concluded that the Avalon Peninsula was never invaded by northwest ice; instead, it was an area of Wisconsinan ice accumulation which gave rise to a vigorous independent ice cap. Eastward flowing ice was diverted from the Avalon by moving northeast and southwest down Trinity and Placentia Bays. The northern half of the Isthmus of Avalon may have been covered by ice from the northwest (Henderson, 1972).

The ice centre in Henderson's (1972) reconstruction was in the basin of St. Mary's Bay. It radiated outward in all directions and attained a thickness of at least 2000 ft (approximately 620 m), a height necessary to have glaciated surrounding highlands on Placentia Peninsula such as the Beaver Pond Hills with an elevation of 275 m. The ice attained this thickness because it was restricted from moving southward (Henderson, 1972).

According to Henderson's (1972) reconstruction, during deglaciation the ice centre moved northwards from the mouth to the head of St. Mary's Bay while southerly drainage increased out of St. Mary's and Placentia Bays. The westward flow of ice over the Placentia Peninsula diminished. The west facing slopes along the Placentia Peninsula coast became ice-free first. Meltwater deposits were laid down and meltwater channels were eroded on ice-free slopes west of the north-south divide. As deglaciation progressed the

ice centre moved to the Trepassey Peninsula. The depositional and erosional features on the Placentia Peninsula were not affected by this move or by later glacial events.

Recently, Catto (1992a; 1992b) mapped the surficial geology of the southwestern Avalon Peninsula. Through analysis of striae, geomorphology and sediments, Catto has concluded that separate ice caps occupied the Isthmus of Avalon and that the St. Mary's ice cap, centred at the head of the St. Mary's Bay, extended to the southwest, west, northwest, and northeast. Both Henderson and Catto have thus established that the direction of ice flow on the eastern shore of Placentia Bay was westward from centres in St. Mary's Bay and on the Placentia Peninsula.

The coastal areas of western Placentia Peninsula often contain complex sedimentary sequences in the incised valleys (Catto, 1992a). At Big Barasway, marine sediments extend into the valley reaching elevations of 10 m and overlie till and glaciofluvial materials. Farther up the valley an organic veneer overlies a glaciofluvial apron. On the valley sides colluvial and till veneers overlie bedrock. On the high grounds between and behind the valleys, organic veneers overlying bedrock and/or till dominate (Catto, 1992b). The till consists mainly of large clasts, pebbles, cobbles and boulders with a sandy matrix. At present, a detailed investigation of the bluff at Big Barasway is being undertaken (House, in preparation). This bluff, approximately 70 m high, is located westward of a bedrock outcrop. Within the barrier complex at Big Barasway, there is a vegetated section overlying diamicton. Adjacent to the northern end of the barrier, a marine terrace of gravel at approximately 5 m overlies till and glaciofluvial sediments.

The base of the valley at Ship Cove is similar to that at Big Barasway. The valley sides are less steep and are marked by fewer colluvial sediments than at Big Barasway, with exposed bedrock and till veneers dominating (Catto, 1992b). Unconsolidated bluffs of diamicton border both sides of the gravel barrier.

2.6 Holocene Sea-level Changes

A Holocene sea-level curve has not been published for the east coast of Placentia Bay or for other parts of the Avalon Peninsula. Curves have been developed for the northern Northern Peninsula (Grant, 1972; Grant, 1989), Cape Freels in northeast Newfoundland (Shaw and Forbes, 1990), and St. Georges Bay and Port au Port area in southwest Newfoundland (Brookes *et al.*, 1985; Forbes *et al.*, 1993). Until recently, little geomorphological, sedimentological and chronological analysis had been undertaken on the Avalon Peninsula.

The existing curves show that for most of the island of Newfoundland, sea-level rapidly fell initially after deglaciation to below present levels and subsequently rose to present levels. An exception to this general trend is present along the northern part of the Northern Peninsula which has experienced continual emergence following deglaciation (Brookes and Stevens, 1985).

Numerical models have been developed that describe the behaviour of the lithosphere under ice load and the earth's response once that load is removed (Clark, 1980; Clark and Lingle, 1979; Peltier *et al.*, 1978; Quinlan and Beaumont, 1981; 1982). These models indicate that postglacial sea-levels can

be categorized into distinctive zones which depend on the distances from the ice centre. Although the island of Newfoundland supported local ice caps, the effect of the Laurentide Ice Sheet essentially overwhelmed the influences of the local caps (Grant, 1989). Consequently, the island's position at the southeastern margin of the Laurentide Ice Sheet is more important in determining the generalized shapes of sea-level curves. Other factors such as thermal expansion affect sea-level curves; however, the order of magnitude is much smaller than that due to forebulge migration.

In the glacio-isostatic models, the crust deforms under the weight of ice, causing material to move toward the margins of the ice sheet. Ice marginal forebulges, elevated areas with this displaced material, migrate toward the location of the former ice mass as the ice sheet melts during and after deglaciation. The rate and direction of forebulge migration for the island is being studied and, based on marine shell evidence throughout the island, is likely faster than glacio-isostatic models have predicted (Liverman, in press). As the viscoelastic properties of the earth cannot be measured directly, geophysicists require information on glacial extent, the manner and rate of deglaciation, and postglacial sea-level responses.

Quinlan and Beaumont (1981) developed models describing postglacial relative sea-levels in Atlantic Canada and showed four types of sea-level curves that could ensue (Figure 4). These curves range from continual emergence (zone A) to continual submergence (zone D). The two intermediate zones, B and C, are characterized by initial emergence, followed by submergence. However, in zone B, emergence is greater than submergence while in zone C, submergence is greater than emergence. Hence, raised

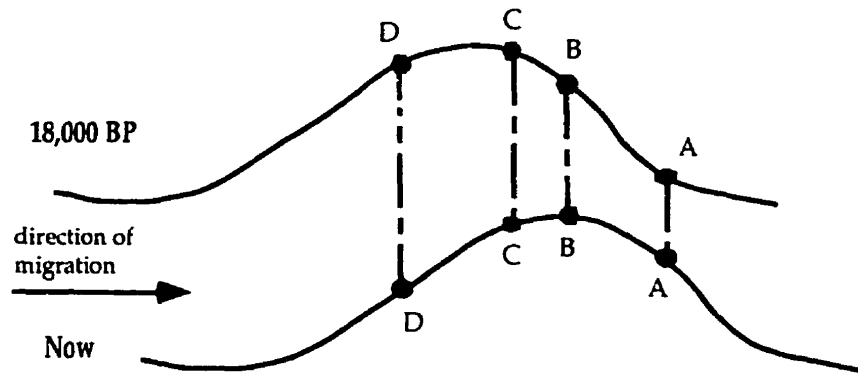


Figure 4a: Schematic diagram of a peripheral bulge at two points in time, 18,000 BP and now. The bulge migrates in the direction of the arrow affecting relative sea-level (RSL) at sites A, B, C, and D, shown in Figure 4b. (after Quinlan and Beaumont, 1981).

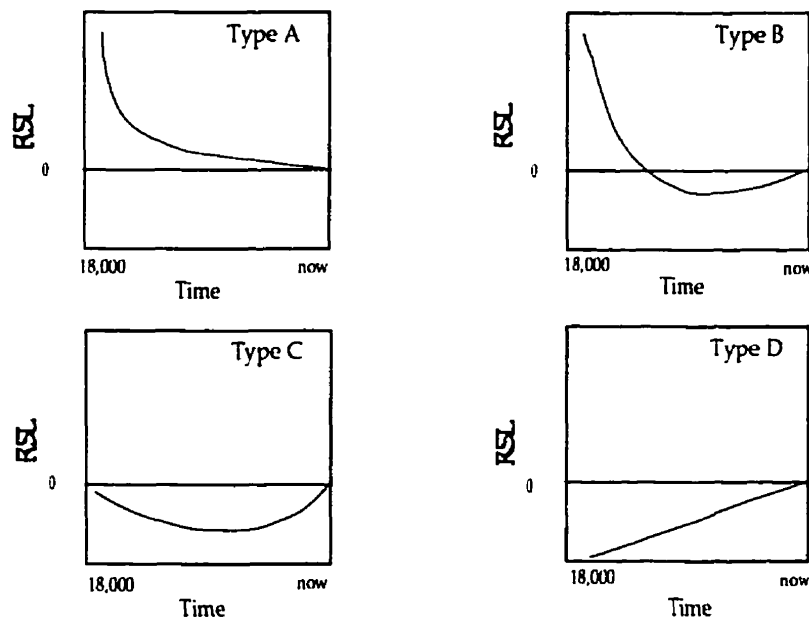


Figure 4b: Schematic diagram showing the RSL history at each of the sites A through D resulting from forebulge migration. These sites and RSL curves are taken as type examples. At location A, the RSL history is characterized by continual emergence, whereas at location D, the RSL history shows continual submergence. At locations B and C, the RSL histories show initial emergence followed by submergence. At location B, the emergence is greater than the submergence, whereas at location C, submergence is greater than emergence. (after Quinlan and Beaumont, 1981).

marine features would be found in zones A and B, whereas zones C and D would show no marine features above present sea-level.

In Quinlan and Beaumont's (1981) model, the Avalon Peninsula was placed within zone D, indicating continual submergence. More recently, Grant (1989) showed the division between type B and type C curves at the Isthmus, thus indicating that the study area falls within either zones C or D. However, the raised marine deposits at 10 m asl at Big Barasway and Ship Cove and the deltaic deposits at Point Verde suggest that the western part of the Avalon Peninsula has undergone emergence. Furthermore, a lowstand at the head of Placentia Bay has been estimated at 8 m below present sea-level (Shaw and Forbes, in press), which in addition to the raised features, indicates that the western part of Placentia Peninsula lies within zone B, as does most of the island.

2.7 Human Activity

The Cape Shore was initially settled during the early nineteenth century by Irish immigrants, principally from the counties of Wexford, Waterford, and Tipperary. The first record of permanent settlement along this coast was at Ship Cove in 1802 (Mannion, 1974). These settlers were isolated, ethnically homogeneous, and subsisted on pastoral farming. Involvement in the commercial fishery increased toward the mid-1800's (Mannion, 1974).

Given the rugged terrain of this shore and the pattern of Irish settlement, homesteads were sparsely scattered in the small, more protected and fertile valleys. These were initially occupied by no more than two

families (Mannion, 1974). With subsequent generations the land units were divided amongst the children, creating a cluster of houses within an ancestral farm unit. The legacy of settlement can still be seen today. The coastline is sparsely populated with pockets of families within the valleys, such as at Little Barasway and Ship Cove with only one to three families.

Compared to more developed areas the beaches at Ship Cove and Big Barasway have experienced relatively minor anthropogenic influence. However, at Ship Cove the removal of aggregate adjacent to the beach for road construction in the 1960's and 1970's and a forced northerly relocation of the outlet in the mid 1960's have affected the beach morphology.

Chapter 3

Methods

3.1 Characteristics of Barrier Sediment

3.1.1 *Clast Shape*

Clast shape analysis is frequently used in Quaternary studies to determine the palaeoenvironmental conditions of deposition. It is particularly important for distinguishing between beach and fluvial deposits, for the former may be used to determine a palaeoshoreline (Howard, 1992). However, the parameters and the definitions of these parameters are not universally accepted (Barrett, 1980). In this research, clast-shape description involved three major components: roundness, sphericity and overall shape.

The roundness measurements employed the scale developed by Powers (1953), where 0.1 to 0.3 is angular, 0.3 to 0.5 is subangular, 0.5 to 0.7 is subrounded and 0.7 to 0.9 is well rounded. The degree of roundness was assessed qualitatively in the field and estimated to the nearest 0.1 division. Clasts with sharp surfaces created by fractures, but showing well-rounded surfaces over most of their areas, were considered well-rounded. At each sample site, a total of 25 randomly selected clasts were assigned Powers roundness grades. The grades were then combined and the modal roundness of the assemblage described in qualitative terms. This procedure allows the relative degree of abrasion to be assessed between the two beach systems at Big Barasway and Ship Cove, as well as permitting the assessment of differences within the individual beaches.

Sphericity is a measure of the ratio of the three mutually perpendicular axial lengths of a clast. The concept was originally developed by Wadell (1935) and modified by Krumbein and Pettijohn (1938). In this study, clasts were described as having either low, medium, or high sphericity. Clasts with a low shortest axis:longest axis ratio are described as having low sphericity. In contrast, clasts with axes of approximately equal length are classified as having high sphericity. As with the evaluation of roundness, the classifications obtained from 25 randomly selected clasts at each sample site were combined and the modal sphericity assessed qualitatively.

The Zingg (1935) classification was used to determine overall clast shape. The divisions are based on intermediate:long axis ratio and short:intermediate axis ratio. Clasts are defined as either discoid, for which the intermediate:long axes ratio is greater than 2/3; bladed, for which both ratios are less than 2/3; roller, for which for the short:intermediate axis ratio is greater than 2/3; or equant, for which both ratios are greater than 2/3. The oblate-prolate index developed by Dobkins and Folk (1970) is preferred by some researchers, for example, Barrett (1980) and Gale (1990), for distinguishing depositional environments. However, this method does not distinguish between rollers and equants, therefore limiting its use as a general descriptive tool.

The axial lengths of the clasts were not measured numerically, and the assignment of the Zingg shapes was done visually in the field. The proportion of the clasts which fell into each shape category at each sample site are reported. Although this procedure does not allow rigorous statistical

analysis, it does permit semi-quantitative comparisons among different locations between and within the beaches at Ship Cove and Big Barasway.

3.1.2 Sediment Texture

Since the majority of sediment within both beaches is coarser than medium-sized pebbles, it is impractical to obtain samples for laboratory analysis that contain enough pebbles, cobbles and boulders for a statistically meaningful result (Catto, 1989; Gomez, 1983). Gale and Hoare (1992) evaluated existing sampling methods and discussed the difficulty of determining the mass of sample required to obtain a representative sample of each size fraction present in a coarse-clastic deposit. For example, Church *et al.* (1987) recommend a minimum sample size of 1000 kg to adequately categorize gravel deposits containing a maximum particle diameter of 100 mm. The beaches at Big Barasway and Ship Cove contain clasts > 256 mm, and thus each textural sample size would have to be much larger than 1000 kg in order to obtain statistically valid results from textural analysis (Gale and Hoare, 1992). Consequently, visual estimates of volume percentages of clasts of each grain size were made in the field using the charts developed for the estimation of mineral percentages by Shvetsov (1954). Size categories were based on the logarithmic (to the base 2) modified Wentworth-Udden Scale (Udden, 1898; Wentworth, 1922; Krumbein, 1934).

3.1.3 Clast Fabrics

Clast fabrics were taken along the beaches at Ship Cove and Big Barasway. Visual examination at the onset of the study revealed strong clast

imbrication along the beaches, particularly along berm crests. Imbrication was consistently seaward and varied at individual locations up to $\pm 45^\circ$ from the trend of the shoreline.

Upon preliminary examination, it was apparent that imbrication varied with clast shape. Discoid clasts consistently showed imbrication patterns with seaward dipping a/b planes, a common pattern noted in other beaches (Bourgeois and Leithold, 1984; Jennings and Smyth, 1990; Reineck and Singh, 1975). In contrast, elongated clasts (rollers and blades) appeared to demonstrate non-random patterns of a-axis imbrication. It was decided, therefore, to evaluate the usefulness of the fabric method involving analysis of the orientation and plunge of the a-axes (Mark 1973; Woodcock 1977; Rappol 1985), in environments where the orientations of the beaches and the direction of wave approaches are known. Thus, the data obtained by a-axis fabric analysis can be compared with the orientations of the strongly imbricated a/b planes of the discoid clasts.

Clast fabrics involving a-axis determinations were taken along the barriers following the method described by Catto (1989). At each site a sample of 25 clasts was chosen from within an area of 1/2 m x 1/2 m. Although the sediment along the beaches at both locations contains large percentages of discoid clasts (see chapters 5 and 7), the majority of sites contained a mixed population, with discs and spheres totaling $\leq 50\%$ of the total proportion of clast shapes. Sites marked by concentrations of discs and spheres in excess of 50% of the total clast assemblage were not tested. The imbrication of the a/b planes of discoid clasts at all sites were noted. Clasts of similar sizes were chosen for analysis, predominately large pebbles and cobbles. All clasts were

taken from the surface layer, except for the fabrics taken from natural cut banks present along stream outlets.

A Brunton pocket transit was used for the measurements. The trends and plunges of the a-axes were measured. Clasts were chosen that had a-axes at least 1.5 times longer than the intermediate b-axes. Despite the large percentages of discs and spheres, a sufficient number of clasts fulfilling the shape criteria were available within each of the small grid areas analyzed.

The results were plotted on a Schmidt equal area stereonet and statistically analyzed using the Stereo package for the Apple Macintosh Computer (McEachran, 1989). With the stereonet, clasts with shallow angles of a-axis plunge plot toward the edge of the circle whereas those with steep angles plot toward the centre. Clasts with a northward or southward trend plot along the y-axis whereas those with a more east-west trend plot along the x-axis on the stereonet. The azimuths of the clasts can be estimated by reading the graduations along the margin of the net.

The Stereo package calculates the mean linear trend and dip, the normalized eigenvalues, and K values based on eigenvector and eigenvalue methods described by Mark (1973), Woodcock (1977), and Rappol (1985). The normalized eigenvalues ($S_i = \lambda_i/n$) describe the strength of the clast orientation, where $S_1 + S_2 + S_3 = 1$. The normalized eigenvalues can range from 0.33 to 1, where 0.33 represents randomness and 1.0 indicates perfect orientation. Values of 0.6 and greater are considered moderately strong values for the littoral environments being studied in this research.

Another statistical parameter, K, where $K = \ln(S_1/S_2) / \ln(S_2/S_3)$, describes the overall shape of the distribution. K values less than 1 indicate a

girdle distribution, values greater than 1 show a cluster distribution. Where $K = 1$, distributions have equal girdle and cluster tendencies (Woodcock, 1977).

3.2 Tracer Clasts

Use of marked, painted, radioactive, or lithologically distinct tracer clasts has been a common procedure in marine beach studies (Boon, 1969; Donoghue and Greenfield, 1991; Sherman *et al.* 1989; Sherman *et al.*, 1990). These clasts, if recovered along the shore, can be used to assess the direction and velocity of sediment migration. In September 1991 a 1 m x 1 m area with mainly small to large pebbles exposed on the surface along the mid-beachface along zone A at Ship Cove, and a 1 m x 1 m area of similar clasts along the upper-beachface near transect BB- 30 along zone D at Big Barasway, were painted with Armor Coat Interior/Exterior Fluorescent Spray Paint. After three days, the paint on the clasts at Ship Cove had been extensively eroded. No painted clasts could be seen on a visit to the beach at Ship Cove two weeks after the initial painting, and none were subsequently recovered on any visits. Approximately 25 clasts with paint could be seen at Big Barasway after two weeks and 6 clasts were visible throughout the subsequent months. Paint was being removed from the clasts at Big Barasway, but the rate was less than that at Ship Cove.

In March 1992, 4 samples of 250 pebbles each were taken from zones A and C at Ship Cove and from zones A and C at Big Barasway. These clasts were thoroughly dried and then painted with Matchless™ Alkyd Marine Paint. The samples of clasts were returned to the zones from which they were

taken and placed in the intertidal zone. Two colours, yellow and red, were used at each beach. A visit to the beaches one week later, as well as subsequent visits, resulted in no siting of painted clasts.

The clasts were painted in attempts to trace the movement of clasts; however, it appears that the paints used could not withstand the constant wave action. The few clasts that retained the paint were located along the backbarrier at Big Barasway and were thus removed from the wear of wave action.

In August 1992 two samples of 250 white granite clasts each, obtained from a beach near Musgrave Harbour, Newfoundland, were deposited in the intertidal areas of zone A at Ship Cove and zone C at Big Barasway. As these granitic clasts are not indigenous to the study area and differ lithologically from the local clasts, it was hoped that they could be located during subsequent visits. Unfortunately, none were found. The clasts were either moved offshore or were covered by locally derived clasts.

3.3 Profile Measurements

Transects were spaced 20 m apart at both Ship Cove and Big Barasway, with the exception of transects BB-15 and BB-18 along zone C at Big Barasway (Figures 5 and 6). These transects were spaced 40 m apart. The orientations of the transects were aligned normal to the beach trend. Divisions along each transect were based on either slope or sediment textural changes. Horizontal distances were taken using a measuring tape and a clinometer was used to measure slope angles. Estimates of mean water level initially were determined from tide tables for Argentia, located to the north of the study

area, and subsequently from direct observation at the sites. Profiles were plotted based on height above mean sea-level.

In July 1993, a coastal monitoring program was initiated jointly by the Newfoundland and Labrador Department of Mines and Energy and the Geological Survey of Canada. Three transects were established along Big Barasway and one at Ship Cove. Repetitive measurements on several occasions were made using a simple paired-staff leveling and tape system. Two of the GSC transects at Big Barasway correspond to BB-10 and BB-34. The transect at Ship Cove corresponds to SC-11. The profiles of the GSC boulder site transect and GSC-393 (BB-10) measured in February 1994 show the location of the ice foot. When measurements were taken during February, the surveying rod was pushed through the snow on top of the foot until the ice prevented further penetration.

Transect measurement of BB-10 in June 1993 using the method employed in this study revealed a height of 3.1 m and a backbarrier width of 42 m. The height of the GSC profile taken at the same location in July 1993 revealed a height of 2.8 m and a backbarrier width of 43 m. The two methods yield a difference in height of 0.3 m and in width of 1 m. Observations by the author on both occasions indicated that the beach in this area had altered little between June and July 1993. The GSC method has been in use for over 10 years and has been checked by electrical surveying equipment. The accuracy of the beach elevations is estimated at ± 10 cm (D. Forbes, Atlantic Geosciences Centre, personal communication).

Taking repeated measurements using the clinometer and tape method between July 1991 and September 1991 (during a time period marked by no

crestal breaching by waves) of transects that had undergone no alteration in height and backbarrier width revealed similar barrier heights. Profiles of transect SC-11 show a difference of 0.4 m between the profiles taken in July 1991 and in September 1991. Transect SC-17 shows a difference of 10 cm between the profile taken in July 1991 and the one in September 1991. The accuracy of angle measurements taken using the clinometer is within $\pm 0.5^\circ$. Using the overall beachface and backbarrier slopes yields an error of ± 0.5 m in barrier height.

Detailed profile data and sediment descriptions were executed during July 1991 and September 1991. Following this, the barriers were visited regularly at least once every six weeks to a maximum of once a week between September 1991 and March 1993. In May 1992, the beaches were visited for five consecutive days. Profile measurements were taken when time and assistance were available. The generalizations in patterns or trends in sediment structure and morphology presented in this thesis are based on actual measurements and visual observations.

3.4 Echo Sounding Measurements

Echo sounding measurements were taken using a "MX-2250" White Line/Straight Line Chart Recorder September 5, 1992 when Placentia Bay was calm and the visibility was clear. The locations of the boat offshore were fixed using two positions along the barrier. Brunton pocket transits were used by shore-based observers to take the bearings of the boat from the barrier locations. The two beach positions were fixed using a theodolite and surveying rods. At Big Barasway the zero angle for the theodolite was based

on two locations: one at the end of Otter Point (Figure 7) and the second at the northern end of the bridge (not shown on Figure 7). A surveying rod was used to measure the distance between the base location at Otter Point and the locations on the barrier. The theodolite was positioned on the locations on the barrier and distances and angular measurements were taken to cross-check the first measurements based at Otter Point. Distances between locations were measured to the nearest metre, giving an error of ± 0.5 m for the positions used for offshore bearings. At Ship Cove the theodolite was positioned on the northern end of the bridge. The zero angle for the theodolite was based on the line drawn between the northern headland and the northern end of the bridge. As at Big Barasway the theodolite was positioned on the locations of the barrier and distances and angular measurements were taken to cross-check the first measurements.

The error associated with a bearing using the Brunton pocket transit is estimated at $\pm 1^\circ$. The error associated with an offshore fixing (using simple trigonometry) increases with distance and smaller angles. After plotting the offshore positions, the position (point C on Figure 5) marked by the largest distances from the fixed positions on shore and the smallest angular bearing was chosen to estimate the largest error associated with the offshore positions used in this study.

Figure 5 illustrates the calculation of error for point C at Big Barasway. The distance between points A and B on shore is 231 ± 1 m. The bearing taken by the observer at point A gave an angle of $28^\circ \pm 1^\circ$ for $\angle CAB$, whereas the bearing taken at point B gave an angle of $140^\circ \pm 1^\circ$ for $\angle ABC$. Determining one-half of the difference in the distances of X (the line

perpendicular to line AB) between the two cases where the errors are greatest will give an estimate of the error. Thus:

$$\tan 27^\circ = X/(230 + Y); \text{ and}$$

$$\tan 39^\circ = X/Y, \text{ or } Y \tan 39^\circ = X.$$

Substituting one equation into the other and solving results in $Y = 391 \text{ m}$ and $X = 317 \text{ m}$.

Likewise, for the other case of theoretical extreme error:

$$\tan 29^\circ = X/(232 + Y); \text{ and}$$

$$\tan 41^\circ = X/Y.$$

Substitution then results in $Y = 400 \text{ m}$ and $X = 348 \text{ m}$. This gives a difference of 31 m for X. Thus, the maximum error associated with the offshore positions determined at Ship Cove and Big Barasway is estimated at $\pm 16 \text{ m}$. Most offshore sites, marked by more central positions and larger bearing angles, had smaller theoretical maximum errors associated with their precise locations.

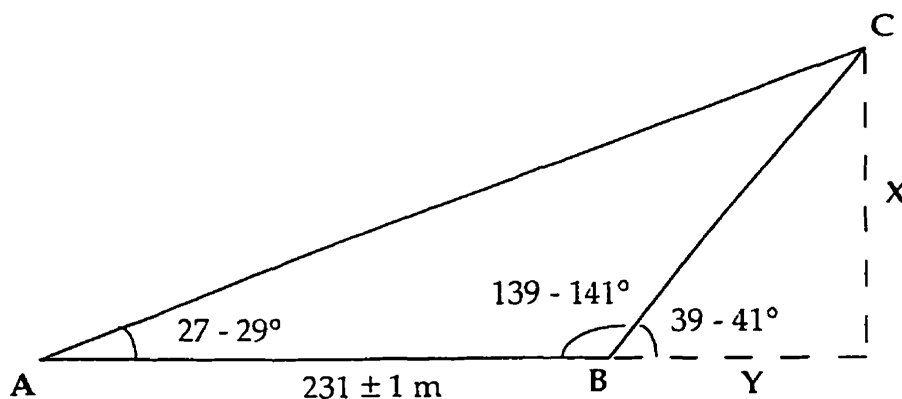


Figure 5: Sketch showing the calculation of error associated with location of the offshore position, point C. Points A and B are the positions on land. The determination of X is explained in the text.

3.5 Cores

Four cores were taken from the lagoon at Big Barasway using a modified Livingstone corer on October 14, 1992. The locations are shown on Figure 7. Textural analyses of the core samples entailed sieve analysis and hydrometer suspension analysis (ASTM 1964). Grain size designations were based on the modified Wentworth-Udden scale (Krumbein, 1934).

3.6 Exposures

Two naturally exposed cut banks were examined. The thicknesses, structure, and textures of the sedimentary units and the fossil composition of the organic units of the stratigraphic sequences were described using the methods outlined previously. The modes of formation of the peats were determined by analysis of their composition and by comparison with modern peats in the study area. N.R. Catto identified the species of marine shells. Two samples of wood fragments with bark were dated by gasometric ^{14}C analysis at the laboratory of the Geological Survey of Canada in Ottawa.

3.7 Cliff Erosion

The bluffs bordering both Ship Cove and Big Barasway are actively eroding. To estimate the rate of cliff retreat, seventeen sites were established at Ship Cove and 21 sites at Big Barasway. Two markers were placed at each site. Orientation to the cliff edge was determined at each site and the distance was measured using a tape. The short duration of the study precludes accurate assessment of long term retreat. However, these measurements, in addition to comparison of 1948 and 1980 air photos and estimates by residents

who have lived in the cove communities for over 40 years, allowed estimates of the rate of cliff retreat.

3.8 Aerial Photos

Longer term comparisons of the morphology are possible using successive air photos taken in 1948, 1967 and 1980. The small scales of the 1948 (1:40,000) and the 1980 (1:56,000) air photos and the size of the gravel barriers make it difficult to accurately quantify the changes in barrier widths and lengths along the zones, as well as the landward displacement. A inaccuracy in the measurement of two points of 1 mm on the 1:56,000 scale of the 1980 air photo would result in an error of ± 56 m. The 1:17,000 scale of the 1967 air photo shows more detail, and a 1 mm inaccuracy would result in an error of ± 17 m. Comparison of morphological changes of the barriers at Ship Cove and Big Barasway in the air photos in addition to changes observed during the study allow an estimate of landward retreat. This estimate is supplemented by observations made by residents who have lived in the communities for more than 40 years.

Chapter 4

¹⁴C Age Determinations and Holocene Sea-level

4.1 Description

Two samples of autochthonous forest peat containing arboreal wood fragments were submitted for gasometric ¹⁴C analysis to the laboratory of the Geological Survey of Canada in Ottawa. At Ship Cove (Figure 6), an autochthonous fibric peat unit 25 cm thick is present at sea-level in a natural cut bank adjacent to the lagoon (Catto, in press; Catto and Thistle, 1993; Catto *et al.*, 1994). The peat contains *Picea mariana* (black spruce) fragments, many of which are covered with adhering bark. This unit contains no marine fossils, and is similar in its organic content and degree of decomposition to fibric peats developed under modern black spruce-tamarack forests in the Ship Cove area, including those adjacent to the present coast (Catto, 1992 a, b). Analysis indicated a ¹⁴C age of 1340 ±70 B.P. (GSC-5306; Catto, in press; Catto and Thistle, 1993; Catto *et al.*, 1994).

At Big Barasway, a sample was obtained from an autochthonous peat layer capping a naturally-eroded sedimentary exposure 2.5 m above sea-level backing the zone B segment of coastline (Figure 7). This peat unit contained bark-covered fragments of *Picea mariana* as well as *Abies balsamea* (balsam fir), lacked marine fossils, and resembled both modern forest peats mapped in the vicinity (Catto, 1992 a; b) and the forest peat which underlies the

tuckamore vegetation present on the shore of the lagoon along the landward side of the Zone B segment of coastline. The peat sample yielded a gasometric ^{14}C age determination of 3480 ± 60 B.P. (GSC-5319; Catto and Thistle, 1993; Catto *et al.*, 1994; Catto, in press).

Figures 8 (Ship Cove) and 9 (Big Barasway) illustrate the stratigraphic successions in which the samples were located. At Ship Cove, unit 1 consists of a laterally discontinuous bed of subrounded and rounded imbricated pebbles and cobbles, underlying 25 cm of peat (unit 2). The sample which was ^{14}C -analyzed was taken from the base of the peat unit at the present mean sea-level. The peat is overlain successively by 30 cm of sand (unit 3) and 35 cm of peat (unit 4). The succession is capped by a 10 cm thick layer of silt (unit 5), overlain by anthropogenically disturbed sediment and soil. The silt contained shell fragments of the extant mollusc *Mytilus*, and badly decomposed fragments of marine rockweed, possibly *Ascophyllum* (Catto, N., personal communication). At Big Barasway, the 46 cm thick peat layer directly overlies diamicton, and is capped by modern organic material developed under coastal grasses and herbaceous vegetation.

4.2 Discussion

The similarity of the peat deposit at Ship Cove to modern peats forming under terrestrial forest deposits and the lack of marine fossils indicate that the peat unit at Ship Cove represents an *in situ* terrestrial forest deposit. Its position at mean sea-level suggests formation when relative sea-level was at an elevation lower than that of the present sea-level. The autochthonous terrestrial peat present at Big Barasway suggests that

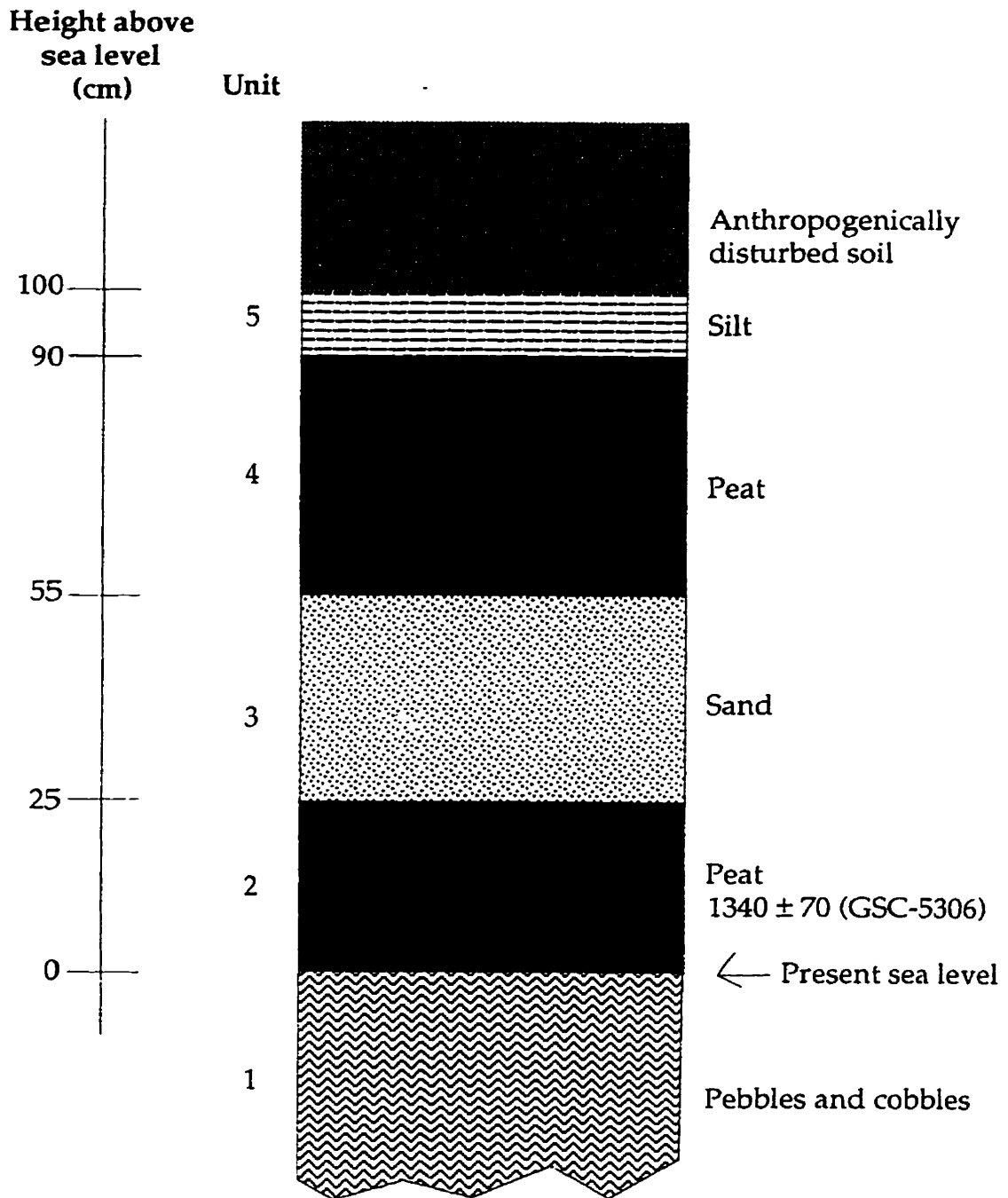


Figure 8: Stratigraphic Sequence at Ship Cove

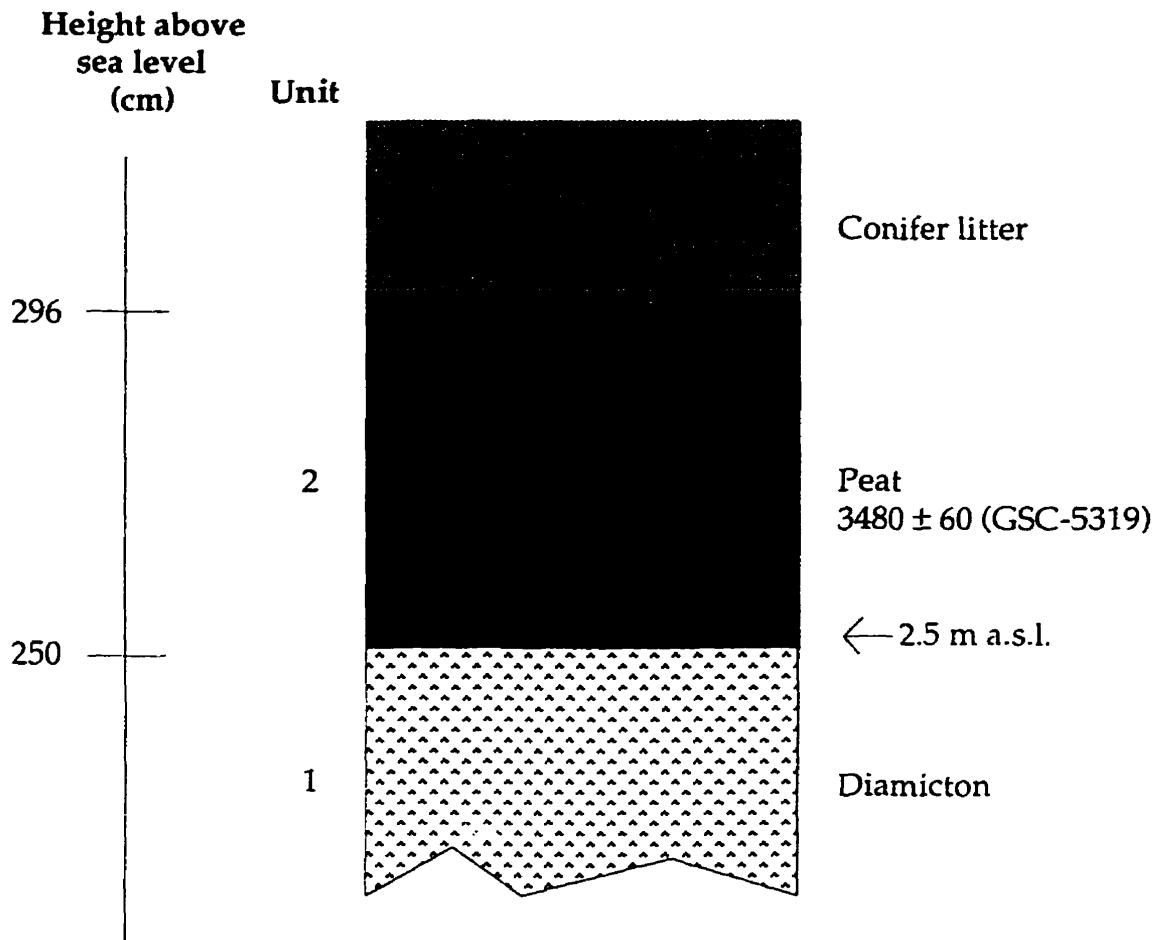


Figure 9: Stratigraphic Sequence at Big Barasway

relative sea-level was below 2.5 m elevation approximately 3480 B.P. A peat sample taken from a coastal bluff 10.5 m above present sea-level at Point Verde, to the north of the study area, has yielded a ^{14}C age of 6130 ± 80 B.P. (GSC-5158). Along the Cape Shore, other ^{14}C analyzed terrestrial peat deposits from Patrick's Cove (7660 ± 90 , GSC-5414), Little Barasway (5600 ± 60 , GSC-5580), and Fox Harbour (5150 ± 80 , GSC - 5169) indicate that sea-levels were at or below present throughout the early- and mid-Holocene (Catto and Thistle, 1993; Catto *et al.*, 1994; Catto, in press). The emerged marine deposits at 10 m a.s.l. underlying the peat unit at Point Verde indicate that, shortly after deglaciation, sea-level was above the present level (Catto, 1992a; Catto and Thistle, 1993). During the early Holocene sea-level dropped rapidly, reaching a lowstand of -8 m a.s.l. at the head of Placentia Bay approximately 7,000 B.P. (Shaw and Forbes, in press). The locations of the terrestrial peat sites along the Cape Shore in exposed marine environments where coastal erosion is evident suggest that transgression subsequently occurred along Placentia Bay, and that relative sea-level did not reach its present position until some time after 3,480 B.P.

The imbricated pebble and cobble unit at the base of the sequence at Ship Cove could have been deposited in either a fluvial or marine beach environment. The gravel shows textural similarities to the beach deposits associated with the modern barrier; however, the clasts are less rounded and the beds are laterally discontinuous. A fluvial origin for this gravel is thus a likely explanation. As at Big Barasway, the sedimentary characteristics of the peat indicate that it is autochthonous.

The silt layer (unit 5) at Ship Cove could be either a marine or an aeolian deposit. If the deposit is aeolian, however, the presence of the marine shell and rockweed fragments would require deposition by onshore winds. In the present environment, little (if any) silt is exposed along the beach for transportation by wind. Along the Cape Shore, aeolian deposition of silt is associated with cliff-top settings such as at the tip of Point Verde, rather than in coves (Catto and Thistle, 1993). Although the shell and rockweed fragments could have been deposited by birds, animals, or humans, the position of the organic fragments interspersed with the silt in unit 5 suggests simultaneous deposition of both silt and fragments. Furthermore, if humans were responsible for the deposition of the rockweed (which is commonly used for fertilizer in gardens by residents of the Cape Shore), larger clasts would likely be deposited also. Mixtures of marine plant matter and pebbles commonly mark areas where rockweeds have been applied as fertilizer, as has been noted at Little Barasway (Catto, personal communication) and at several seacoast localities along the eastern Burin Peninsula (Ruffman, A., Geomarine Associates, personal communication).

During this study, high lagoon levels at Ship Cove, reaching 90 cm above mean sea-level and near the base of unit 5 have occurred. These higher lagoon levels develop when the stream outlet was closed, the height being limited by the hydraulic head. Deposits resulting from outlet closure and consequent increased elevation of the surface level of the lagoon waters, however, would likely contain wood fragments derived from erosion. The silt layer lacks any terrestrial wood fragments. Destruction of the barrier and subsequent opening of the lagoon to marine infiltration at the present (or

lower) sea-level would necessitate a large storm event. The low-energy deposition indicated by the silt, however, requires the presence of a protective barrier. Deposits associated with storm overwash along the barrier and in the lagoon are dominated by coarse clasts and contain large driftwood fragments, frequently of tree species not native to Newfoundland (Catto, in press), and fine sediment is not present.

An outlet could possibly open during a storm, exposing the lagoon to marine infiltration, and then close shortly after or during the waning stages of the storm. If the discharge of the stream were low, marine water could then be trapped in the lagoon and a low-energy depositional environment would temporarily exist. This sequence of events could occur if sea-level was either at its present position, or if the level was slightly lower.

Low energy marine deposition could also reflect higher lagoon levels resulting from higher sea-levels (Catto, in press). If this is the case, another possible explanation for the ^{14}C ages of the terrestrial peats and the sequences at Ship Cove and Big Barasway is that a transgression occurred after 3480 B.P., and continued until it reached a maximum of at least 75 cm but less than 2.5 m above modern sea-level, at some time after 1340 B.P. Following this, sea-level fell to at least the present level.

Regardless of which explanation is the correct one for the deposition of the silt layer, regional evidence (Catto, in press; Catto and Thistle, 1993; Catto *et al.*, 1994) indicates that sea-level has been rising throughout the past 1000 years. A fragment of *Picea* (spruce) associated with autochthonous forest peat found 0.5 m below sea-level at Biscay Bay Brook, southeast of the study area, has been ^{14}C dated at 750 ± 90 B.P. (GSC-5414; Catto, in press). On the western

side of Placentia Bay, 0.5 km south of Little St. Lawrence on the Burin Peninsula, peat with wood fragments was found 1.7 m below the high water level (Tucker *et al.*, 1982). The peat was determined to have a ^{14}C age of 970 ± 50 B.P. (GSC-2569) and the wood 1080 ± 50 B.P. (GSC-2617). Also on the Burin Peninsula, rooted stumps and other *in situ* wood deposits have been found in several locations (Grant, 1989, 1991; Liverman, personal communication). *In situ* wood situated at 1.22 m below highest tide level and overlain by salt marsh peat was ^{14}C dated at 970 ± 80 B.P. (Grant, 1991). These terrestrial deposits indicate a 1-2 m rise in sea-level over the last 1000 years. Intertidal autochthonous forest peat and rooted stumps along the east coast of Prince Edward Island indicate similar rates and timing of submergence (Frankel and Crowl, 1961; Grant, 1970, 1989). In July 1994, the discovery of four rooted *Picea* stumps between mean high and mean low tide levels at Mobile, Newfoundland, south of St. John's, indicates that sea-level has also risen along the eastern Avalon coast. A sample from one of these stumps has been submitted to the Geological Survey of Canada for ^{14}C analysis (Catto, personal communication).

Archaeological evidence also suggests recent rises in relative sea-level. A fragment of a wall at Fort Frederick, Placentia, has been located approximately 2 m below present sea-level (Royce Gaines, personal communication to Catto, 1993; Catto, in press; Catto and Thistle, 1993). This fort was constructed in 1722, and the position of the wall thus suggests that sea-level may be currently rising at approximately 0.7 cm per year at Placentia. Archaeological evidence has been used to date submergence at Fortress Louisbourg, Nova Scotia, as well as a submerged corduroy road near Fort

Beausejour, New Brunswick (Grant, 1970, 1989). Seventeenth century structures recently excavated at Ferryland, Newfoundland, also suggest recent submergence in this area (Catto and Thistle, 1993). The possibility of local subsidence surrounding the Fort Frederick wall, induced by its own weight, and the additional possibility that the original wall may have been built to extend below sea-level create difficulties in assessing the true rate of submergence. The actual rate is probably between 0.3 - 0.6 cm/year (Catto, in press; Catto *et al.*, 1994), a rate similar to that occurring along the coast of Nova Scotia (Shaw *et al.*, 1993). Further research is needed to quantify the true rate of rise. Notwithstanding the difficulties involved in determining the precise numerical rate of transgression, the interpretations of the behaviour and sedimentology of the barriers at Ship Cove and Big Barasway have demonstrated that a transgression is presently occurring.

Chapter 5

Description of the Barrier at Ship Cove

5.1 Morphology

The beach at Ship Cove is 0.5 km long (Figure 6). The northern 200 m consists of a bayhead barrier with widths that range between 26 and 60 m and heights that range between 2 and 5.5 m above mean sea-level. The greatest heights of 6 m are reached not on the barrier itself but on the beach adjacent to the southern end of the barrier. Headlands bordering the north and south sides have a layer of diamicton, with thicknesses ranging between a thin veneer to 5 m, overlying siltstone and sandstone of the Musgravetown Group (King, 1988). Echo sounding measurements revealed depths of 14 m at the mouth of the cove. The echo sounder profiles show a steeper gradient of 0.1 towards the northern side of the cove and a gentler gradient of 0.02 towards the south side of the cove. The beach is influenced by plunging breakers which generally break 2 to 15 m from the shoreline. Plates 1 and 2 show an overview of the barrier and lagoon.

Twenty transverse profiles taken in July, 1991 and May, 1992 are shown in Figures 10 - 18. Table 5 shows the transect trend, the height, the foreshore and backshore widths, the foreshore and backshore slopes, and the total width for each transect, taken in July, 1991. Nine of these transects (SC-11 to SC-19) were taken on the bayhead barrier. Ten (SC-1 to SC-10) were taken along the southern half of the beach, and one transect, SC-20, was taken to the north of the barrier.

Plate 1: Overview of the barrier at Ship Cove, looking south. May 1992.

Plate 2: Backbarrier and lagoon at Ship Cove, July 1991. Also shown is the location of GSC-5306.

<u>Transect</u>	<u>Trend (°)</u>	<u>Height (m)</u>	<u>Foreshore Width (m)</u>	<u>Slope (°)</u>	<u>Backshore Width (m)</u>	<u>Slope (°)</u>	<u>Total Width (m)</u>
SC - 1	297	2.6	25.1	5.9			25.1
SC - 2	293	3.2	29.2	6.2	pit		29.2
SC - 3	296	3.4	29.5	6.5	pit		29.5
SC - 4	290	3.5	21.8	9.2			21.8
SC - 5	293	4.4	24.0	10.2			24.0
SC - 6	291	4.5	20.6	12.3			20.6
SC - 7	289	4.9	25.5	10.8			25.5
SC - 8	287	5.4	29.4	10.5			29.4
SC - 9	287	6.0	28.3	12.1			28.3
SC - 10	280	5.8	27.3	12.0			27.3
SC - 11	279	5.5	25.9	12.0	24.0	5.8	49.9
SC - 12	278	5.5	28.7	11.0	28.9	11.0	57.6
SC - 13	278	5.3	27.7	10.9	31.7	9.6	59.4
SC - 14	278	4.7	23.1	11.5	25.2	10.6	48.3
SC - 15	272	5.0	25.1	11.2	20.3	13.7	45.4
SC - 16	269	5.0	27.8	10.2	18.1	15.4	45.9
SC - 17	267	4.9	23.6	11.7	21.8	12.7	45.4
SC - 18	263	4.1	33.5	7.0	12.4	18.3	45.9
SC - 19	259	2.7	13.7	11.0	12.4	12.2	26.1
SC - 20	253	2.3	15.1	8.7	10.0	2.3	26.1

Table 5: Dimensions of the barrier beach at Ship Cove.

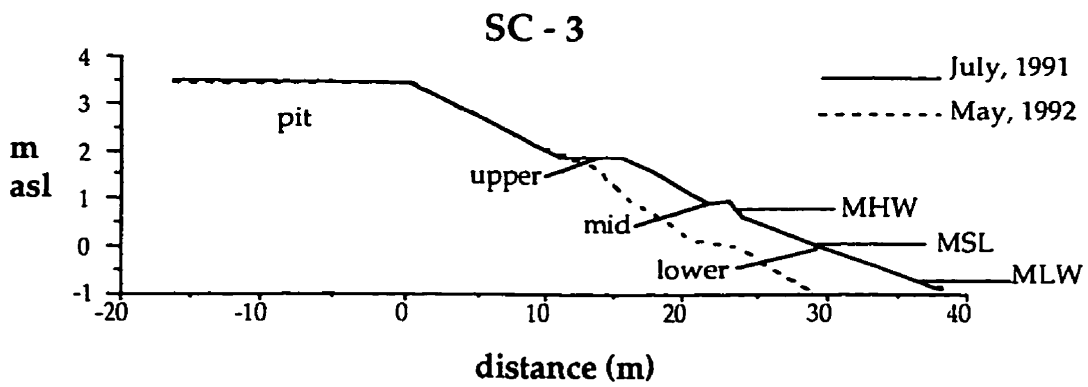
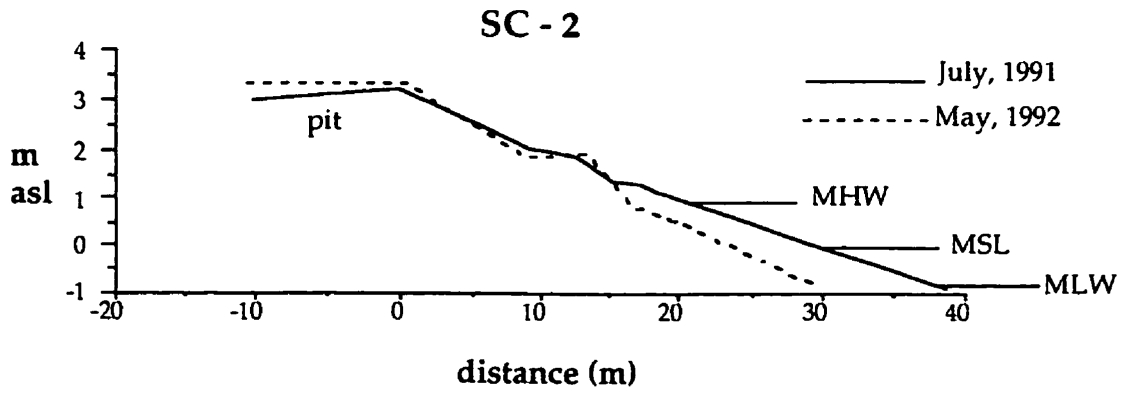
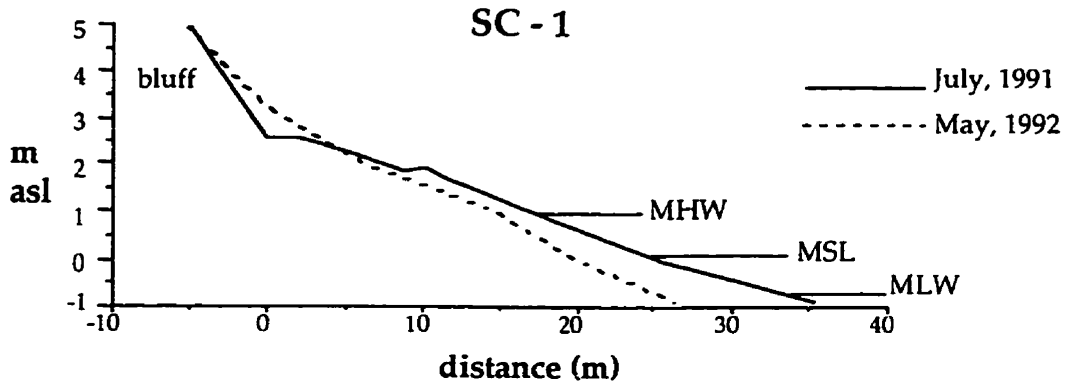


Figure 10: Profiles of transects SC-1 - SC-3, Ship Cove.

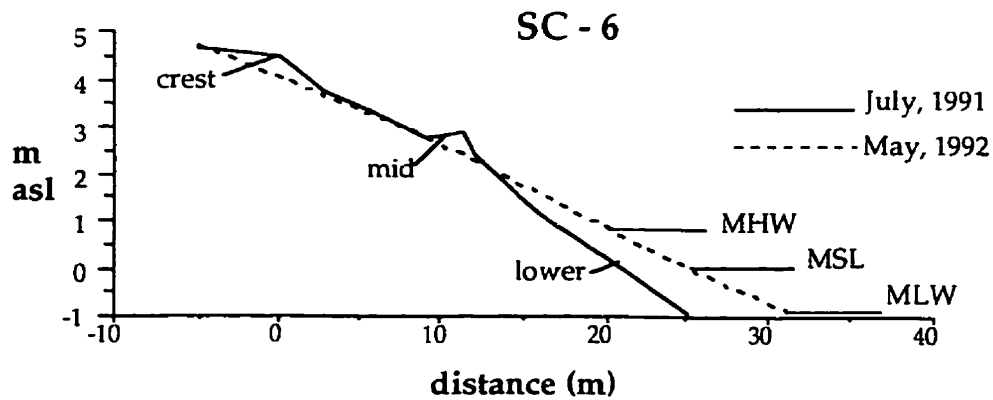
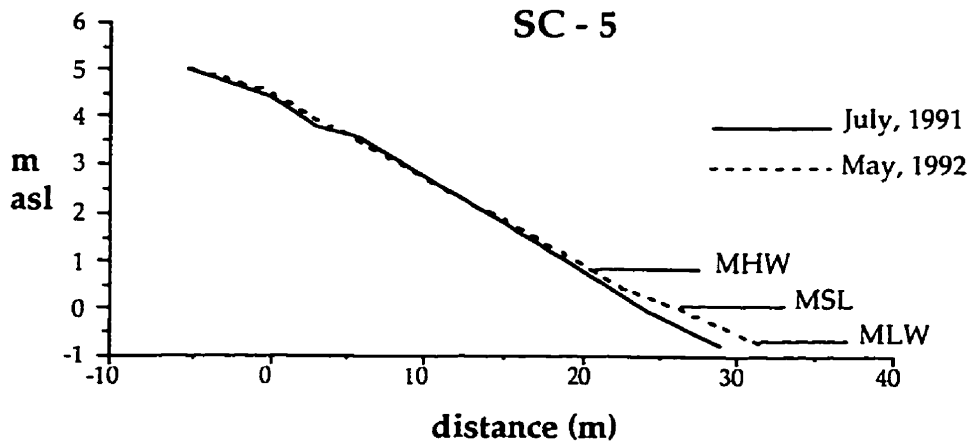
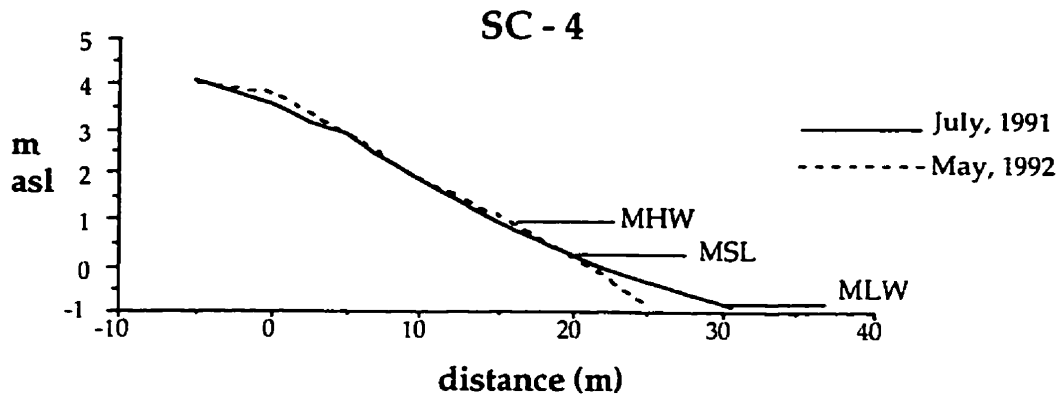


Figure 11: Profiles of transects SC-4 - SC-6, Ship Cove.

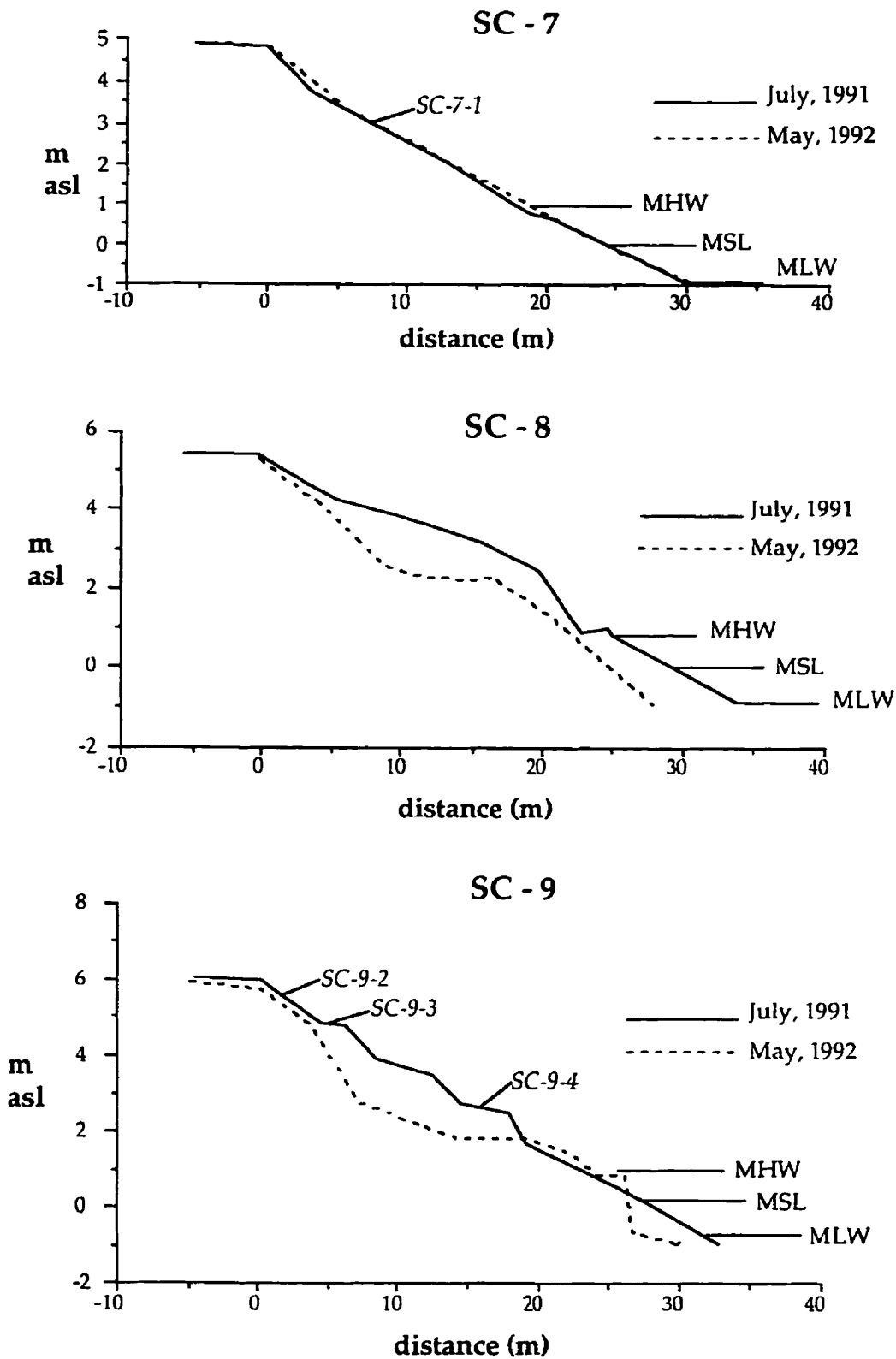


Figure 12: Profiles of transects SC-7 - SC-9, Ship Cove.

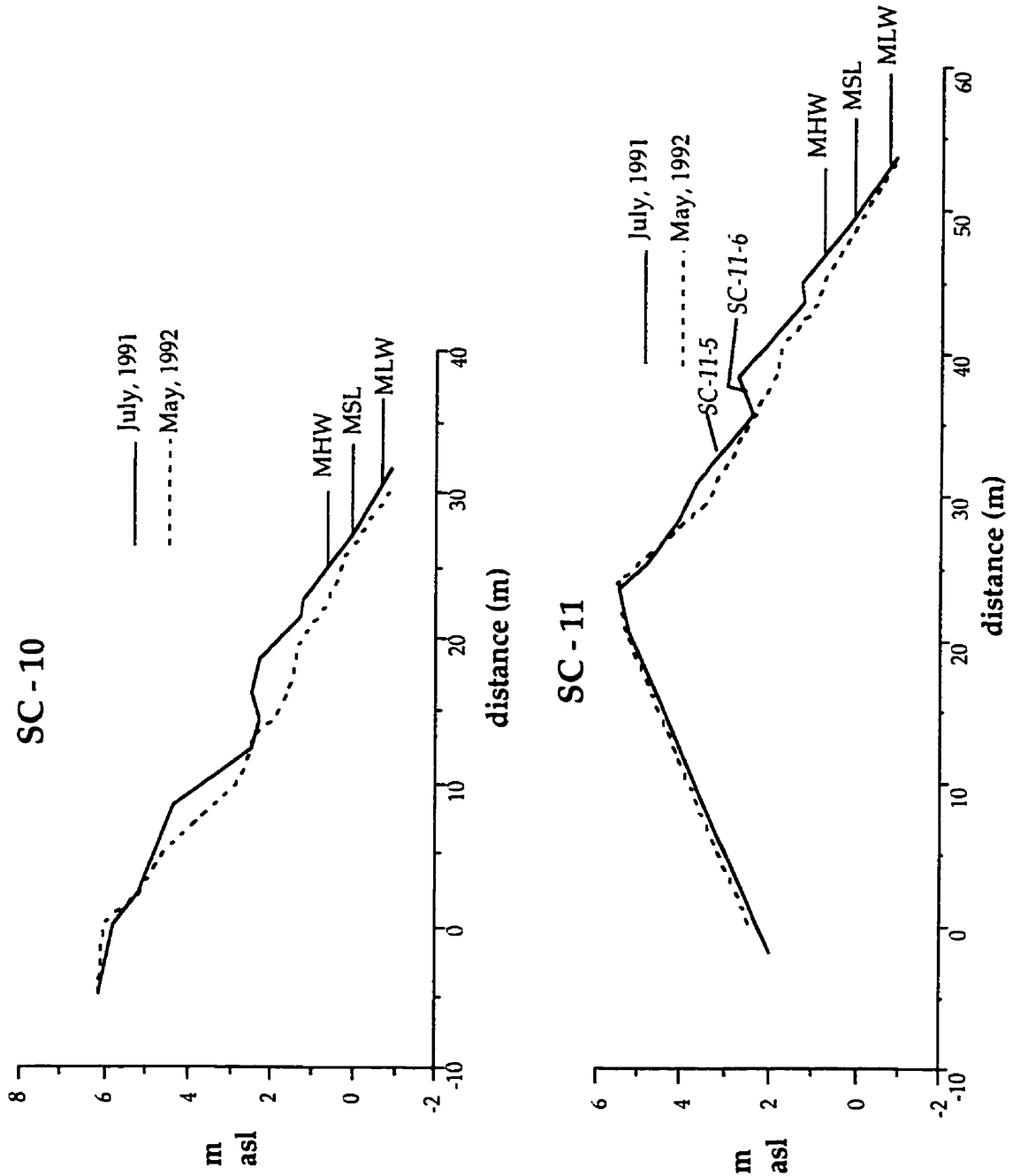


Figure 13: Profiles of transects SC-10 and SC-11, Ship Cove.

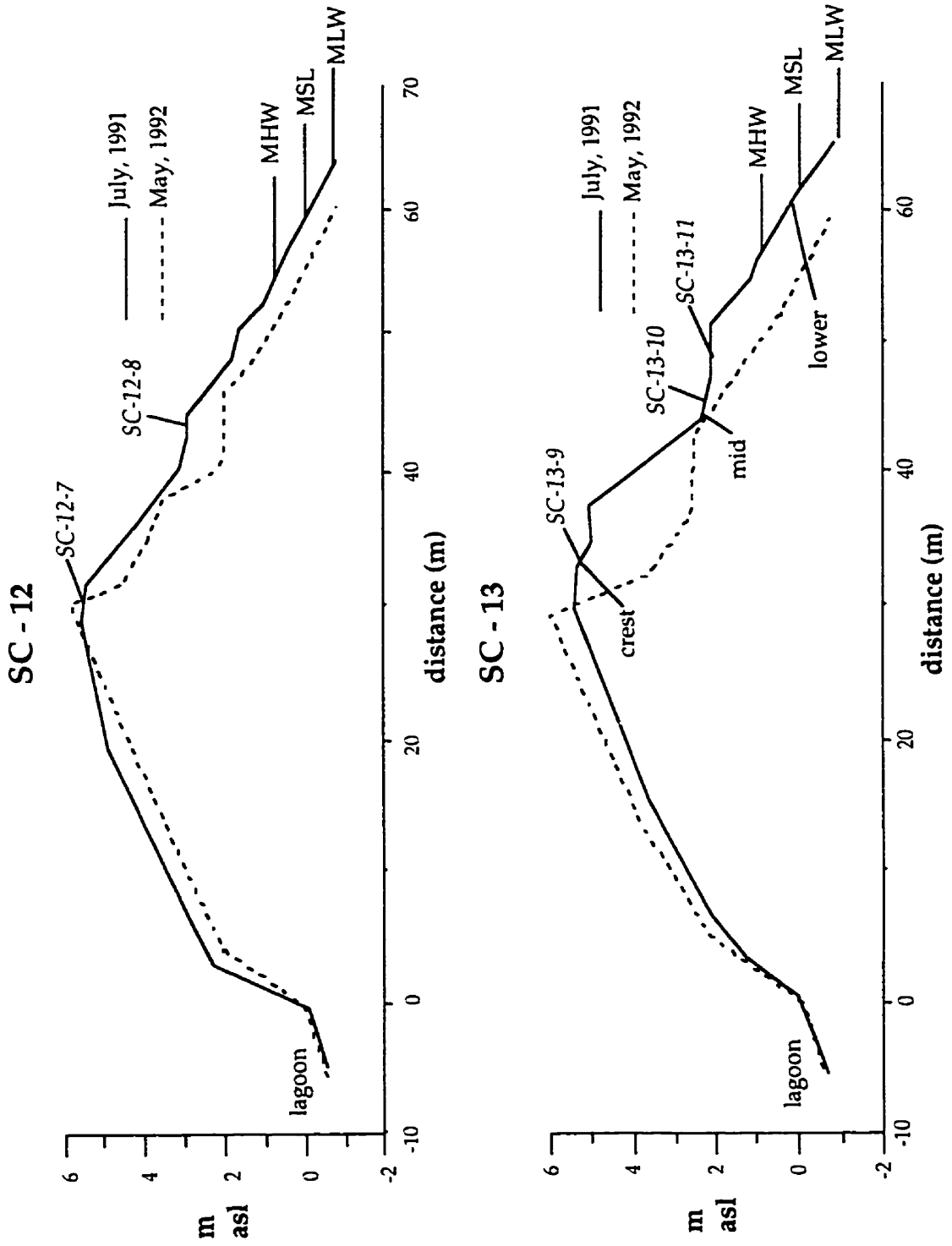


Figure 14: Profiles of transects SC-12 and SC-13, Ship Cove.

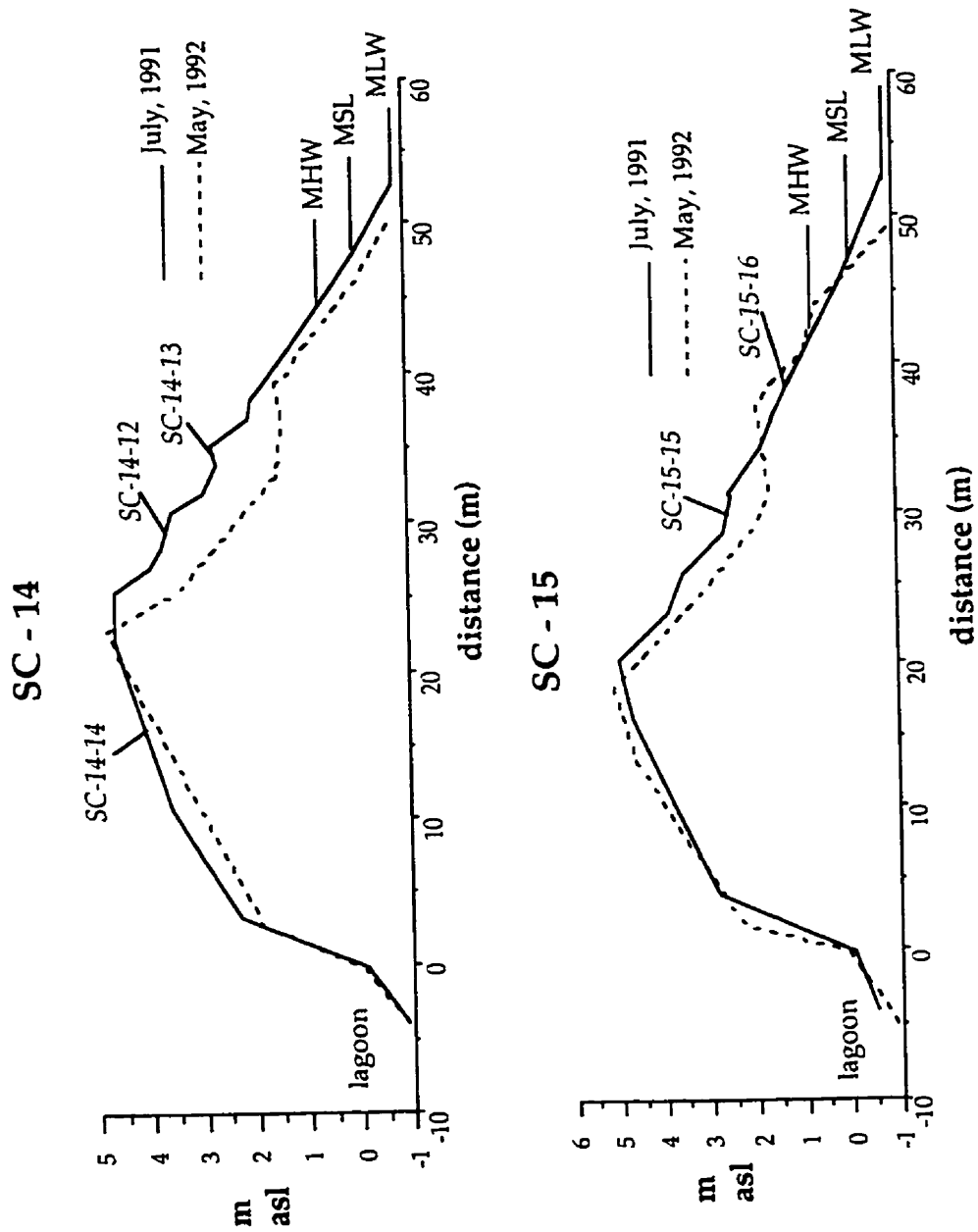


Figure 15: Profiles of transects SC-14 and SC-15, Ship Cove

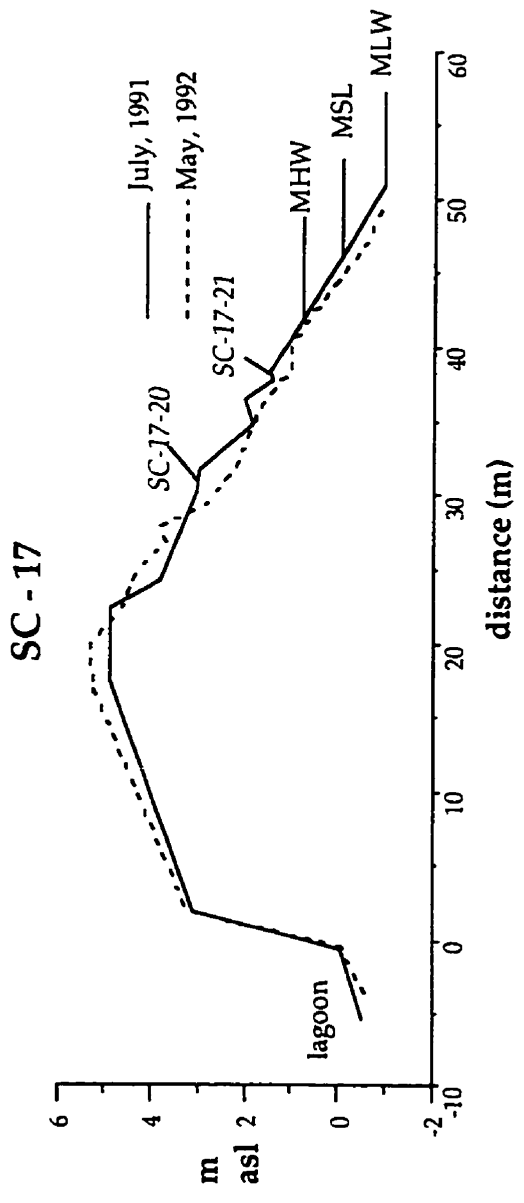
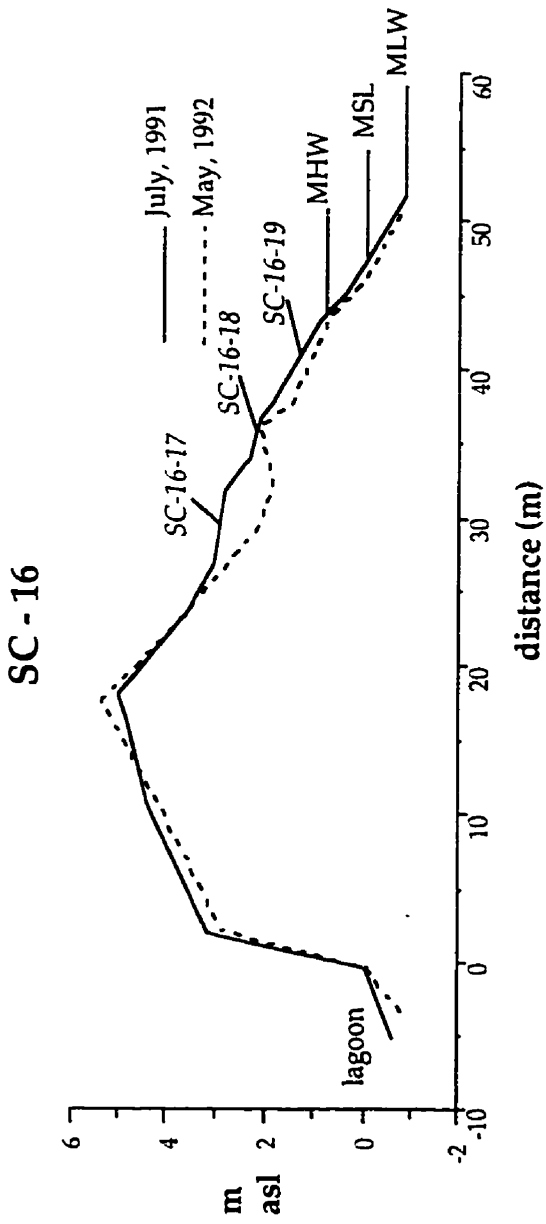


Figure 16: Profiles of transects SC-16 and SC-17, Ship Cove.

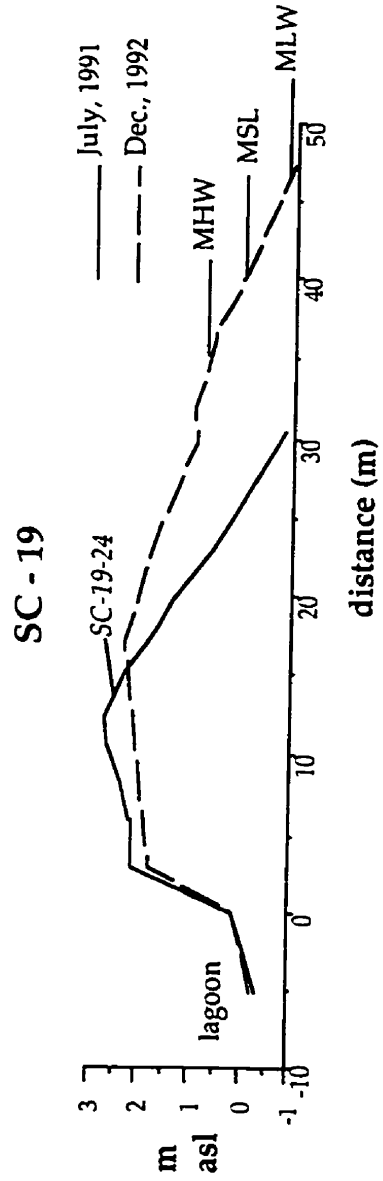
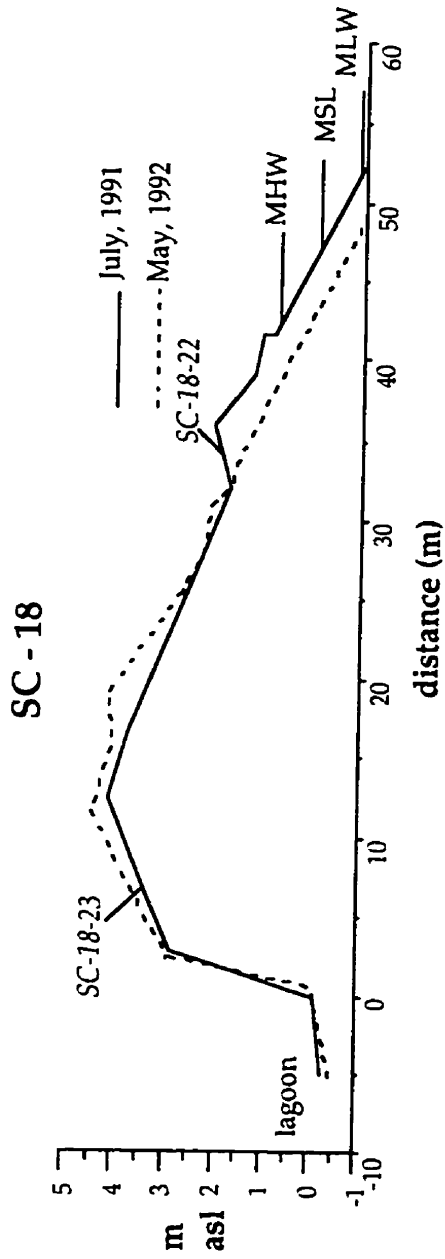


Figure 17: Profiles of transects SC-18 and SC-19, Ship Cove.

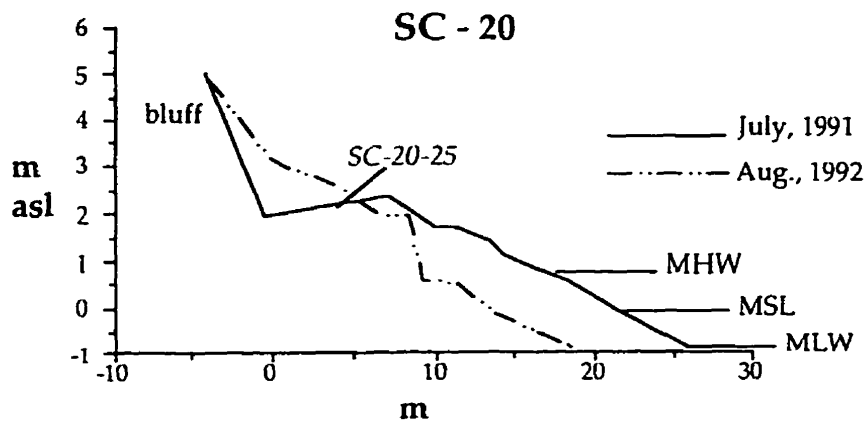


Figure 18: Profiles of transect SC-20, Ship Cove.

For convenience, the beach will be discussed in three sections, arranged from south to north. Zone A is comprised by transects SC-1 to SC-3; zone B, SC-4 to SC-7; and the third, zone C, SC-8 to SC-20.

During July 1991, the southern section (zone A) was characterized by comparatively gentle foreshore slopes of approximately 6° . Heights were approximately 3 m. A storm berm was present at 1.5 - 2 m asl. Shallow cusps were present with wavelengths of 6.5 - 11.7 m and heights of 0.3 - 0.7 m. This section of the beach is used by caplin to spawn during the summer. Landward of transects SC-2 and SC-3 there is an artificial pit filled mainly with granules. This pit was the result of aggregate removal for highway construction in the 1960's and 1970's. Subsequently, beach processes deposited granules and filled in the pit (Plate 3).

Although deviations from the general pattern occur, repetitive observations through 1991, 1992 and 1993 revealed granule-sized sediment removal along this reach of the beach occurs during the months of September to December. This results in exposure of the underlying pebble and cobble framework of the beach and steepening of the profile.

Plate 3: Overview of Ship Cove, looking north. Zone A is in the foreground with the pit landward. Zones B and C are in the background. July 1991.

During July 1991, the central section (zone B; SC-4 to SC-7) was characterized mainly by a linear profile with a 10-12° slope. A berm was present in the mid- to upper-beachface along SC-6. An actively eroding small bluff (< 1 m high), consisting mainly of pebbles and cobbles with a sandy matrix, bounded the back of the beach. Transects SC-5 and SC-7 bisect cusped features that extended the width of the beach. The bluff behind these

transects is eroding more extensively than elsewhere along this section. Repetitive observations during 1991, 1992 and 1993 revealed that the removal of fine clasts from this boulder-dominated zone resulted in little change in the overall beach shape throughout the seasons (Plate 4).

Plate 4: The eroding bluff bounding zone B and sediment along the upper beachface. July 1991.

In the northern section (zone C) of the beach, the area represented by transects SC-8 to SC-10 has no back beach. SC-11 marks the southern edge of the barrier part of the system. Transects 19 and 20 were taken in the vicinity of the outlet. The highest elevations of 6 m occur in this section of the beach. During July, 1991 the overall beachface slopes were between 10 and 12° (Plate 5).

During July 1991, this section was characterized by tiers of cusps. As many as four tiers were present between transects SC-10 and SC-15 (Table 6). Figures 19a and 19b show schematic diagrams of cusp morphology and terminology. The upper level cusps located in the upper-beachface reached the barrier crest, 6 m asl, and had wavelengths (measured from horn to adjacent horn) of 15 - 28.6 m and heights (vertical distance) of 2-3 m. The cusp embayments had steep slopes, 20-25°, and were shallow with small cusp horns along the crest.

Plate 5: Lower-beachface cusps along zone C and eroding bluff bounding the northern end of the barrier. July 1991.

The middle two levels (the second and third level cusps located in the mid-beachface) had undergone modification and were not as clearly defined.

	Wavelength (m)	Vertical Height (m)	Width (m)
Zone A			
	9.1	0.5	5.2
	9.1	0.3	3.3
	11.7	0.4	3.9
	6.5	0.4	4.0
	7.8	0.4	7.8
	9.1	0.7	6.5
mean	8.9	0.5	5.1
s.d.	1.7	0.1	1.7
Zone C			
<i>upper tier</i>			
	21.5	2.5	
	19.5	2.1	12.4
	28.6	3.0	9.1
	18.9	2.0	
	15.0	2.5	7.9
mean	20.7	2.4	
s.d.	5.0	0.4	
<i>middle tiers</i>			
	9.8	1.1	8.5
	13.0	1.4	
	13.0	1.2	11.1
	11.0	1.6	9.8
	11.1	1.4	8.4
	11.7	1.2	3.9
mean	11.6	1.3	
s.d.	1.2	0.2	
<i>lower tier</i>			
	5.8		
	3.3		
	2.0		
	7.2		
	3.9		
	3.3		
	8.5		
	8.5		
	3.9		
	8.5		
	3.9		
	7.2		
mean	5.5		
s.d.	2.4		

Table 6: Dimensions of cusps at Ship Cove, July 1991.

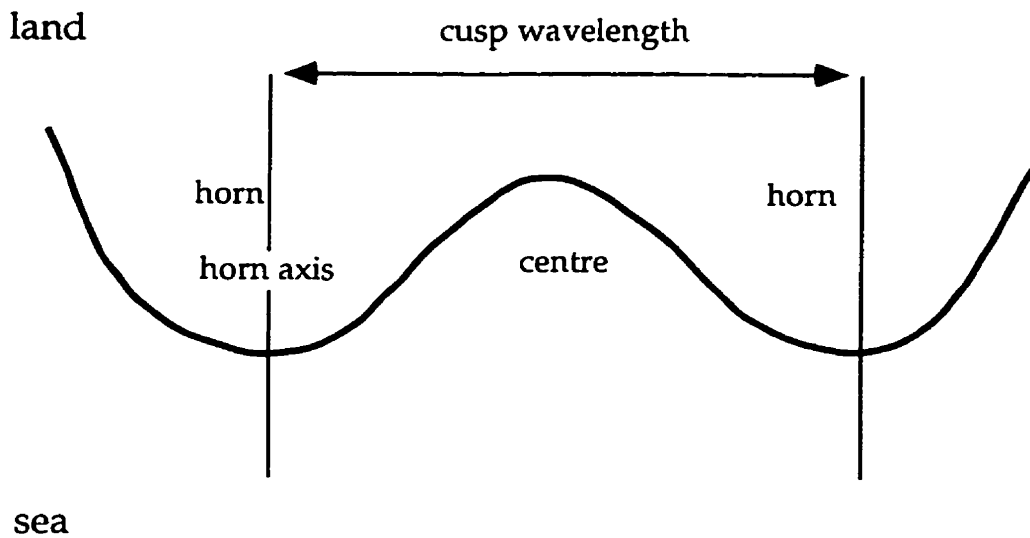


Figure 19a: Schematic planar view of cusp morphology. The cusp horn is an accumulation of sediment extending seaward. The cusp centre is the embayed region between adjacent horns. Cusp wavelength is defined as the distance between the axes of adjacent horns.

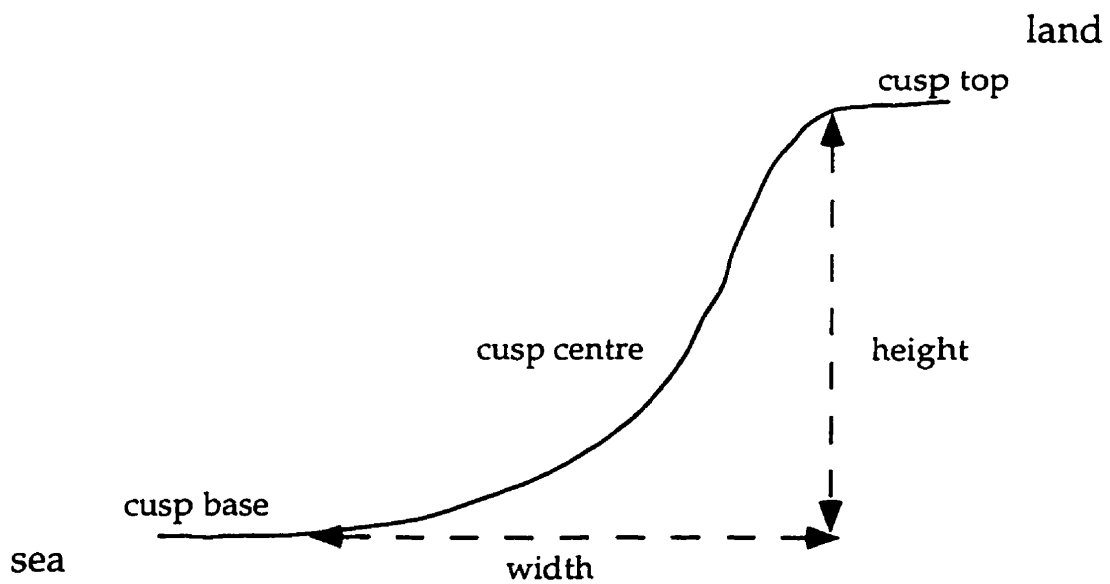


Figure 19b: Schematic cross-section of a cusp. The height is the vertical distance between the cusp base and the cusp top. The width is the horizontal distance between the cusp base and cusp top.

These two levels of cusps were not in phase with each other and in places the third level cusps merged with the second. The cusps in the mid-beachface had deeper embayments with pronounced horns. As the summer progressed and the beachface increased in steepness, the horns of the mid-beachface cusps developed a distinct landward dip. Both middle levels had wavelengths of 9 - 14 m and heights of 1.5 m. The third level reached a height of 4 m asl and the base of the second level was at 0.5 - 1 m asl. The lowest level cusps located within the intertidal zone had wavelengths of 2.0 - 8.5 m and heights of approximately 0.5 m and became very elongated when the tide was low (Plate 5).

Plate 6: Cusps along zone C. August 1991.

Cusps occur frequently throughout the year, although only one to three tiers were observed in 1992 and 1993. The upper, largest cusps were destroyed during a storm on Christmas Day, 1991. On 15 December 1993, large cusps similar to those present along the upper tier in July 1991 were observed. These cusps extended throughout the beachface and reached to 0.5 - 1 m below the beach crest. The lengths ranged between 23 and 29 m.

As cusps were prevalent features along this section of the beach during July 1991, the profiles of the beachface are marked by berms at different elevations along each transect. The number of berms varies between individual profiles. The variances are a result of which section of the cusp morphology individual transects intersected. A transect intersecting a cusp horn will have a berm on its profile unlike the profile of a transect that intersects a cusp centre.

During July 1991, as well as during 1992 and 1993, the backbeach was characterized by extremely steep slopes ($30 - 45^\circ$) directly adjacent to the lagoon. This steeply-sloping area has a maximum height between 2 and 3 m asl. The area of the backbeach between the steep section and the barrier crest has slopes ranging from 6° to 11° .

In general, during the summer months (May/June through August/September), the profiles have an overall convex shape resulting from net sediment accumulation. As the summer progresses the beachface increases in steepness, as sediment is moved landward. This pattern can be seen in the profiles of SC-11 and SC-17 (Figures 20 and 21). With net sediment removal during the autumn months, the beachface takes on a more concave shape. Between late January and March an ice foot develops in the

mid- and upper-beachface. The active sediment zone is confined mainly to the intertidal zone. Sediment is thrown on top of the ice foot; however, the ice protects the sediment within the mid- and upper-regions of the barrier. Blocks of ice with sediment overtop the barrier. With spring thaw, this resulted in mounds of small- and medium-sized pebbles on top of the cobble-dominated barrier crest (Plate 7).

Plate 7: Circular mound of pebbles amongst the cobble-dominated beach crest after spring thaw. April 1992.

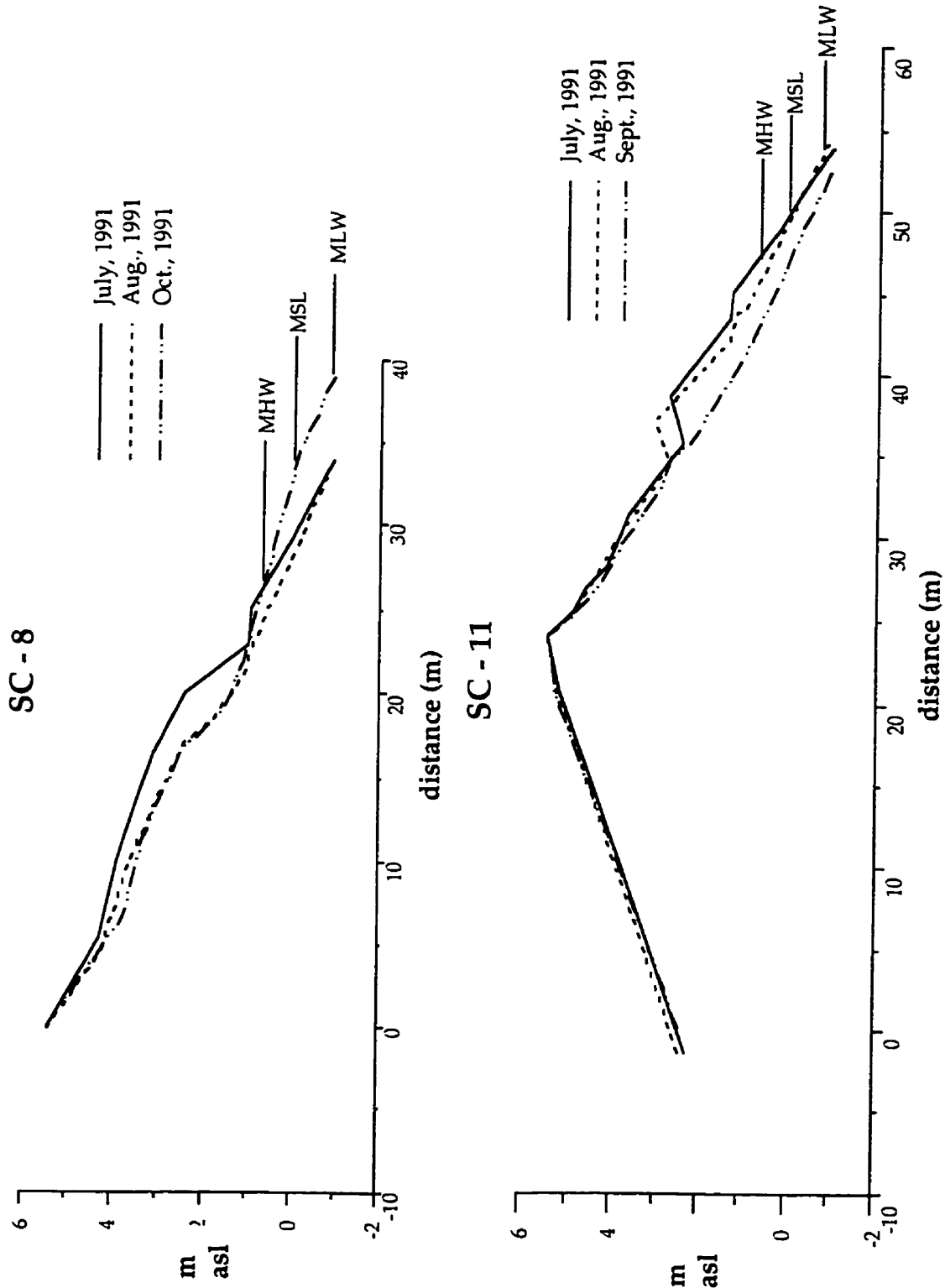


Figure 20: Comparison of profiles of transects SC-8 and SC-11 measured July, August, and September or October 1991.

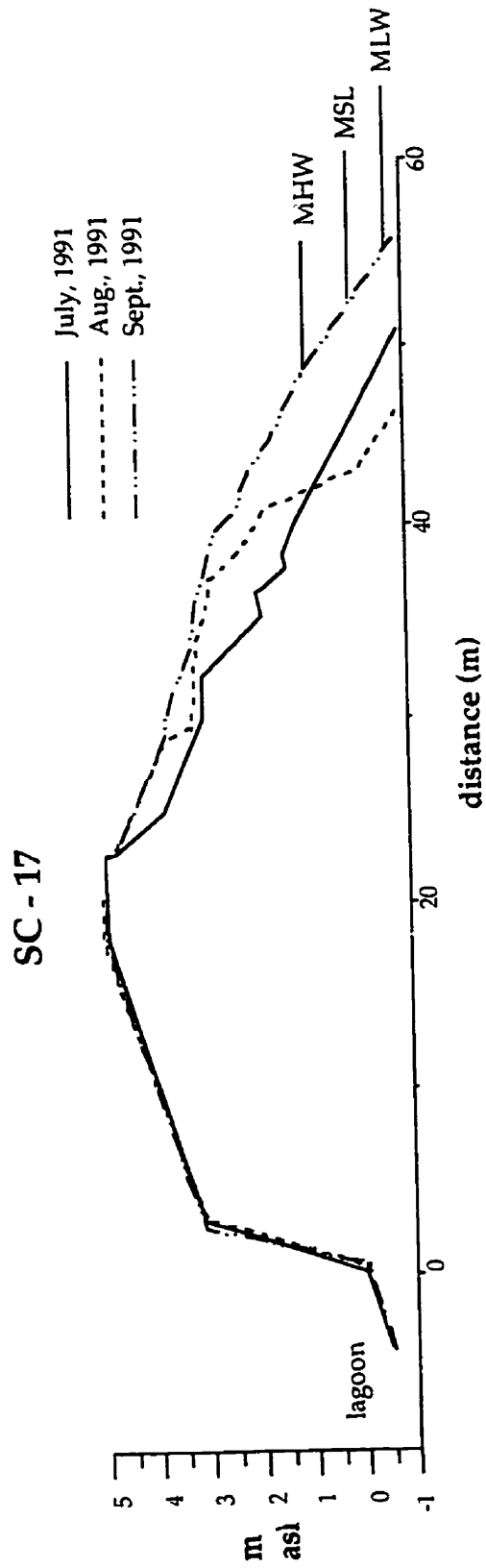


Figure 21: Comparison of profiles of transect SC-17 measured July, August and September 1991.

The major storm event on Christmas Day, 1991, marked by southwesterly winds, caused the removal of large amounts of sediment and exposed underlying cobbles and boulders. The barrier along the entire northern section had a regular concave shape throughout its height (Plate 8). Overtopping had occurred, with sediment being deposited on the barrier crest, in addition to sediment removal from the front (Figures 22 and 23). The profiles taken in May, 1992, show the effects of this storm and other events during the winter and spring of 1991 - 1992. The profiles of transects SC-14 and SC-17 taken in July 1991, May and December 1992 (Figure 23) also show an increase of barrier height by 0.2 - 0.5 m, a decrease of backbarrier widths by approximately 3 - 4 m, and an increase of backbarrier slopes. Although the profiles of transect SC-11 (Figure 22) do not show an increase of height between July 1991 and May 1992, the decrease in backbarrier width is evident. The profiles of SC-11 show a removal of sediment between July 1991 and December 1992. The profiles of transect SC-2 (Figure 22) reveal an increase of height.

In July 1993, a transect was established by the Newfoundland Department of Mines and Energy near transect SC-11. Since July 1993, profiles have been taken in August, September, December and February 1994. The results are shown in Figure 24. The profiles taken in July, August and September 1993 show steep, erosive upper-beachfaces, similar to that seen in the upper-beachface of the profiles taken in May 1992 and December 1992. The mid- to lower-beachface in the July, August, and September 1993 profiles

Plate 8: Convex beachface profile after winter storms along zone C. December 1991.

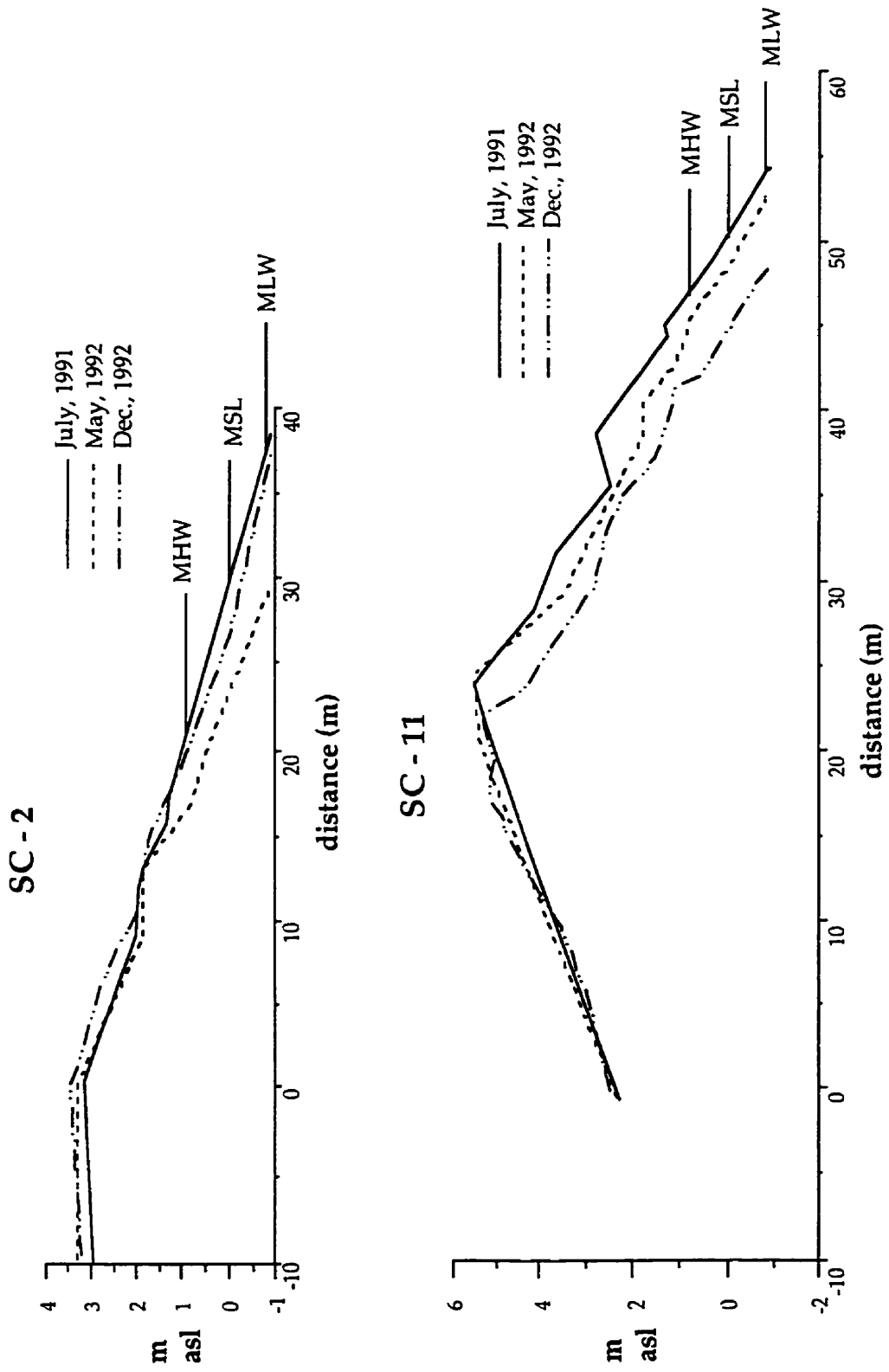


Figure 22: Comparison of profiles of transects SC-2 and SC-11 measured July 1991, May 1992 and December 1992.

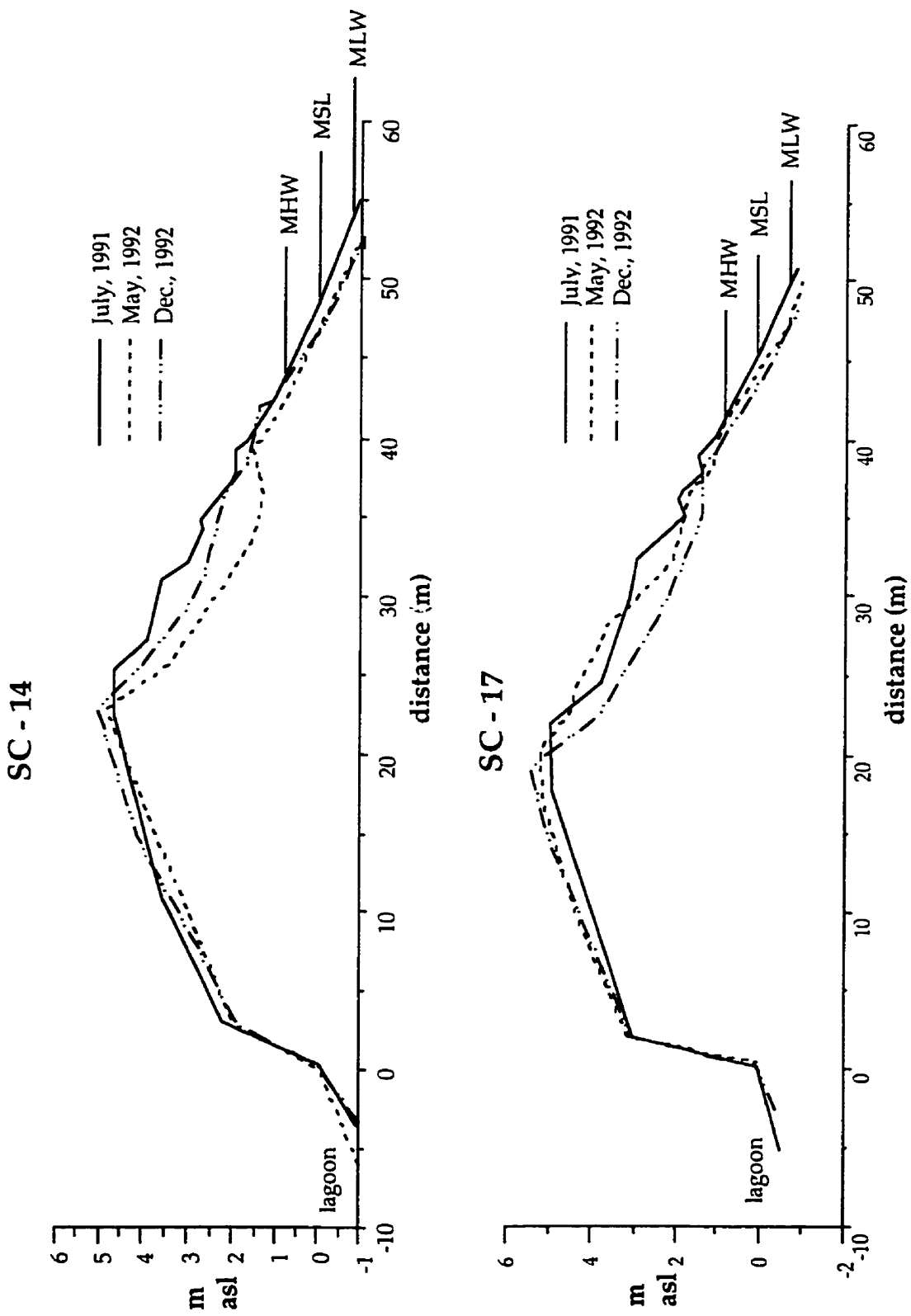


Figure 23: Comparison of profiles of transects SC-14 and SC-17 measured July 1991, May 1992 and December 1992

Ship Cove, GSC-394

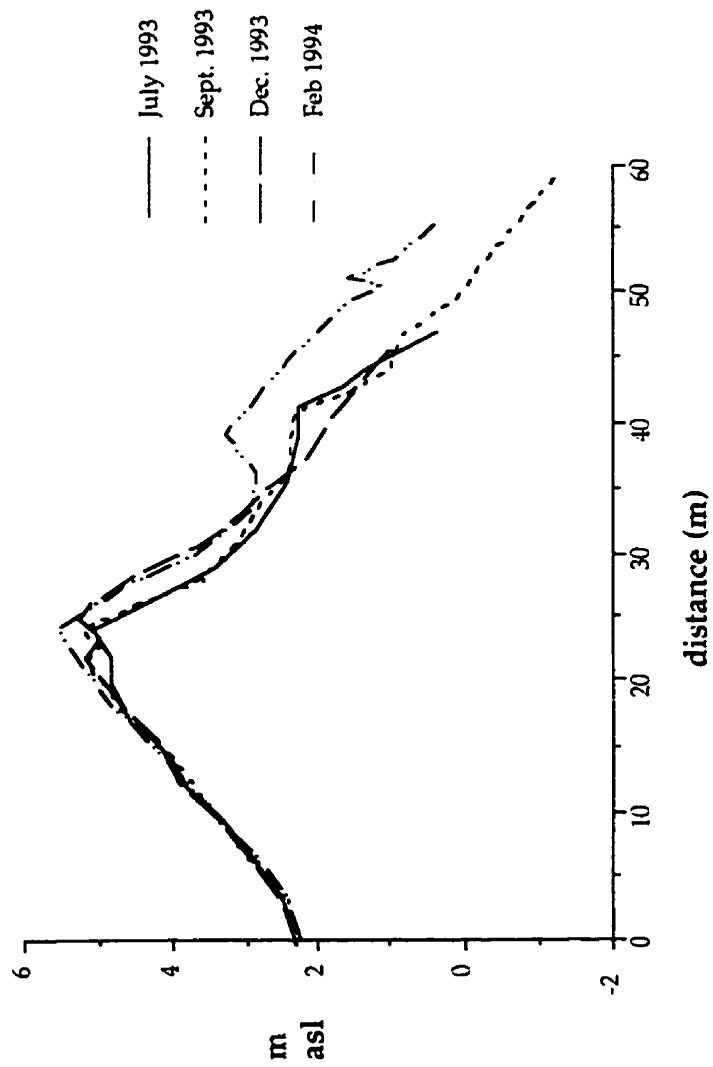


Figure 24: Profiles of GSC-394 measured July, September and December 1993 and February 1994.

show an accumulation of sediment that has been removed in the December 1993 profile. The profile taken in February 1994 shows the results of overtopping. Sediment had been transported over the crest and the barrier height increased by approximately 0.4 m. The mid- and lower-beachface of the profile taken in February 1994 may not reflect sediment accumulation for a pronounced ice foot was present at the time measurements were taken.

Toward the northern end of the barrier, near transect SC-12, the one overwash channel seen over the course of the study was formed between 14 March and 28 March 1992. The channel measured 5.2 m wide and 0.5 m deep (Plate 9). The base of the channel contained imbricated granules and pebbles. The long axis of the channel was oriented at 249°. This channel was most likely formed during a period of prolonged storm activity, between March 19-24 1992, which was marked by strong westerly and southerly winds (AES, unpublished). An overwash fan formed but did not remain, as the sediment that was transported landward was transported seaward again by the stream. On 28 March 1992, the stream flowed through a comparatively wide outlet, 6 m, and had a estimated velocity of 1.7 m/s.

The outlet at Ship Cove is unstable. It opens and closes on a daily basis during the summer months, depending on fluvial discharge and wave activity. Plate 10 shows an outlet in the process of opening in August 1991. Plate 11 shows a large outlet and swash bars in October 1992. The short duration of the study limits generalizing the pattern of outlet status (whether open or closed) throughout the course of a year; however, over the time period of the study, a pattern was emerging. During the periods between September and December, and between April and May, the outlet is generally

open. Between June and August, the outlet is generally closed. Between January and March the outlet is variable, but tends to be open more than closed. Table 7 shows selected dates when the outlet was open or closed during the study. When it is closed seepage occurs throughout the barrier front, although less seepage occurs in the winter months when the lagoon and interstitial water within the barrier are frozen. Air photos taken in 1967 show that the position of the outlet was located at the southerly end of the lagoon adjacent to transect SC-11. In 1973 or 1974, the northern end of the barrier was subjected to explosives (Tobin, S., Ship Cove, personal communication). This caused the outlet to move to its present more northerly position.

The extent of lateral transport of the sediment at the mouth bars, as well as elsewhere along the beach, is not known. Clasts that were painted and placed along transects SC-9 and SC-4 were not found subsequently. However, the swash alignment of the beach to the incident waves indicates that the majority of movement is offshore/onshore. The angle between wave swash/backwash interactions show a northerly direction of less than 45°. An obtuse swash/backwash angle indicates strong longshore drift (Antia, 1989) Consequently, little longshore transport is expected for the sediment at the swash bars or elsewhere along the beach.

Comparison of 1948 and 1980 air photos reveals a landward movement of the barrier of approximately 10 - 25 m (Figure 25). The meadow adjacent to the stream and lagoon has been overtopped by the barrier. According to Mr. Stan Tobin, a local resident, 20 - 30 m of the meadow have been covered or eroded by the stream at its present outlet. After extensive overwashing by a

major storm on 14 - 15 February 1982, fence posts were exposed along the barrier top in the vicinity of SC-16 - SC-18. Mr. Tobin remembers the date well for this was the storm associated with the loss of the oil drill rig, Ocean Ranger, and its crew.

Plate 9: Overwash channel. March 1992.

Plate 10: An outlet forming. August 1991.

Plate 11: Swash bars along outlet. October 1992.

<u>Date</u>	<u>Outlet</u>	<u>Channel Width (m)</u>	<u>Depth (m)</u>
Jul-91	c		
30/7/91	c		
22/8/91	o	0.5	0.2
23/8/91	o	2.5	0.4
24/8/91	c		
14/9/91	c		
23/9/91	o	2.0	0.3
5/10/91	o	5.0	1.5
6/10/91	o	6.0	0.5
28/10/91	c		
4/11/91	o	4.0	0.5
13/12/91	o	1.0	0.4
17/1/92	c		
27/1/92	o	1.5	0.5
12/2/92	c		
3/1/92	c		
14/3/92	o	3.0	1.0
28/3/92	o	6.0	1.0
21/4/92	o	2.0	1.5
13/5/92	o	1.5	0.5
2/6/92	o	0.5	0.2
30/6/92	c		
25/7/92	c		
5/9/92	c		
10/10/92	o	3.0	0.5
14/10/92	o	5.0	1.5
16/12/92	c		
1/15/93	c		
15/2/93	o	4.0	0.5
17/3/93	o	1.0	0.4
28/3/93	c		

c = closed
o = open

Table 7: Status of outlet at Ship Cove on selected dates.

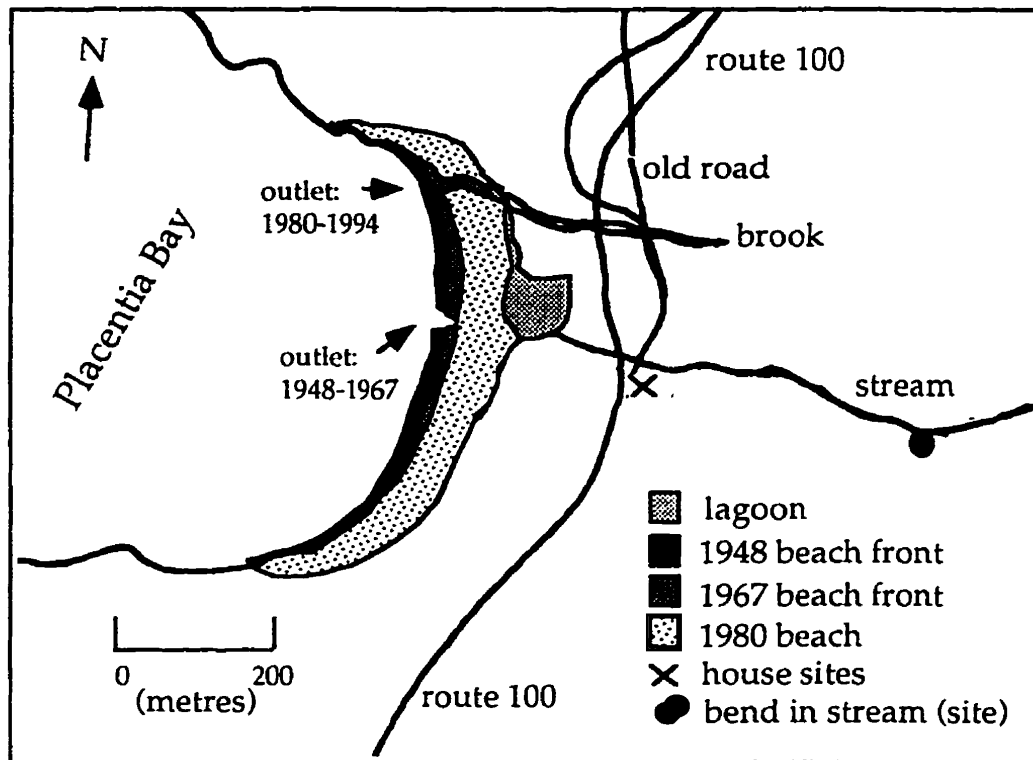


Figure 25: Comparison of 1948, 1967 and 1980 air photos of Ship Cove. Distances were determined from the sites shown. See text for further discussion.

5.2 Clast Lithology

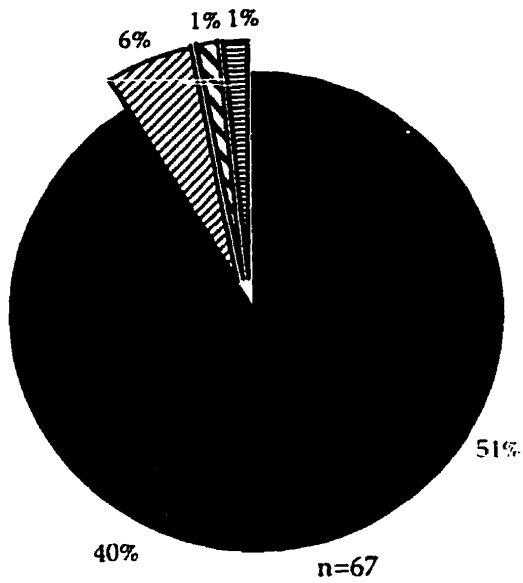
To determine the lithology of the beach clasts, a sample of 67 clasts was taken from the barrier crest and a second sample of 57 was taken at mean sea-level on the stream mouth swash bar along the outlet. Table 8 shows the composition of the samples individually and combined.

	swash bar	crest	combined
siltstone	47%	51%	49%
sandstone	30	40	35
conglomerate	9	0	4
basalt	5	6	6
rhyolite	5	1	3
granite	4	1	2
Total	100%	99%	99%

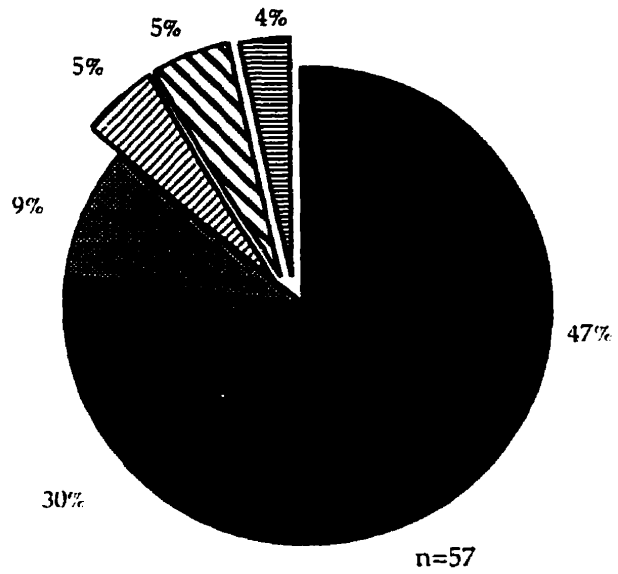
Table 8: Compositions of the clast lithologies for the samples taken from the barrier crest and the swash bar, and for the samples combined.

The igneous component (basalt, rhyolite and granite) of the mouth bar was 14% whereas on the crest it was 8%. The combined clast lithological data show 88% of the clasts to be locally-derived siltstone, sandstone and conglomerate. Basalt, rhyolite, and granite form 12% of the total assemblage (Figure 26).

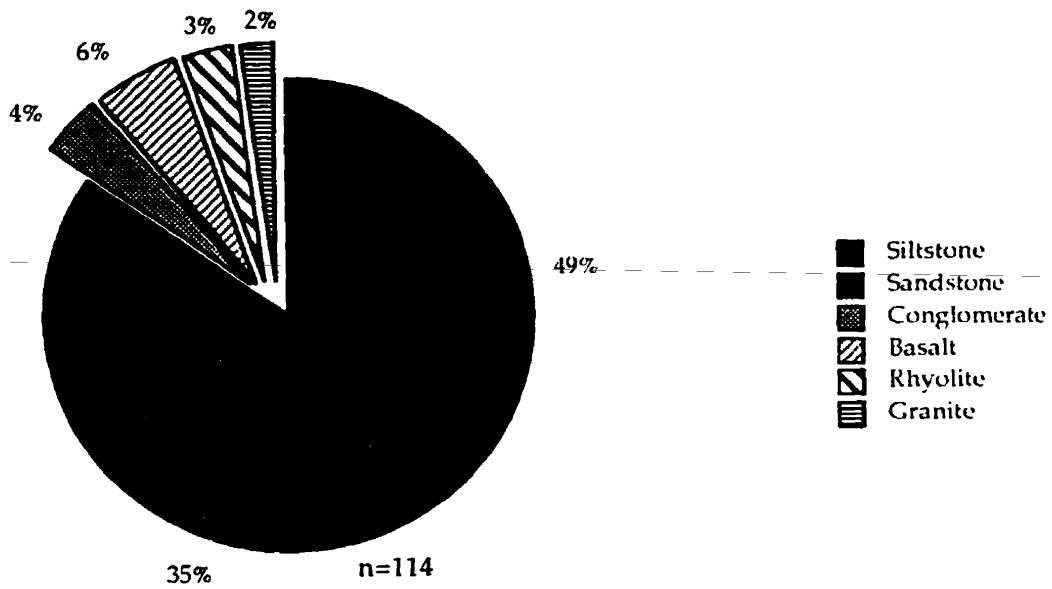
Lithology on Beach Top



Lithology on Swash Bar



Combined Lithologies



- Siltstone
- Sandstone
- Conglomerate
- ▨ Basalt
- ▧ Rhyolite
- ▩ Granite

Figure 26: Lithologies for Ship Cove. The exploded portions show the igneous components.

5.3 Sediment Texture

The beach at Ship Cove shows considerable surface textural differences along its length, as well as across individual transects. Overall, the southern section, zone A, consists mainly of granules and sand; zone B mainly of boulders with an infill of pebbles; and zone C, the northernmost section, of pebbles and cobbles.

Figure 27 shows surface texture analyses from samples taken in July 1991. The samples were taken on the lower-beachface, the mid-beachface area, and the crest. Since the back of SC-3 has been anthropogenically altered, the crest is considered the top of the storm berm. Transects were chosen within each zone; SC-3 for zone A, SC-6 for zone B, and SC-13 for zone C and are used as representative of the zones. Also shown are the textural analyses for the stream mouth swash bar taken in September 1991 and the textural assemblage for the entire beach which includes more data than that obtained from the transects alone. The numerical quantities in the graphs and discussion in chapter 6 are used to indicate qualitatively how the beach sediment varies landward and alongshore.

Along all three transects, estimated clast size increased with increased distance from the water's edge. Along transect SC-3, cobbles dominated the storm berm (70%) whereas small-sized pebbles mainly composed the mid-beachface area (80%) and sand and granules dominated the lower-beachface (95%). Along transect SC-6, boulders dominated throughout the beachface. Cobbles, however, decreased from 25% on the crest to 5% along the lower-beachface, as smaller clasts increased seaward. Cobbles decreased from 95% on the crest to 60% midway to 30% near the shore along transect SC-13. Plate 12

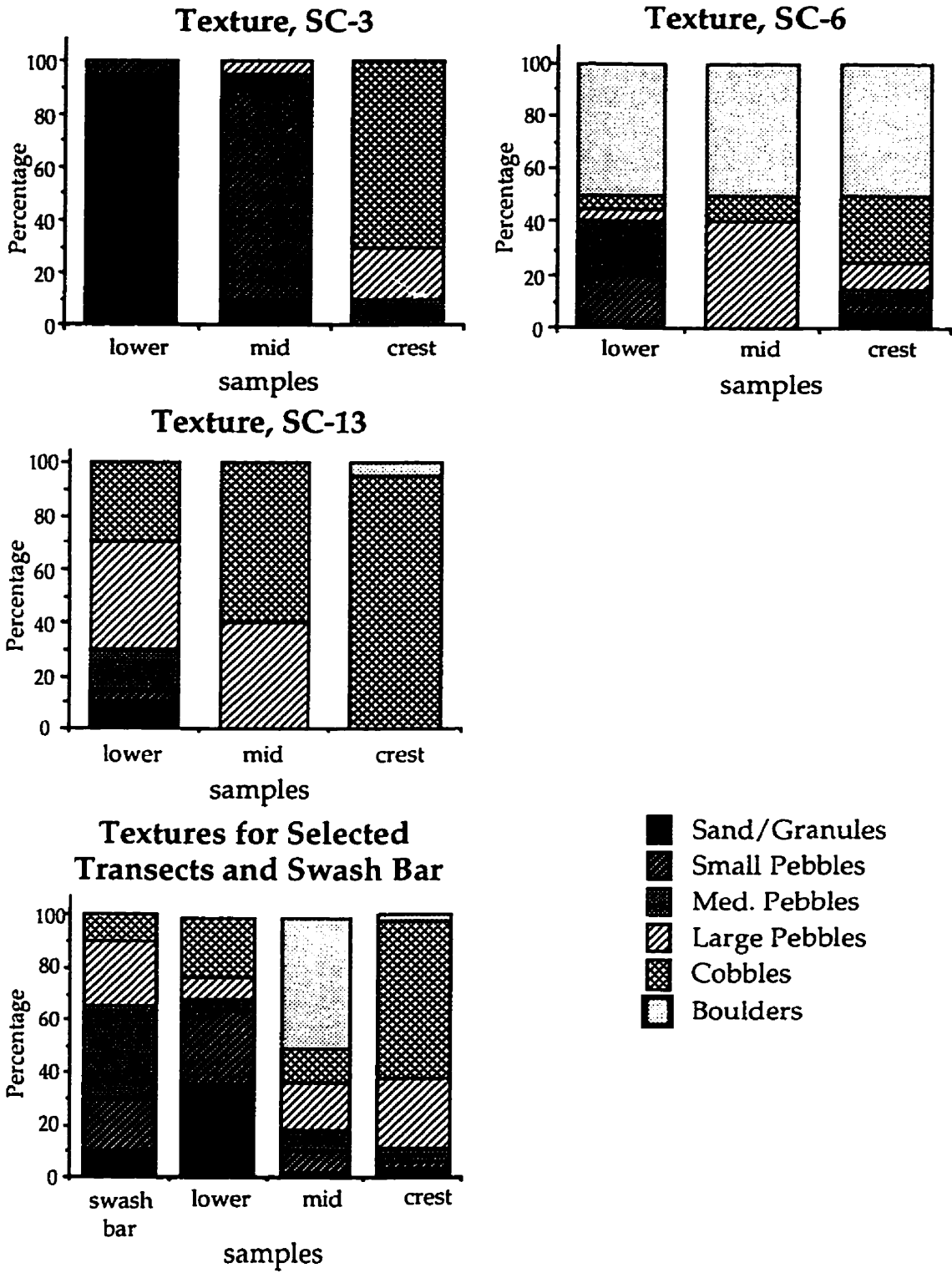


Figure 27: Sediment textures for Ship Cove.

shows the imbricated cobble-dominated clasts on the barrier crest along zone C. Landward of the crest on the overwash fans, the sediment composition is similar to that of the crest and is dominated by cobbles.

Plate 12: Imbricated cobbles along the beach crest. July 1991.

The sediment on the stream mouth bar shows an unsorted mix of clast sizes, ranging from sand to cobbles. The samples along the transects show a high degree of sorting by size, except for the crest of SC-6 that was estimated to consist of a mixture of 5% granules, 5% small-sized pebbles, 5% medium-sized pebbles, 10% large-sized pebbles, and 25% cobbles in addition to the boulder frame. The beach as a whole was dominated by cobbles (estimated 41%) in July 1991. Small to large-sized pebbles combined formed an estimate of 47% and sand and granules 10%.

Cuspate features showed sorting of sediment. Although the upper cusp showed little sorting of sediment by shape or size between the horn and centre, more spherical clasts accumulated at the base of the steep slopes of the centre. The mid-beachface cusps showed imbricated large pebbles and cobbles on the horns, imbricated medium to large pebbles at the base and disorganized pebbles in the centre. The cusps along the lower-beachface in the intertidal zone were shallow and had distinct clast zonation. Imbricated medium- to large-sized pebbles formed the horns, small- to medium-sized pebbles lined the edge of the cusp embayment, and sand and granules were present elsewhere, except for a channel of large pebbles and cobbles bisecting the centre (refer to Plate 5 for lower-level cusps).

As the morphology changes with seasons and storm activity, variability was seen in the texture. After storm events, such as the Christmas Day storm of 1991, large amounts of pebbles were removed, exposing mainly cobbles and boulders. The beach was visited two days after the Christmas Day event. At this time, the beachface was characterized by a convex shape.

In contrast, however, two days after the March 15, 1993 the intertidal area contained sand while pebble and cobble cusps were present along the mid- and upper-beachface along zone C, the northern section. In addition, although sediment was removed along zones A and B exposing boulders along the lower-beachface of zone A and more of the boulders in zone B, a layer of sand and granules was deposited.

In general between November and March, underlying cobbles and boulders dominate throughout zone C with pebbles, granules, and sand increasing during the other months. Along zones A and B, net sediment

removal occurs between November and March, although great variability exists with onshore and offshore transport of sands and granules. An excavation into the lower-beachface along the southern section in October 1991 revealed alternating strata of coarse sand and granules overlying pebbles and granules. Figure 28 shows this sequence.

At times, when the outlet opened, sedimentary structures within the barrier were exposed by erosion. On 22 August 1991, three units were exposed on the barrier along the northern side of the outlet, 1 m asl (exposure A, Figure 29; Plate 13). The basal unit consisted mainly of seaward-imbricated open-work pebbles and cobbles with a minimum thickness of 10 cm. A 2 cm thick stratum (unit 2) of open-work granules overlay the lower unit along a sharp contact. This in turn was overlain sharply by a 15 - 20 cm thick unit of seaward-imbricated pebbles and cobbles with a 5% infill of sand, granules, and detrital seaweed. The thickness of the unit increased landward. The beds dipped 10 - 15° seaward.

Also on the northern side of the outlet on August 22, a distinct 15-20 cm thick stratum of open-work imbricated cobbles was exposed between layers of imbricated pebbles containing a sandy and organic matrix at 0.5 m asl (exposure B, Plate 14). The beds dipped 15 - 20°.

On June 2, 1992 an exposure (exposure C, Figure 30) revealed a minimum of 13 cm of imbricated open-work cobbles at the base. Unit 1 was overlain by 17 cm of imbricated pebbles with an infill of granules (unit 2), in turn capped by a 12 cm layer similar to unit 1. The beds dipped 10 - 15° seaward and, similar to the other exposures, the contacts were sharp.

Plate 13: Exposure A. The pencil measures 13 cm.

Plate 14: Exposure B. The pencil measures 13 cm.

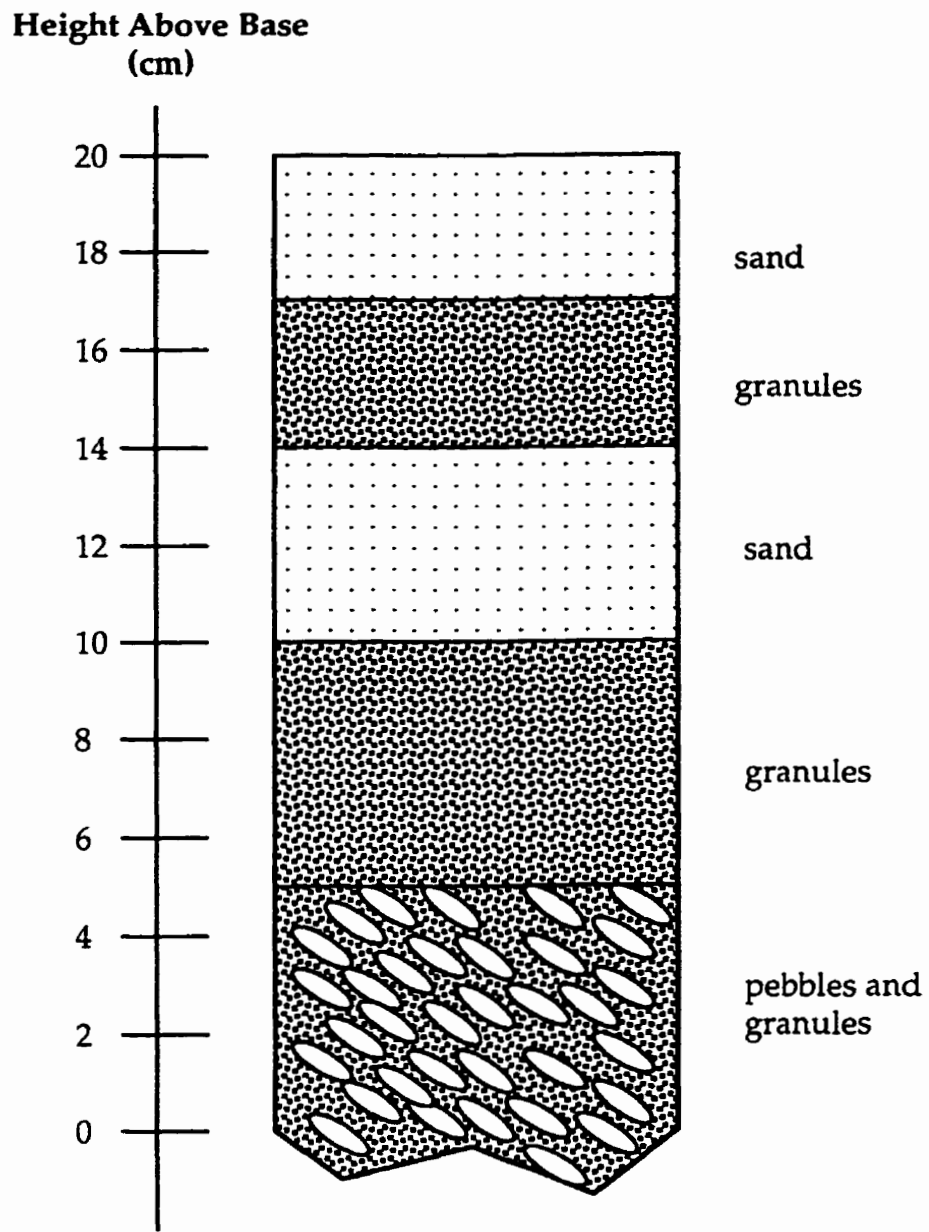


Figure 28: Sedimentary sequence along zone A, Ship Cove.

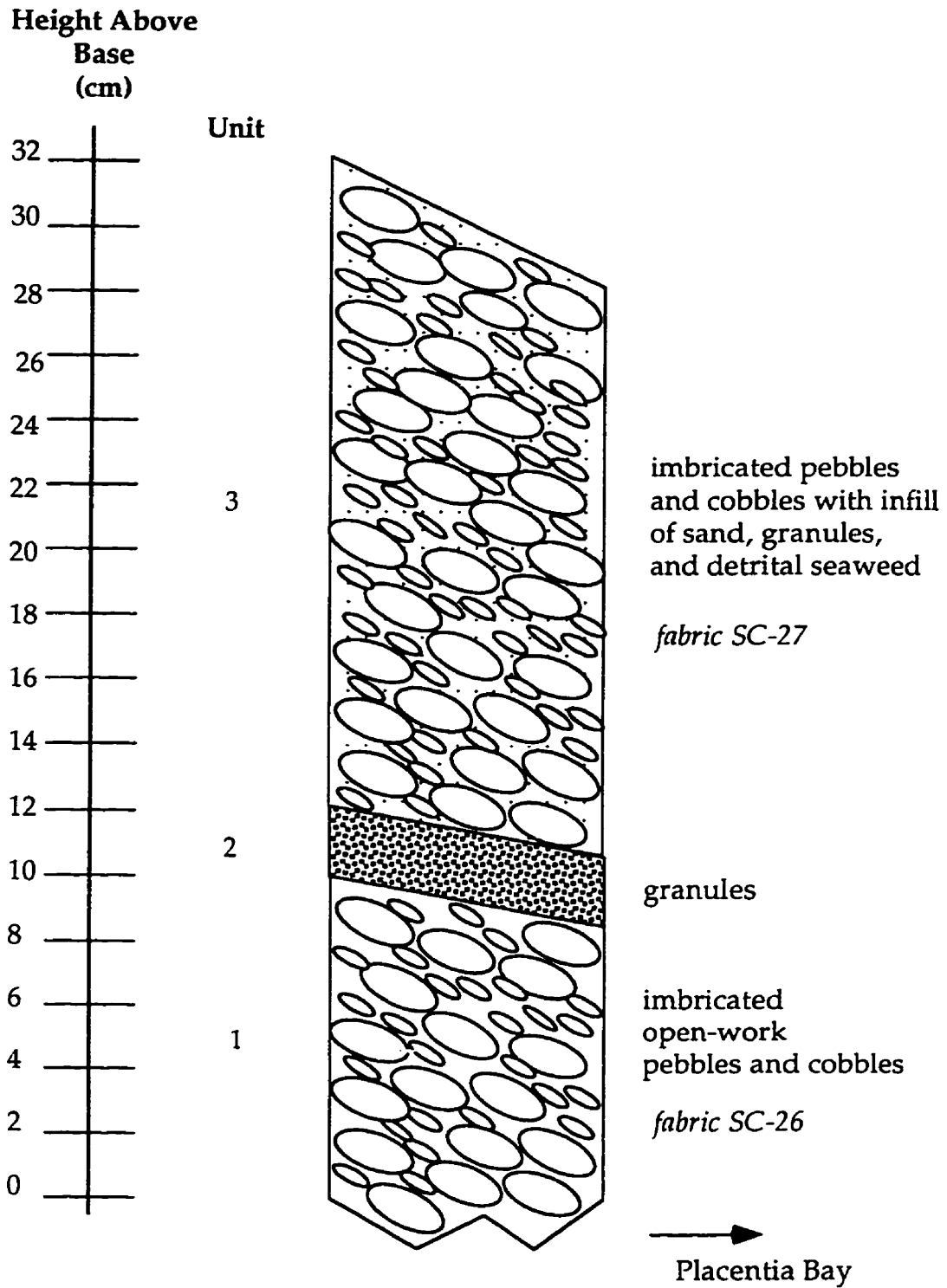


Figure 29: Exposure A, Ship Cove.

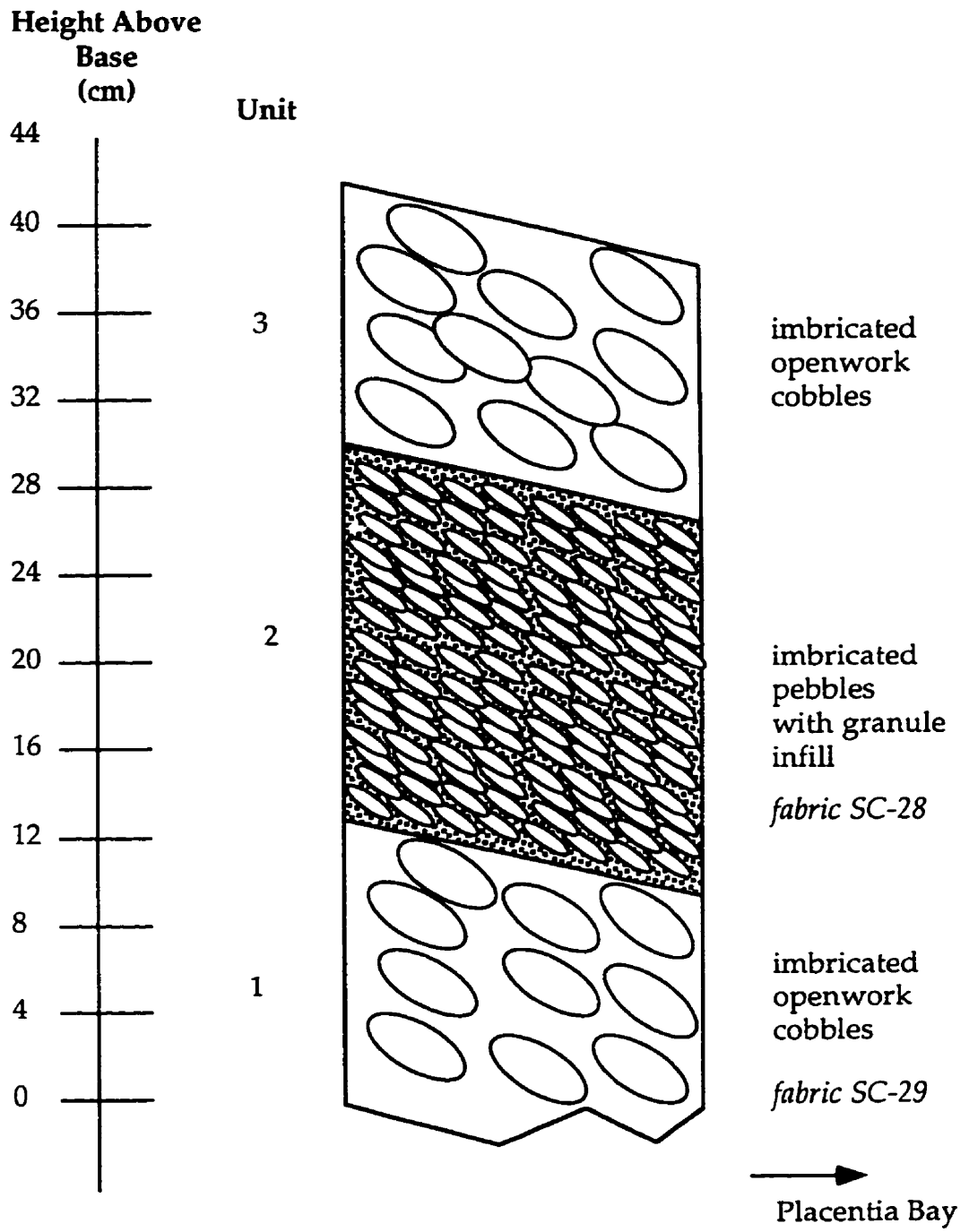


Figure 30: Exposure C, Ship Cove.

5.4 Clast Shape

Figure 31 shows the clast shape analysis of the four samples taken on the crest, mid-, and lower-beachface along transects SC-3, SC-6, and SC-13. These transects were chosen as representatives of the zones in which each is located. In addition, clast shape analysis of a sample from a stream mouth bar was performed. Also shown in Figure 31 are the estimated clast shape compositions of each transect, combining the samples along each transect width and the clast shape composition of the entire beach which includes the total samples taken in July 1991 ($n = 163$), than those discussed in detail here.

Discs and blades formed of at least 80% of the composition for each sample along the transects whereas rollers and equants comprised less than 20%. The crests, however, had a slightly lower proportion of rollers and equants. Along transect SC-3, rollers and equants comprised 6% of the assemblage at the crest, and 12% and 19% on the mid- and lower-beachface sections, respectively. Transect SC-6 had no rollers or equants on the crest whereas the mid-area had 8% and the lower had 7%. Lastly, transect SC-13 had 4% of these shapes on the crest whereas the mid- and lower-beachface sections consisted of 20% and 12% respectively. In addition, although not shown graphically, the percentages of equants and roller increased from 4% along the crest to 12% along the edge of the barrier on the overwash fan. For the combined clast assemblage of each transect, transect SC-6 had a lower percentage of rollers and equants, 5% compared to 17% and 13%.

The clast shape assemblage on the stream mouth bar was distinct. Discs and blades composed 59% of the total assemblage with rollers and equants comprising 41%.

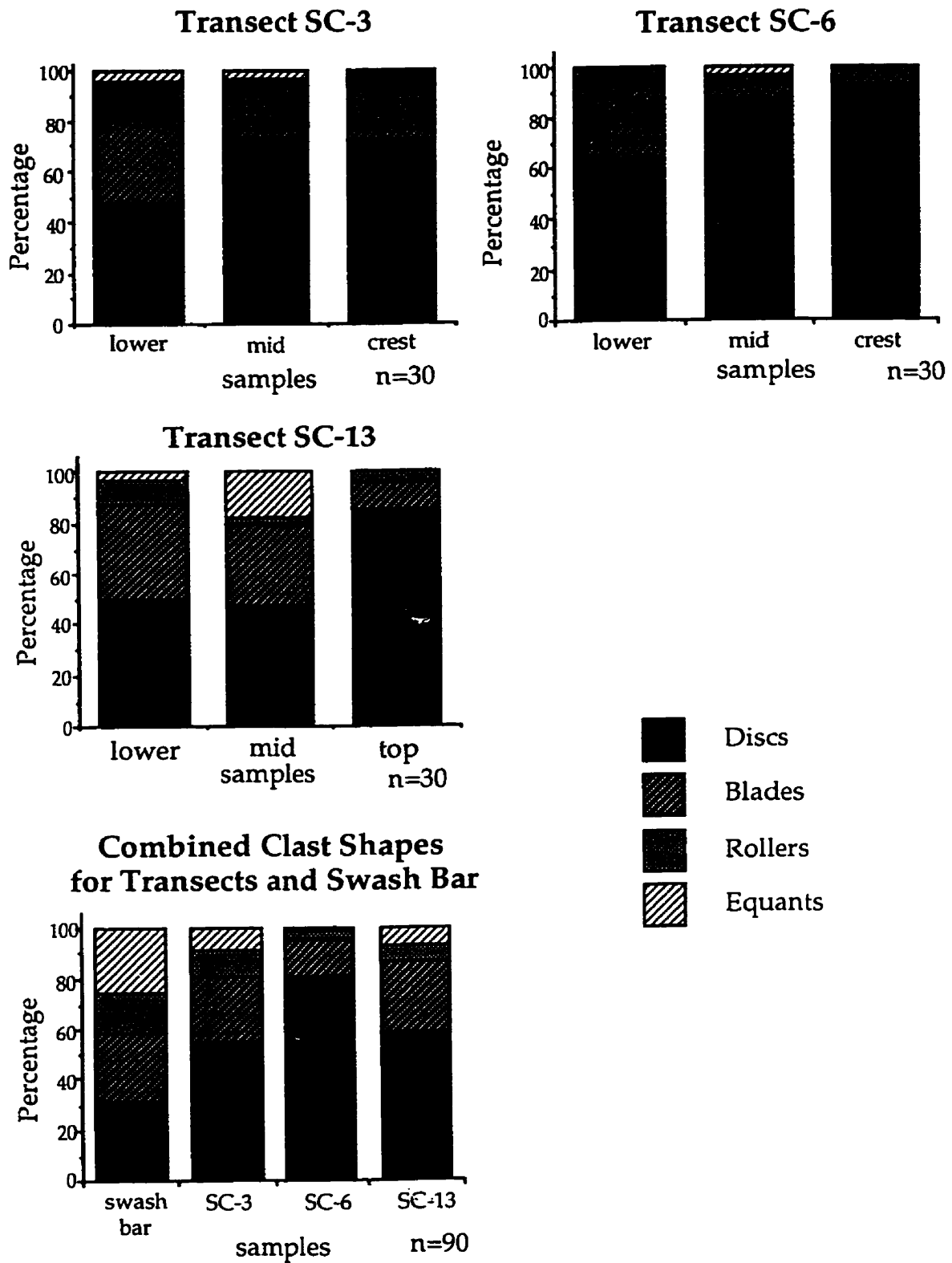


Figure 31: Clast shape analysis for Ship Cove.

With few exceptions, the clasts are rounded to well rounded throughout the width and length of the beach. With the exception of those in the vicinity of the present location of the outlet (the mouth bar) the clasts are characterized by low sphericity. Around the outlet, the clasts are mainly moderately spherical.

5.5 Fabric Analysis

The a/b planes of the discoid clasts had a strong seaward imbrication on the berm crests, the barrier crest and backbarrier. At these locations along the barrier, the orientations of the a/b planes ranged between $\pm 45^\circ$ of the transect trend and the plunges generally ranged between 15 - 30°. At the base of and along steeply-dipping berm scarps, the imbrication of the a/b planes were less well defined and the plunges were gentler, ranging between 0 - 15°.

Thirty-two a-axis clast fabrics were taken from the beach sediments at Ship Cove. Figures 32 - 39 show the plots of these fabrics. Table 9 shows the statistical values, the transects along which the fabrics were taken, the transect trend, and the deviation of the fabric trend from the transect trend. Negative values indicate a trend deviation to the north whereas positive values indicate a trend deviation to the south. The first twenty-five fabrics were taken along the transects during July 1991. The locations are shown on the profiles of the transects (Figures 10 - 18). Seven fabrics (SC-26 to SC-32) not associated with transects were taken at later dates from the sediment in the vicinity of the outlet. Consequently, the columns for transect trend and deviation are blank in Table 9.

The principal eigenvalues range between 0.524 and 0.813, with a mean of 0.644 and a standard deviation of 0.066. Eight of the thirty-two fabrics have principal eigenvalues less than 0.6, eighteen have values between 0.6 and 0.7, and six are greater than 0.7.

Three fabric patterns have K values greater than 1. The others show girdle distributions with K values less than 1. The plunge values range between 3.9° and 37.7°. The majority, 24 out of 32, have values between 10° and 25°.

Five of the 25 fabrics taken along the transects have net trends which show little deviation ($< \pm 5^\circ$) from the transect trends, and are thus aligned perpendicular to the shoreline. Twelve show deviations to the south. Of these twelve, seven show comparatively large deviations (36.7° to 58.9°). The other five have deviations between 11.4° and 26.4°. Of the eight fabrics that deviate to the north, two have large deviations, -39.4° and -55.2°. The other six fall between -13.3° and -29.7°.

When the fabrics were taken in July 1991, the beach was characterized by tiers of cusps. Consequently, most fabrics were taken along a part of the cusp form with the majority taken on the crests or on the bases of cusps that had been filled and modified by lower level, seaward cusps.

Two fabrics, SC-14-14 and SC-18-23 with trends of 295.2° and 244.2° and plunges of 25.8° and 15.5° respectively, were taken along the backbeach. Their S_1 values are similar, 0.673 and 0.687, as are the absolute values of the deviations from their respective transect trends, 17.2° and 18.8° respectively. However, the trend of fabric SC-14-14 deviates to the north, whereas that of SC-18-23 deviates to the south.

Number	Trend	Plunge	S1	S3	K	Tran Trend	Deviation
SC - 7 - 1	241.7	17.3	0.674	0.036	0.40	289	47.3
SC - 9 - 2	245.9	23.7	0.669	0.078	0.83	287	41.1
SC - 9 - 3	290.8	14.2	0.604	0.038	0.23	287	-3.4
SC - 9 - 4	240.2	13.5	0.624	0.300	0.24	287	46.8
SC - 11 - 5	242.3	20.8	0.611	0.027	0.20	279	36.7
SC - 11 - 6	292.3	21.2	0.707	0.037	0.52	279	-13.3
SC - 12 - 7	274.1	16.7	0.674	0.034	0.39	278	3.9
SC - 12 - 8	259.2	14.1	0.555	0.021	0.09	278	18.8
SC - 13 - 9	274.1	17.2	0.587	0.078	0.38	278	3.9
SC - 13 - 10	281.3	19.2	0.638	0.034	0.29	278	-3.3
SC - 13 - 11	225.8	20.4	0.626	0.043	0.32	278	52.2
SC - 14 - 12	251.6	11.8	0.565	0.018	0.10	278	26.4
SC - 14 - 13	317.4	19.1	0.581	0.065	0.30	278	-39.4
SC - 14 - 14	295.2	25.8	0.673	0.054	0.55	278	-17.2
SC - 15 - 15	260.6	11.1	0.758	0.027	0.60	272	11.4
SC - 15 - 16	327.2	9.2	0.634	0.051	0.39	272	-55.2
SC - 16 - 17	268.4	29.8	0.652	0.117	1.51	269	0.6
SC - 16 - 18	216.1	10.2	0.605	0.013	0.14	269	52.9
SC - 16 - 19	246.2	16.8	0.599	0.083	0.47	269	22.8
SC - 17 - 20	292.6	25.0	0.732	0.043	0.72	267	-25.6
SC - 17 - 21	208.1	7.7	0.615	0.055	0.35	267	58.9
SC - 18 - 22	292.7	14.9	0.591	0.043	0.23	263	-29.7
SC - 18 - 23	244.2	15.5	0.687	0.057	0.66	263	18.8
SC - 19 - 24	276.9	24.9	0.749	0.057	1.10	259	-17.9
SC - 20 - 25	280.2	19.1	0.739	0.037	0.67	253	-27.2
SC - 26	205.4	8.1	0.690	0.040	0.49	exposure	
SC - 27	164.0	3.9	0.606	0.045	0.27	exposure	
SC - 28	253.7	9.1	0.574	0.051	0.21	exposure	
SC - 29	218.3	10.8	0.661	0.023	0.28	exposure	
SC - 30	311.6	17.9	0.524	0.075	0.16	fan	
SC - 31	345.3	12.7	0.600	0.030	0.19	fan	
SC - 32	236.7	37.7	0.813	0.065	2.99	adjacent to outlet	
min	164.0	3.9	0.524	0.013	0.09		
max	345.3	37.7	0.813	0.300	2.99		
mean	261.9	16.9	0.644	0.055	0.51		
s. d.	38.8	7.1	0.066	0.050	0.54		

Table 9: Clast fabric data for Ship Cove.

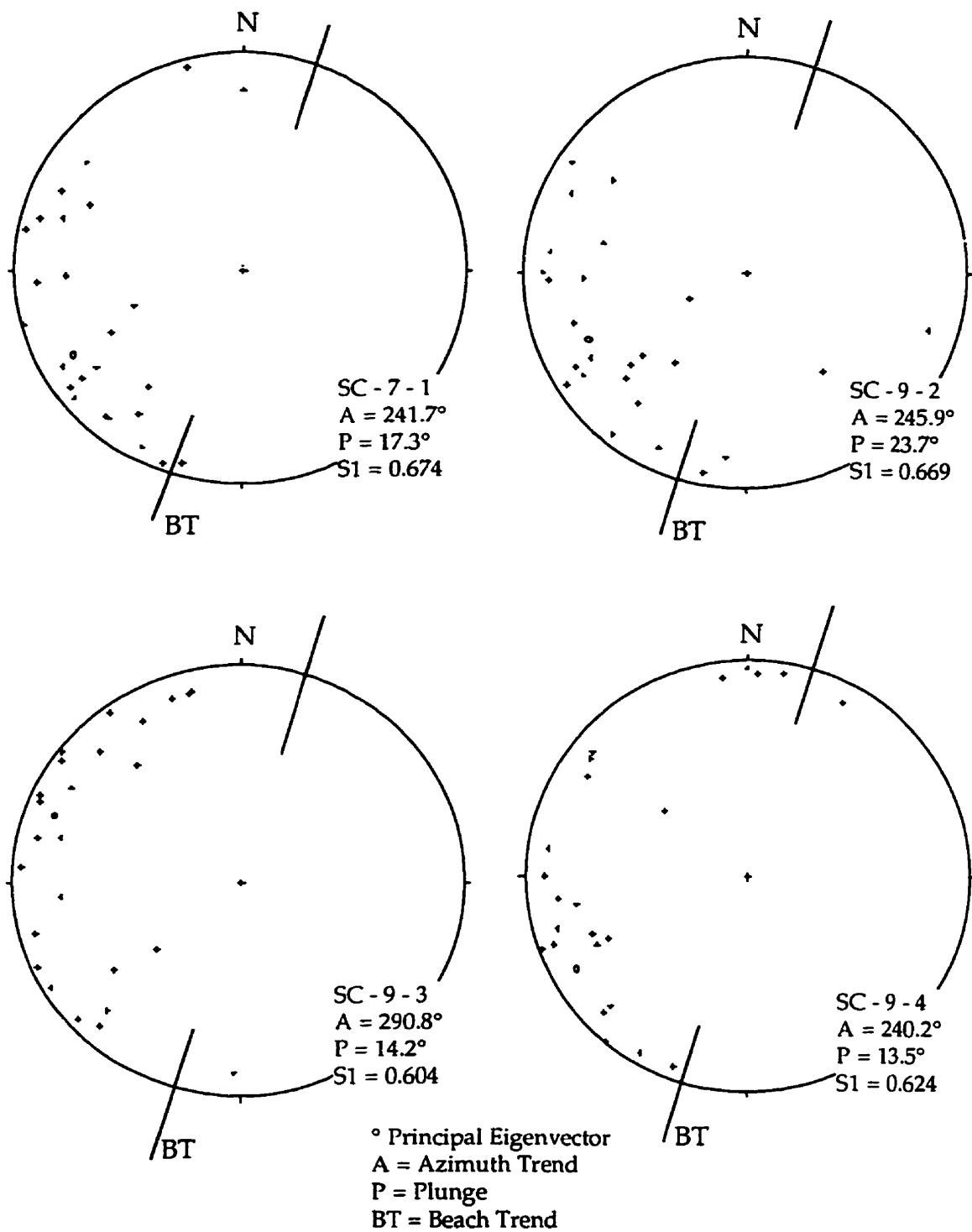


Figure 32: Clast fabrics, Ship Cove.

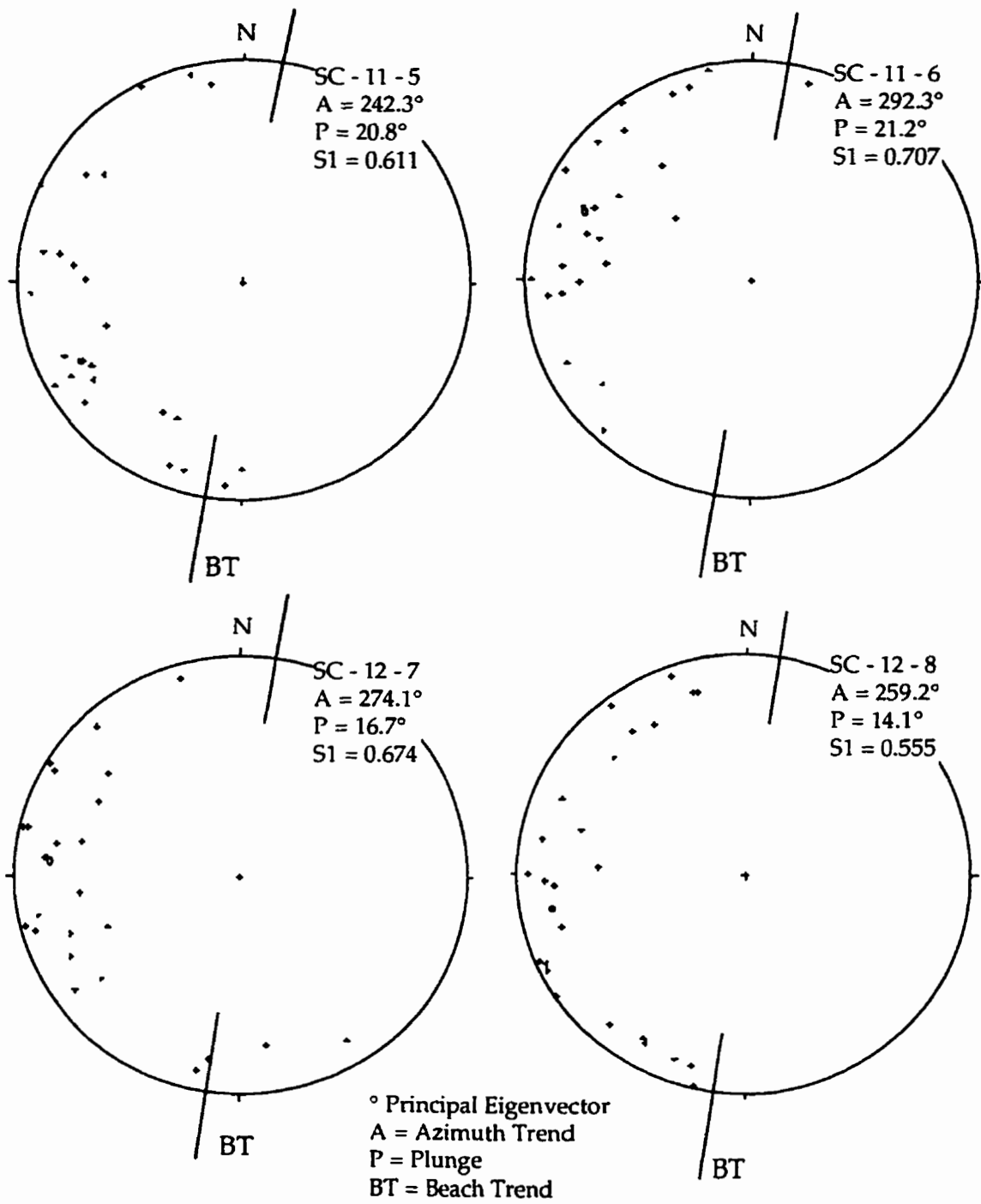


Figure 33: Clast fabrics, Ship Cove.

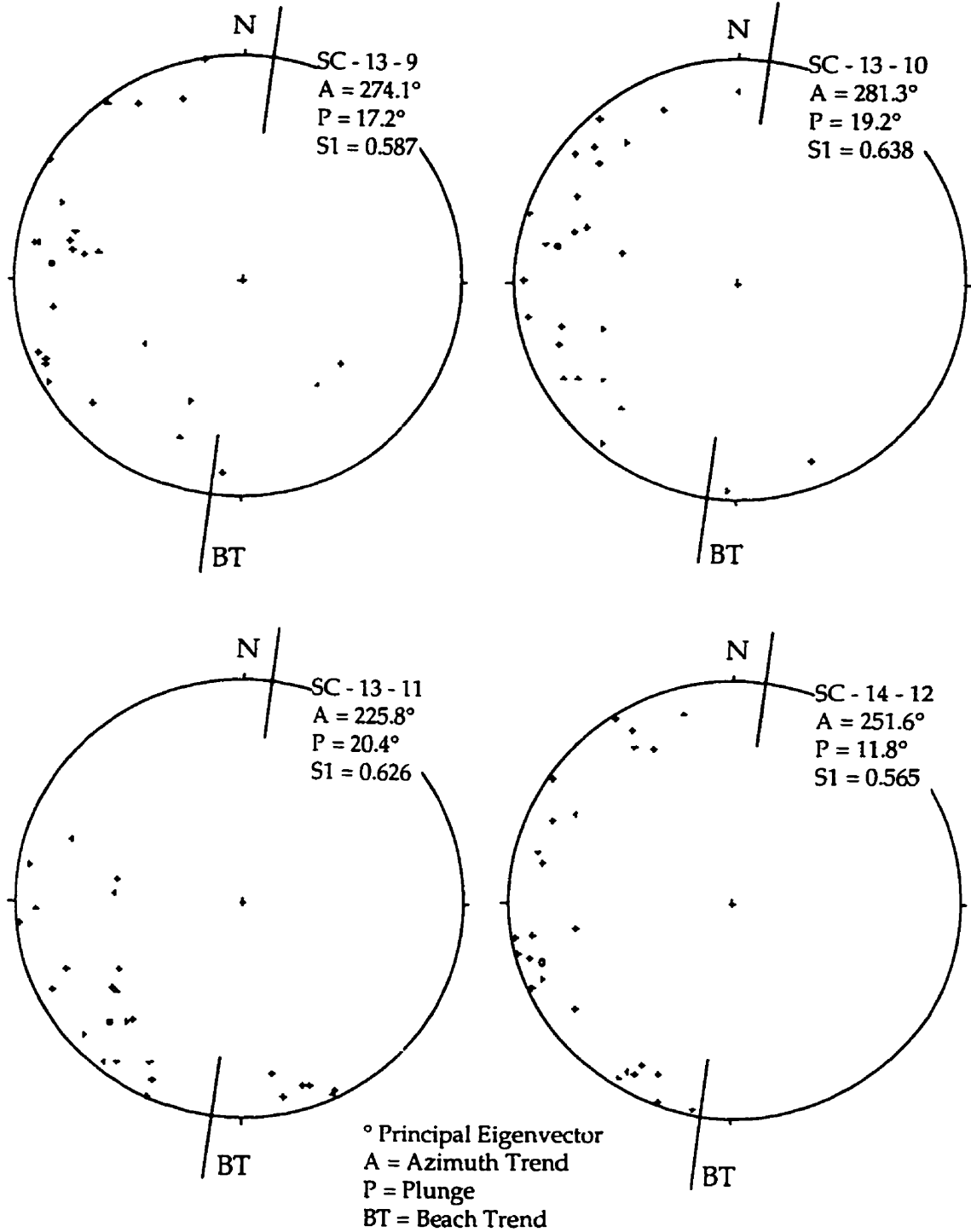


Figure 34: Clast fabrics, Ship Cove.

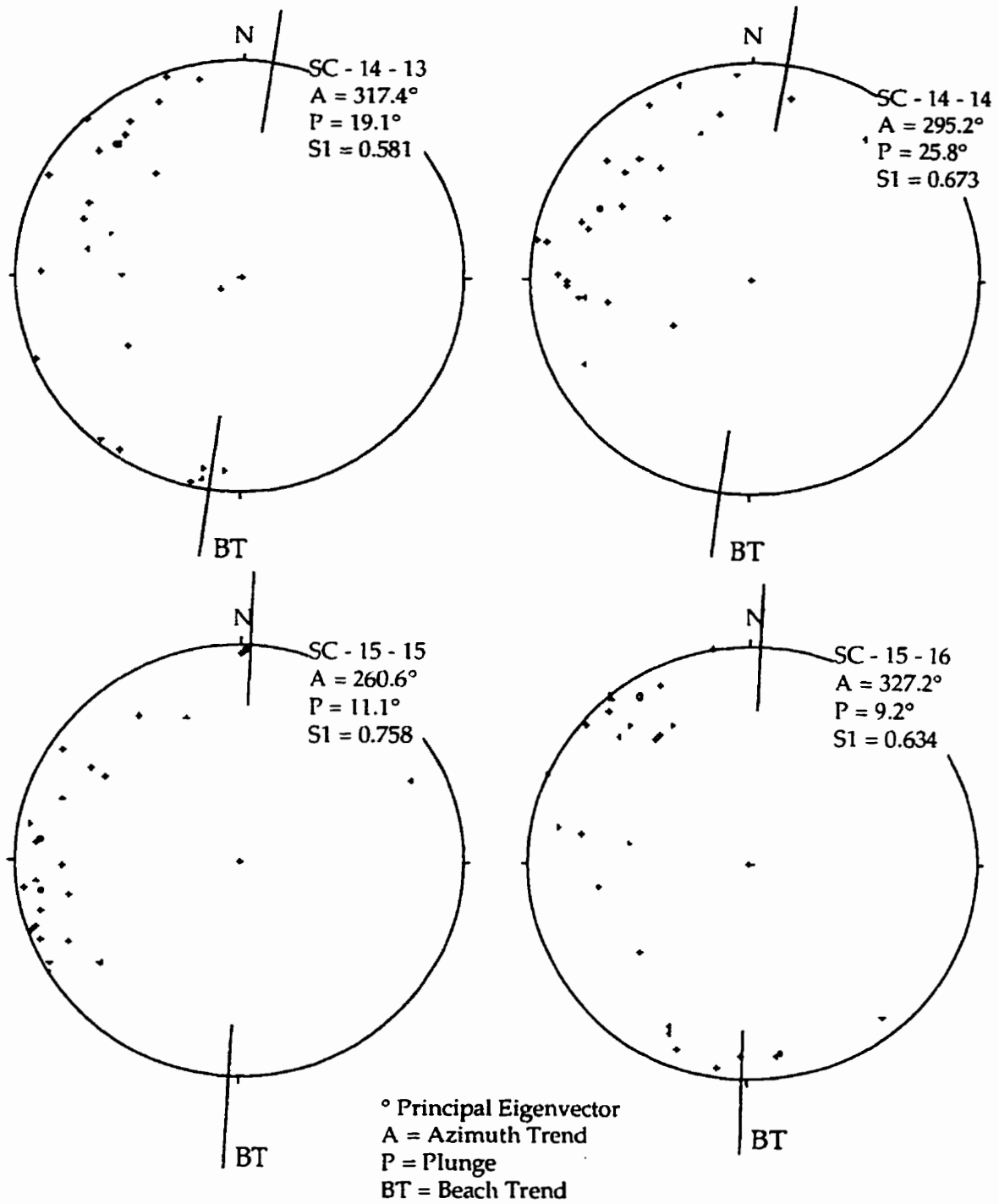


Figure 35: Clast fabrics, Ship Cove.

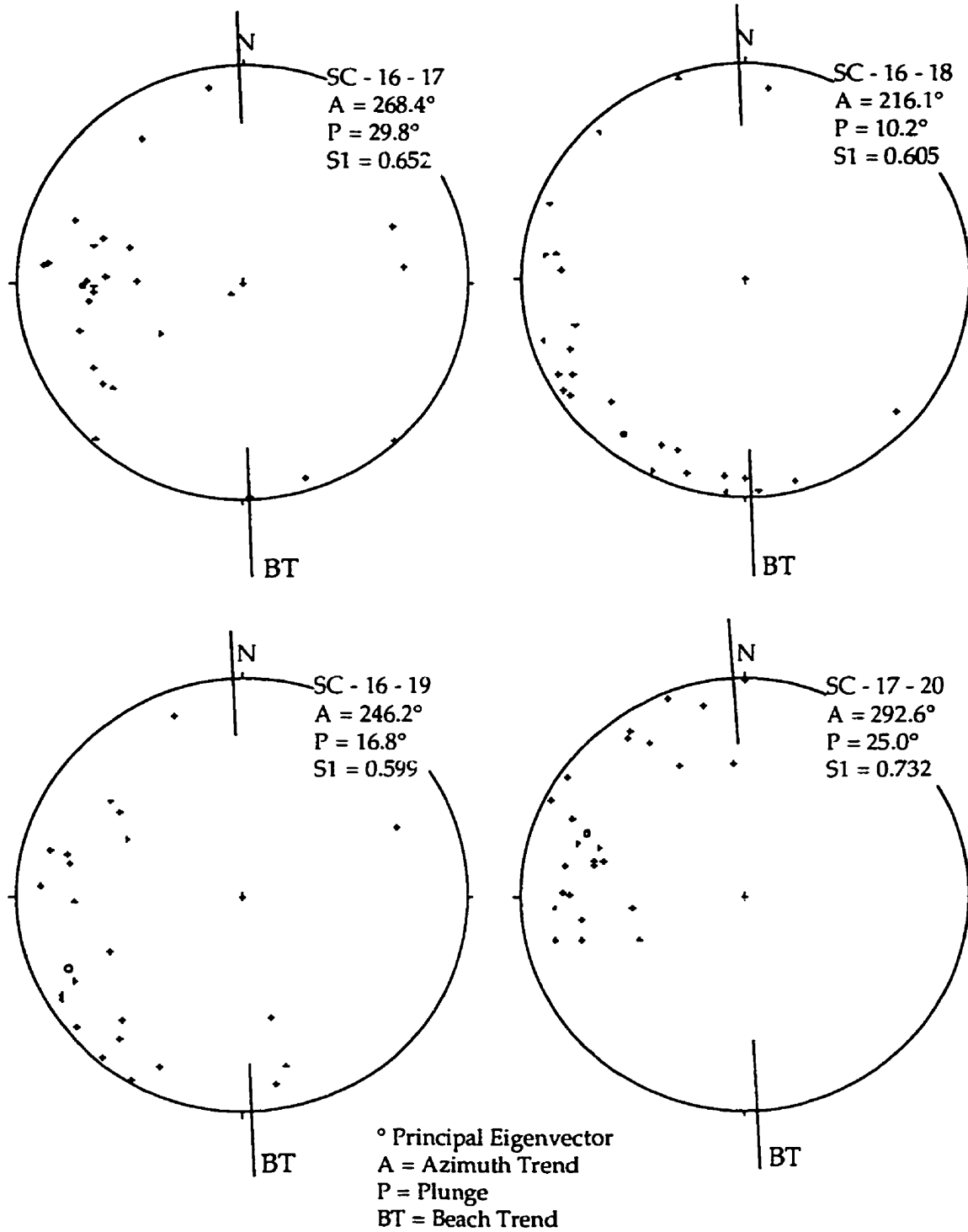


Figure 36: Clast fabrics, Ship Cove.

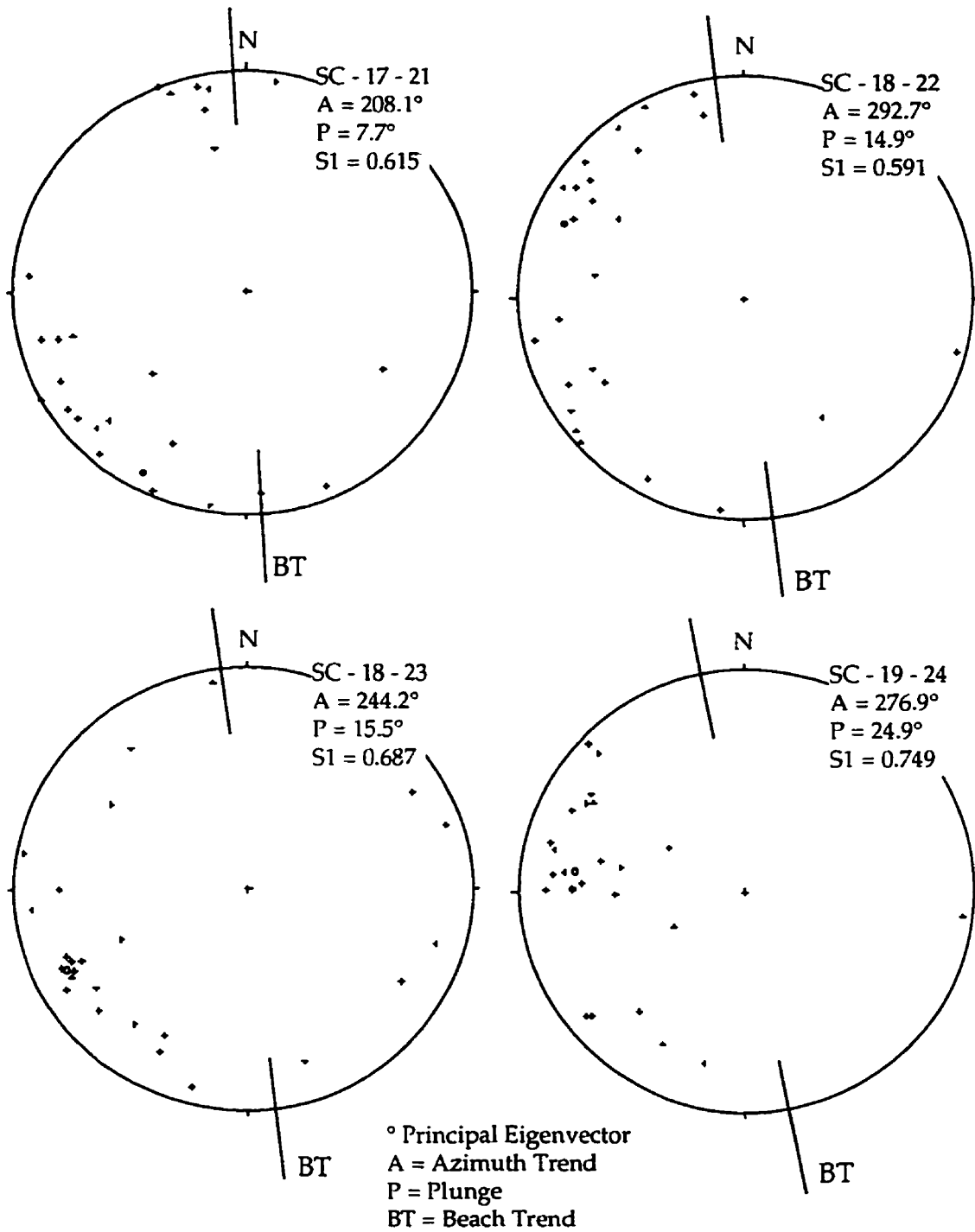


Figure 37: Clast fabrics, Ship Cove.

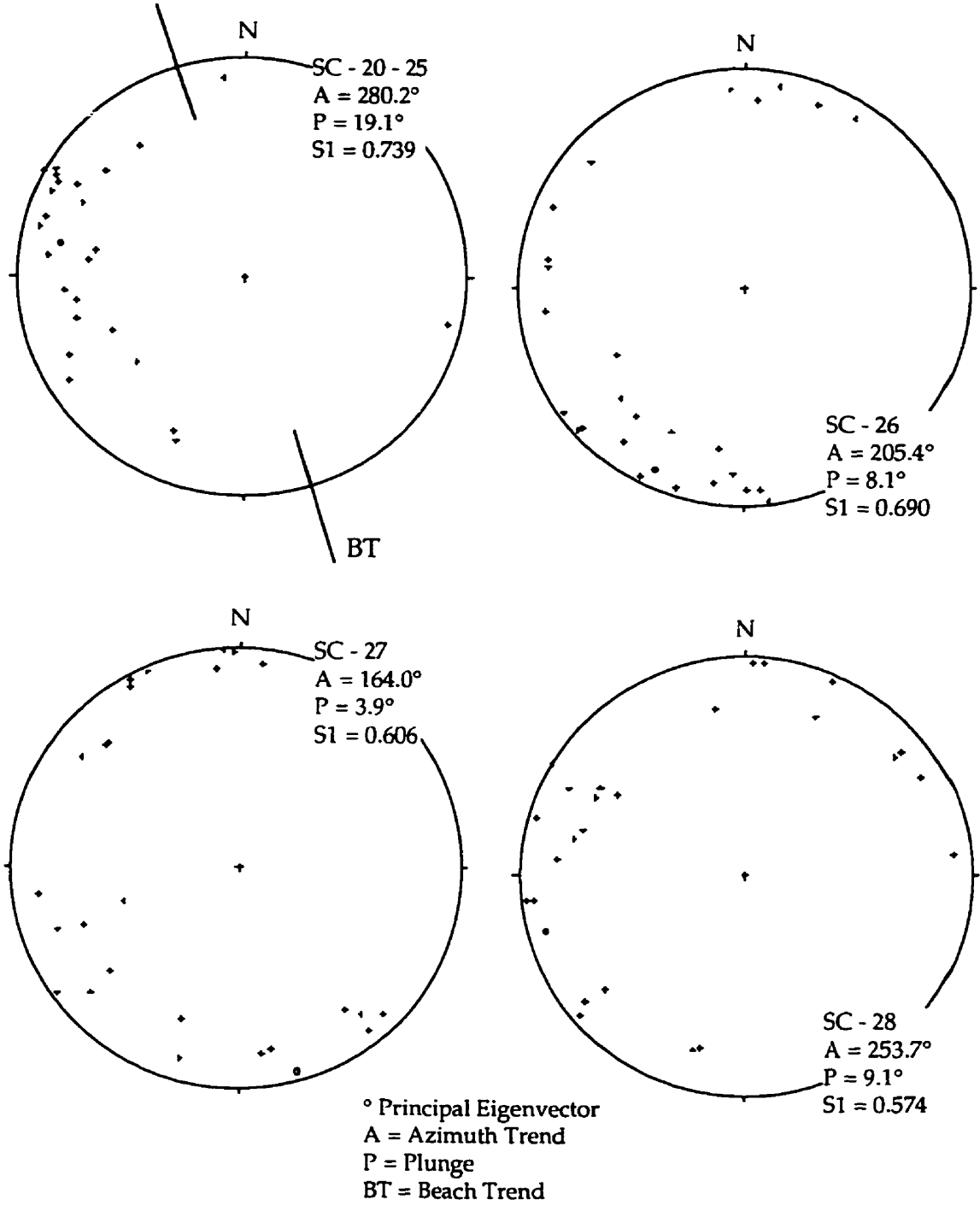


Figure 38: Clast fabrics, Ship Cove.

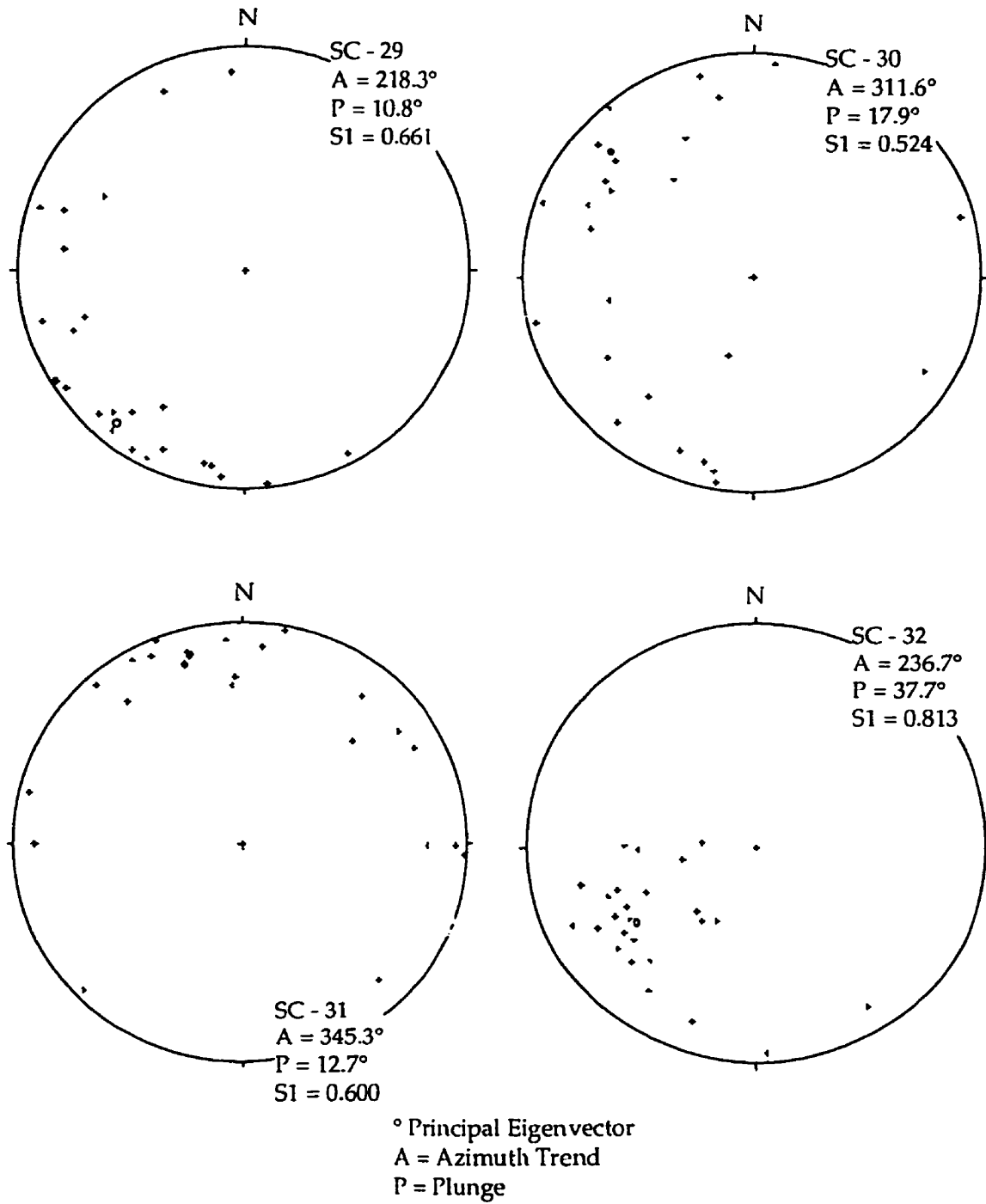


Figure 39: Clast fabrics, Ship Cove.

No explicit pattern of increasing plunge values with distance from the sea is evident. For example, moving landward along transect SC-9, the plunge values of fabrics SC-9-4, SC-9-3 and SC-9-2 are 13.5°, 14.2°, and 23.7°. The lower two values are similar whereas the upper one is distinct. Other transects show increasing plunge values, but the differences are not strong. Furthermore, along transect SC-13 the plunge value of the fabric taken on the barrier crest, SC-13-9, is 17.2° whereas the other two fabrics, SC-13-10 and SC-13-11 have plunge values of 19.2° and 20.4° respectively. The differences in these three values are insignificant.

The magnitude and direction of deviation of fabric trend from the transect orientation shows no discernible pattern with distance from the sea. Frequently, fabrics taken at similar elevations and similar positions on cusate features show differing trends. For example, SC-13-10 was taken at the base of a steep slope and has a trend of 281.3°, whereas SC-13-11, taken along the same transect at approximately 20 cm lower elevation, has a trend of 225.8°.

The trend value largely depends on the position on the cusps where the fabric determinations were made. The shape of the cusp, whether symmetrical or asymmetrical, also influences the measured trend. For example, SC-16-19 was taken towards the centre of an asymmetrical cusp crest with the elongated end towards the north. In contrast, SC-16-18 was taken along the southern margin of the same cusate feature. The trend of SC-16-19 is 246.2° with a deviation of 22.8°. The trend of SC-16-18 is 216.1° with a deviation of 52.9°. Both fabrics deviate to the south, with fabric SC-16-18 (taken at the margin) having a stronger southerly component.

Clast fabric SC-17-20 was taken to the south of the centre of a symmetrical cusp crest, and had a trend value of 292.7° with a deviation of -25.6° . Along this cusp, the imbrication of the a/b planes of the discoid clasts was structured. The clasts toward the centre were imbricated parallel to the transect trend, whereas to the south the imbrication was aligned to the north. Clasts located north of the centre of the cusp showed a southerly imbrication (Figure 40).

Clast fabrics SC-26, SC-27, SC-28, and SC-29 were taken on exposures along the barrier formed by the opening of the stream outlet. SC-26 and SC-27 were taken in August 1991, whereas SC-28 and SC-29 were taken in July 1992 on separate strata within the same exposure (detailed descriptions are in the texture section). SC-26 has trend of 205.4° , a plunge of 8.1° and an S_1 of 0.690. SC-27 has a trend of 164.0° , a plunge of 3.9° and an S_1 of 0.606. SC-28 has a trend of 253.7° , a plunge of 9.1° and an S_1 of 0.574. Fabric SC-29 has a trend of 218.3° , a plunge of 10.8° and an S_1 of 0.661.

The principal eigenvalues of the fabrics taken from the exposures of sediment adjacent to the outlet are similar to those found on the existing beach surface. The trend orientations for SC-26 and SC-28 are similar to those taken along the transects, but that of SC-27 (164.0°) is more southerly. Although two of the fabrics taken along the transects have low plunges ($< 10^\circ$), the majority (23/25) have plunges greater than 10° . The fabrics taken from the exposures all have low plunges.

Clast fabrics SC-30 and SC-31 were obtained from two separate fans which closed the outlet in July 1992. The S_1 values are 0.524 and 0.600,

respectively. The trends are 311.6° and 345.3° , and the plunges are 17.9° and 12.7° respectively.

The last clast fabric, SC-32, was taken directly to the south of the open outlet in August 1991. It has the highest S_1 value (0.813), the highest plunge (37.7°) and the highest K value (2.99). The trend is 236.7° .

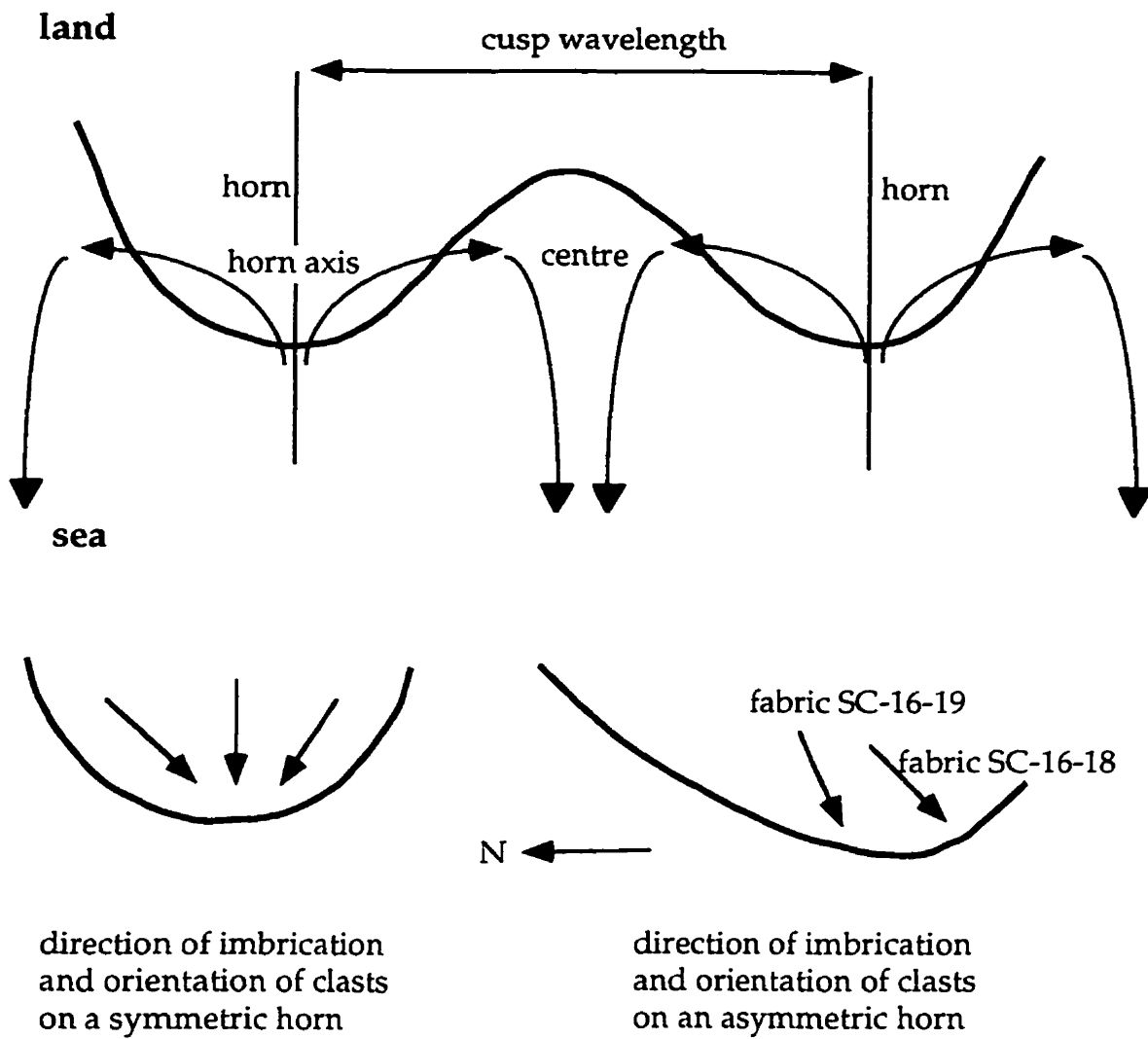


Figure 40: *Top*: Schematic diagram showing pattern of water flowing through cusp centre. *Bottom*: Orientation of clasts observed on symmetric and asymmetric cusp horns; explanation in text.

Chapter 6

Discussion of the Barrier at Ship Cove

6.1 Morphology

6.1.1 Cusp Formation

Tiers of beach cusps have been observed on the beach at Ship Cove. Along zone C, each tier had progressively larger wavelengths farther up the beachface. In July, 1991, the uppermost tier had a mean wavelength of 20.7 m and height of 2.4 m. The mid-beachface cusps had a mean wavelength of 11.6 m and height of 1.3 m, and the lower had a mean wavelength of 5.5 m and height of 0.5 m. The cusps along zone A had a mean wavelength of 8.9 m and height of 0.5 m.

Field observations of cusp formation in the lower- and mid-beachface showed a circulation where the swash action ran up the beachface, became divided at the horns and flowed seaward in the embayments (Figure 40). Backwash flow, particularly evident in the lower-beachface at low tide, concentrated in the centre of the embayments and removed finer sediment, leaving large pebbles and cobbles exposed. Similar observations were made by Longuet-Higgins and Parkin (1962), Russel and McIntire (1965), and Worrall (1969). However, other observations have shown a reverse circulation where flow moves from the embayments to the horns (Norris, 1956; Komar, 1971; and Williams, 1973).

Cusp formation involves both erosional and depositional processes. Assuming accretion occurs when swash action overrides backwash action and

erosion when backwash overrides swash, then deposition in this case occurs on the horns and erosion in the troughs (Sallenger, 1979). It is likely that the well-sorted imbricated cobbles in a seaward-dipping bed in exposure B were from a cusp horn. Deposition would also occur on the base, or floor, of the embayment (Allen, 1984). This leads to the possibility of preserving whole depositional structures superimposed over erosional forms (Otvos, 1964).

The most widely used theory for the origin and spacing of cusps involves alongshore standing waves, and was originally proposed by Longuet-Higgins and Parkin (1962). In the most accepted theory, cusps result mainly from subharmonic, or less frequently, synchronous edge waves (Inman and Guza, 1982). Other explanations describe cusp formation as an interaction between swash action and beach morphology (Werner and Fink, 1993) and by intersecting progressive waves of the same period. The latter cause periodic longshore variations in water levels and rip currents which can then create cusped forms on shore (Dalrymple and Lanan, 1976).

Edge waves are formed by wave motion that becomes trapped against the shoreline by refraction and then moves alongshore. The interaction of the edge wave and the incident wave cause perturbations in the wave height (Sallenger, 1979). The spacing of the perturbations depends on the wavelength of the edge wave which is expressed in the wavelength of the cusps. Synchronous edge waves occur when the edge wave period equals the incident wave period and, the cusps that result will be equal to one edge wave wavelength. Subharmonic edge waves have periods twice that of the incident waves; consequently wave height maximums alternate with wave height minimums with the passage of every incident wave crest. The

resulting cusps will have wavelengths one-half that of the edge waves (Sallenger, 1979). It is speculated that edge waves are necessary to initiate cusp development but are not required to develop the mature cusp topography (Inman and Guza, 1982). Edge waves are initiated during fair weather or storm decay swells and may help to channel wave run-up over the barrier crest (Orford and Carter, 1984).

The formulas formulated by Inman and Guza (1982) used to approximate edge wavelength are:

$$l_c = L_e/2 = (g/\pi)(T_i^2) \tan b, \text{ subharmonic}$$

and,

$$l_c = L_e = (g/2\pi)(T_i^2) \tan b, \text{ synchronous;}$$

where:

l_c = the cusp wavelength,

L_e = longshore wavelength,

g = gravity

T_i = incident wave period.

$\tan b$ = the slope of the beach.

The predicted values roughly approximate observed cusp wavelengths along many beaches (Inman and Guza, 1982). At Ship Cove the incident wave periods are not known for the upper-beachface cusps. Assuming the cusp wavelengths approximate one-half the more common subharmonic edge waves, then the incident waves had periods of 5.3 s (using a slope of 20°) for the upper cusps.

The cusps shown in Plate 6 were taken during the waning stages of Hurricane Bob on 24 August 1991. The resulting cusps had wavelengths of approximately 12 m. Visual estimates showed an incident wave period of 8 s. Using a beach slope of 11° gives a predicted value of 4.5 s, a value lower than observed. For the lower-level cusps, the predicted value is 3 s (using a beach slope of 11°). Observed wave periods were 6 or 7 s. For the cusps in zone A, the predicted incident wave period is 5.1 s, again lower than the observed values of 6 to 7 s. Comparisons of the observed and predicted incident wave periods better approximate the less frequent synchronous waves where the cusp wavelength equals the edge wavelength. The beaches discussed by Inman and Guza (1982), for the most part, are composed of sand and located along long beaches exposed to ocean waves where edge waves can fully mature. Ship Cove, in contrast, is enclosed, small, and composed of large-sized clasts.

Inman and Guza (1982) relate maximum cusp vertical height with wavelength by the formula:

$$g_c = 0.24Kl_c \tan b;$$

where:

g_c = maximum cusp vertical height,

K = constant, function of breaker height, beach slope, permeability, etc., on the order of 1 (i.e. $K = 1$).

Using this formula gives maximum cusp heights of 1.19 m for the upper cusps, 0.54 m for the middle cusps, and 0.25 for the lower cusps along zone C. The calculated height for the cusps at zone A is 0.23. All of these values are

less than observed and likely result from inadequacies of applying this formula to a gravel-dominated pocket beach.

6.1.2 Outlet Stability

The status and position of the outlet has important consequences for the nearshore wave dynamics because it influences edge wave development and subsequent cusp formation (Orford *et al.*, 1988). An open outlet also allows a seaward transfer of sediment, although this may not be as important a factor in the morphodynamic development as in sand-dominated environments where tidal sediment exchange plays an important role (Hayes, 1991; Chasten and Seabergh, 1993). In this area, the microtidal to low mesotidal range, small drainage basin, low discharge, and a high proportion of large clasts in the surrounding diamicton, result in little seaward transport of sediment.

When the outlet is closed, seepage occurs, particularly at low tide when the hydraulic head (the difference between the lagoon level and the sea-level) is greatest. Seepage discharge occurs throughout the barrier but is greatest at the present northern location of the outlet and at the former position along the southern edge of the lagoon. The main factors controlling the discharge of seepage are the permeability of the sediment within the barrier, the potential cross-barrier head, and the discharge of the drainage basin (Carter *et al.*, 1984). The potential cross-barrier head decreases with increased barrier width and increases with increased hydraulic head differential. Given the predominance of large-sized clasts and the small barrier widths of 25 - 60 m,

the barrier at Ship Cove is susceptible to seepage when a channel is not present.

Using the discharge values at Little Barasway Brook suggests an estimated discharge of 1.4 cumecs for the stream at Ship Cove. In examples from Ireland it was found that discrete channels formed in barriers when stream discharges exceeded 1.0 - 1.5 cumecs (Carter *et al.*, 1984). The estimate of discharge at Ship Cove falls within this range. Since 1.4 cumecs is an average value, seasonal variability will cause the stream flow to exceed this value (primarily in the spring and fall months) while at other times, the discharge will fall below this mean.

Table 7 shows the status of the outlet on several dates and the channel dimensions. In general, the outlet was closed during July and August and parts of June and September. During the months of March through May and October through November, it was open. Conditions during the other months were variable.

Deviations from this general trend can be seen, however. Since the soil capacity for water retention is low and the channel gradient relatively high, stream discharge responds rapidly to rainfall events. For example after the passage of Hurricane Bob on August 19 and 20, 1991, which produced the extreme daily precipitation of 13 mm on August 19 for that month, the stream outlet was open and reached a width of 2.5 m on August 23. Subsequently, with little or no rain on the days following the passage of the storm, the outlet closed on 24 August 1991. Seaweed that had been thrown ashore during the storm acted as a binding agent for the clasts and helped create a more effective outlet plug. Seaweed matter was found within some

of the strata exposed within the barrier along the outlet at later dates. This was associated with deposition around storm events and/or outlet closure.

The mean discharge at Little Barasway Brook was 0.227 cumecs for August 1991, and the total August precipitation at Big Barasway was 50.8 mm (Table 7). This suggests a proportional discharge of 0.2 cumecs at Ship Cove, a value well below the Carter *et al.* (1984) estimate of 1.0 - 1.5 cumecs required for channelization. In contrast, in November 1991 the mean discharge for Little Barasway Brook was 2.02 cumecs, giving a proportional discharge of 1.8 cumecs for the stream at Ship Cove. The outlet was open when visited on 4 November 1991.

On 28 October 1991, however, the outlet was closed. The mean discharge for October 1991 at Little Barasway Brook was 2.16 cumecs, a larger quantity than in November 1991. The days with higher discharge were early in the month, particularly October 4 and 8. Consequently, with relatively mild wave conditions and low to moderate rainfall, the outlet had closed by October 28. A large rainfall event, 36 mm on 1 November 1991, contributed to the opening of the outlet as seen on 4 November.

Development of the outlet favours places where barriers are least coherent and where barrier heights are lowest as a consequence of reduced breaking wave heights (Lowry and Carter, 1982). Given the present morphology of the barrier at Ship Cove, the highest elevations of 5.3 - 5.5 m asl are between transects SC-11 and SC-13. Beach overtopping was found at higher elevations of 6 m between transects SC-9 and SC-10, but these sites are not on the barrier itself. This would indicate that the area toward the centre of the cove receives the highest wave run-up. The general configuration of

the cove causes lower waves to reach both ends. Furthermore, the ridge seen in the 9 and 12 m bathymetric contours (Figure 6) may promote wave-focusing in the centre. This causes an increase of wave run-up and as a consequence, the present northern position of the outlet is in an area which receives comparatively reduced wave run-up.

Prior to the forced relocation of the outlet to the north, the outlet was located between SC-11 and SC-12, in the higher energy areas. The 1948 and 1967 air photos and the 1954 photograph show a small outlet at this central location. Given its small size and location it is likely the outlet was unstable then, as it is now. The forced relocation of the outlet created a channel behind the barrier that extended from the lagoon to the northern end of the cove. The creation of this channel has allowed the outlet to favour the northerly location where waves reaching the barrier are lower. Also shown in the air photos is a small lagoon formed by a brook to the north behind the present outlet location (Figure 25). Overwash fans can be seen between the two lagoons.

When the outlet was diverted to the north, it stayed at that location, as it is now located in an area where wave run-up is generally lower compared to the central portion of the cove. With the northerly stream flow behind the barrier, erosion has increased along the pasture land adjacent to the lagoon and has eroded the overwash fans shown in the 1954 photo. Undercutting of fence posts can be seen along the edge of the meadow. This may be providing minor amounts of sand and silt to the beach system.

Whenever the outlet was open during this study, mouth or swash bars formed and extended below mean sea-level. The size varied to a maximum

length and width of approximately 15 m depending on the intensity of stream discharge and wave activity. The increased sphericity of the clasts on the bars may indicate a stronger fluvial influence than elsewhere on the beach.

Similar features formed by fluvial flood events are described by Cooper (1990) along the Natal coast of southeast Africa. Over time, wave activity moved the sediment landward and eventually closed the outlet.

Plate 15: Overview of the beach at Ship Cove looking south, taken in August 1954. The stream outlet was located at the southern end of the lagoon. Overwash fans are present in the foreground of the photo.

6.1.3 *Seasonal Change, Storm Response, and Recent Evolution*

May through late summer is a period of net sediment accretion. Tiers of cusped features are prevalent and the outlet is generally closed. Along zone C, the mid- and lower-beachface steepens as sediment is transported landward. Berms along the mid-beachface develop a distinct landward dip. As wave energies increase with the frequency and intensity of storms, the combined effect of increased backwash and gravity from the steepened slopes causes progressive undercutting of the berms in the mid-beachface, and removal of sediment. With more intense storms more sediment is removed, cusps form and crestal overtopping occurs, transporting sediment landward. This results in an increase of barrier height and a narrowing of backbarrier widths. During January, February, and parts of March, ice foot development protects the barrier from overtopping and erosion from the mid- and upper-beachface. The active sediment zone is then in the intertidal area below the ice foot. With warming during March, wave activity undercuts the foot and aids in its destruction.

However, ice foot development appears to have been more common in the past five years than between 1975 - 1988 (Catto, in press; Catto and Hooper, 1994; Catto *et al.*, 1994). If this is so, then the morphodynamics would have differed, particularly in January, when storm activity can be the most intense. Overwashing would have been more frequent.

Periods of accretion do occur between October and April and allow cusp and berm development along the mid- and lower-beach zones. As noted by Carr *et al.* (1982) in beaches in England and Wales, profile variation is greater in the 'winter' months. Nonetheless these winter oscillations fit within a

larger seasonal cycle. Periods of erosion can occur in the 'summer' but are not prolonged, and the beach recovers relatively quickly. Furthermore, within the seasonal fluctuations, the barrier is moving landward as a response to overtopping and overwashing events that occur mainly in the fall and spring months.

The removal of finer sediment from the beach, resulting from the infilling of the pit behind zone A, would have affected the lower-beachface in particular, and consequently, the shoaling process and run-up ability would have changed. Beach slopes likely would have increased, the waves would have broken closer to shore and the waves would have been able to reach farther up the beach. Subsequent to aggregate removal, it was likely the barrier front increased in steepness and height.

6.2 Sedimentology

6.2.1 Cross-shore Shape and Size Sorting

Low-sphericity, well-rounded, bladed and discoid clasts dominate throughout the entire length and width of the beach at Ship Cove. During the time of detailed study in July and August 1991, the proportions of rollers and equants were consistently lower on the beach crest than along the mid- and lower-beachface. However, the pattern in which the proportions of these shapes increased down beach differed. Along transect SC - 3, rollers and equants formed an estimate of 12% on the mid-section and increased to an estimate of 19% along the lower-beachface. Transect SC-6, in contrast, showed little change in shape composition, 8% to 7%, between the mid- and lower sections. Transect SC-13 showed an estimated decrease of rollers and

equants from 20% midway to 12% along the lower-beachface. These relative proportions indicate that the shape composition along the crest was distinct from the mid- and lower-beachface sections, whereas the mid- and lower areas showed greater variability and were not distinct from one another. Discoid clasts are more efficiently transported in suspension enabling farther transport by wave or swash turbulence than is the case for rollers or equants (Orford, 1975). As a consequence, more discs overtop the beach crest during storm events.

In July 1991, the beach was characterized by tiers of berms and cusps throughout the beachface. Shape sorting was evident between the berm crests (or cusp horns) and the bases of the berm scarps (or bases of cusps). The berm crests showed lower proportions of higher sphericity rollers and equants than did the bases. For example, along transect SC-13 the mid-beachface sample was taken from the base of a steep cusp centre and contained comparatively high proportions of equants and rollers. Towards the seaward edge of the cusp base, fewer equants and rollers were found. The more pivotable rollers and equants move seaward under gravity flow during backwash (Orford, 1975). Consequently, at the base of steep cusp embayments, more spherical clasts were found. With cusped development along the lower level, where the base of the upper cusp becomes the crest of that below, less spherical clasts dominate. As a result of cusped berm development along the beachface, secondary shape sorting exists within the primary down-beach shape sorting pattern (Williams and Caldwell, 1988).

The swash bar at the mouth of the outlet showed the greatest percentage of rollers and equants. This assemblage was distinct along the

beach. The clast shape distribution indicates a greater fluvial component than elsewhere along the beach. Although the swash/backwash motions remain the most dominant force in shape segregation and modification, the rolling motion of bedload in unidirectional flow has influenced the composition of the assemblage, by partially dampening the oscillatory flow.

Locally-derived sedimentary sandstone and siltstone form the largest fraction of the clast lithology in the samples taken on the swash bar and beach crest. This contributes to the predominance of low-spherical shapes characteristic of this beach. However, the igneous clast component was larger on the swash bar than along the crest. The igneous clasts are more resistant to abrasion and are unlikely to form low-sphericity discoids. Thus, the igneous clasts may contribute more to the roller and equant shape fraction than to the blade and disc component. Abrasion on a cobble and boulder-dominated pocket beach in Maine resulted in the preferential modification of isotropic (having no preferred mineral orientation) granitic clasts into compact (equant) forms (Waag and Ogren, 1984). In part, as a result of lithological control, larger percentages of more pivotable roller- and equant-shaped igneous clasts are present in the mid- and lower-beachface at Ship Cove.

The beach at Ship Cove showed landward coarsening with cobbles dominating the upper-beach and crest, similar to the pattern found along most beaches, such as Chesil Beach, England (Carr, 1969). Seaward coarsening, though, has been observed on beaches along Nova Scotia (Bryant, E., 1983; Taylor *et al.*, 1985) Pebbles increased proportionally along the mid- and lower-beachface and sand was present in the intertidal zone. During the summer of 1991, the mid- and lower-beachface along zone C showed distinct inverse

grading of small-, medium-, and large-sized pebbles. With removal of sediment during seasonal change and storm events, an underlying cobble-dominated framework was exposed along zone A and C (compare Plates 5 and 8). Zone B mainly contained large boulders in the framework and at the surface. The larger clasts of the framework in all three zones during the summer months had higher sphericity and contained more rollers and equants than did the surface sediments.

Bluck (1967) discussed clast size and shape zonation on gravel beaches in South Wales. He found beach clasts organized into four zones down beach. The upper berm crest (zone 1) mainly contained cobble-sized discs. Successive zones were comprised by imbricated disc-shaped pebbles (zone 2); an infill towards the base where pebble-sized equants and rollers filled in a framework of cobble-sized equants (zone 3) , and an outer frame at the base made up of equant cobbles (zone 4).

The beach along zone C at Ship Cove shows similarities to that described by Bluck (1967). The crest and backbarrier contain imbricated open-work blade and disc-shaped cobbles, corresponding to Bluck's zone 1. The upper-beachface (zone 2 of Bluck) contained mainly blade- and disc-shaped cobbles, with imbrication being less well developed than in Bluck's model due to the presence of seaward-dipping steep slopes inside cusp centres. The mid-beachface (zone 3) contained higher percentages of roller and equant pebble- and cobble-sized clasts, overlying larger cobbles of higher sphericity. The lower-beachface in the intertidal zone contained sand and imbricated pebbles. The outer zone consisting mainly of pebbles and cobbles, and the

cobble and boulder-dominated nearshore zone correspond to zone 4 of Bluck's model.

In Bluck's (1967) model, clast shape was a more important depositional factor than was size. In addition, the clast shape was not primarily the result of wave abrasion. Deposits of pre-existing clasts were reworked by waves, and the interaction of clast shapes and the relative amount of energies reaching across the beachface determined the clast shape and size zonations. Dobkins and Folk (1970), however, showed the importance of wave action in clast shape determination along basalt-dominated beaches in Tahiti.

The high wave energies of this environment and the limited sediment supply allow a high degree of reworking of the sediment. This, in addition to the sedimentary origin of the clasts, results in discs and blades. Both sediment source and process are thus important in particle shape distributions on gravel beaches, as noted by Kirk (1980).

The swash bars are temporary features as the outlet opens and closes depending on the dynamic interplay of marine and fluvial activity. When the outlet is closed, the sediment on the swash bars is moved landward. Preservation of these sediments in the geologic record is thus limited in this wave-dominated swash-aligned environment; however, increased proportions of rollers and spheres are seen in the vicinity of the outlet even when the outlet is closed. These findings may be useful when examining pre-Holocene deposits. If comparisons of shape distributions taken from lateral sections at similar elevations along a sedimentary unit reveal a distinct clast group of increased rollers and equants and higher sphericity, then this may indicate the presence of an outlet within a beach environment.

Furthermore, the lack of an overlying discoid layer corresponding to the beach crest in a vertical sequence marks a fluvial component. These findings correspond to those of Hobday and Banks (1971) from a pocket beach in Norway. There, the beach had similar shape zonations to that of Bluck's (1967) model but the swash bars showed less distinct shape assemblages.

6.2.2 Lateral Textural Variation

In addition to cross-shore size sorting, the clast-size distributions showed textural compartmentalization, with the southern end of the cove (zone A) dominated by sand and granules. A large proportion of finer clasts are also found in zone B, amongst the boulder framework. Pebbles, cobbles and large boulders form the underlying framework of the beach along zone A and are exposed after extreme storm events. The overlying finer sediment is moved offshore, forming a bar in the nearshore zone. With sediment aggregation the sand and granules move onshore again.

Sand is present in the lower-beachface along zone C, but proportionally less than the other zones. It is unlikely that the sediments of zone C are completely isolated from zones A and B. As a consequence of protection by the headlands on the southern side of the cove from the dominant southwesterly waves and the gentler nearshore gradient along zone A, this section of the beach receives less wave energy, and finer sediment dominates.

6.2.3 *Fabric Analysis*

The orientation, plunge, strength, and distribution of clast fabrics in beach environments are the result of complex interactions of the hydrodynamics, morphology and sediment. Johansson (1965, p. 19) states:

The orientation is thus influenced by the following main hydrodynamic conditions, eg. the direction, height, length and period of the incoming waves, the velocity, depth and flow properties of the uprush and backwash (which may not have the opposite direction, owing to the direction of the incoming waves and the percolation of the swash water into the foreshore.

At Ship Cove, the seaward-imbricated a/b planes of the discoid clasts on berm crests, barrier crest and backbarrier were well organized and varied generally within $\pm 45^\circ$ of the transect trends. The angle of imbrication varied between 15 and 30°. The high energy, reflective nature, and cusp development of a swash-aligned, coarse-sediment beach results in the creation of girdle-shaped a-axis fabrics with a mean principal eigenvalue of 0.644. The coarse texture allows high percolation of swash waves and thus significantly diminishes backwash flow. Hence, the clast fabrics are oriented with moderate principal eigenvalue strengths.

Prentice (1993) obtained similar principal eigenvalues, K values, and deviations of a-axis fabric orientations from transect trends for clast fabrics taken on the gravel barrier at Topsail Beach, Newfoundland. Sixty percent of the clast fabrics on Topsail Beach showed a directional component of the dominant westerly wave front. The others were oriented parallel to the shoreline or landward.

Prior to the work of Prentice (1993), Norrman (1964) showed that four preferred orientations occurred in a cobble-dominated bay: one parallel to the shoreline, two oblique at approximately 45° to the shoreline and one parallel to the wave front. Fraser (1935) and Williams and Gulbrandsen (1977) reported gravels oriented parallel to shoreline trend.

Norrman (1964) attributed the oblique positions to swash action and the perpendicular positions to cobbles that are aligned, but not transported by, wave action. The beach at Ship Cove must be exposed to higher wave energies than the beach described by Norrman, as cobbles are not only re-aligned but are transported by wave action. Clast-size distributions did not have a profound effect on the resulting clast fabrics, as the cobble-dominated beach crest has similar trends, plunges and statistics as the fabrics taken on the pebble-dominated mid- and lower-beachface.

At Ship Cove, however, except for fabric SC-27 taken along an exposure, none of the mean orientations were parallel to the shoreline or oriented landward. This may be attributed, partly, to the low sphericity bladed clasts common here. Although blade-shaped clasts are common at Topsail Beach, the clast sphericity is greater there than at Ship Cove (Prentice, 1993). Consequently, the clasts at Topsail Beach can pivot more easily and respond more to gravity in conjunction with backwash flow than at Ship Cove. The similar coarse sediment textures at both beaches indicate that the backwash flows are weak in both locations. The lack of parallel orientations are primarily a response to a lack of more pivotable clasts and secondarily to the hydrodynamic, morphological and lithological reasons which initially contribute to clast-shape distribution.

The organization of the imbrication of the a/b planes and the a-axis plunges show similarities. The plunges determined from the a-axis fabric method, as well as the imbrications of the a/b planes of the discoid clasts in the sample grids, do not show a distinct increase in angle farther up the beachface such as was noted at Little Sister Bay, Wisconsin by Krumbein (1939). Instead, the plunges demonstrate cross-shore variability with a mean of 16.9°. The low-sphericity, bladed and discoid shapes allow a tight packing of clasts with individual areas of steep plunges (Sanderson and Donovan, 1974).

Cusate features play an important role in determining the a-axis orientation of clast fabrics of the bladed and roller clasts, as well as the imbrications of the a/b planes of the discoid clasts. Cusps allow a focusing of wave energy as swash action moves up the beach. Swash action strikes and overtops the sides of the cusp horn at different angles. Hence, the position on the cusp where the fabric is taken will influence the mean clast orientation. Asymmetric cusps with the elongated end downdrift of the swash direction will have a stronger orientation toward the swash than elsewhere on the cusp (clast fabrics SC-16-18 and SC-16-19).

On symmetric cusp horns, the clasts along the centre axis of the horn were aligned parallel to the transect trend (or wave direction), whereas to the south of the horn axis, clasts were aligned to the north of its axis (or transect trend). Likewise, clasts located to the north of the axis of the horn deviated to the south of the horn axis trend (Figure 40).

The clast orientations follow the movement and focusing of waves up cusp centres (Figure 40). As waves move up cusp centres along both sides of

the horn, the cusp along the southern side of the horn causes the clasts to have a trend towards the north along the southern side of the horn. In contrast, the cusp centre to the north results in the clasts oriented more to the south along the northern edge of the horn as waves become directed from the cusp sides to the cusp centres. The orientations of the a-axis fabrics and the directions of the imbrications of the a/b planes of the discoids in the grid samples illustrate the same transport regime.

A clast fabric taken on a swash bar had the strongest eigenvalue, 0.813, of all the fabrics taken on the beach. It also had the highest plunge value, 37.7° and the highest K value of 2.99. These statistics suggest a high-energy fluvial environment. However, the orientation of the fabric is 236.7° indicating deposition from seaward flow. This fabric was taken at low tide on a day when wave activity and stream velocities were low. It may be that this strong fabric was formed when flood tidal flow overrode the oscillatory waves and created a unidirectional flow. If an outlet already existed before the flood tidal flow, the flood flow would have been strongest along the sides of the stream, as stream velocities would be higher in the centre of the thalweg. As the tide rose, the stream velocities would decrease as the gradient between the lagoon and sea-level decreased. Undercutting along the sides of the channel would cause slumping of sediment into the channel which could then be remobilized by tidal flow. Weaker ebb flow would have used the existing stream channel and not destroyed the flood deposits.

The strong orientation could also have been created by tidal flow cutting into the barrier and forming an outlet. In this way the faster-moving tidal flow within the cut bank area can create a strong orientation.

Clast fabrics taken from fans which closed the outlet had weaker eigenvalues than along the swash bar, 0.524 and 0.600 and had girdle distributions with K values less than 1. These characteristics are similar to the fabrics taken along the beachface and cannot be used to distinguish between these morphological features on the beach.

6.2.4 *Exposures*

Due to the unconsolidated nature of the sediments, it was impossible to examine extensive lateral and vertical exposures. The seaward open-work pebbles and cobbles in the lower unit along exposure A, examined on 22 August 1991, had a more southerly orientation (164°) and lower plunge (3.9°) than values typical of the beach. The seaward-imbricated pebbles and cobbles that overlay the layer of open-work granules show an overpassing event.

Overpassing, or bed armouring, has been described under conditions of unidirectional flow (eg., Allen; 1983, Everts, 1973; Foley, 1977). Larger-sized particles gain momentum by their high exposure in the boundary layers, become entrained in fast-moving flow, and roll over the underlying smaller clasts. Everts (1973) suggested that the grain size difference between the layers must be small, otherwise the underlying bed would be eroded. In Foley's (1977) and Allen's (1983) descriptions, particle size differences may be large. These models are most applicable to roller- or equant-shaped particles, as these shapes are more likely to roll in traction. The pivoting angles of equants are less than that of angular clasts or imbricated ellipsoids and thus require lower velocity flows for entrainment than the latter types (Komar,

1987; Komar and Li, 1986). However, once in motion, discoid clasts can move easily and rapidly (Allen, 1983).

Isla (1993) proposed an explanation for overpassing in beach environments. During the stronger swash flow, entrainment of mixed-sized sediment distribution is set in motion. During backwash, declining flow velocities favour inverse grading whereby finer particles (sand and granules) become trapped between the larger particles with higher inertia. A point is reached during the initial stages of backwash when the finer particles are deposited and the larger ones roll over them. When bed flow decreases below that necessary to maintain overpassing of the larger particles, deposition of these larger clasts occurs.

In Isla's model, spherical clasts were considered, and the applicability of the model to low-sphericity discs and blades is not discussed. The evidence from Ship Cove, however, indicates that this process likely occurs. The higher flows necessary to initiate movement in imbricated discs and blades would result in higher inertia. With declining flows during the initial stages of backwash, the inertial motion of the imbricated discs and blades may allow them to continue moving landward for a short time.

The infill of sand and granules in this overpassing layer could either result from simultaneous deposition of all clast sizes, or could have filtered down from later overlying deposits not clearly seen in this exposure. Similar processes have been demonstrated in fluvial environments (Frostick *et al.*, 1984; Beschta and Jackson, 1978). Organic matter, mostly seaweed, was present throughout the unit and likely was deposited with the imbricated discs during a high-energy storm event, perhaps resulting in closure of the outlet.

The fabric in this unit (SC-28) is similar to those taken on fans (SC-30 and SC-31) which caused the closure of the outlet. However, as noted above, the fabrics on the fans are not distinct from those taken on cusps along the beachface.

The open-work nature of the imbricated cobble layer in exposure B likely indicates a cusp horn area where kinetic sieving has moved finer materials downward (Orford and Carter, 1982b). It is probable that similar conditions prevailed when units 1 and 3 of exposure C were deposited. The granule infill of unit 2 may have been partly deposited simultaneously with the pebbles and partly by kinetic sieving. These granules may have become trapped within the pebble layer and not moved farther down.

6.2.5 Summary of Sediment Distribution

Given the strong differences between the southern end (zone A) and the northern section (zone C), two types of sedimentation occur on the beach. Zone B is transitional between zones A and C.

Zone A:

The storm berm along the upper-beachface consists of stratified, seaward-imbricated discoid and bladed pebbles and cobbles. The mid- and lower-beach consists of alternating strata of granules and sand overlying roller and equant cobbles.

Zone C (Gravel Barrier):

(1) The crest and backbarrier contain crudely stratified, landward-dipping strongly seaward-imbricated open-work blade- and disc-shaped cobbles. (2) The upper-beachface contains mainly blade- and disc-shaped cobbles, not as well imbricated due to the presence of seaward-dipping steep (20 - 25°) slopes inside cusp centres. This area is characterized by erosional surfaces. (3) The mid-beachface contains stratified seaward-dipping pebbles with higher proportions of roller and equant clasts than on the crest, overlying large cobbles of higher sphericity. This is the most laterally changeable section of the beach, for depositional surfaces alternate with erosional surfaces with cusp development. (4) The lower-beachface in the intertidal zone is composed of stratified beds of imbricated pebbles and sand dipping at 8 - 12°. (5) The outer zone or step contains mainly pebbles and cobbles. (6) Lastly, the nearshore zone is dominated by cobbles and boulders. Table 10 summarizes the sedimentary characteristics of Ship Cove.

These findings are very similar to the characteristics of the barrier at Mutton Bay (Forbes and Taylor, 1987). Both the Mutton Bay and Ship Cove barriers are compartmented by prominent headlands which limit sediment availability by impeding longshore transport. Both barriers are highly reflective and reach similar heights of 5 - 6 m above mean sea-level.

<u>Number</u>	<u>Unit</u>	<u>Zone</u>	<u>Slope</u>	<u>Structure/texture</u>
1	backbarrier	supratidal	8-10° (landward)	stratified, seaward-imbricated; open-work blade and disc cobbles
2	upper- beachface	supratidal	20° (seaward)	erosional surfaces caused by large cusps; mainly blade and discs; poor to chaotic clast orientation
3	mid-beach	supratidal	10-15° (seaward)	stratified imbricated pebbles and cobbles; cusp development; higher percentages of equants and rollers
4	lower- beachface	intertidal	8-12° (seaward)	stratified, imbricated pebbles and sand
5	step	subtidal	4-6° (seaward)	stratified, pebbles and cobbles
6	nearshore	subtidal	5-8° (seaward)	cobbles and boulders

Table 10: Summary of the sedimentary characteristics along zone C, Ship Cove.

Chapter 7

Description of the Barrier System at Big Barasway

7.1 Introduction

The 1.3 km long gravel beach system at Big Barasway consists of two baymouth barrier beaches separated by a 200 m-long vegetated island (Woody Island). The overall shape of this barrier differs from most other barriers along the eastern shore of Placentia Bay, as it forms an undulating seaward arc (Plate 16). The headlands that border the southern end of the beach are flanked by bluffs of unconsolidated diamicton with thicknesses that range between 1 and 5 m overlying bedrock. To the north of Big Barasway, the gravel beach continues for 1.5 km. The shore in this area is flanked by a 70 m high-bluff of unconsolidated diamicton .

A continuous lagoon flanks the landward side of the barrier and is fed by an unnamed stream. The stream enters the lagoon at its northern end, flows south within the lagoonal area for approximately 400 m, and exits into Placentia Bay.

Although the beach overall consists mostly of large pebbles and cobbles, there are lateral differences in morphodynamics and in the sediment shapes and textures. Based on these differences, the beach is divided into four zones: A, B, C, and D, as shown in Figure 7. The sedimentology and morphodynamics of each of these zones initially will be discussed separately.

Following consideration of each zone, a comparative analysis will be presented.

Plate 16: Overview of the barrier at Big Barasway looking south. Zone D is in the foreground. Zone C is to the south of the outlet, followed by zone B, the vegetated section. Zone A is in the background. July 1991.

7.2 Zone A

7.2.1 Morphology

The beach in this zone is aligned SSE-NNW, and is 325 m-long of which the barrier forms the northern 200 m. Fourteen transverse profiles, taken between July 27 and July 30, 1991, are illustrated in Figures 41 - 46. Table 11 lists the azimuth of each transect, the total width, the foreshore and

<u>Transect</u>	<u>Azimuth</u>	<u>Height (m)</u>	<u>Foreshore (m)</u>	<u>Slope (°)</u>	<u>Backshore (m)</u>	<u>Slope (°)</u>	<u>Total Width (m)</u>
BB - 1	263	3.8	21.5	10.0	0.0		21.5
BB - 2	259	3.9	19.0	11.6	0.0		19.0
BB - 3	256	4.0	17.5	12.9	0.0		17.5
BB - 4	254	3.9	17.5	12.6	7.0	6.5	24.5
BB - 5	247	4.0	17.0	13.2	10.0	4.6	27.0
BB - 6	246	4.6	23.5	11.1	20.8	12.5	44.3
BB - 7	250	4.5	24.4	10.4	30.1	8.5	54.5
BB - 8	242	3.6	21.7	8.6	29.9	6.9	51.6
BB - 9	242	3.3	31.3	6.0	54.8	3.4	86.1
BB - 10	242	3.1	38.7	4.6	40.6	4.4	79.3
BB - 11	247	2.6	32.0	4.6	48.7	3.1	80.7
BB - 12	256	2.5	21.1	6.8	39.3	3.6	60.4
BB - 13	253	2.3	19.3	6.8	25.0	5.3	44.3
BB - 14	267	2.3	12.6	10.3	39.0	3.4	51.6

Table 11: Dimensions of the barrier along zone A, Big Barasway.

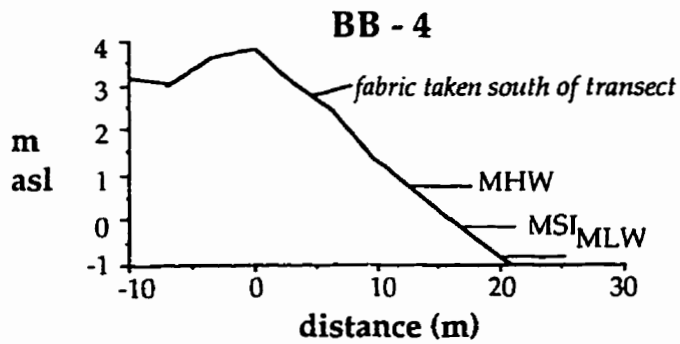
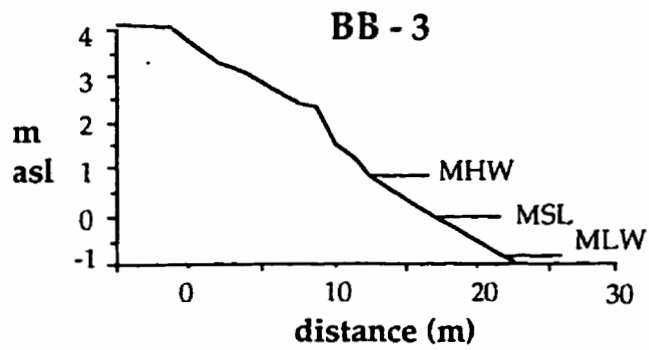
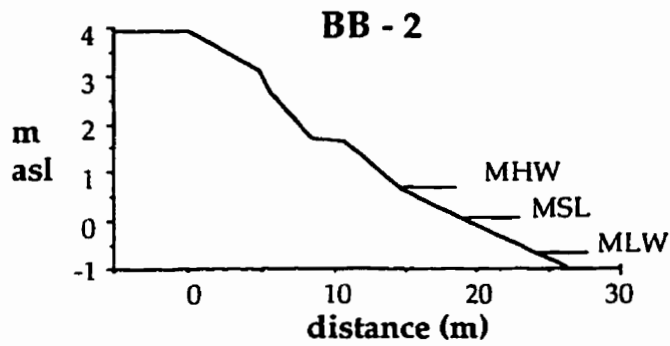
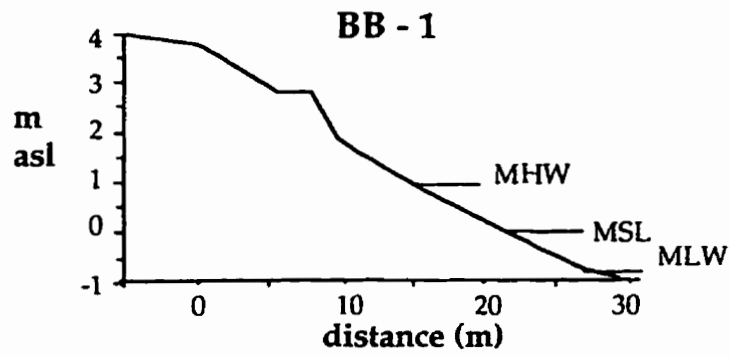
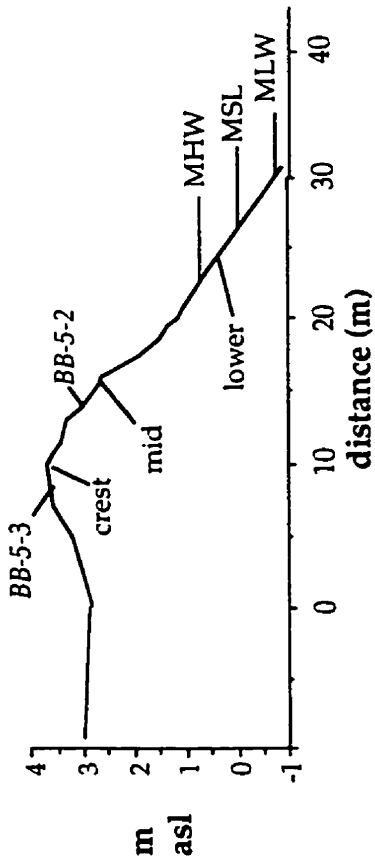


Figure 41: Profiles of transects BB-1 - BB-4;
zone A, Big Barasway

BB - 5



BB - 6

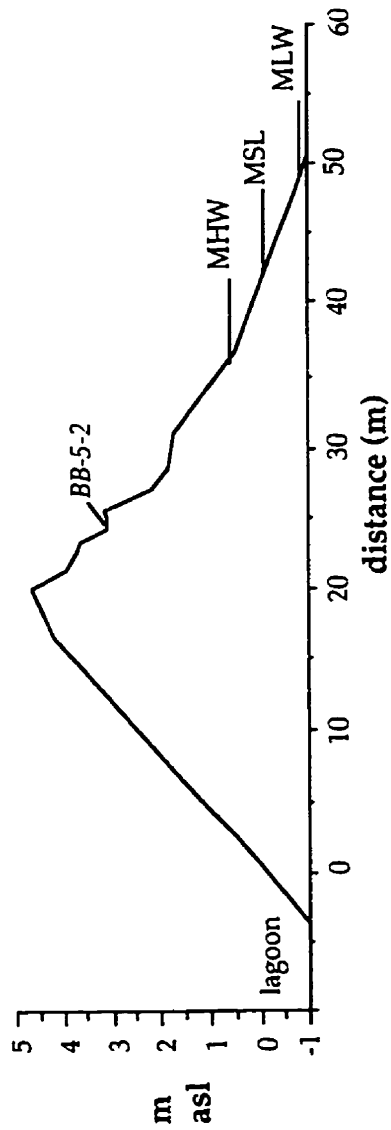


Figure 42: Profiles of transects BB-5 and BB-6; zone A, Big Barasway

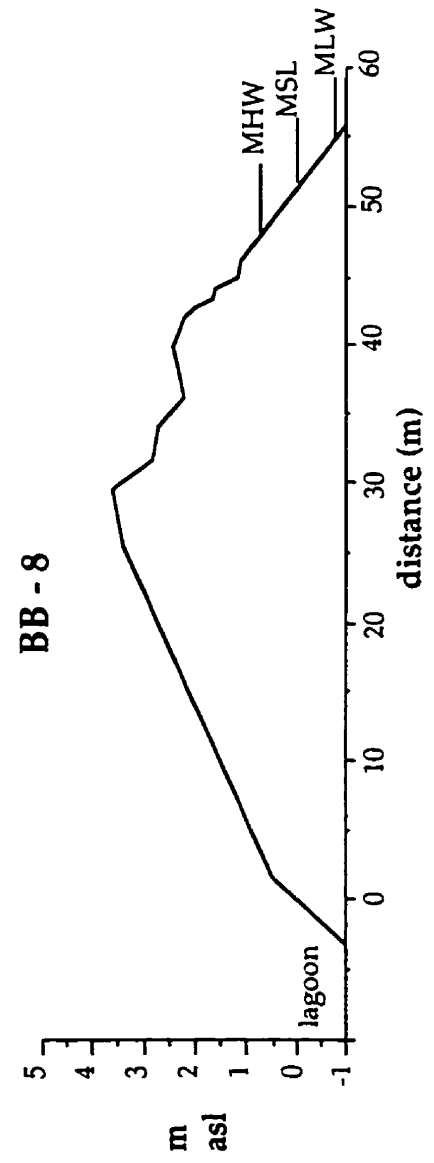
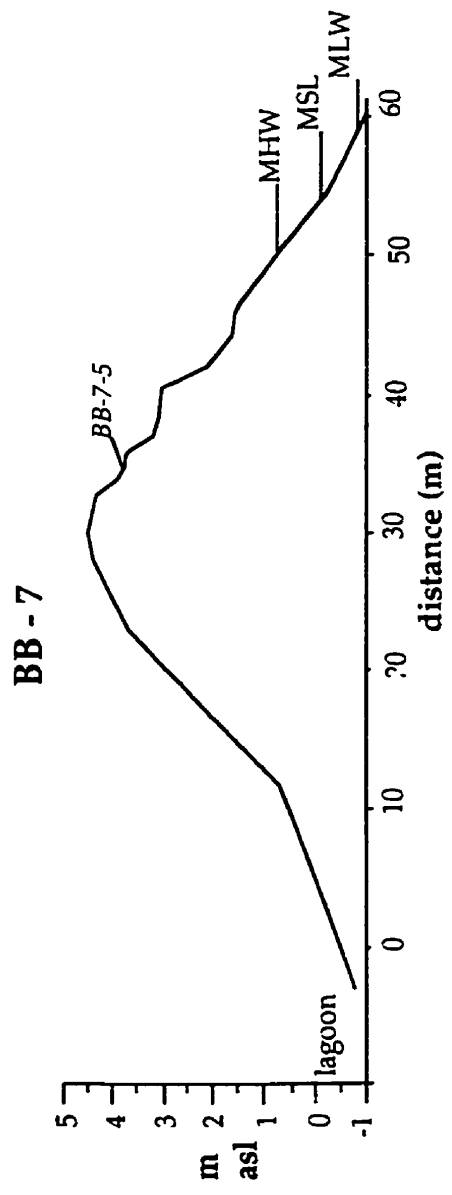


Figure 43: Profiles of transects BB-7 and BB-8; zone A, Big Barasway.

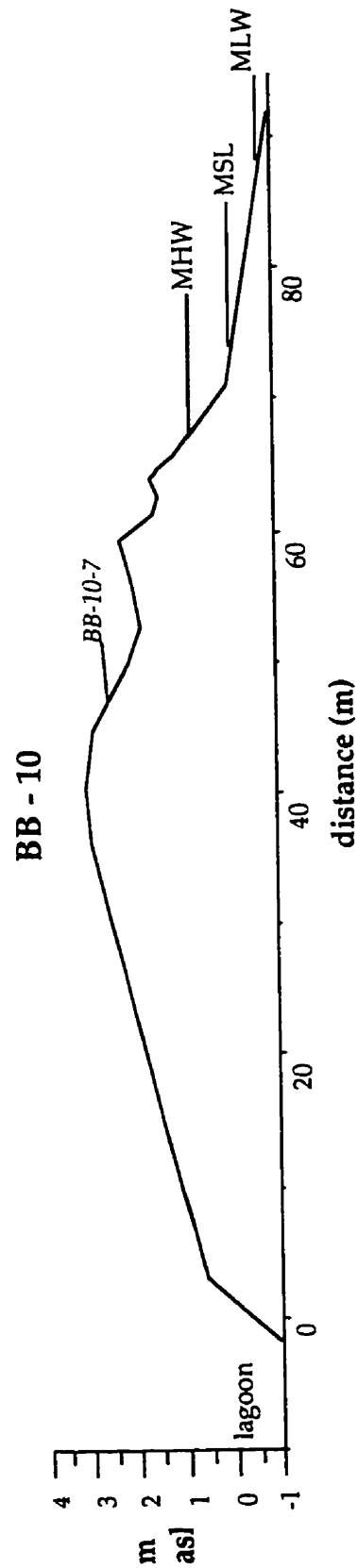
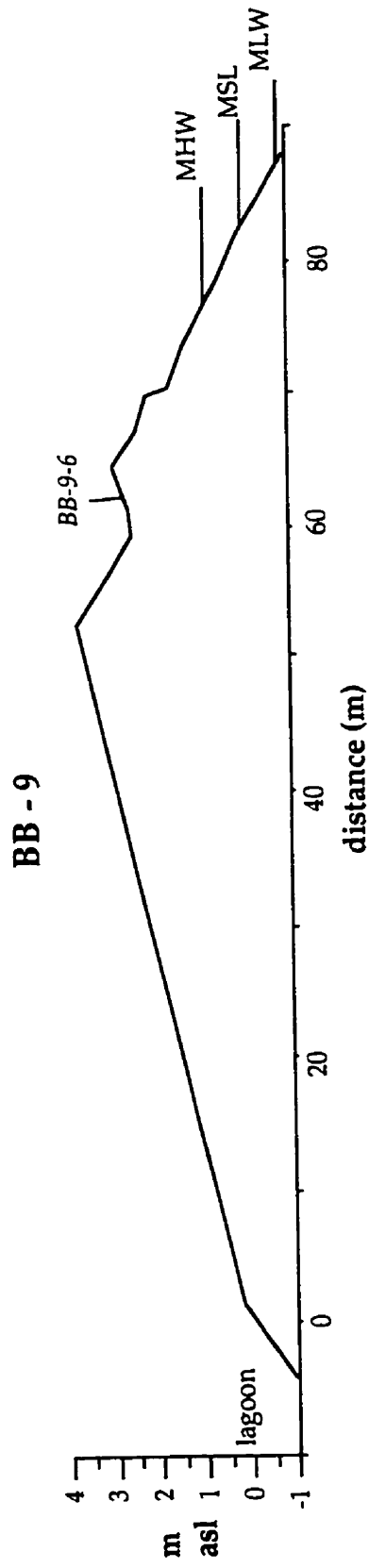


Figure 44: Profiles of transects BB-9 and BB-10; zone A, Big Barasway.

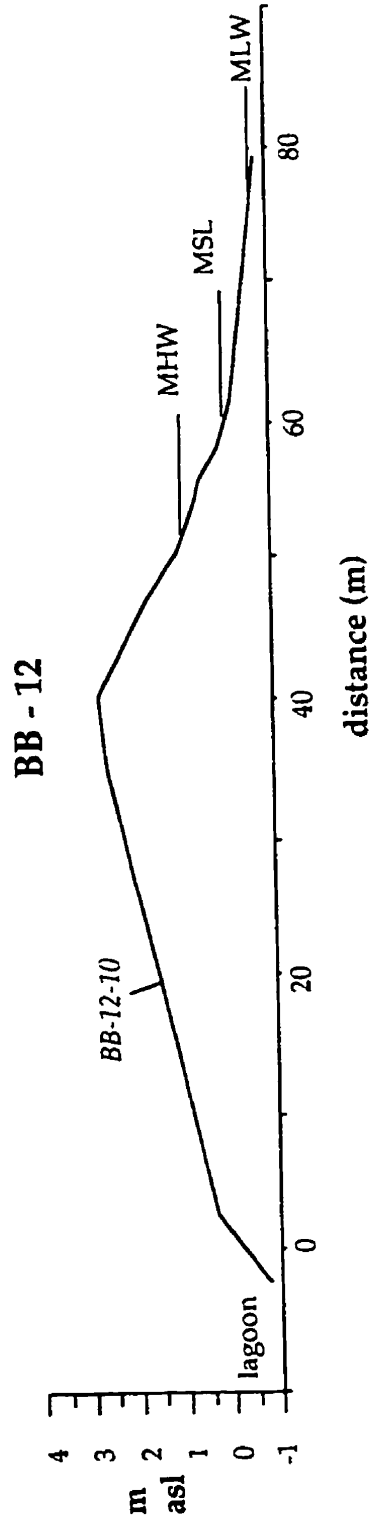
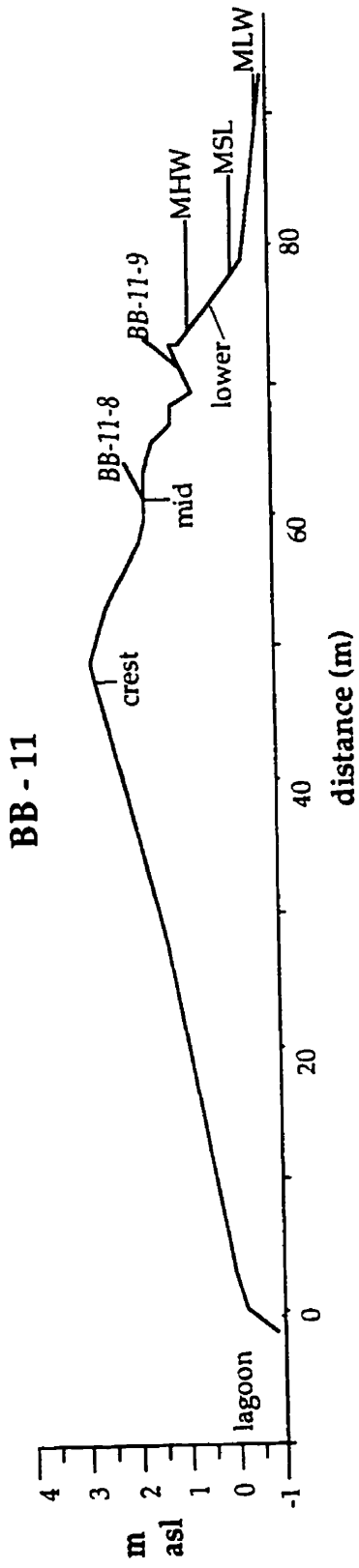


Figure 45: Profiles of transects BB-11 and BB-12; zone A, Big Barasway.

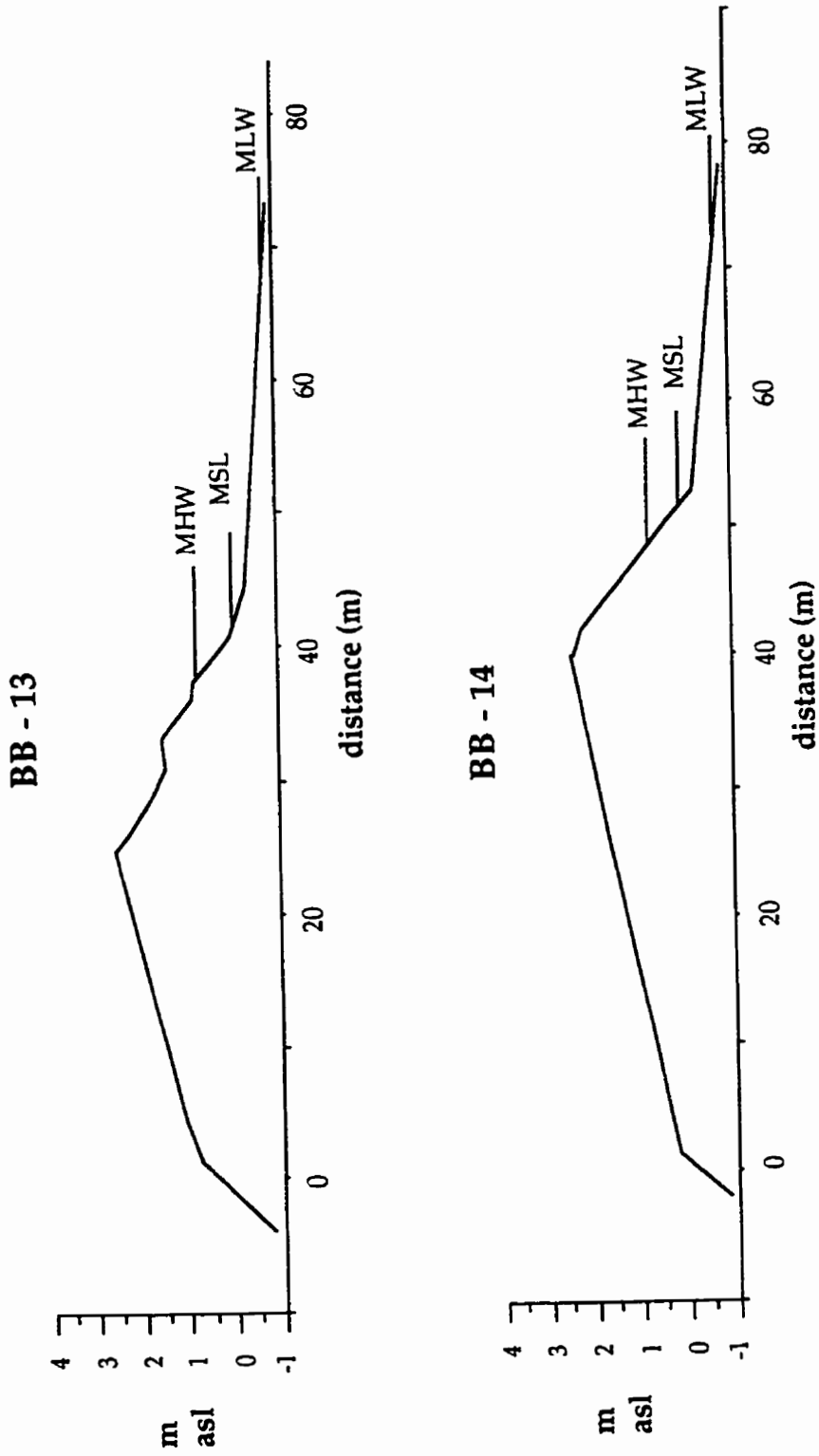


Figure 46: Profiles of transects BB-13 and BB-14; zone A, Big Barasway

backshore widths, the height above mean sea-level, and the overall back and foreshore slopes.

For convenience, zone A is discussed as a single unit, although morphological variations are present. The southern half of the beach, comprised by transects BB-1 through BB-7, is characterized by relatively high elevations (3.8 to 4.0 m asl), and steep foreshore slopes, 10.0° to 13.2°. At the southern end, transects BB-1 through BB-5 are marked by little or no backbarrier area. Consequently, they are narrow in comparison to the other profiles. The lagoon flanks the landward end of transects BB-6 and BB-7. These represent the beginning of the barrier system that continues to the north. These transects have comparatively steep backshore slopes of 8.5° and 12.5°, and the widths of the backshore along these transects are 20.8 and 30.1 m, respectively.

The northern half of zone A, comprised by transects BB-8 through BB-14, is characterized by lower elevations (2.3 to 3.6 m asl) gentler foreshore slopes (4.6° to 10.3°) and gentler backshore slopes (3.1° to 6.9°). The widths of the backshore range between 25 and 54.8 m. Two large overwash fans are present. One fan is located between transects BB-8 and BB-10, and the other is located between BB-11 and BB-13.

The profiles of the transects along the southern half show a storm ridge at approximately 3 m asl. The beachface below this ridge is distinctly concave along transects BB-1, BB-2, BB-6, and BB-7. Transect BB-4 shows a subtle concave shape whereas BB-3 has a more linear shape in this beachface area. These differences are attributable to the presence of cusped features. When measured in July 1991, the transects marked by distinct concave beachfaces

bisected the embayments of cusps. BB-4 was aligned through the margin of a cusp embayment whereas BB-3 traversed the crest of a cusp. The cusps along this segment of beach towards the upper-beachface had wavelengths of 7 - 9 m and heights of 1.2 m. The shape of the mid- and upper-beachface along profile BB-5 shows the presence of large boulders and does not clearly reflect the presence of cusps.

Between 1.5 and 2 m asl, transects BB-2, BB-3, BB-4 and BB-6 show slightly concave lower beach profiles. These shapes show the presence of lower beach cusps with wavelengths of 5 - 6 m and heights of 0.8 - 1 m asl. These concave shapes, however, are not as distinct as those on the upper-beachfaces and show modification by more recent wave activity.

Comparison of the profiles of transects BB-7 and BB-8 reveals a transition between the southern and northern parts of zone A. In addition to the storm berm ridge and the morphological features associated with cusps, a second ridge, below a cusp, is evident at 1.5 m asl in transect BB-7. This represents the initial upshore development of a linear ridge, which became very pronounced between BB-8 and BB-11. North of transect 11, the ridge declines in prominence and does not appear on the profile of transect BB-14.

On transect BB-9, a third linear ridge was evident in summer 1991 at 1 m asl. This ridge became prominent between transects BB-10 and BB-11. To the north of BB-11, this ridge decreases in height and, as in the case of the second linear ridge, was not recorded on transect BB-14 (Plate 17).

In the summer of 1993, a coastal monitoring program was initiated jointly by the provincial Geological Survey Branch and federal Geological Survey of Canada. Two transects were established along zone A. One

(referred to as the boulder site) is located south of transect BB-6 and the second is located along transect BB-10. Figure 47 illustrates the profiles for July, September, and December 1993 and February 1994.

Plate 17: Northward transport of sediment along the northern end of zone A. July 1991.

Gravel cones and depressions, similar to those described by Eyles (1976) at Holyrood Pond, Newfoundland, were observed along the back-beach between transects BB-9 and BB-12 (Plate 18). Also seen were sand/granule ridges leeward of larger clasts. Circular depressions and cones reached 25 cm in width at the base and 15 cm in height. The discoid clasts tended to have a seaward imbrication whereas the other shaped clasts lacked imbrication.

Plate 18: Gravel cones and depressions on the backbarrier along zone A. June 1993.

7.2.2 Morphological Variation

The beach in this zone showed a yearly cyclical pattern in morphology, although deviations from the general trend occurred. During July, August and September, the slope of the beachface increased to 17 - 20° at the southern end and 9 - 12° at the northern end. This was followed by a decrease in foreshore slope and a straight or concave foreshore profile as sediment was moved offshore (Plate 19).

Plate 19: Overview of the southern end of zone A. July 1992.

Figure 48 compares the profiles taken on October 1991 of BB-3 and BB-8 with those taken in July 1991. These two transects show the general trend of morphological change in the southern and northern beach sections.

The profile of BB-8 shows a slight increase in slope. The ridge at approximately 2 m elevation had been pushed landwards and upwards. As well, sediment from the seaward edge of this ridge had been removed. This shows the transition from sediment accumulation to sediment erosion. Prior to July 1991, sediment was pushed landward. Between July and October, sediment removal began. The profile of BB-3 shows removal of sediment and the development of a concave shape for the lower three-quarters of the profile. Although not clearly demonstrated in the profile taken in October,

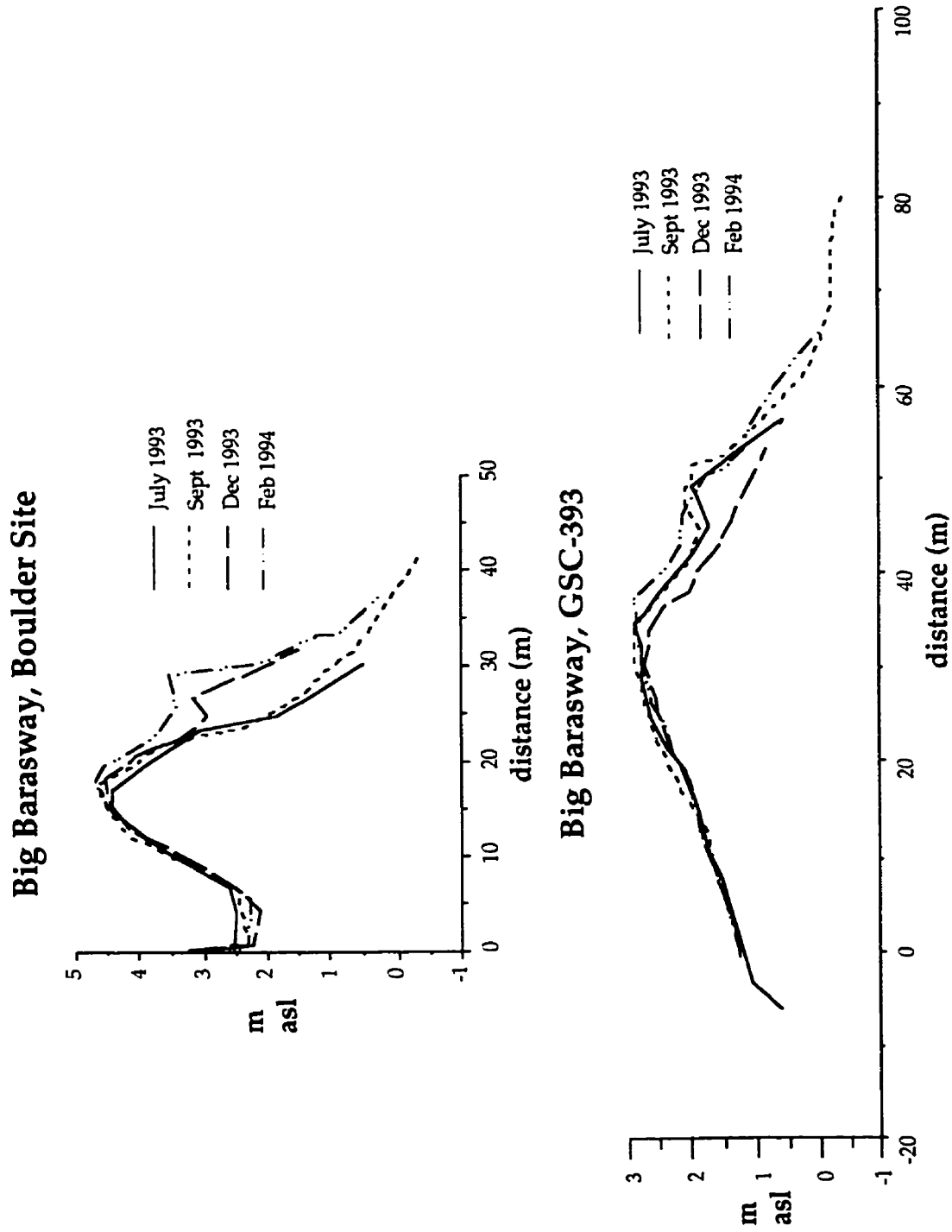


Figure 47: Profiles of Boulder Site and GSC-393 measured July, September and December 1993 and February 1994.

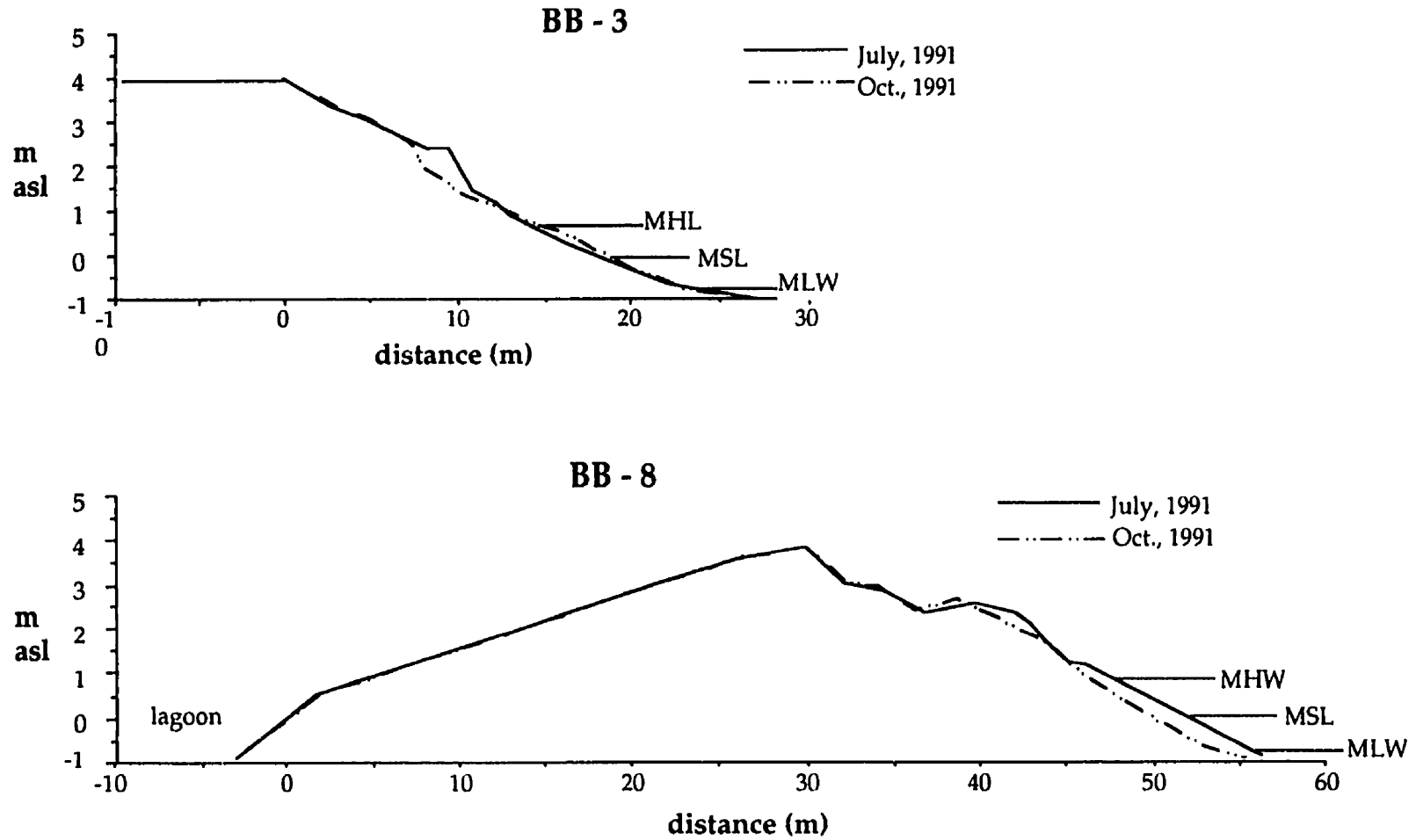


Figure 48: Comparison of profiles of transects BB-3 and BB-8 measured July and October 1991.

the beachface of the southern end had increased in steepness throughout the late summer and early autumn. Sediment removal continues through December although, within this general pattern, episodes of accumulation occur. For example, the GSC profile for the boulder site in December 1993 shows a large accumulation of sediment along a linear ridge that extended along the southern half of this zone.

During the months of mid- to late January through mid-March, a prominent ice foot developed in the mid-beachface area along the length of the beach (Plate 20). The profiles of the boulder site and GSC-393 (BB-10) in February 1994 show the location of the ice foot. Interstitial ice within the sediment and the ice foot itself influence the shape of the barrier. The active area of sediment movement is confined to the intertidal zone. April through June showed an overall sediment accumulation, resulting in more convex beachface profiles.

Two major southwesterly storm events on 25 December 1991 and 15 March 1993 caused extensive removal of sediment throughout the beachface. These events resulted in a distinct concave profile forming at the southern end and formation of a slightly concave to straight profile at the northern end. On 17 March 1993, the sediment removed from the beachface could be seen directly below the low tide mark along the southern end. This resulted in the waves breaking farther (approximately 15 - 25 m) from the shoreline than the average of 5 - 15 m.

Figures 49 and 50 compare profiles of transects BB-3, BB-6 and BB-10 taken in July 1991, December 1992, and June 1993. A cycle of accumulation and erosion is evident in these profiles. The profiles of BB-10 show the

largest transport of sediment as a linear ridge was formed, removed, and re-formed. Although not as dramatic as BB-10, BB-3 and BB-6 show alternating episodes of accumulation and erosion. In particular, a more pronounced concave shape extends from the beach crest to the mid-beachface area on the profiles taken in December, whereas the ones taken in June and July show berm development higher up the beachface.

Overwashing was confined to the northern end. Crestal topping occurred at the southern end but transported little sediment. Although little landward movement of the barrier was observed during the study, comparison of 1948 and 1980 air photos allows estimates of a landward movement of 10 - 25 m (Figure 51).

Plate 20: Ice foot development along zone A. February 1992.

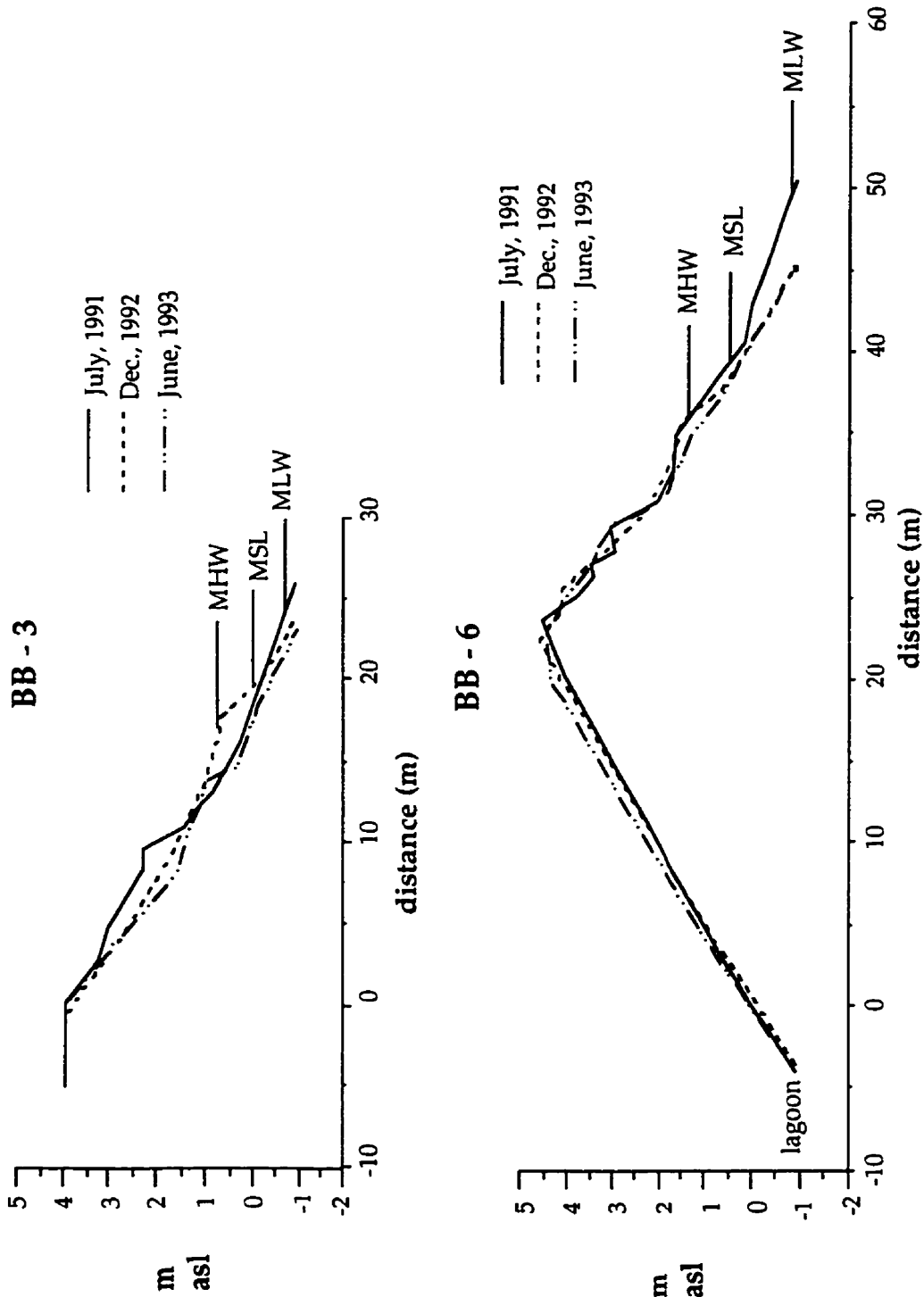


Figure 49: Comparison of profiles of transects BB-3 and BB-6 measured in July 1991, December 1992 and June 1993.

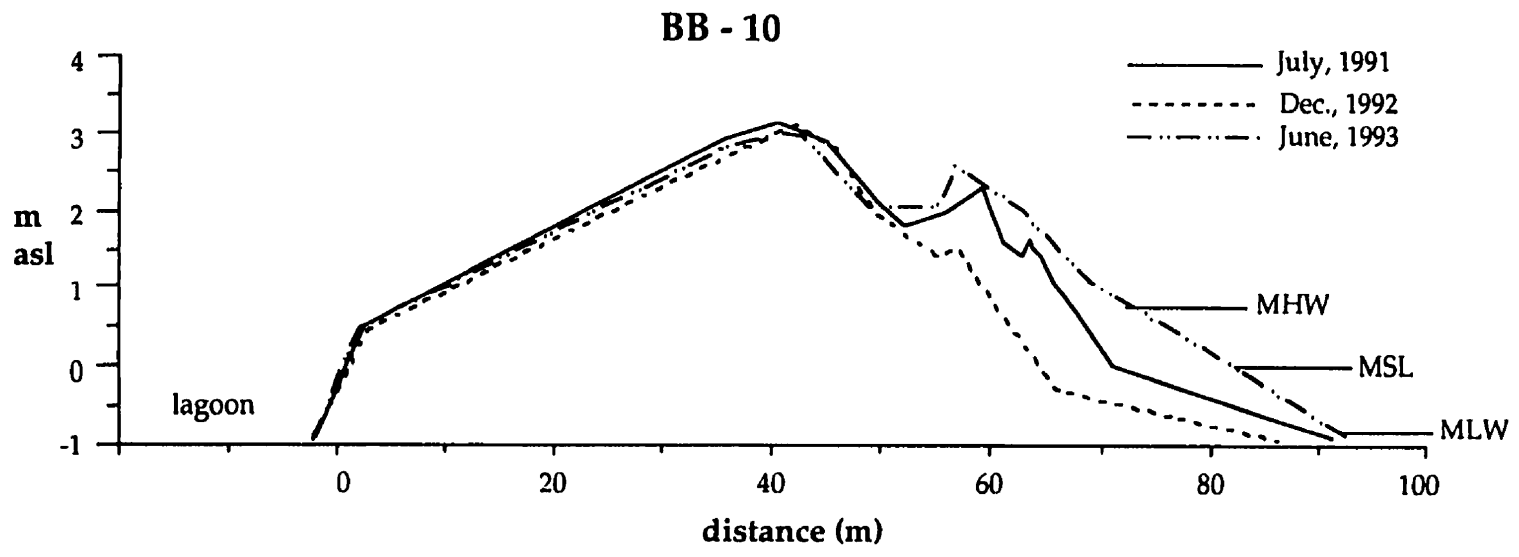


Figure 50: Comparison of profiles of transect BB-10 measured July 1991, December 1992 and June 1993.

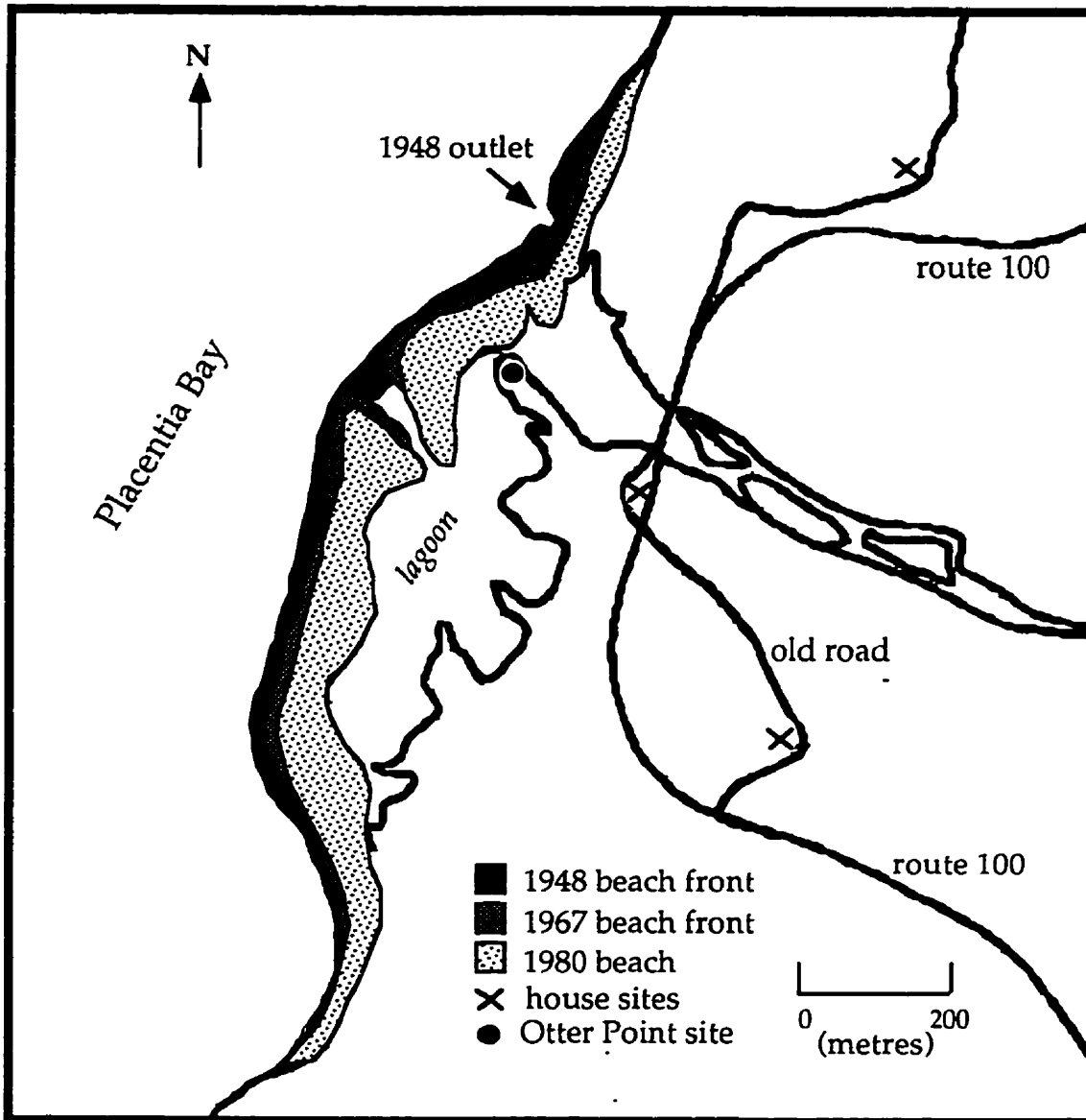


Figure 51: Comparison of 1948, 1967 and 1980 air photos of Big Barasway. Distances were determined from the sites shown. See text for further discussion.

7.2.3 *Clast Lithology*

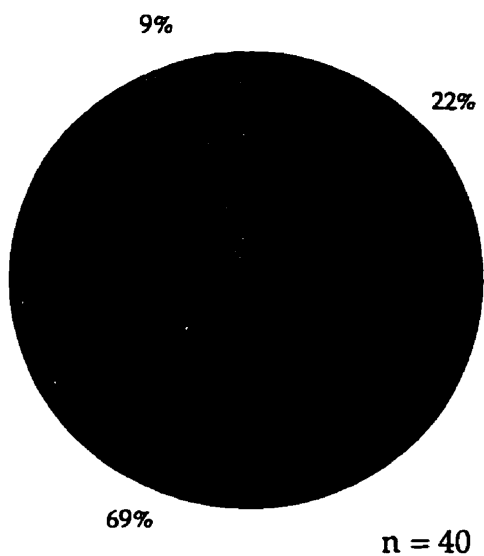
Samples of 40 clasts were taken at the crest and along the lower-beachface to determine the lithology of the beach clasts. The samples were analyzed separately and the results then combined to determine the lithological assemblage of the entire zone. The results are shown in Figure 52. The sample taken at the crest of the beach was composed of 69% sandstone, 22% siltstone, and 9% basalt clasts. In contrast, the sample taken on the lower-beachface contained a large component of igneous clasts (26% basalt, 13% rhyolite, and 6% granite), in addition to sedimentary clasts. Also found were minor amounts of breccia, ironstone, and quartzite. The combined clast lithological data show 66% of the clasts to be siltstone, sandstone, or conglomerate. Volcanic basalt and rhyolite clasts represent 27% of the total assemblage.

7.2.4 *Sediment Texture*

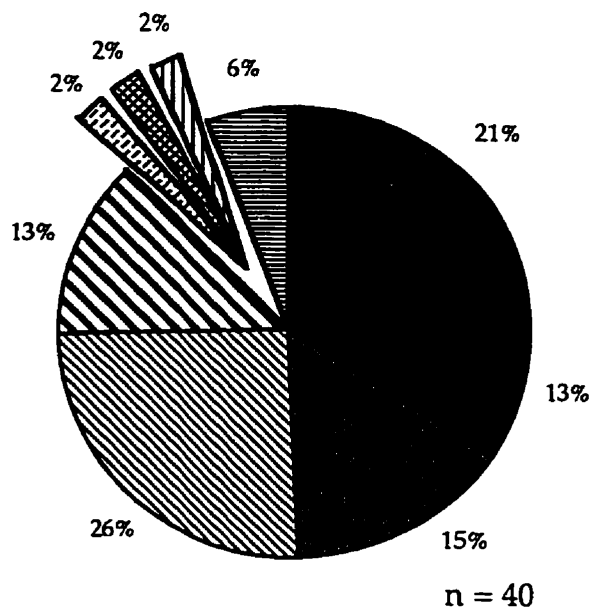
As well as morphological variation, zone A shows textural variations along the length of beach and across individual transects. Along the entire length of the zone, cobbles and boulders dominate the beachface from the subtidal zone to slightly above mean sea-level. The textural analyses involve samples taken above this area.

Figure 53 shows the results of surface texture analyses taken in July 1991. The samples were taken at the lower-beachface above the cobble and boulder step, mid-beachface, and the beach crest along transects BB-5 and BB-11. These transects are representative of the northern and southern sections,

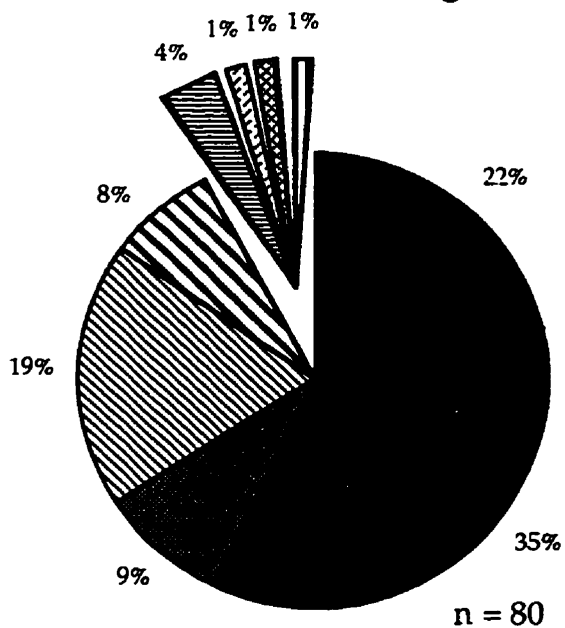
Lithology on Beach Top



Lithology on Lower-Beachface



Combined Lithologies












-  Siltstone
-  Sandstone
-  Conglomerate
-  Basalt
-  Rhyolite
-  Granite
-  Breccia
-  Ironstone
-  Quartzite

Figure 52: Lithologies for zone A, Big Barasway

although sediment texture varied slightly within both sections and the transition between the northern and southern sections is gradational. The sediment texture composition of the crest along BB-11 is similar to that observed along the width of the backbarrier along this transect. BB-11 intersects an overwash fan and thus the textural composition of the crest indicates the composition of an overwash fan.

Transect BB-5, located toward the southern end of the zone, is composed mostly of large pebbles and cobbles. In contrast, BB-11, taken toward the northern end, shows a high percentage of sand, granules, and small and medium pebbles. As in the analysis of the sediment at Ship Cove, the numerical quantities are used to indicate qualitative differences in sediment on the beach. This is then used to interpret differences in barrier morphodynamics.

Along transect BB-5, the proportion of cobbles increases from 2% on the lower beach to 41% midway to 88% at the beach top. BB-11 does not show a distinct increase in grain size with elevation on the beachface. Large percentages of small- and medium-sized pebbles (80%) form the lower-beachface along a linear ridge from which the sample was taken. The mid-beachface sample is dominated by large pebbles, cobbles and boulders (70%). The top shows mainly sand and granules (50%). Additionally, in all samples there is a wide range of clast sizes, from sand to boulders.

With removal of sediment during the fall and winter months, the surface sediment texture along the entire beachface changed. The exposed clasts throughout the width and length of the beachface were dominated by 80 - 90% cobbles and boulders.

7.2.5 *Clast Shape*

Figure 54 shows the results of clast shape analyses for the surface samples at the three sites along transects BB-5 and BB-11. Also shown are the results for the three sites along each transect combined. This gives overall estimated clast-shape distributions for each transect.

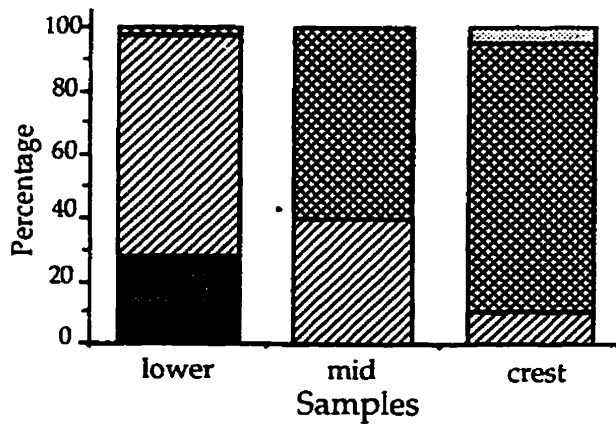
Transect BB-5 shows an increase of discs and a decrease in equants with distance from the seaward edge. In contrast, the relative proportions of clast shapes remain approximately constant along transect BB-11. When the results of the three sites for each transect are combined, no significant change in shape is evident between the clasts of transects BB-5 and BB-11.

Figure 55 shows the histograms for clast roundness and sphericity. Along BB-11, the clasts are less rounded and slightly more spherical than along BB-5. No angular or subangular clasts were present along BB-5.

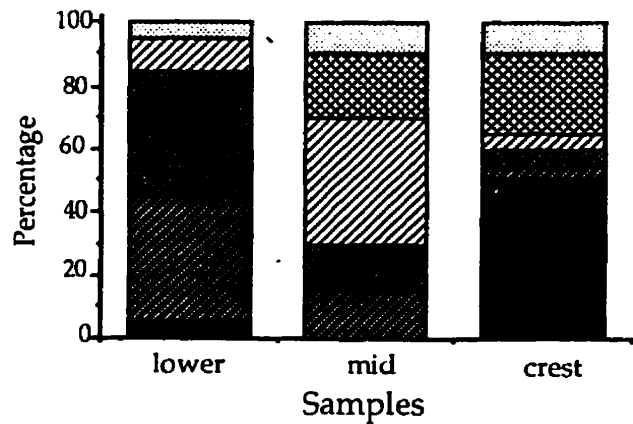
The cobble and boulder-dominated lower-beach step is largely composed of blades, rollers and equants. With removal of sediment during the fall and storm events, the underlying large cobbles and boulders are exposed in the mid-beachface area and show an increase in equants and rollers. In general, the larger clasts show greater sphericity and lower percentages of discs.

With removal of sediment, clast-shape zonations are more pronounced. Discs dominate the upper-beachface and crest while the clasts in the mid- and lower-beach areas are mainly rollers and equants.

Texture, BB - 5



Texture, BB - 11



- Sand/Granules
- Small Pebbles
- Medium Pebbles
- Large Pebbles
- Cobbles
- Boulders

Textures for Selected Transects

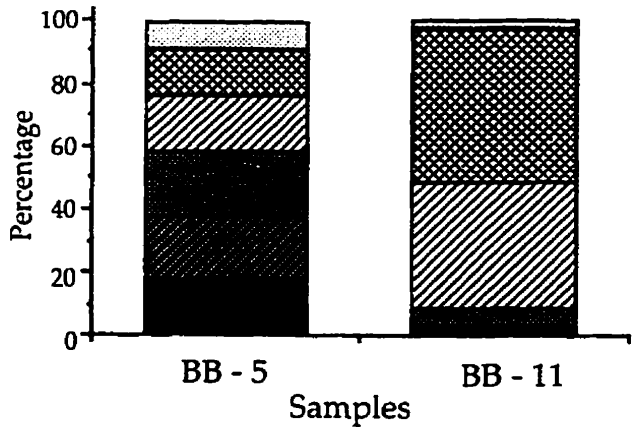


Figure 53: Sediment textures for zone A, Big Barasway.

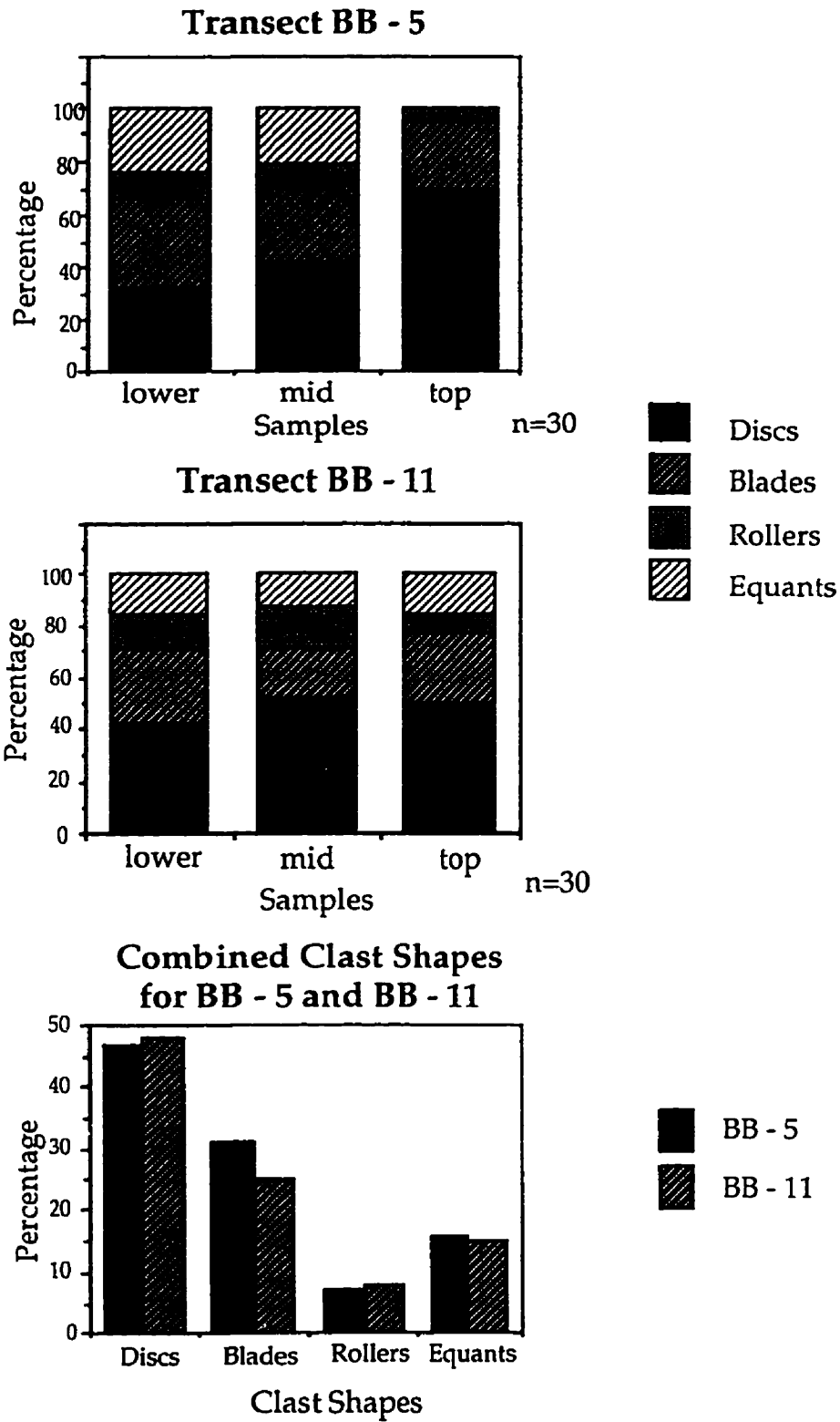


Figure 54: Clast shape analysis for zone A, Big Barasway

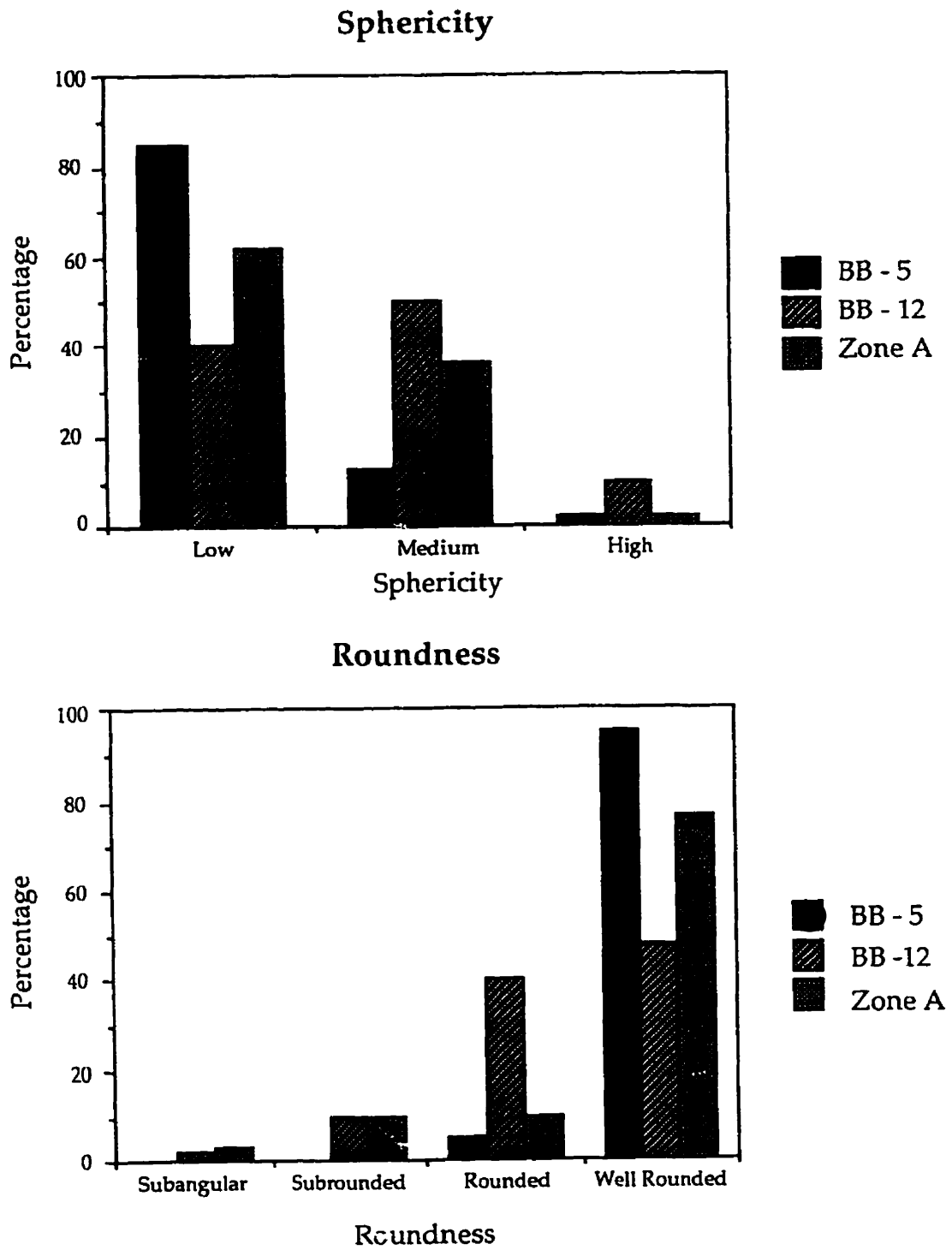


Figure 55: Sphericity and roundness analyses for zone A, Big Barasway.

7.2.6 Fabric Analysis

Ten clast fabrics using the a-axis method were taken on the beach within zone A (Figures 56 - 58). The direction of imbrication of the a/b planes of the discoid clasts ranged between $\pm 45^\circ$ of the transect trend along the southern end and deviated more commonly by $\leq 30^\circ$ to the south of the transect trend along the northern end, although isolated areas in the northern end had deviations to the north of the transect trend. As at Ship Cove, the seaward plunges of the a/b planes generally ranged between 15 - 30°. Table 12 shows the statistics, the transects along which the a-axis fabrics were taken, the transect trend, and the deviation of the fabric trend from the transect trend. Negative values indicate a trend deviation to the north, whereas positive values indicate a trend deviation to the south. The designations of the fabrics indicate the transect along which they were taken.

<u>Number</u>	<u>Trend</u>	<u>Plunge</u>	<u>S1</u>	<u>S3</u>	<u>K</u>	<u>Tran Trend</u>	<u>Deviation</u>
BB-4-1	253.9	33.1	0.653	0.053	0.46	254	0.1
BB-5-2	292.8	7.5	0.550	0.135	0.66	247	-45.8
BB-5-3	291.9	13.2	0.653	0.071	0.64	247	-44.9
BB-6-4	255.2	22.3	0.691	0.065	0.80	246	-9.2
BB-7-5	263.9	16.1	0.617	0.080	0.54	250	-13.9
BB-9-6	296.6	17.7	0.683	0.078	0.93	242	-54.6
BB-10-7	225.9	19.1	0.513	0.065	0.11	242	16.1
BB-11-8	235.1	27.8	0.472	0.093	0.05	247	11.9
BB-11-9	226.8	17.8	0.746	0.036	0.69	247	20.2
BB-12-10	276.3	15.9	0.550	0.063	0.19	256	-20.3
		mean E1	s.d. E1				
south		0.633	0.053				
north		0.593	0.117				
all		0.613	0.088				

Table 12: Clast fabric data for zone A, Big Barasway.

The principal eigenvalues range between 0.472 and 0.746. Fabrics BB-5-2, BB-10-7, BB-11-8, and BB-12-10 with eigenvalues of 0.550, 0.513, 0.472 and 0.550 respectively, are weakly oriented. The other fabrics show moderate to strong orientations. The K values for all the fabrics are less than 1, and thus they represent girdle distributions.

The clast fabrics were taken on different morphological features along the beach. The locations where the fabrics were taken are shown on the profiles of the transects. Fabric BB-4-1 with an S_1 of 0.653, a plunge of 33.1° and a deviation of 0.1° from the transect trend was taken on the centre of a cusp horn.

Clast fabric BB-5-2 with a low plunge value of 7.5° was taken at the base of a steep beach berm scarp. Clasts from the scarp above had fallen into this area. This fabric has a relatively low S_1 of 0.550 and a large deviation of -45.8° from the transect trend. Fabric BB-5-3 was taken on the beach top. Although it has a similar trend to BB-5-2, the plunge of 13.2° and S_1 of 0.653 differ.

Clast fabrics BB-6-4, BB-7-5, and BB-9-6 were located along the landward trough of the linear berm ridge where the beach profiles slope landward. The plunges for these are similar, 22.3°, 16.1° and 17.7°; as are the eigenvalues, 0.691, 0.617, and 0.683 respectively. The trend of BB-9-6 deviates -54.6° from the transect trend, whereas BB-6-4 and BB-7-5 deviate -9.2° and -13.9° respectively.

Fabric BB-10-7 was taken toward the upper-beachface. It has an S_1 value of 0.513, a plunge of 19.1°, and a deviation of 16.1°. Fabric BB-11-8 was taken on a berm located 1 m asl. It has the lowest S_1 value, 0.472, of all the

clast fabrics and a high plunge value of 27.8°. It deviates from the transect trend by 11.9°.

Fabric BB-11-9, taken on a recently formed berm above the high tide mark along transect BB-11, has an S_1 of 0.746, the strongest S_1 recorded in zone A. It has a plunge of 17.8° and deviates from the transect trend by 20.2°.

Clast fabric, BB-12-10, was taken on the back of the barrier. Its plunge, 15.9°, is similar to fabric BB-5-3, also taken at the back of the barrier. BB-12-10 shows a weaker orientation, however, with an S_1 of 0.550. It deviates from the transect trend by -20.3°.

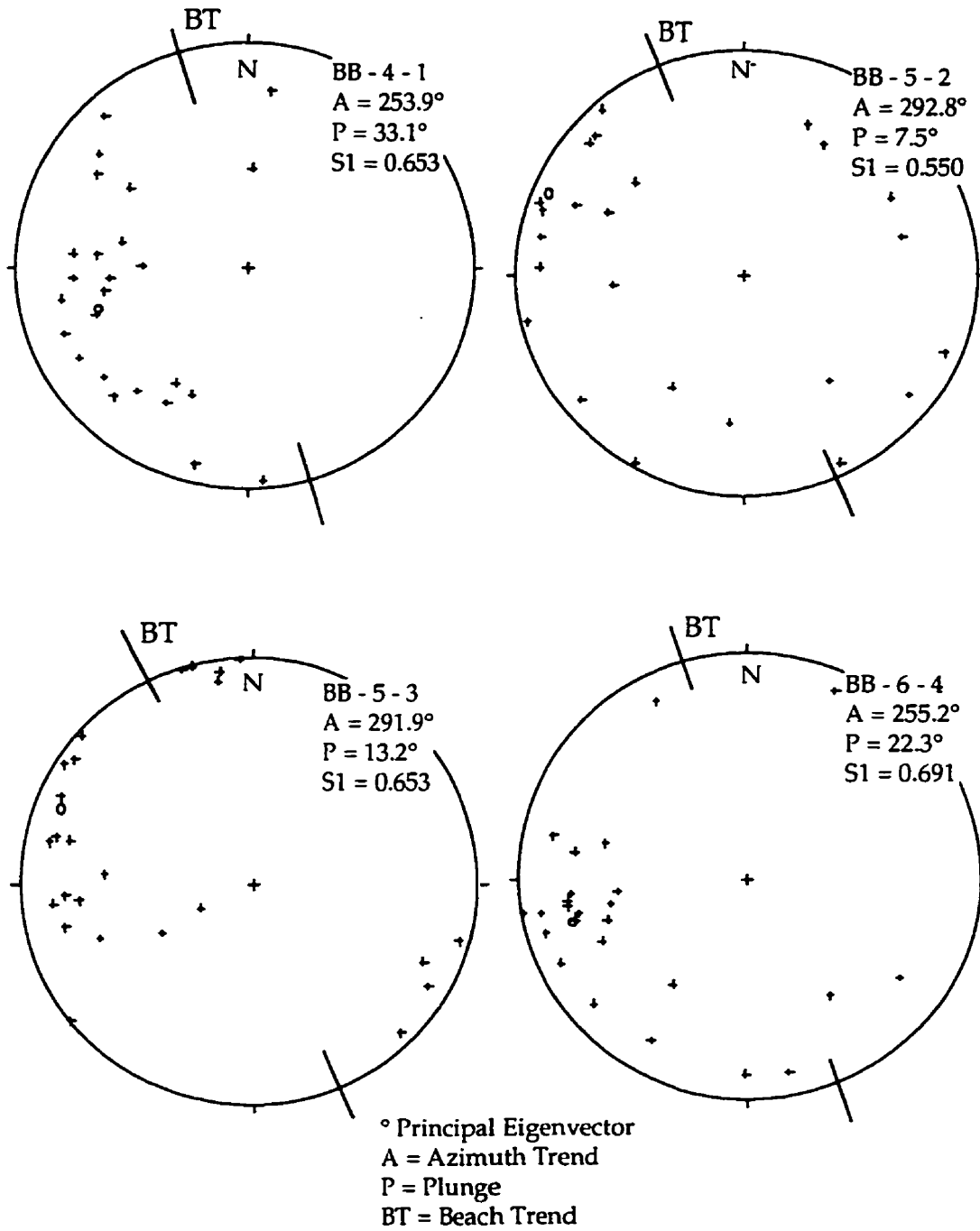


Figure 56: Clast fabrics, zone A, Big Barasway

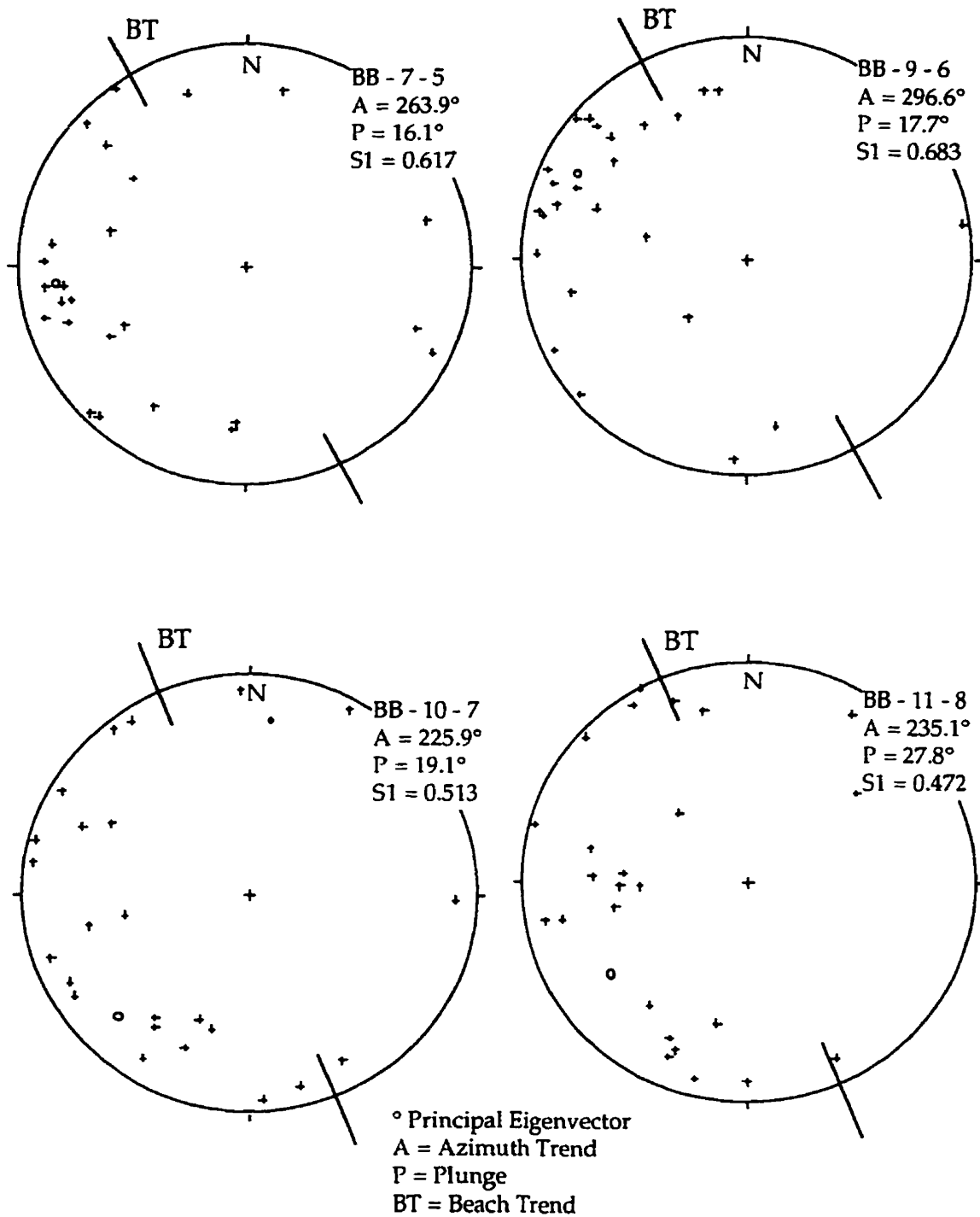


Figure 57: Clast fabrics, zone A, Big Barasway

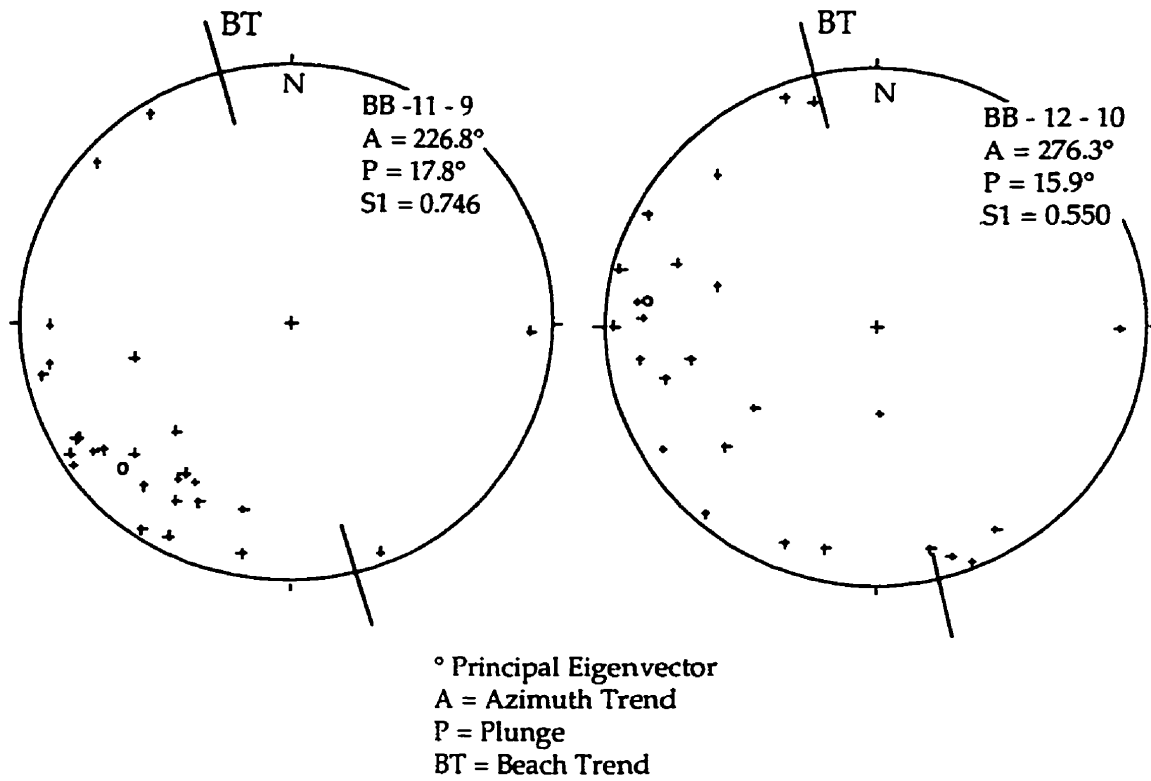


Figure 58: Clast fabrics, zone A, Big Barasway

7.3 Zone B

This zone measures 200 m long (Plate 21). One profile was measured along this stretch of the beach (Figure 59). It has a height of 3 m above mean sea-level and a width of 19.8 m. It has a linear to slightly concave foreshore profile with a slope of 8.5°. This profile is characteristic of the entire length of this zone. Little seasonal variability has been observed. This section of the beach has maintained a linear front throughout seasonal changes during the study. The sediment consists mainly of boulders with an infill of subangular to subrounded granules, pebbles and cobbles. Elongated cusate features extending in a northerly direction indicate a northward transport of sediment.

Plate 21: Overview of zone B. GSC-5319 was taken from the peat bounding the beach. August 1992.

The sedimentary bluff at the back of the beach consists of diamicton ranging between 0.5 to 2.5 m thick, capped by peat. This area is actively eroding, losing between 0.5 to 1 m per year at the seaward edge between 1990 and 1993. Air photos reveal a landward retreat of 10 - 25 m between 1948 and 1980, a rate of 0.3 - 0.8 m per year (Figure 51).

The top of the bluff is vegetated with grasses seaward and spruce landward. Beach clasts are interspersed with vegetation toward the southern end. Cores were taken from three living trees using a Swedish Increment Borer. Counting the tree rings revealed ages of 54, 63 and 88 years. The girths of the trees were 70 cm, 70 cm, and 97.5 cm respectively.

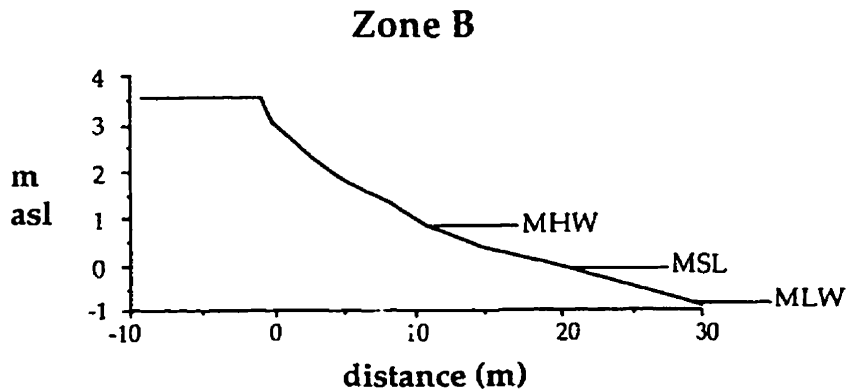


Figure 59: Profile of transect along zone B, Big Barasway.

7.4 Zone C

7.4.1 Morphology

The segment of the barrier representing zone C is 180 m long (Plate 22). The southern half is aligned north-south. The northern half forms a convex-seaward curve from north to east, terminating at the stream outlet. Six transverse profiles, taken on 23 and 24 August 1991, are illustrated in Figures 58 and 59. Transects BB-15, BB-16, BB-17 and BB-18 are spaced 40 m apart, whereas transects BB-18, BB-19 and BB-20 are spaced 20 m apart. Table 13 lists the azimuth, height, foreshore and backshore widths and slopes, and the total width for each transect. The height of the barrier in this section ranges between 3.1 and 3.7 m asl. The total widths range between 33.4 and 67 m. Below mean sea-level there is a gently-sloping (<2°) platform along the northern half. During low tides a lateral bar is exposed along the outlet (Plate 23).

Plate 22: Overview of zone C. July 1991.

<u>Transect</u>	<u>Azimuth</u>	<u>Height (m)</u>	<u>Foreshore (m)</u>	<u>Slope (°)</u>	<u>Backshore (m)</u>	<u>Slope (°)</u>	<u>Total Width (m)</u>
BB - 15	283	3.2	17.5	10.3	22.4	8.1	39.9
BB - 16	274	3.7	15.2	13.7	18.2	11.5	33.4
BB - 17	301	3.6	26.0	7.9	20.5	10.0	46.5
BB - 18	325	3.1	43.2	4.1	23.8	7.4	67.0
BB - 19	350	3.1	38.6	4.6	27.8	6.3	66.4
BB - 20	64	3.1	9.9	17.4	26.6	6.6	36.5

Table 13: Dimensions of the barrier along zone C, Big Barasway.

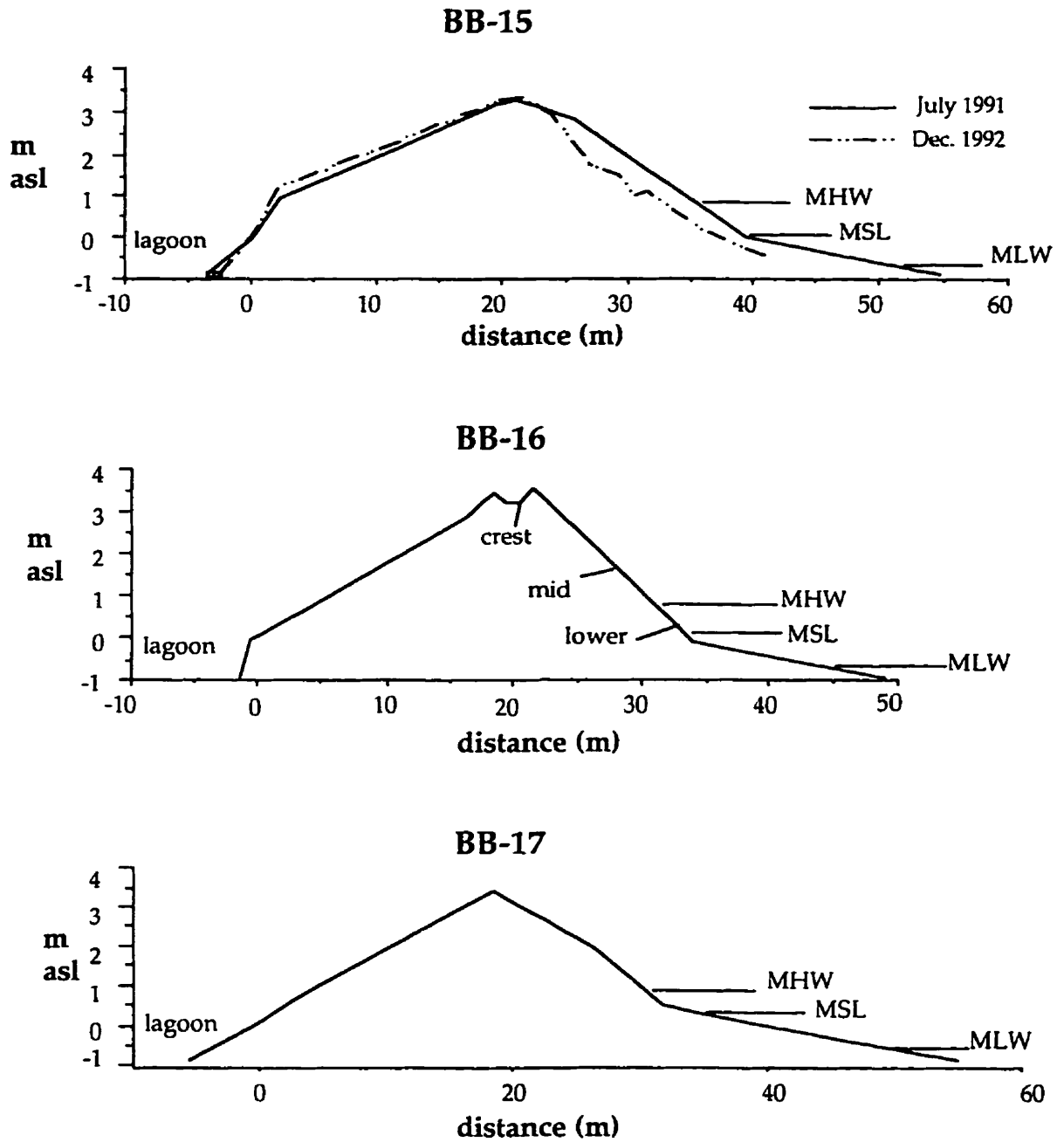


Figure 60: Profiles of transects BB-15 - BB-18, zone C, Big Barasway.

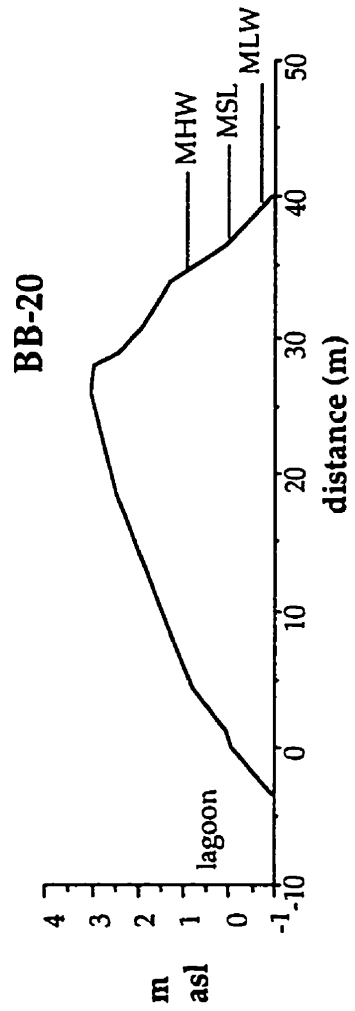
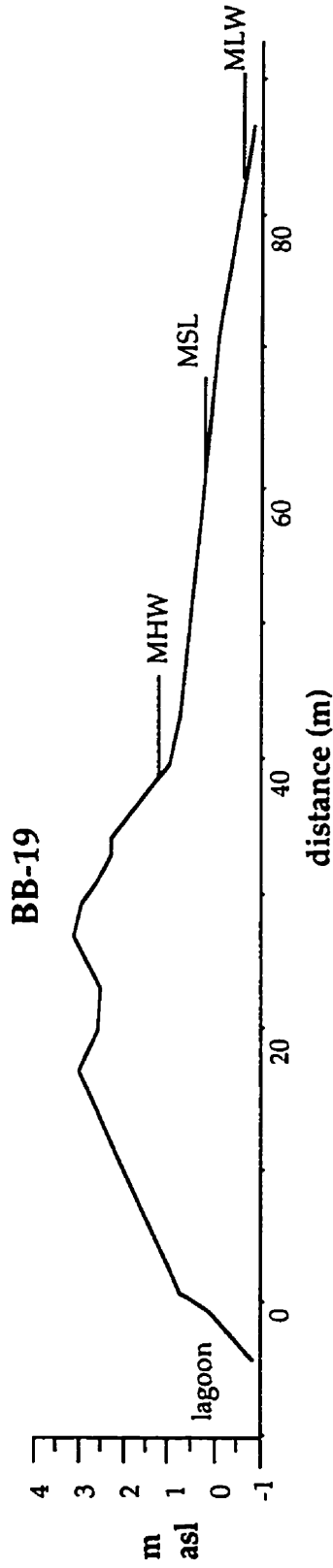
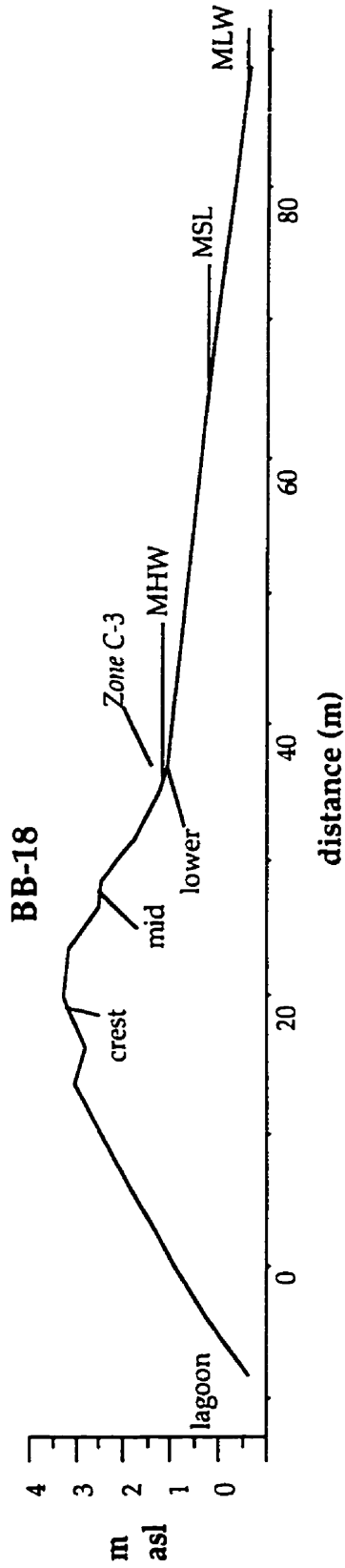


Figure 61: Profiles of transects
BB-18 - BB-20, zone C,
Big Barasway.

Plate 23: Lateral bar along the southern side (zone C) of outlet exposed during low tide. July 1992.

As with zone A, the barrier along zone C shows lateral differences. The southern half, illustrated by transects BB-15 and BB-16, has linear foreshore profiles, with slopes of 10.3° and 13.7° along the respective transects. The backshores are characterized by linear profiles similar to the foreshores, with slopes of 8.1° and 11.5° .

Transects BB-18 and BB-19 have a convex foreshore profile with a linear ridge dominating the mid-beachface. Also present on these two profiles were two pronounced ridges on the top of the barrier. The landward ridge is at a slightly lower elevation than the seaward one.

Transect BB-17 shows a transition between the south and north sections. It has a linear foreshore as do the transects to the south, but the

foreshore slope is gentler at 7.9° The backshore slopes linearly at 10°, similar to the transects to the south.

Transect BB-20 was taken along the margin of the stream outlet. This profile is marked by a relatively short (9.9 m) and steep (17.4°) foreshore. The backshore is similar to transects BB-19 and BB-20 with a width of 26.6 m and a slope of 6.6°.

The barrier in zone C showed only slight profile changes during the duration of the study. Sediment was removed from the southern half during the fall and winter months and the beachface became slightly concave. At the northern end sediment was removed from the mid-beachface ridge. The beach maintained a convex shape throughout the year, however.

Plate 24: Erosion of the barrier near the outlet, zone C. The lateral bar is in the background. July 1992.

The barrier around the outlet is undergoing modification. The stream is eroding the barrier along this zone as it widens in a southerly direction. Approximately 10 m of the length of the barrier was removed between July 1991 and June 1993 (Plate 24). Some of this sediment has been transported landward. A pronounced hook has formed in the backbarrier area of zone C along the southern margin of the stream outlet.

7.4.2 *Clast Lithology*

A sample of 71 clasts taken along the beach crest from zone C contained 48% sandstone, 35% siltstone, 6% conglomerate, 6% basalt, 3% granite, and 3% quartzite. Figure 62 illustrates the lithological analysis. The 88% of sedimentary origin here is similar to the 91% of sedimentary origin along the crest in zone A.

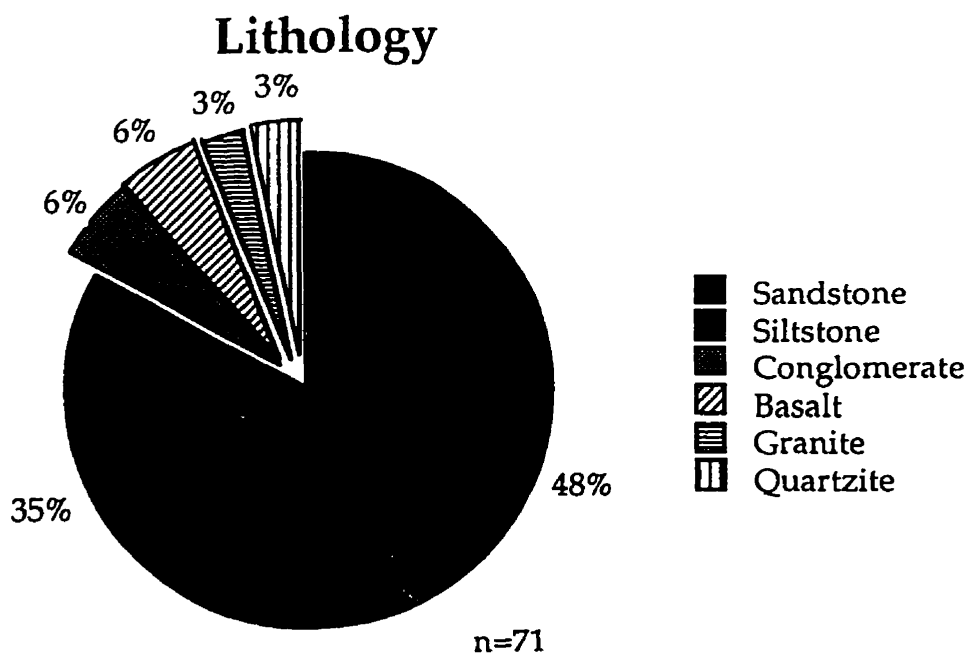


Figure 62: Lithology for zone C, Big Barasway.

7.4.3 *Sediment Texture*

The sediment texture differs between the south and north sections (Figure 63). As with previous sections discussing sediment texture, the numerical quantities are used to indicate general increasing or decreasing of sediment clast sizes. Transect BB-16, typical of the southern section, is composed mostly of boulders and cobbles. Along this transect the relative proportion of boulders and cobbles vary with the lower beach composed of 80% boulders, 10% cobbles and 10% small to large pebbles. The mid-beachface shows an increase of cobbles to 40% and an increase of pebbles to 30%. The barrier top is composed of 70% cobbles, 20% boulders, and 10% pebbles. On the lower slopes of the backbarrier, the texture is marked by a 10% increase of smaller pebbles and granules.

Transect BB-18, typical of the northern segment, contains more pebbles and fewer large clasts. The lower-beachface is composed of 40% boulders, 30% cobbles, 10% small pebbles, and 20% granules. The mid-beachface sample, taken along the ridge, is entirely composed of pebbles, with 20% large, 40% medium and 40% small. The top of the beach contains 40% cobbles, 50% large pebbles, and 10% medium pebbles.

The sediment textures varied relatively little over the duration of the study. In particular, the southern sections of zone C remained essentially unchanged. With removal of small and medium pebbles from the mid-beachface ridge in the northern sections during storm events, larger-sized pebbles were exposed.

Erosion of the barrier along the outlet, exposed a cross-section of the interior stratigraphy. This exposure was located near the top of the barrier,

landward of the ridges shown on profiles BB-18 and BB-19. It measured 30 cm in height. The sediment was loose and unstable, precluding further excavation. The section, illustrated in Figure 64, consisted of 5 - 8° landward dipping planar beds. The lowermost exposed stratum consisted of open work pebbles and cobbles with granules infilling the voids. This stratum was successively overlain by 2.5 cm of granules, a 3.5 cm bed of small- and medium-sized pebbles, 1.5 cm of granules and small-sized pebbles and 4.0 cm of granules. Capping the sequence was a cobble stratum with a granule infill.

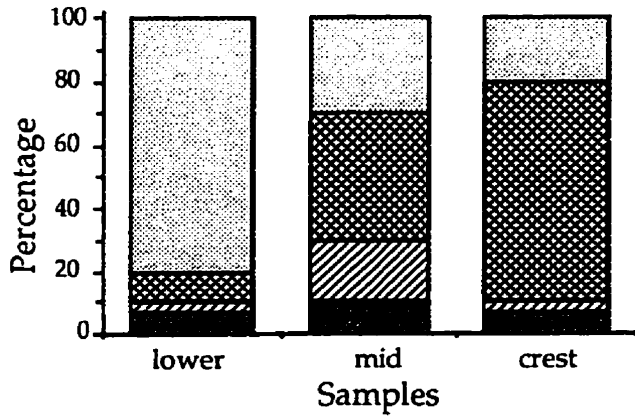
7.4.4 *Clast Shape*

Figure 65 illustrates estimates of the overall clast shape analysis for three sites along transects BB-16 and BB-18. The lower site of BB-16 showed 33% discs, 31% blades, 3% rollers and 33% equants. The mid-beachface site contained 33% discs, 37% blades, 4% rollers and 26% equants, whereas the beach crest showed 37% discs, 50% blades, 0% rollers and 13% equants.

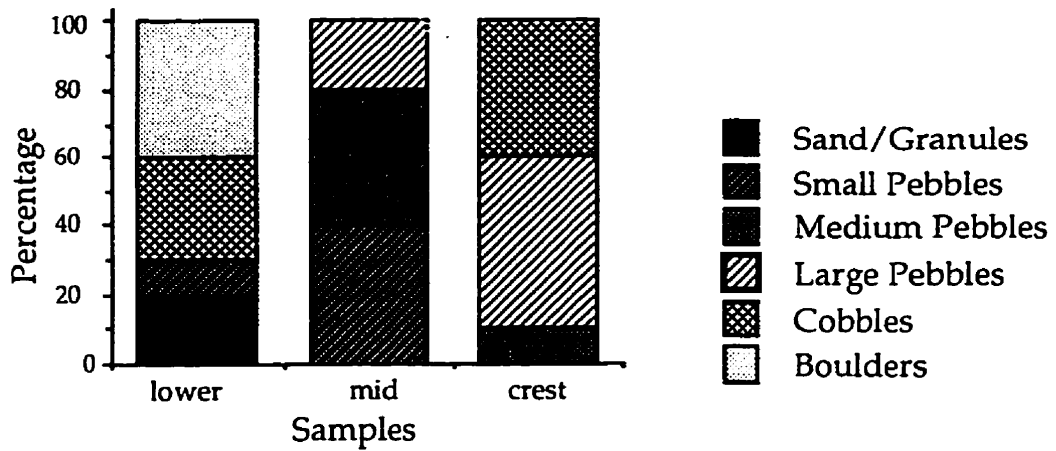
The lower site of BB-18 was composed of 29% discs, 42% blades, 19% rollers and 10% equants. The mid-beachface contained 48% discs, 48% blades and 4% equants, whereas the top was composed of 52% discs, 30% blades, 4% rollers and 15% equants. Along both transects the proportion of rollers and equants was significantly less on the crest than on the lower- and mid-beachface.

The roundness and sphericity change between the north and south sections. The clasts to the south near zone B were largely angular to subangular with moderate to high sphericity. In contrast, clasts to the north are subangular to subrounded with low to moderate sphericity. In addition,

Texture, BB-16



Texture, BB-18



Textures for Selected Transects

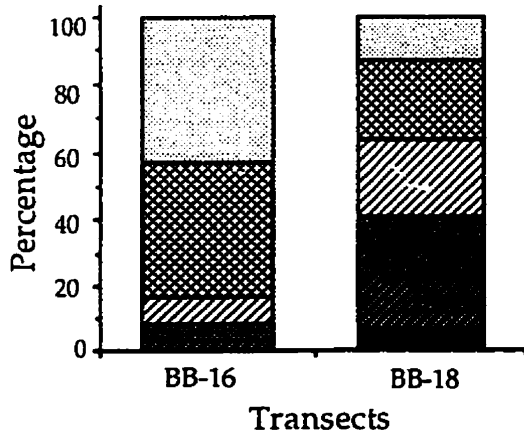


Figure 63: Sediment texture for zone C, Big Barasway.

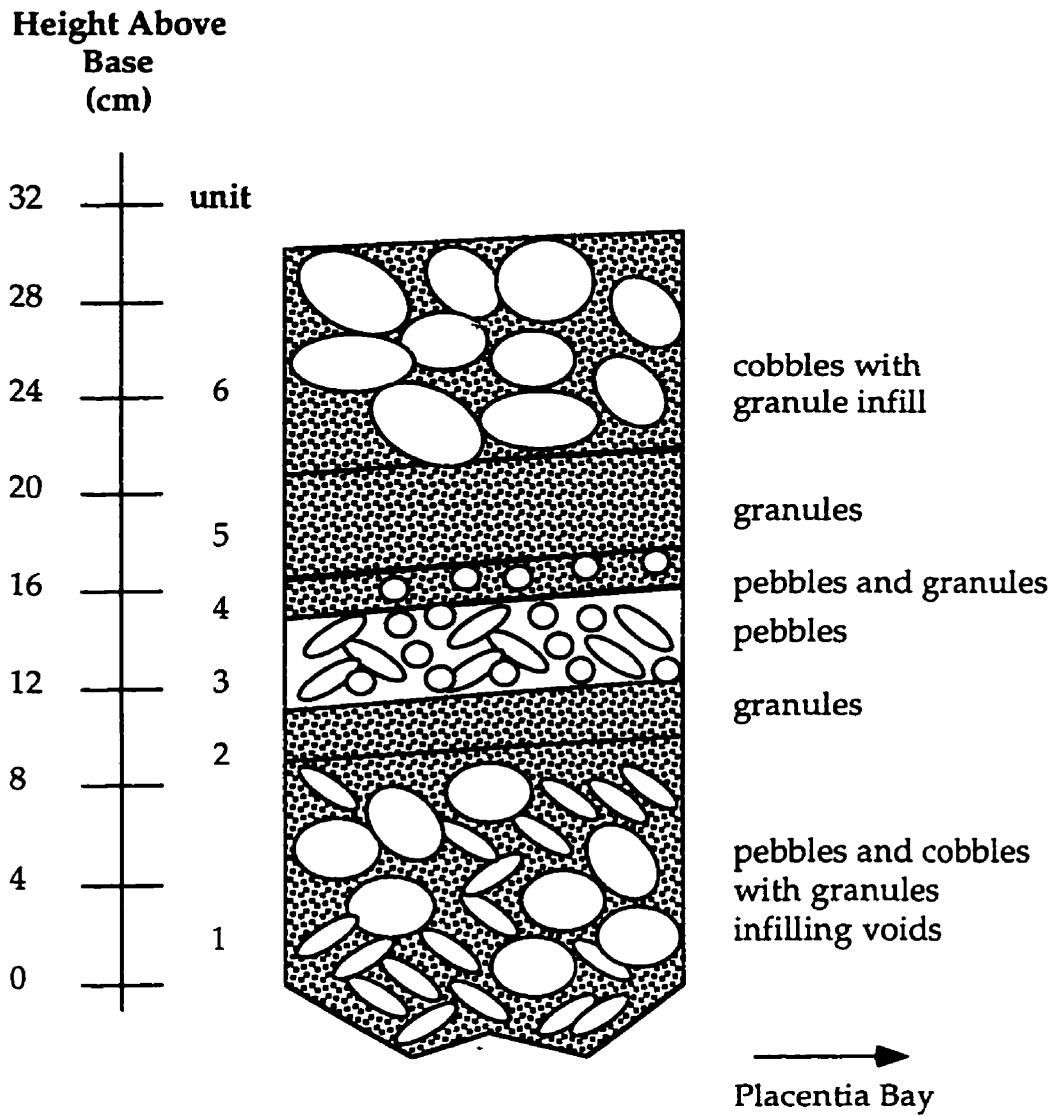
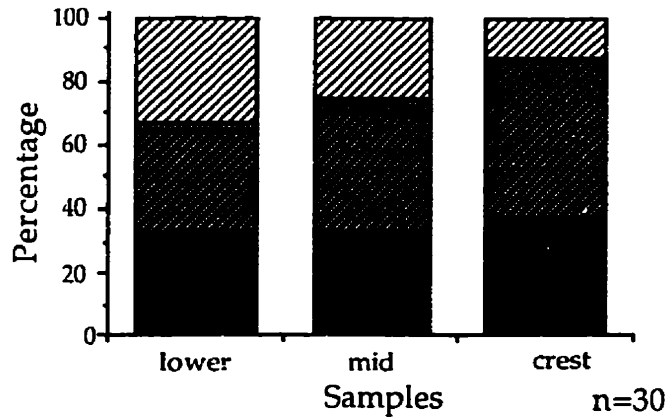
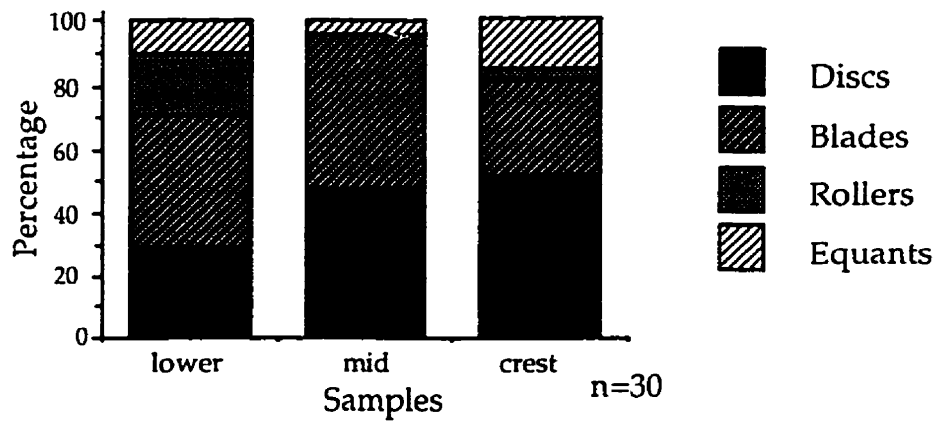


Figure 64: Exposure, zone C, Big Barasway.

Clast Shapes, BB-16



Clast Shapes, BB-18



Clast Shapes for Selected Transects

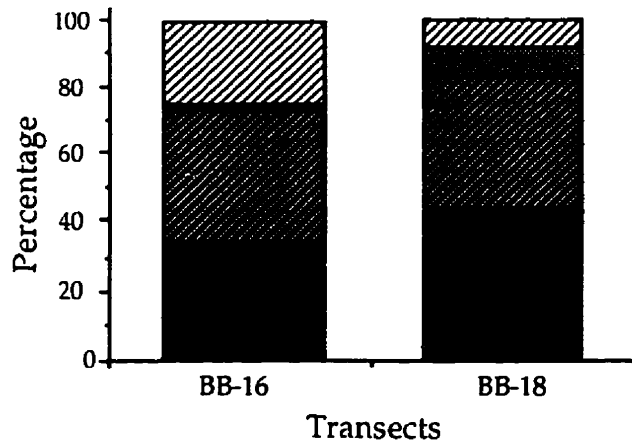


Figure 65: Clast shape analysis for zone C, Big Barasway.

combining the shape compositions for the three samples along each transect reveals a decrease of rollers and equants from 26% at BB-16 to 17% at BB-18.

7.4.5 Fabric Analysis

Three a-axis clast fabrics were taken from this zone (Table 14, Figure 66). The imbrication of the a/b plane of the disc component of the sample sites were noted. Clast fabric C-1 was taken on the lateral bar during low tide. It has an azimuth of 320.1° and a plunge of 13.5° (seaward). The S_1 is 0.619 and the K value is 0.22.

Clast fabric C-2 was taken within the pebble and cobble lower layer of the exposed section along the bank. This yielded an azimuth of 104.8° and a plunge of 9.2° (landward). The S_1 is 0.596 and the K value is 0.23.

Clast fabric C-3 was taken at the base of the barrier along transect BB-19. It has an azimuth of 007° which is a 17° deviation from the transect azimuth, and a plunge of 15.9°. It has an S_1 of 0.720 and a K value of 0.5.

<u>Number</u>	<u>Trend</u>	<u>Plunge</u>	<u>S1</u>	<u>S3</u>	<u>K</u>	<u>Tran Trend</u>	<u>Deviation</u>
Zone C-1	320.1	13.5	0.619	0.027	0.22		
Zone C-2	104.8	9.2	0.596	0.043	0.23		
Zone C-3	7.0	15.9	0.720	0.030	0.50	350	-17

Table 14: Clast fabric data for zone C, Big Barasway.

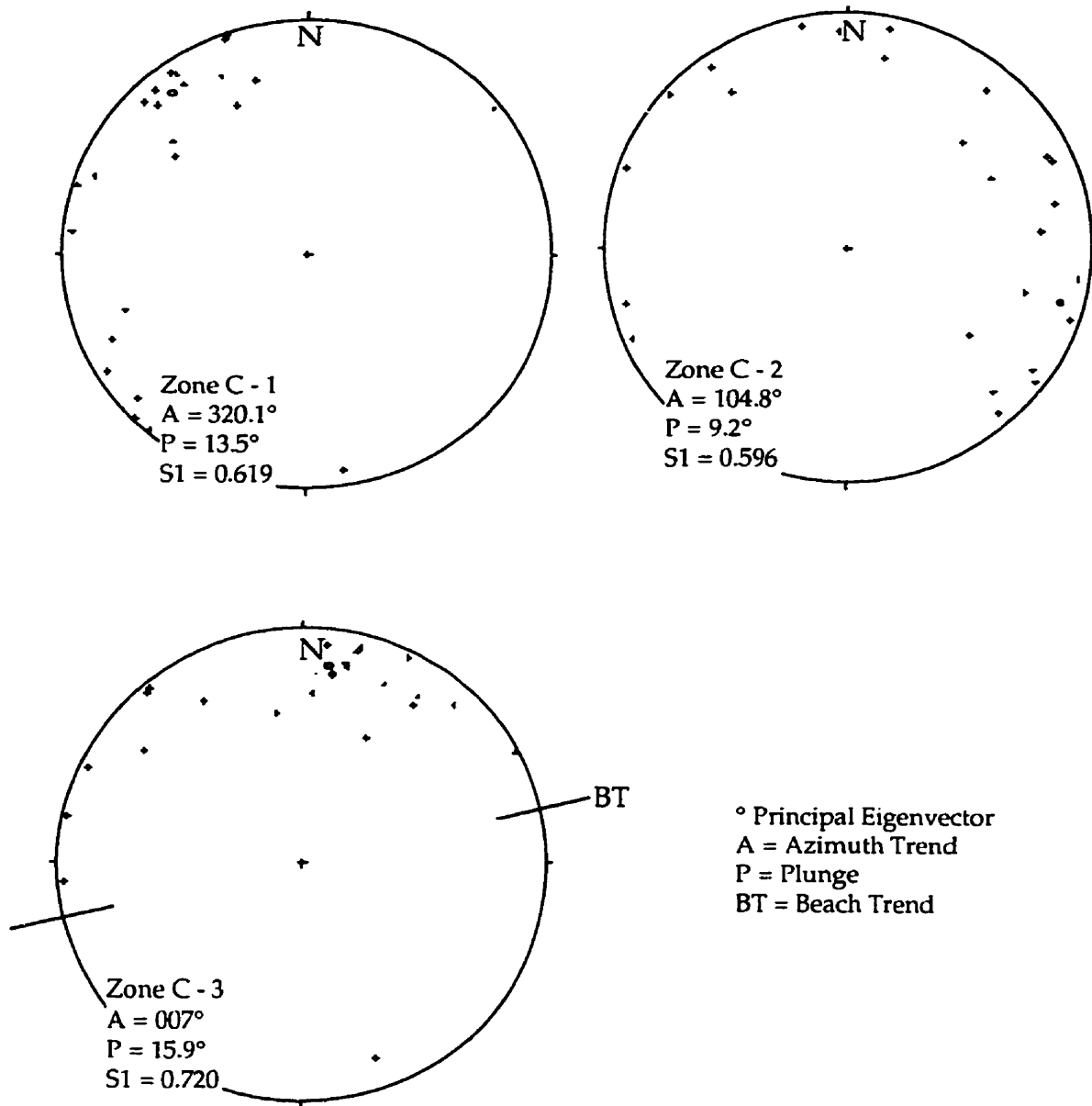


Figure 66: Clast fabrics, zone C, Big Barasway.

7.5 Zone D

7.5.1 Morphology

This segment of the beach is 420 m long. Heights range between 3 and 3.5 m asl. The outlet bounds this zone to the south. To the north a beach extends 1.5 km at the base of a 70 m high bluff of diamicton. Twenty transverse profiles spaced 20 m apart, taken in July 1991, are illustrated in Figures 67 - 74. Table 15 lists the azimuth, the height, foreshore and backshore widths and slopes, and the total width for each transect. The lagoon extends north from the outlet to south of transect BB-38. Transects BB-38 through BB-40 have minor or no backshores.

For convenience, the morphology will be discussed in four sections. The first, most southerly section near the outlet, is comprised by transects BB-21 to BB-24. The second section consists of transects BB-25 to BB-29. The third consists of transects BB-30 to BB-34, and the fourth and most northerly section, is comprised by transects BB-35 to BB-40.

A sinusoidal shape characterized the southern section as the N-S trend at BB-21 curves toward a SSW-NNE trend at BB-22, and back to N-S trend at transects BB-23 and BB-24. During July 1991, the foreshore slopes ranged between 8.7° and 13.6°, whereas the backshore slopes ranged between 9.9° and 12.6°. The overall widths ranged between 25.8 and 36.7 m. On the crest and back beach area, *Cakile edentula* (sea rocket), *Lathyrus japonicus* (beach pea), and *Mertensia maritima* (sea mertensia) grow during the summer and cover approximately 5% of the crest and backbeach area in this section. Little or no vegetation was seen along zones A and C.

<u>Transect</u>	<u>Azimuth</u>	<u>Height (m)</u>	<u>Foreshore (m)</u>	<u>Slope (°)</u>	<u>Backshore (m)</u>	<u>Slope (°)</u>	<u>Total Width (m)</u>
BB - 21	266	3.1	17.2	10.2	16.1	10.9	33.3
BB - 22	290	3.0	18.2	9.4	16.1	10.6	34.3
BB - 23	278	3.0	12.4	13.6	13.4	9.9	25.8
BB - 24	264	3.0	19.5	8.7	17.2	12.6	36.7
BB - 25	292	3.1	45.4	3.9	20.6	8.6	66.0
BB - 26	311	3.3	55.1	3.4	18.2	10.3	73.3
BB - 27	340	3.4	46.2	4.2	18.2	10.6	64.4
BB - 28	330	3.3	44.1	4.3	19.6	9.6	63.7
BB - 29	333	3.2	37.4	4.9	25.9	7.0	63.3
BB - 30	327	3.4	22.2	8.7	21.9	8.8	44.1
BB - 31	330	3.0	18.2	9.4	19.8	8.6	38.0
BB - 32	329	3.4	18.6	10.7	52.5	3.7	71.1
BB - 33	333	3.5	19.5	10.2	40.1	5.0	59.6
BB - 34	315	3.2	18.0	10.1	27.2	6.7	45.2
BB - 35	309	3.1	20.9	8.4	14.7	11.9	35.6
BB - 36	299	3.2	19.4	9.4	15.6	11.6	35.0
BB - 37	297	3.5	24.5	8.1	13.9	14.1	38.4
BB - 38	296	3.3	14.6	12.7	22.6		37.2
BB - 39	296	3.3	24.8	7.6	7.0		31.8
BB - 40	300	2.8	19.4	8.2	0.0		19.4

Table 15: Dimensions of the barrier along zone D, Big Barasway.

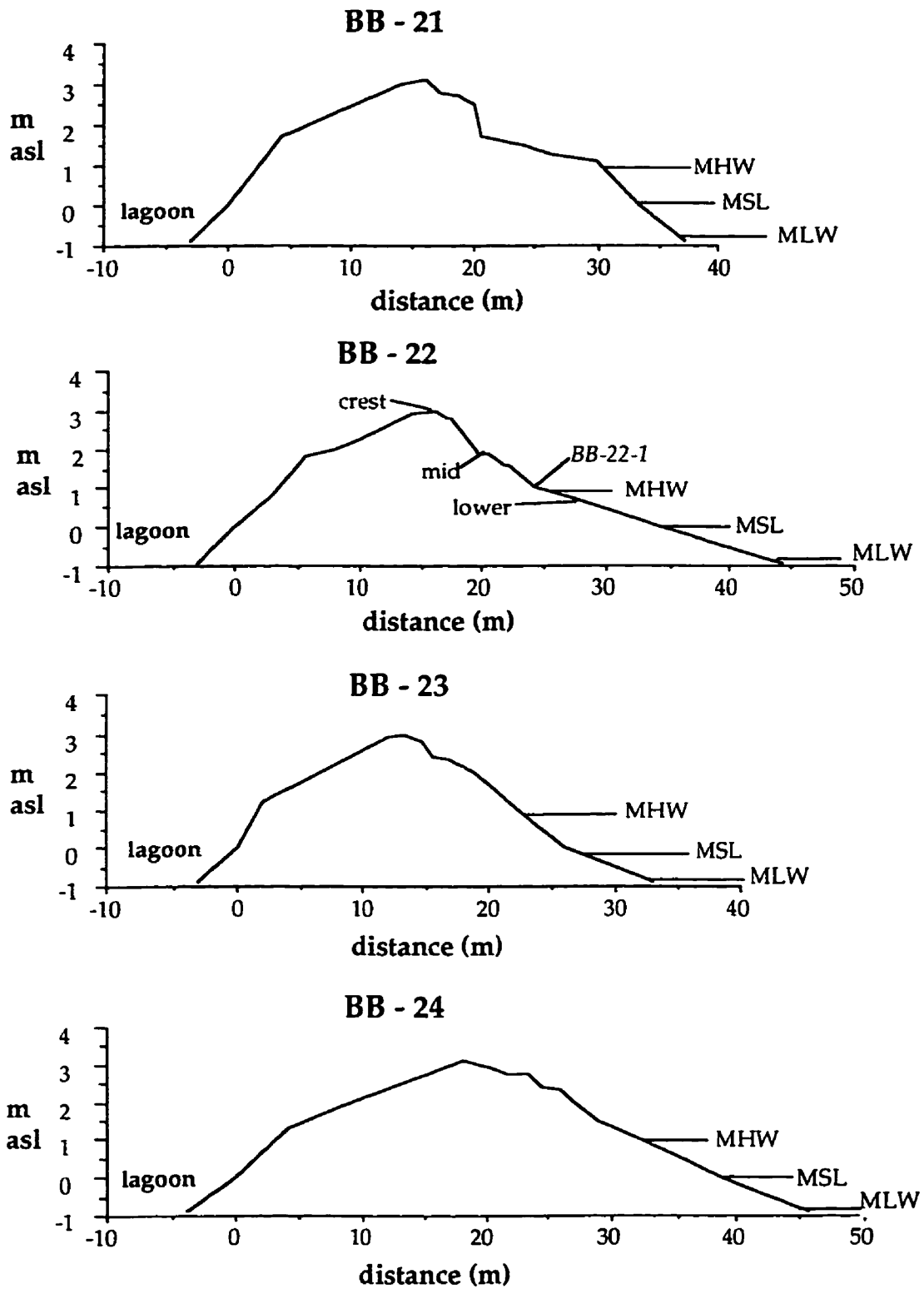


Figure 67: Profiles of transects BB-21 - BB-24, zone D, Big Barasway.

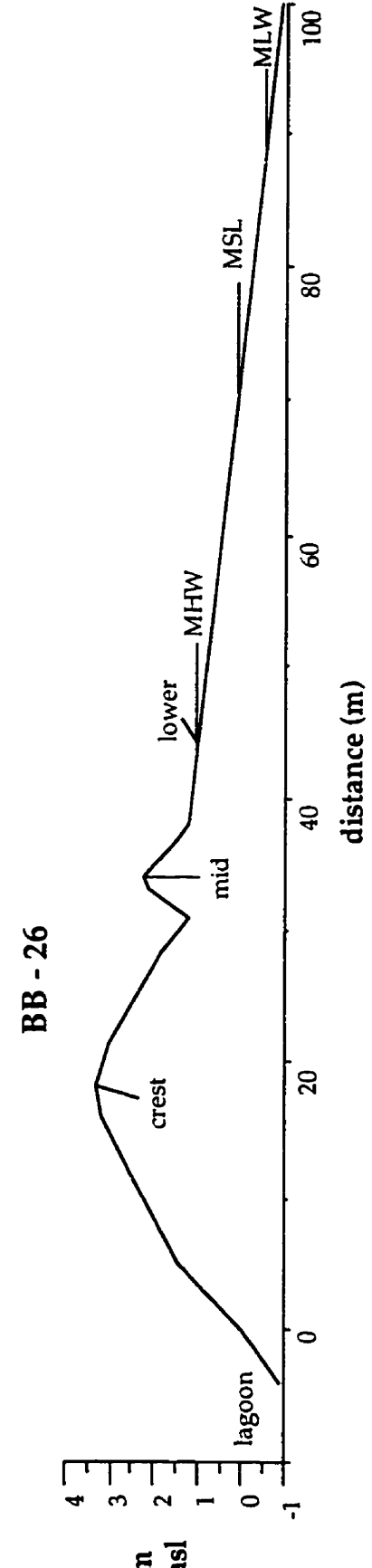
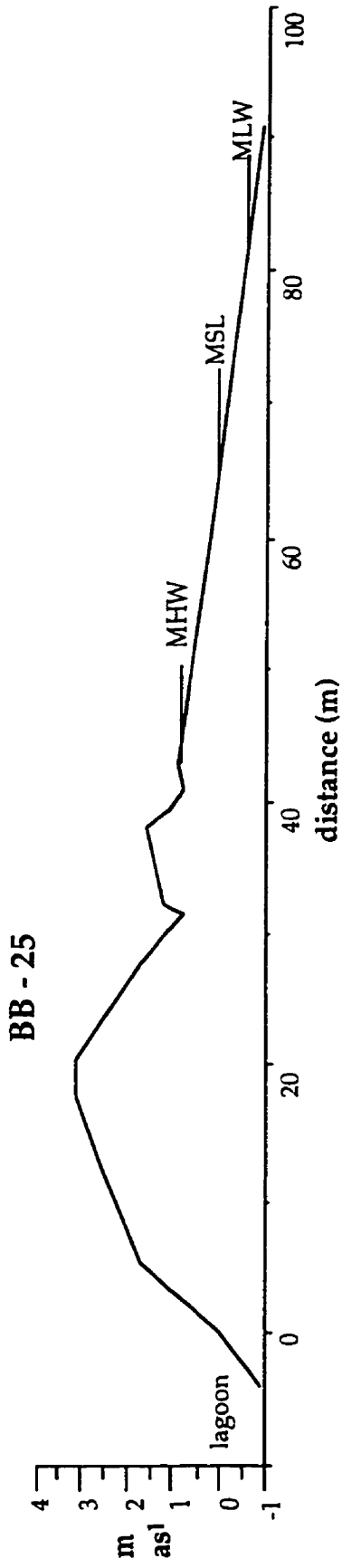


Figure 68: Profiles of transects BB-25 and BB-26, zone D, Big Barasway.

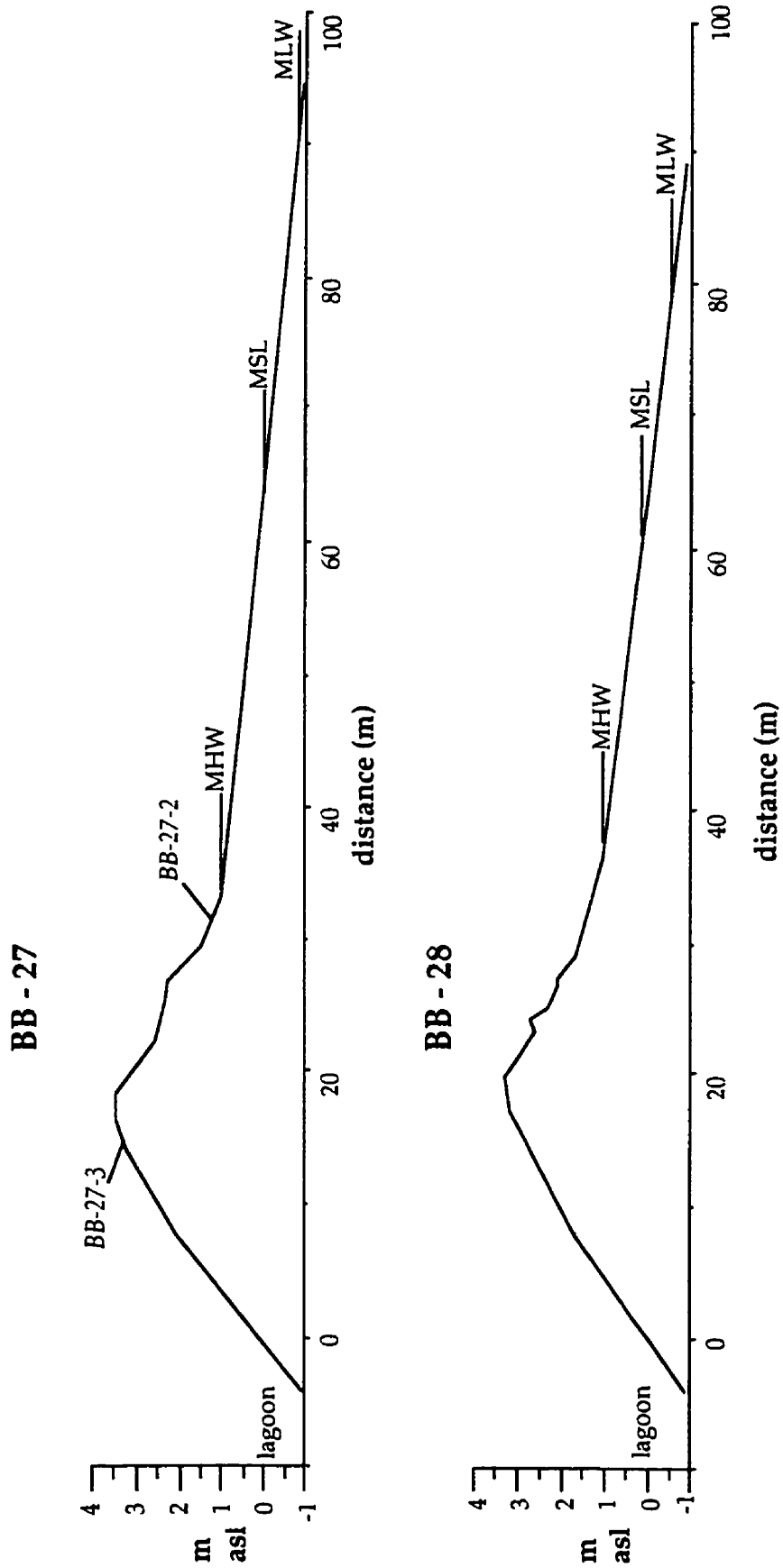


Figure 69: Profiles of transects BB-27 and BB-28, zone D, Big Barasway.

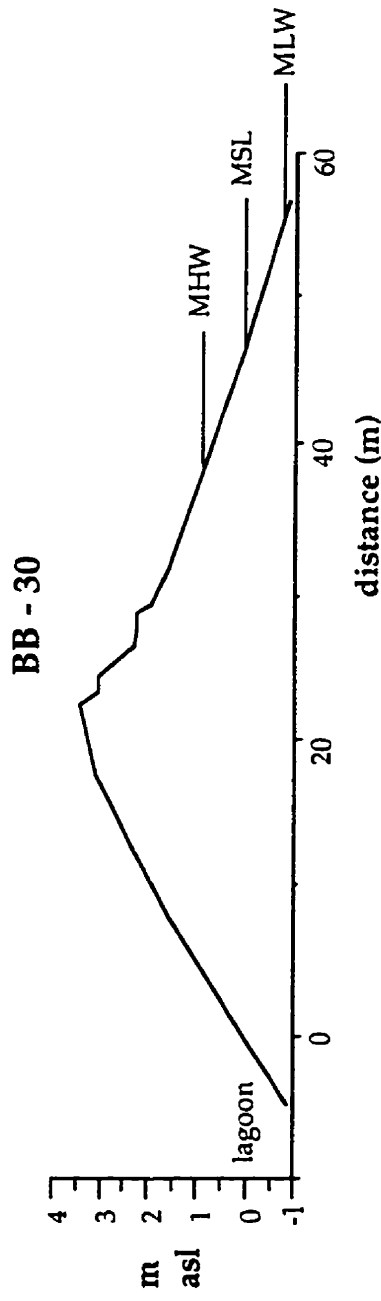
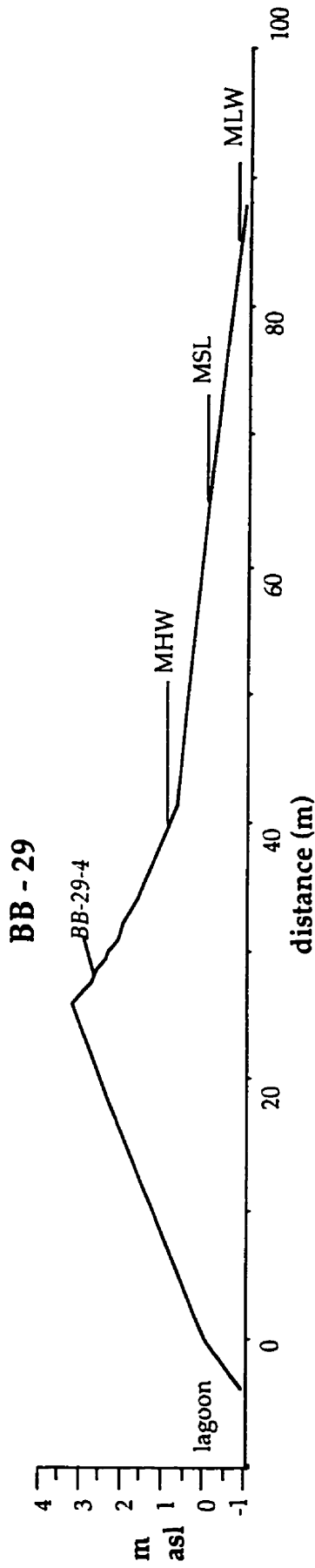


Figure 70: Profiles of transects BB-29 and BB-30, zone D, Big Barasway.

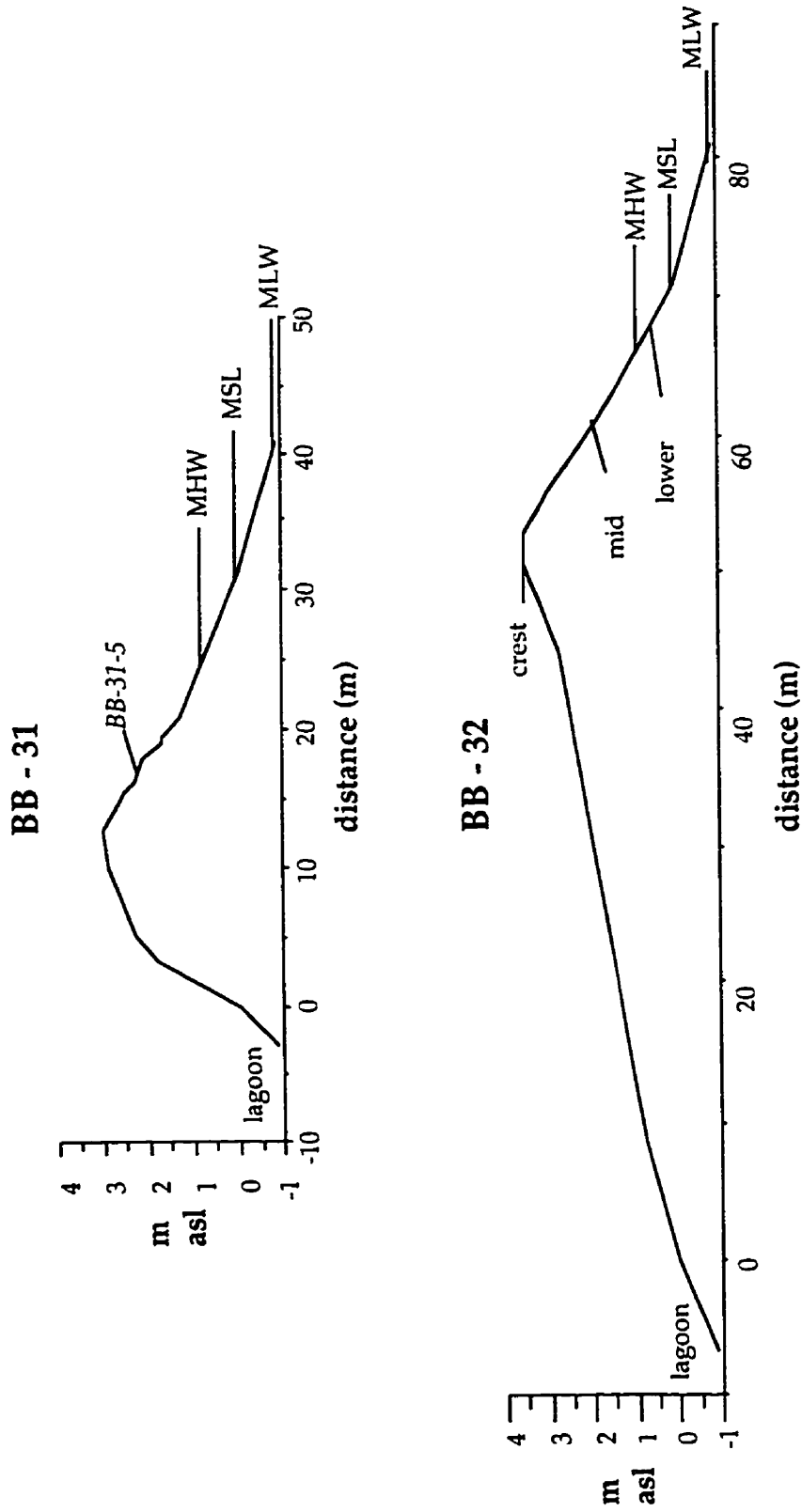


Figure 71: Profiles of transects BB-31 and BB-32, zone D, Big Barasway.

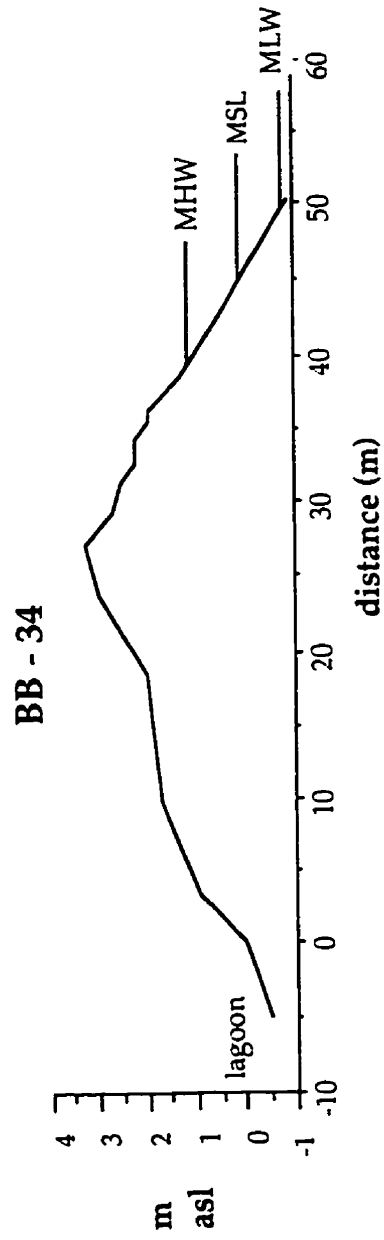
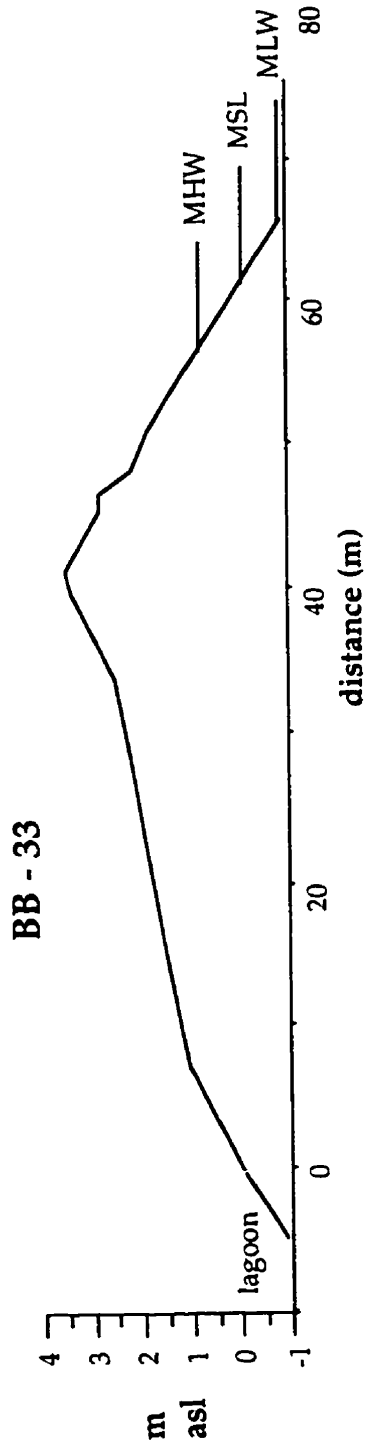


Figure 72: Profiles of transects BB-33 and BB-34, zone D, Big Barasway.

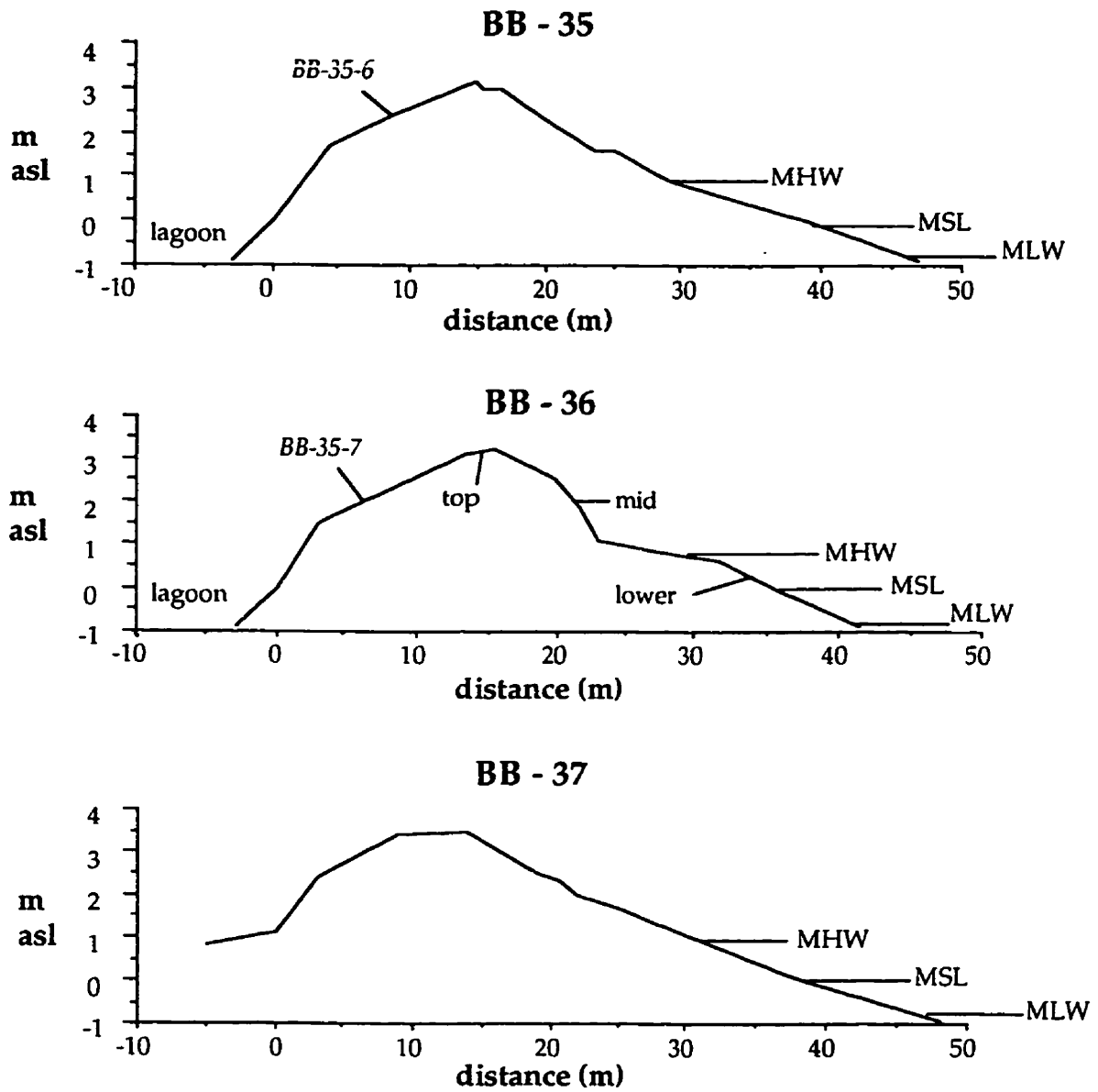


Figure 73: Profiles of transects BB-35 - BB-37, zone D, Big Barasway.

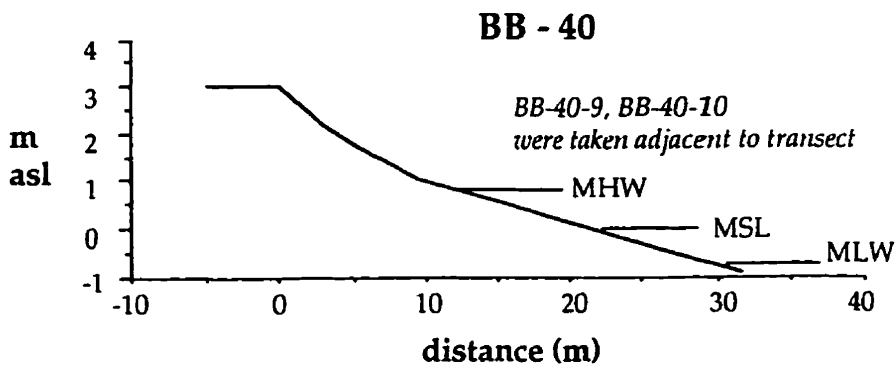
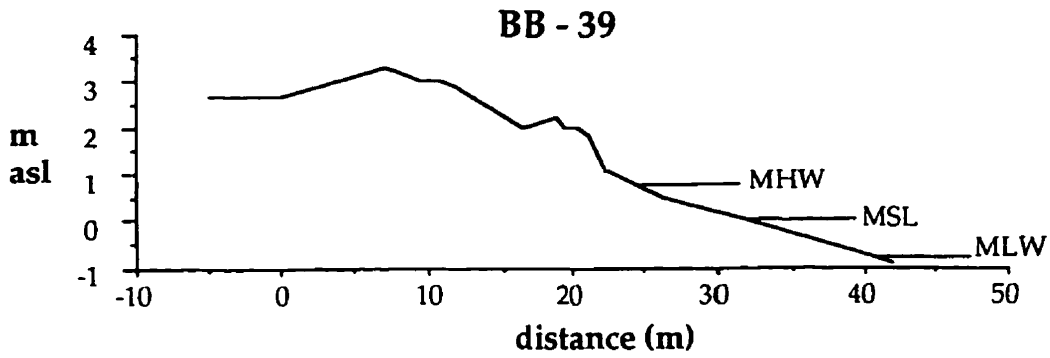
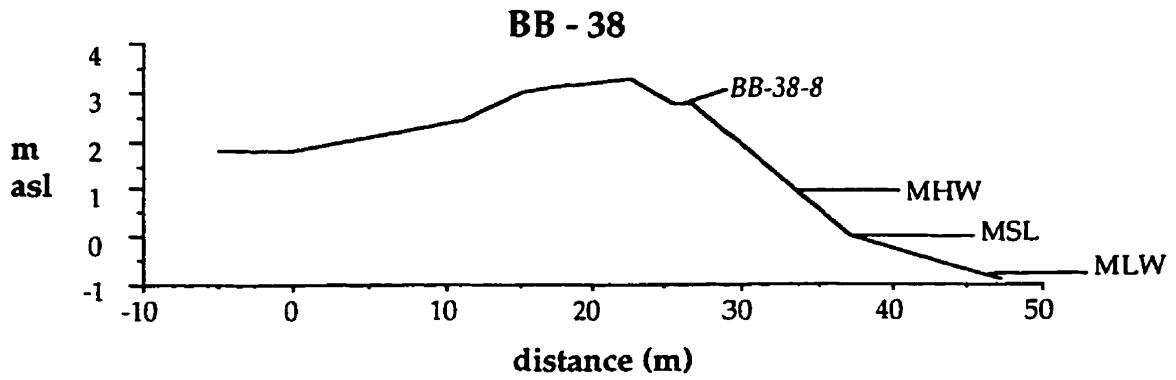


Figure 74: Profiles of transects BB-38 - BB-40, zone D, Big Barasway.

The barrier extends 18 m to the south of transect BB-21. At the tip of the barrier, a hooked spit composed of granules and small pebbles curving toward the back of the barrier, was present during the summer of 1991. During the fall of 1991, this feature was eroded and was completely removed by November 1991. The feature had reformed by the summer of 1992 and had eroded, as in 1991, in the autumn of 1992. This pattern was repeated again in 1993.

The foreshores in the southernmost section were characterized by linear to convex profiles in July 1991. Small linear ridges were present. The profile of transect BB-21 shows a modification of this overall shape. A 5 m-wide berm was present in the upper-beachface, the steep berm scarp topped a relatively gently-sloping mid-beachface area and the lower-beachface dropped sharply to the outlet. The crest and foreshore area were modified to some extent as a result of all-terrain vehicle traffic.

The section to the north (BB-25 - BB-29) is characterized by a gently-sloping ($< 2^\circ$) boulder and cobble platform in the intertidal zone. The shoreline trend curves from SSW-NNE at transect BB-25 to WSW-ENE toward transect BB-27. During July 1991, the overall foreshore slopes ranged between 3.9° and 4.9° , whereas the backshore slopes ranged between 7° and 10.6° . The total widths ranged between 63.3 and 73.3 m. Summer vegetation cover on the barrier crest and backbarrier area here is estimated at 5%.

A pronounced spit of small- and medium-sized pebbles dominated the foreshore morphology during the summer of 1991 in the area of transects BB-25 and BB-26. It reached a height of 2.5 m asl and widths of 10 m. The spit followed the curvature of the barrier and continued as a linear ridge to the

north. The ridge was most distinct at transect BB-27 and lessened northward at transects BB-29 and BB-30. Directly landward of the spit, small overwash fans were present and contained small- and medium-sized pebbles, similar to that observed on the crest and front of the spit. During the autumn of 1991, sediment from this feature was moved landward and northward. The spit merged with the barrier, producing convex profiles for the foreshores of transects BB-25 and BB-26, as shown in Figure 75. No similar spits developed during the summers of 1992 or 1993.

Between transects BB-27 and BB-29, elongated cusps with a northerly alignment occur sporadically. These have wavelengths of 9 to 12 m and heights of 0.5 m. These cusped features indicate a northward transport of sediment, similar to those observed along zone B (Plate 25).

Plate 25: Elongated cusps becoming backwash channels along zone D. July 1992.

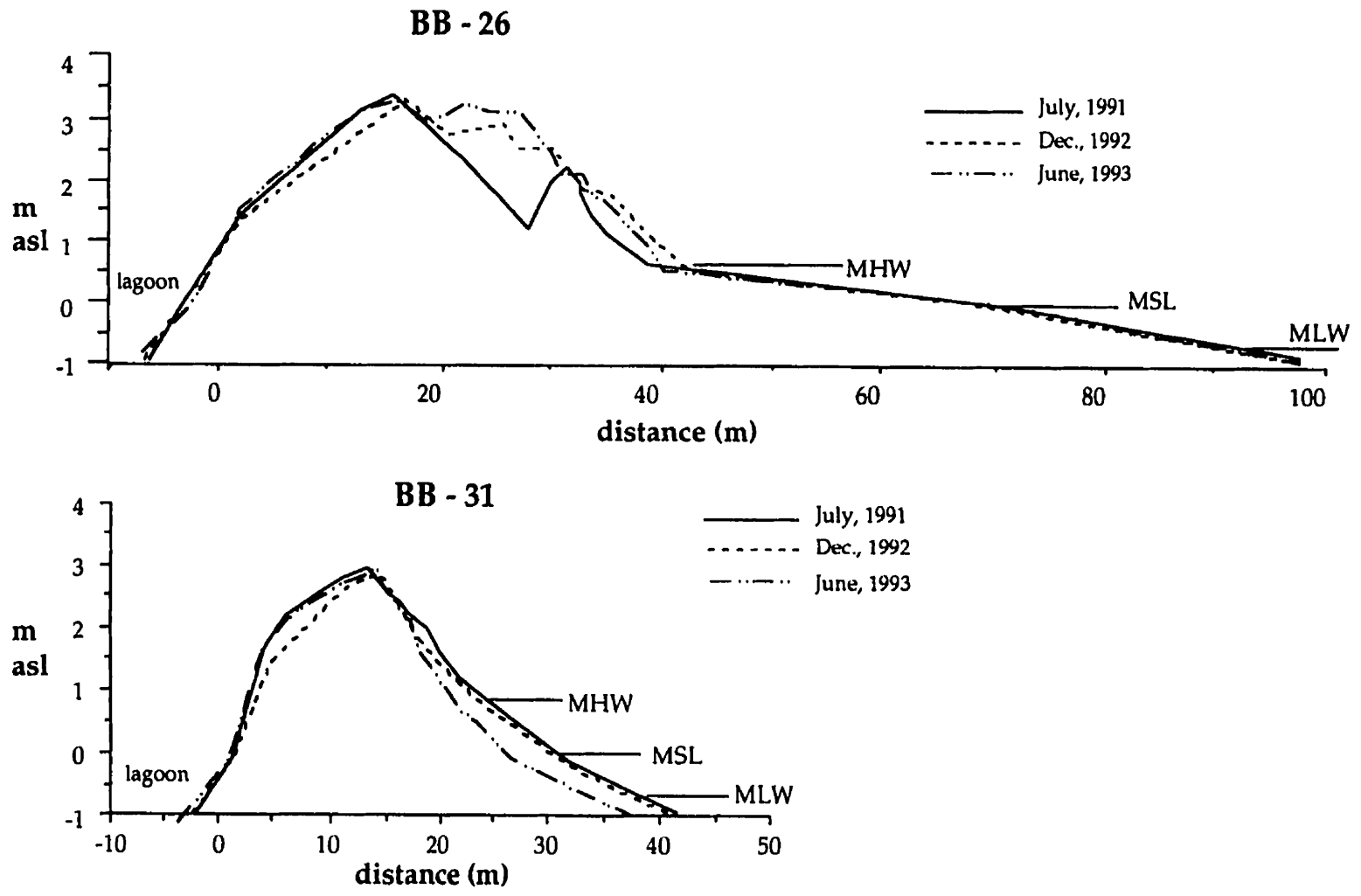


Figure 75: Comparison of profiles of transects BB-26 and BB-31 measured July 1991, December 1992 and June 1993.

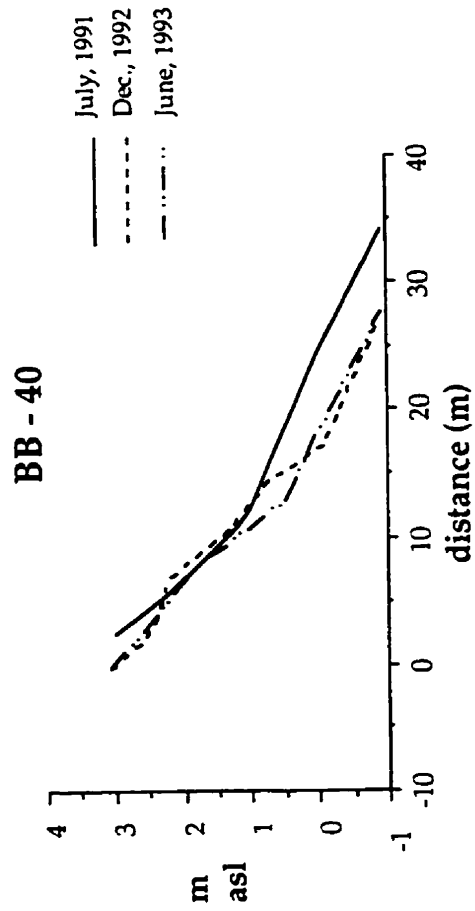
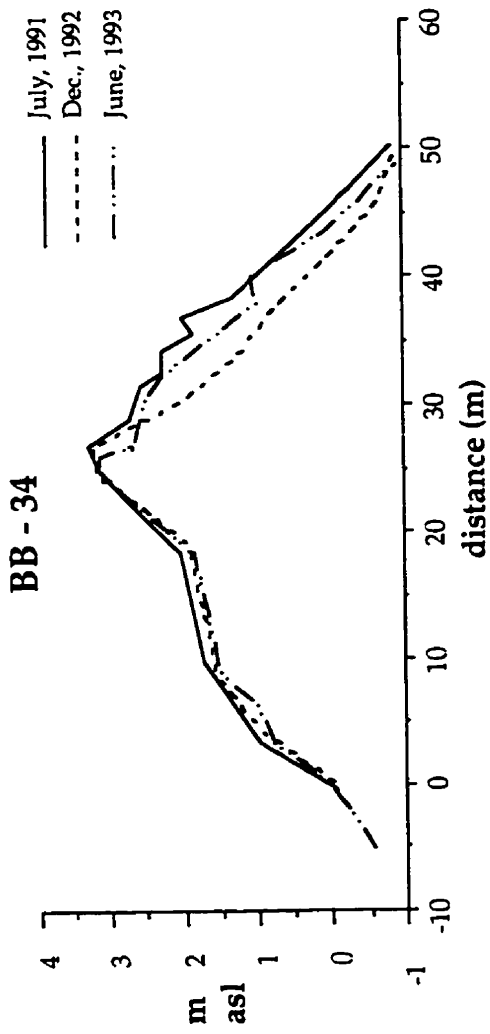


Figure 76: Comparison of profiles of transects BB-34 and BB-40 measured July 1991, December 1992 and June 1993.

The third section (BB-30 to BB-34) has a shoreline trend of SW-NE. During July 1991 the foreshore slopes ranged between 8.7° and 10.7° whereas the backshore slopes ranged between 3.7° and 8.8°. The total widths ranged between 38 and 71.1 m. The backshore profiles of transects BB-32, BB-33 and BB-34 show the presence of a large fan. Approximately 60% of the mid- to back areas of the fan is covered by *Angelica atropurpurea* (angelica) during the summer, but seaward of the fan vegetation is absent.

The foreshores in this section had linear profiles during July 1991. Backwash channels with widths between 0.5 and 1 m and heights of 10-25 cm were present in the foreshores of this section. The orientation of these channels varied between 018° and 034° with deviations of 26° to 34° from the shoreline trends. The southward edge of these channels had an armouring of cobbles while the interior of the channels were dominated by medium and small pebbles (Plate 26).

Based on profile measurement and visual inspection throughout 1991-1993, this section has shown an alternating pattern of sediment accumulation during the summer months (May - September) and sediment erosion during the other months, although deviations from this general trend occurred depending on the direction and intensity of wave activity (Plate 27). In addition to seasonal change, examination the beach as a whole and individual profiles indicates that there has been a net loss of sediment along the beachface to the north of BB-30. The profiles of BB-34 show accretion in the mid- and lower-beachface between December 1992 and June 1993 showing seasonal variability while the upper-beachface and crest is retreating consistently (Figure 76). At 0.7 m below the barrier crest along transect BB-34,

Plate 26: Backwash channels farther to the north of Plate 26, zone D. July 1992.

Plate 27: Overview of the beachface along sections 3 and 4, zone D. December 1991.

Plate 28: Exposure of wooden frame along zone D. June 1993.

Plate 29: Overview of the barrier taken August 1954. The wooden frame shown in Plate 29 is the remains of one of the wooden stages on the barrier shown in the 1954 photo. The outlet in 1954 was located at the northern end.

80 cm of wooden frame was exposed by September 1993 (Plate 28). Initial exposure of the frame began during the winter of 1991/1992 and erosion has continued throughout the course of this study. Approximately 1 m of sediment from the barrier front has been removed between 1991 and 1993. In a photo taken on August 23, 1954 (Plate 29) two wooden stages are located on the barrier in the vicinity of BB-34. The frame is probably part of one of the buildings. Evidently, between 1954 and 1991, sediment overtopped and eroded this area as the barrier moved landward.

The fourth section (BB-35 to BB-40) has a SSW-NNE trend. During July 1991 the foreshore slopes ranged between 8.4° and 12.7° whereas the backshore slopes were comparatively steep (11.9° to 14.1°). The total widths ranged between 21.4 and 38.4 m. Approximately 2% of the crest and back beach areas is covered by the same species found in the southern sections.

At the time the profiles were measured in July 1991, large amounts of sediment had accumulated. The profile of transect BB-40 was taken through the centre of a cusp and has a concave shape in the mid- to upper-beachface. The other transects were characterized by linear to convex shapes. A storm berm was present on the upper-beachface of profiles BB-35, BB-36, BB-38 and BB-39. Transect BB-39 shows a pronounced berm in the mid-beachface area while transects BB-35 and BB-37 show a lesser berm at the same elevation. Transect BB-36 shows a steep mid-beachface area.

When these profiles were taken poorly defined cusps were present with wavelengths of 6 to 9 m and heights of 0.5 - 0.75 m. Cusps occurred sporadically throughout the duration of the study with wavelengths that ranged between 5 and 10 m. The cusps generally occur along the mid- to

lower-beachface, are shallow and composed of sand in the centres and small to medium pebbles on the cusp horns.

Plate 30: Southward transport of sediment along section 4, zone D.

In July 1993, transect GSC-392 was established along transect BB-34. Figure 77 illustrates the profiles taken in July, September and December 1993. The profile measured in September 1993 has increased sediment, and more pronounced, higher elevated berm development than that measured in July. The profile taken in December 1993 shows a loss of sediment from September 1993. Although this demonstrates a similar summer/winter cycle as observed at Ship Cove and zone A, Big Barasway, this section of the beach does not show a consistent seasonal accumulation/erosion cycle. The beachface alternates between concave and convex profiles as sediment is either removed or added with wave activity. Linear ridges of sediment initiated at the northern end dissipate towards the southern end of this section (Plate 30).

These ridges occur occasionally and indicate a southward movement of sediment. Frequently after storm events, large amounts of seaweed are present (Plate 31).

Breaching of the barrier crest occurs throughout zone D, although little sediment is transferred landward along most of the barrier for the variations in profiles show little change. Between transects BB-35 and BB-36, more extensive overwashing occurs during storm events. Two small overwash fans are present here and deposition has occurred during the study (Plate 32). Six painted clasts placed between transects BB-30 and BB-31 in September 1991 were found on the fan along the back of transect BB-36 in November 1991.

Plate 31: Large accumulation of seaweed after a storm. November 1992.

Big Barasway, GSC-392

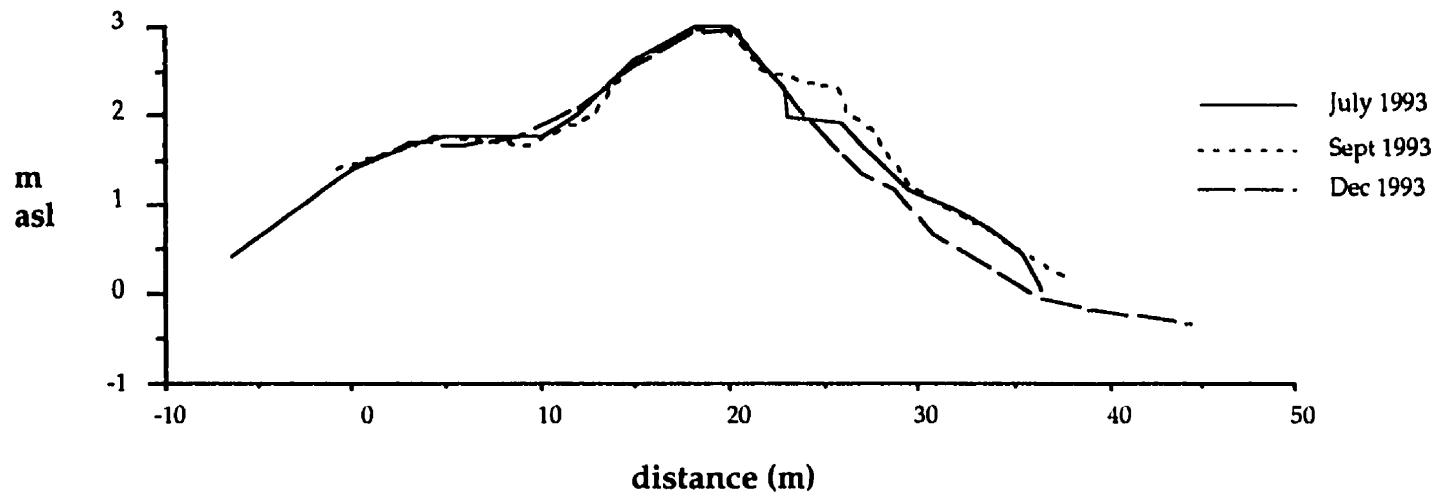


Figure 77: Profiles of GSC-392 measured July, September and December 1993.

Plate 32: Overwashed sediment along the northern end of zone D. June 1993.

7.5.2 Clast Lithology

Samples of 72 clasts were taken along the beach crest and along the lower-beachface to determine the lithological distribution. The samples were analyzed separately and the results then combined to determine the lithological assemblage of the entire zone. The results are shown in Figure 78. The sample taken at the crest was composed of 29% sandstone, 47% siltstone, and 13% conglomerate. Basalt, rhyolite, granite, tuff and quartzite formed 9% of the assemblage. The sample taken along the lower-beachface contained a larger amount and variety of igneous clasts; 13% basalt, 11% rhyolite, 4% granite, and 4% pumice. The pumice is not locally-derived and

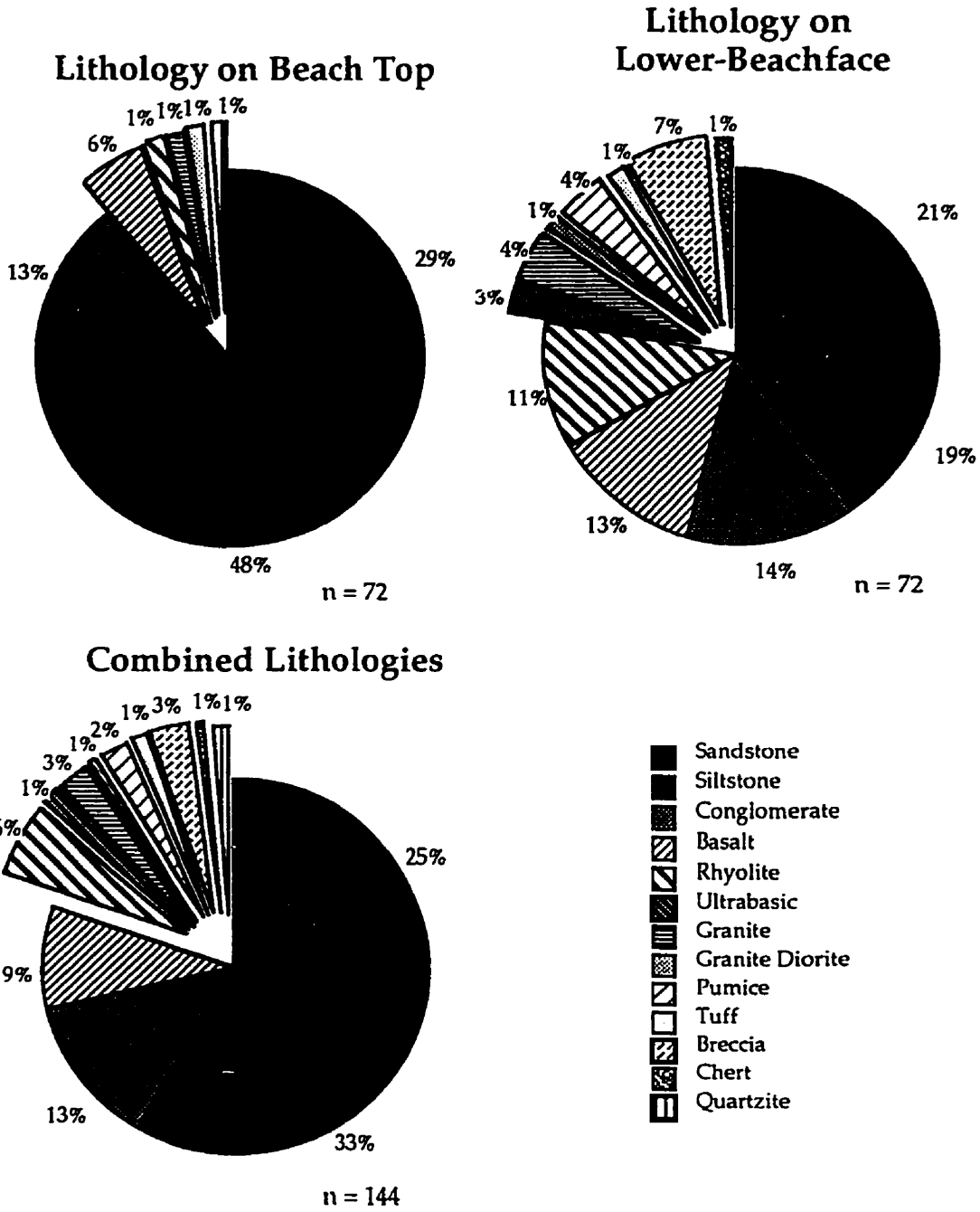


Figure 78: Lithology for zone D, Big Barasway.

most likely arrived as ship ballast or as Gulf Stream flotsam. Also found were ultrabasic, granodiorite, tuff, breccia, and chert clasts. The combined data show a concentration of 71% sandstone, siltstone and conglomerate, 15% basalt and rhyolite, and 14% of a mixture of clast types mentioned above.

7.5.3 *Sediment Texture*

Along the entire length of zone D, cobbles and boulders dominate from the subtidal zone to 0.5 m above mean sea-level. The surface textural analyses were based on samples taken above this area.

Figure 79 shows the estimated texture for transects BB-22, BB-26, BB-32, and BB-36 which are representative of their associated subdivisions. The samples were taken at the lower-beachface above the cobble and boulder step, mid-beachface, and the beach crest. These quantities as at zones A and C and at Ship Cove are intended to illustrate how the barrier sediment composition varies and the patterns that were observed. Along BB-22 the beach crest and lower-beachface were dominated by large pebbles and cobbles, whereas the mid-beachface area consisted mainly of medium-sized pebbles. At BB-26, the clast size increased up the beachface. The lower-beachface was dominated by small pebbles (50%) with no cobbles, the mid-beachface contained an unsorted mix of clast sizes with 20% cobbles, whereas the beach crest consisted of 80% cobbles. Boulders (60%) dominated the lower-beachface of BB-32 in contrast to the mid-beachface which contained 70% small pebbles. The beach crest had a larger component of cobbles (40%) but also a mixture of pebbles sizes. Lastly, BB-36 showed a predominance of sand and granules (50%) in the lower-beachface as well as the mid-beachface (60%). The crest, on the other hand,

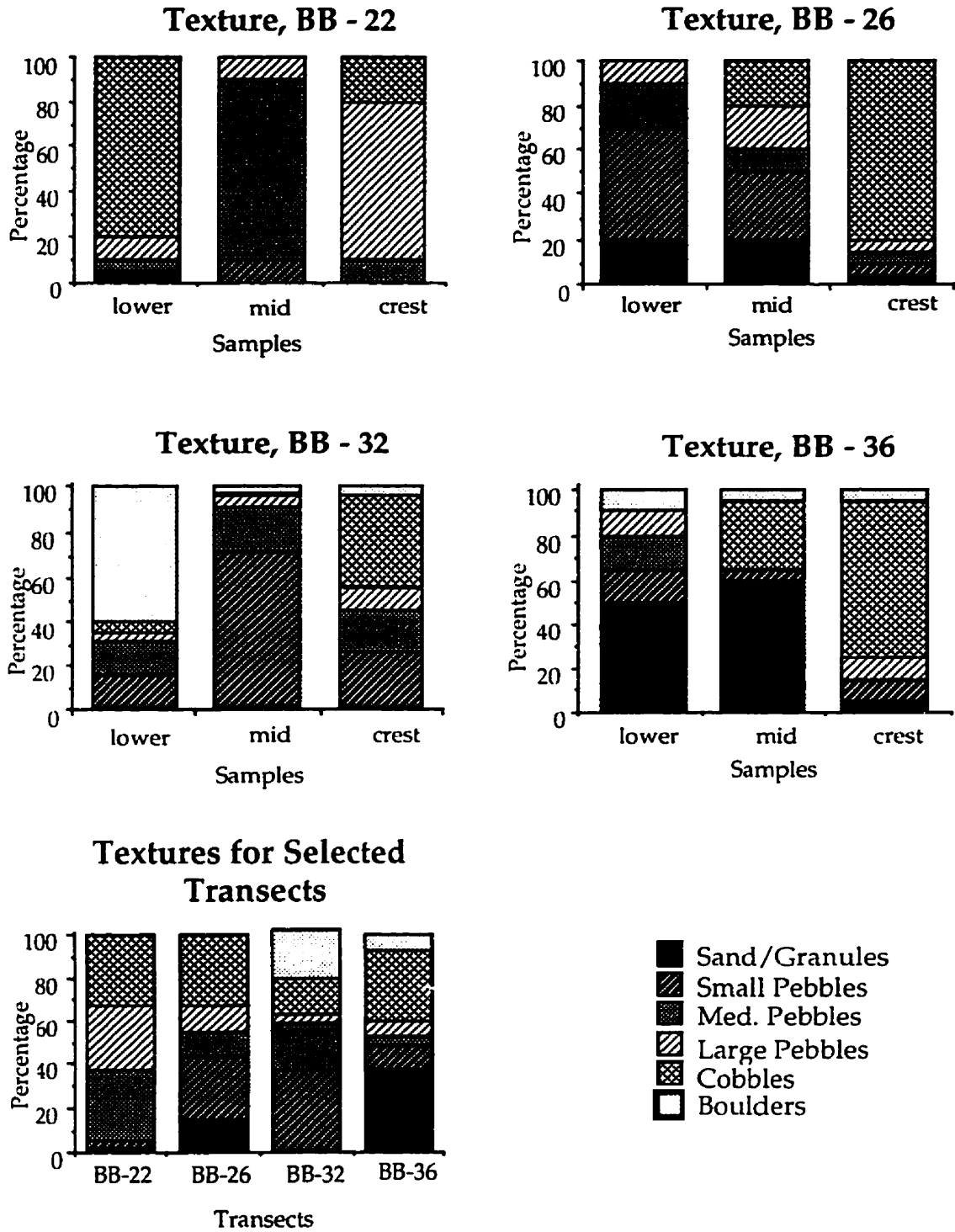


Figure 79: Sediment texture for zone D, Big Barasway.

consisted mainly of cobbles (70%). Plate 32 shows the textural composition of overwashed deposits. Although dominated by cobbles, similar to that observed on the crest of transect BB-36, overwashed sediment contains more smaller-sized clasts, particularly granules and small pebbles.

These textural analyses show the variability and inconsistency along transects and between lateral regions of the barrier. For instance, along BB-26 the sediment size increased from the base to the crest, whereas along BB-36 the sediment size decreased. Furthermore, in most samples, a wide range of clast sizes from sand and granules to cobbles and boulders is found. Also shown in Figure 79 are the textural compositions for the combination of the samples for each transect combined. BB-22 had a nearly even mix of cobbles, large- and medium-sized pebbles; BB-26 had a bimodal distribution of cobbles and small pebbles; BB-32 had a large component of small pebbles, whereas BB-36 had a bimodal distribution of cobbles and sand/granules.

7.5.4 *Clast Shape*

Figure 80 illustrates the results of clast shape analyses for three sites (crest, mid-beachface, lower-beachface) along the four subdivisions in zone D. Results from transect BB-22 represent the clast shape distribution for section 1, those from transect BB-26 for section 2, those from transect BB-32 for section 3 and lastly, those from transect BB-36 for section 4. Also illustrated are the results for the three sites along each transect combined to show the overall clast-shape distributions for each transect. As with the sediment texture analyses, the quantities for clast shape compositions are interpreted qualitatively.

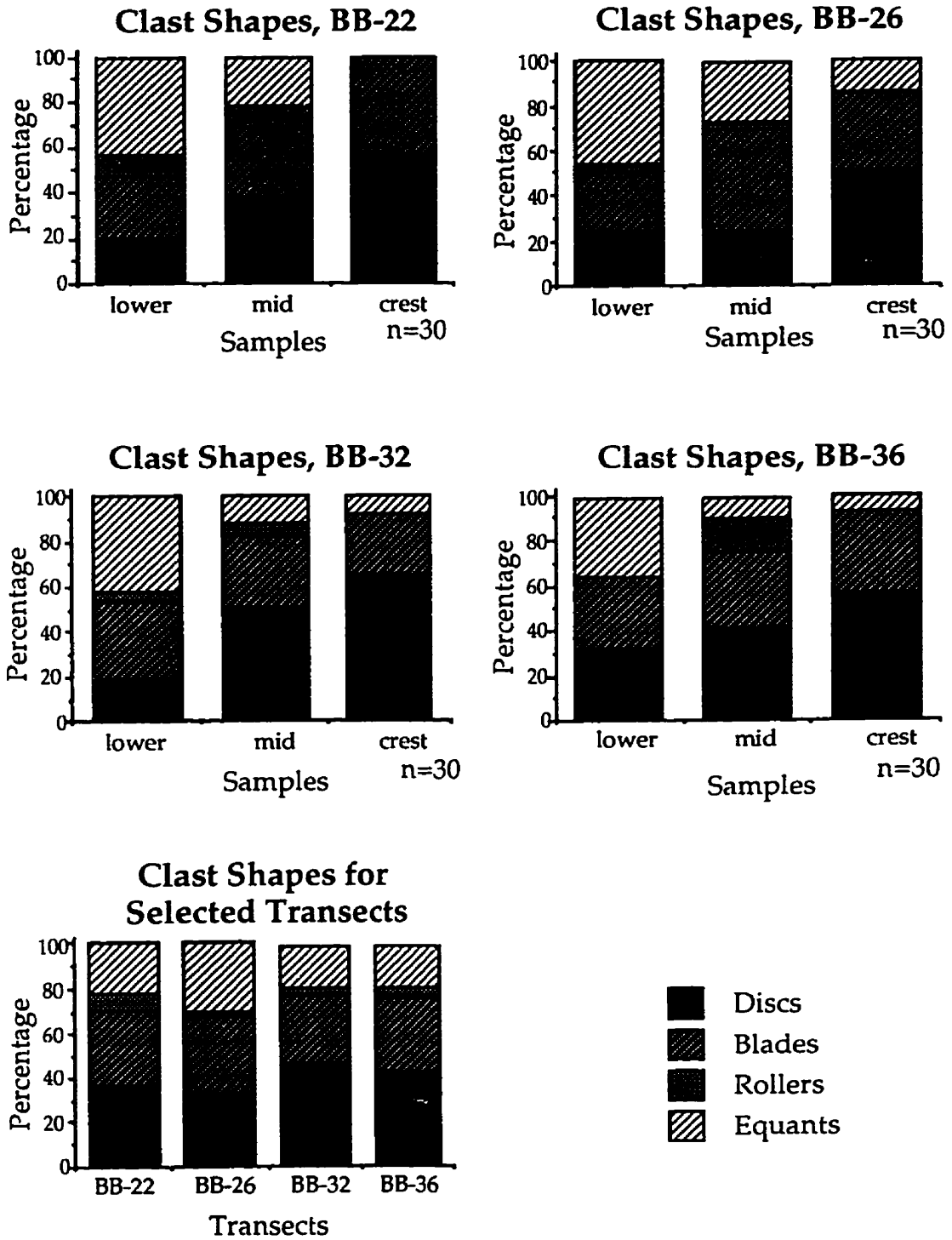


Figure 80: Clast shape analysis for zone D, Big Barasway.

All four transects show an increase of discs and a decrease of equants with distance from the seaward edge. Discs increase from 19% to 57% along transect BB-22, 24% to 50% along transect BB-26, 19% to 65% along transect BB-32, and 32% to 56% along transect BB-36. In contrast, equants decrease from 44% to 0% along transect BB-22, 47% to 14% along transect BB-26, 42% to 8% along transect BB-32, and 35% to 7% along transect BB-36. The percentages of blades show minor changes along the transects, fluctuating between 26% and 43%. Rollers are confined to the mid- and lower-beachface areas. When the results for the three sites along each transect are combined, no significant change in shape is evident among the clasts along the four transects. The overall clast-shape distribution, incorporating data from all transects, is 45% discs, 35% blades, 4% rollers, and 17% equants.

Throughout the four subdivisions the roundness remains similar, with the clasts mostly subrounded (70%) and rounded (25%). Minor amounts of subangular clasts are present.

As with the overall clast shape, there are differences in the sphericity between the lower-beachface and the beach crest. The lower-beachface is characterized by moderate to highly spherical clasts while the crest is dominated by low to moderately spherical clasts.

7.5.5 Fabric Analysis

The imbrications of the a/b planes of the discoid clasts on the barrier along zone D were less defined than at Ship Cove and in zone A at Big Barasway. In most areas, the orientation of imbrication generally deviated between 0 and 30° to the south of the transect trend. The plunges of the

imbrications ranged between 5 and 25° seaward and were gentler than along zone A or at Ship Cove. Ten a-axis clast fabrics were taken on the beach within zone D. Figures 81 - 83 show the plots of the fabrics. Table 16 lists for each fabric the azimuth, plunge, S_1 , S_3 , K, transect trend and deviation of fabric trend from transect trend. All the K values are less than 1.0. The S_1 values range between 0.535 and 0.728.

Both clast fabrics, BB-22-1 and BB-27-2, were taken along the cobble-dominated step located on the lower slopes of the barrier front. The modal azimuths for BB-22-1 and BB-27-2 are 006.5° and 358.7° with deviations of -76.5° and -18.7°, respectively. The plunges are 02.6° and 11.2°, respectively. The S_1 values are 0.651 for BB-22-1 and 0.654 for BB-27-2.

Clast fabric BB-27-3 was taken on the back of the barrier in the centre of an erosional channel, developed from the crest towards the backbarrier area. Seaward of the fabric site a large log lay across the head of the channel. The fabric has an modal azimuth of 297.7°, a plunge of 10.5°, an S_1 value of 0.728 and a deviation of 42.3°.

Clast fabric BB-29-4 was taken along a small berm at the base of a steep slope. It has an azimuth of 225.5°, a plunge of 04.6°, an S_1 of 0.574 and a deviation of 107.5°.

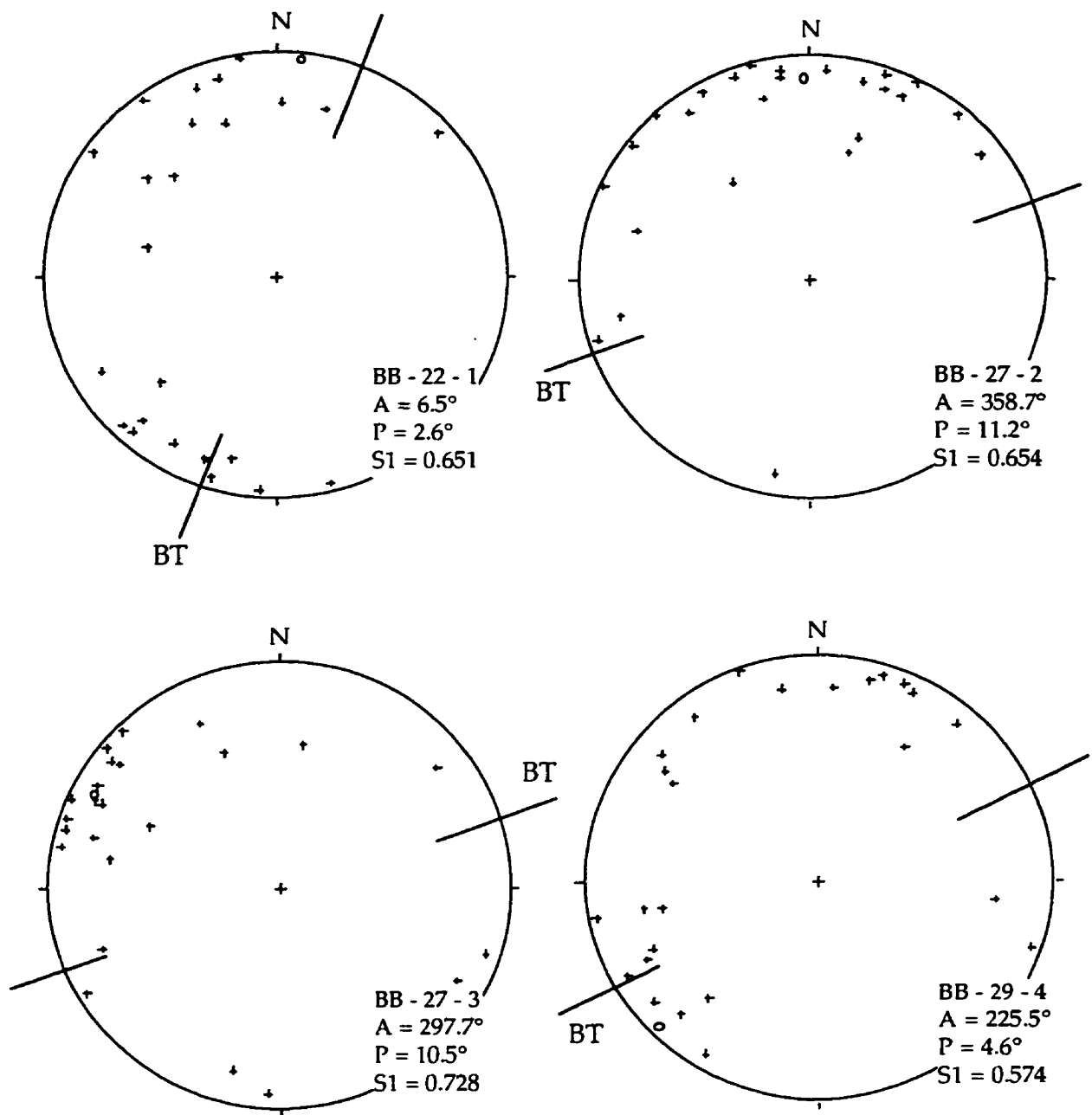
Clast fabric BB-31-5 was taken on a linear berm ridge. It has an azimuth of 319.8°, a plunge of 24.0°, an S_1 of 0.570 and a deviation of 10.2°.

Fabrics BB-35-6 and BB-35-7 were taken on the backbarrier. BB-35-6 has an azimuth of 308.5°, a plunge of 09.3°, an S_1 of 0.619 and a deviation of 0.5°. BB-36-7 was obtained from overwash deposits. It has an azimuth of 163.1°, a plunge of 7.3° (landward), an S_1 of 0.538 and a deviation of 155.9°.

Clast fabrics BB-38-8, BB-40-9, and BB-40-10 were taken on berms. BB-38-8 has an azimuth of 279.4°, a plunge of 21.4°, an S₁ of 0.627 and a deviation of 16.6°. BB-40-9 has an azimuth of 278.8°, a plunge of 20.1°, an S₁ of 0.586 and a deviation of 21.2°. BB-40-10 has an azimuth of 300.1°, a plunge of 21.8°, an S₁ of 0.662 and a deviation of -0.1°.

<u>Number</u>	<u>Trend</u>	<u>Plunge</u>	<u>S1</u>	<u>S3</u>	<u>K</u>	<u>Tran Trend</u>	<u>Deviation</u>
BB-22-1	6.5	2.6	0.651	0.042	0.38	290	-76.5
BB-27-2	358.7	11.2	0.654	0.048	0.43	340	-18.7
BB-27-3	297.7	10.5	0.728	0.055	0.89	340	42.3
BB-29-4	225.5	4.6	0.574	0.057	0.24	333	107.5
BB-31-5	319.8	24.0	0.570	0.035	0.15	330	10.2
BB-35-6	308.5	9.3	0.619	0.056	0.37	309	0.5
BB-36-7	163.1	7.3	0.538	0.036	0.09	299	135.9
BB-38-8	279.4	21.4	0.627	0.061	0.43	296	16.6
BB-40-9	278.8	20.1	0.586	0.044	0.22	300	21.2
BB-40-10	300.1	21.8	0.662	0.064	0.60	300	-0.1
		mean	0.621				
		s.d.	0.056				

Table 16: Clast fabric data for zone D, Big Barasway.



°Principal Eigenvector
 A = Azimuth Trend
 P = Plunge
 BT = Beach Trend

Figure 81: Clast fabrics, zone D, Big Barasway.

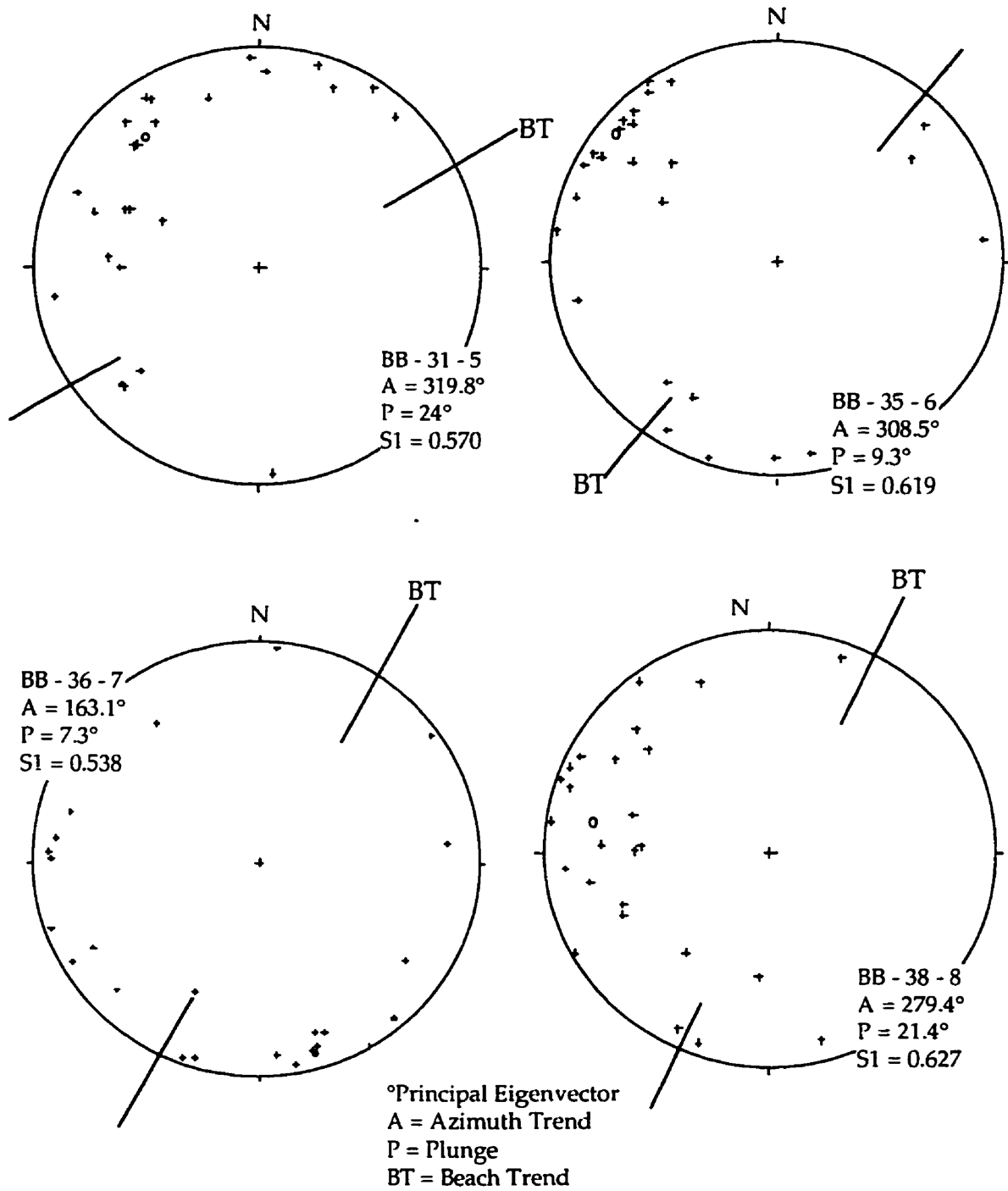
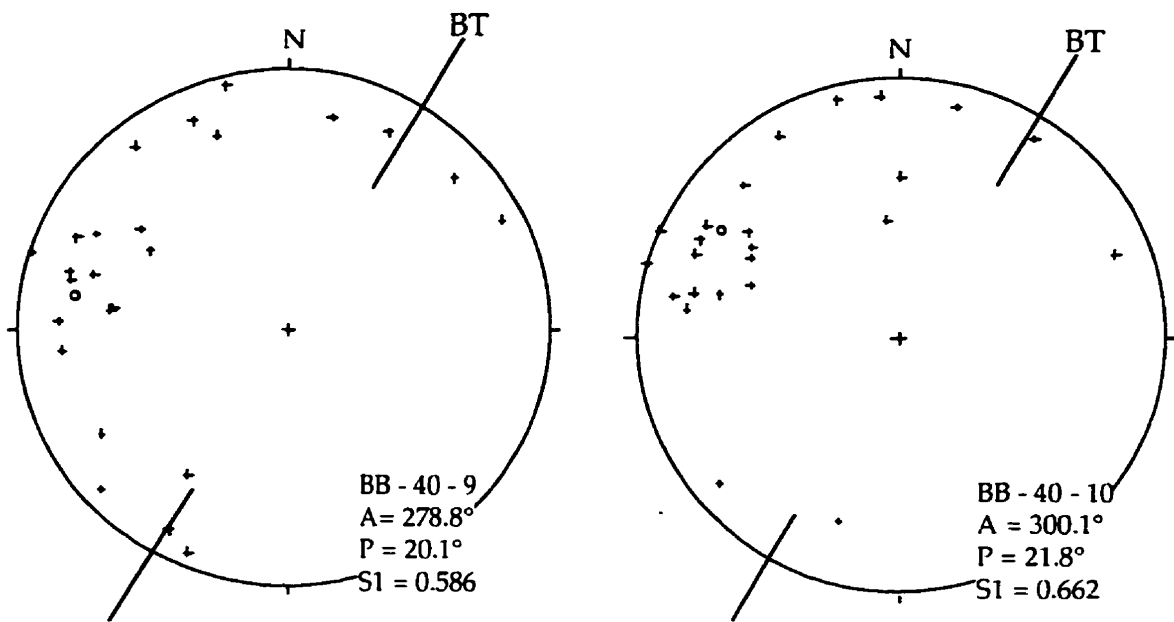


Figure 82: Clast fabrics, zone D, Big Barasway.



°Principal Eigenvector
 A = Azimuth Trend
 P = Plunge
 BT = Beach Trend

Figure 83: Clast fabrics, zone D, Big Barasway.

Chapter 8

Discussion of the Barrier System at Big Barasway

8.1 Introduction

The morphodynamics and sedimentology of the barrier system at Big Barasway are largely controlled by the gently-sloping sub- and intertidal platform situated in the central 800 m. Complex wave refraction patterns result and wave energies reaching the barrier behind and to the sides of the platform are dissipated. Zone B, located directly behind the platform, is not actually part of the barrier itself, but an 'island' separating two barrier systems; the barrier developed in zone A, from another barrier composed of zones C and D. Under the influence of the northerly direction of longshore drift, as shown by the geomorphological evidence of elongated cusps along zone B, sediment from the island is contributing to the barrier along zones C and D to the north. Little or no sediment from zone B is transported to zone A to the south. In addition, as zone A contains higher proportions of clasts with discoid shapes, higher roundness and lower sphericity than that of the clasts along zones B, C and D, it is apparent that zone A contributes minimal (if any) amounts of sediment to the zones to the north.

Boulders and cobbles were seen on the platform during low tides. When taking echo sounding measurements in September 1992, boulders and cobbles were observed in the nearshore zone. Boulders, rather than bedrock strata, were exposed at the base of the bluff along zone B.

The fan shape and its likely composition of unconsolidated sediments indicate that the platform is a modified glacial feature. The large bluff bordering the barrier to the north and the diamicton along zone B were deposited as subaqueous mass movement deposits (House, in preparation). Consequently, during deglaciation, floating ice in the valley may have caused the formation of an underflow fan. With rising sea-levels, the clasts along the fan, capable of being transported by wave action, would have moved landward and formed the barrier leaving the bouldery platform as a lag deposit.

Although Placentia Bay is generally ice-free during the winter months, during other periods in the Holocene, intertidal sea ice may have contributed to the close packing of the cobbles and boulders within finer sediments on the platform and the lower reaches of the barrier. Boulder pavements similar to that seen at Big Barasway are described by Hansom (1983) and McCann *et al.* (1981). However, since wave processes are more important than ice processes in the present environment, ice related features such as striae (Hansom, 1986) would not have been preserved.

As the result of the bathymetry of the relict glacial fan, the two barriers are controlled by separate flow cells. The different hydrodynamic settings cause the barriers to exhibit striking morphological and sedimentological differences. The lithological assemblages are similar between the zones and thus do not contribute to the sedimentary differences. The southern half of zone A shows characteristics of a swash-aligned barrier, whereas the barrier along zones C and D is drift-aligned. The eroding bluff backing zone B supplies sediment to the northern zones and is part of that

flow cell. Since two barriers exist, the organization of the morphodynamics and sedimentary assemblages of zones B, C and D will be discussed together but separately from zone A.

8.2 Zone A

8.2.1 Morphology

Because of the shallow nearshore bathymetry and complex refractory patterns along the platform, edge waves cannot fully develop. Therefore, the cusps along the southern end are poorly formed, infrequent, and confined to a small segment. The lack of complete edge wave development largely accounts for the lower barrier heights here, as compared to Ship Cove, where cusp development from edge waves increases wave run-up. The height of the barrier marks the limit of extreme wave run-up.

With removal of sediment from the beach along the ridges in the autumn and winter months to the nearshore zone, a part of the sediment is transported southward. A northward recycling occurs again during the lower-energy summer months. Given the stronger northward flowing drift, it is unlikely all the sediment undergoes circular transport. The bluffs bordering the southern end supply minor amounts of new sediment. The southern end of the zone, thus either maintains a fixed sediment quantity or experiences a net removal of sediment, while the northern end receives a net gain. This limited (and perhaps depleting) sediment supply along the southern end, in addition to cusped development characteristic of swash-aligned beaches, contributes to the high barrier heights and steep beachface

slopes. These are particularly evident in the upper- and mid-beachface regions above the high tide mark and in the upper-intertidal mark.

Although the duration of the study is short (2 1/2 years) the time series profiles along transect BB-6 show a slight landward movement of sediment and a corresponding flattening of the beach crest. The barrier height has remained essentially the same. Air photo analysis shows that the barrier has moved landward. Ice foot development and relatively quiet wave climate during the study may have dampened the average rate of landward movement.

The mechanism for landward movement of gravel barriers is by rollover (Orford *et al.*, 1991). Sediment along the beachface is reworked, transported to the beach crest and backbarrier, buried, and then exposed again on the beachface as the barrier moves landward. The profiles show that rollover is occurring at a rate of 0.3 - 0.8 m per year, in contrast to rapidly migrating barriers such as that at Story Head, Nova Scotia (Forbes *et al.*, 1991).

Sediment starvation in conjunction with rising sea-levels may eventually lead to instability, whereby the erosive capability of the wave activity will increase. The barrier width and height would decrease in the vicinity of transect BB-6 and an overwash channel or inlet may result during an extreme storm event. Given the extreme southerly position of the lagoon around BB-6 and the entrance of the stream into the lagoon at the northerly extreme, it is unlikely the main stream outlet would reposition itself around BB-6. In addition, a bedrock outcrop located behind transect BB-9 constricts the width of the lagoon. Consequently the main stream outlet or outlets are

confined to positions north of the outcrop, as was an outlet located in the vicinity of transect BB-10 during the last century.

The old outlet location at the northern end of zone A (around BB-10) is in a downdrift location. It is probable that an extreme storm or series of storms deposited sediment and closed the outlet, forming the overwash fan now present in that area. With a large accumulation of sediment here, the stream would have located a weaker position along the barrier and forced an opening. This could have been facilitated by erosive activity by the storm or series of storms along other portions of the barrier, in particular the northern part of zone D, where the outlet was located in 1948.

Although the profiles taken of the northern end do not show landward movement it is likely the northern end is moving at a faster rate than the southern, as the northern end follows the erosion and retreat of the island. Under present hydrodynamic conditions, the ridges along the beachface terminate within zone A and are frequently removed offshore or overwashed during storm events. Under the transgression this region is experiencing, these ridges may be extended into zone B and perhaps farther north as water levels over the boulder platform increase. A rise in sea-level would result in increased erosion along the bluff within zone B and overtopping of the island, which would eventually be incorporated as part of the barrier. The amount of new sediment introduced from the bluffs into the system would be small; however, with increased sea-level rise, landward movement of the barrier would continue along the northern end of zone A. Areas to the south of zone B would be controlled by separate flow cell or cells, as is now the case.

8.2.2 *Cross-shore Clast Shape and Size Sorting*

The sedimentological differences seen along the length of the barrier at zone A reflect changes in nearshore bathymetry. The southern edge of the platform begins around transect BB-9, correspondingly, the type and organization of the sediment changes. During July 1991, the surface sediment along the southern half (BB-1 - BB-7) was dominated by rounded, low-sphericity bladed and discoid clasts. Although the proportions of overall clast shapes remained similar along the length of the barrier, the northern half (BB-7 - BB-14) contained clasts with higher sphericity and lower roundness. In addition, the southern half showed a distinct decrease in equants and rollers along the barrier crest from the mid- and lower-beachface. The northern half, on the other hand, showed little sorting by shape along transects.

The sediment texture along the southern area showed landward coarsening, as seen at Ship Cove, with cobbles dominating the crest and pebbles along the lower sections above the cobble and boulder frame. The northern half showed an unsorted mix of clast sizes throughout the beachface and crest. Overall, higher percentages of smaller clasts were found along the northern half.

The primary factors contributing to the differing sedimentary assemblages are the amounts of wave energy reaching the barrier on a regular basis, and more importantly, the responses to storm events. The amount of new sediment entering the system is negligible, and it is unlikely sediment is moving northward into the other zones. Wave processes are thus reworking a limited sediment supply within a constant area.

Within zone A the linear ridges formed under the lower wave energies of the summer months showed northward movement of sediment. The cusate formation along the southern half, albeit poor, showed a greater swash alignment with a higher component of offshore/onshore movement of sediment. The increased asymmetry of the cusps northward reflect the increased importance of longshore drift along the northern half.

The trend of increasing proportions of small clasts northward reflects lower wave energies resulting from the interaction of the offshore platform; in contrast to the higher energy conditions along the southern end where nearshore bathymetry is deeper. The decreased roundness and increased sphericity northward toward zone B, particularly along the back beach, indicates less abrasion and thus less exposure to wave activity. The clasts more closely resemble those within the diamicton along zone B. Since the linear ridges and northerly-elongated cusps indicate a northward movement of sediment, these clasts are not derived from the south where roundness is greater. These clasts are either relict sediments that were deposited closer to the formation of the barrier and have not been exposed to as much wave activity as those to the south, or they have been introduced to the system more recently from the island.

The latter explanation is more probable. The ^{14}C dates on wood in this region (see chapter 4) indicate that Holocene transgression has occurred here. The relatively high rates of erosion along zone B, the presence of ripped clumps of sod thrown on the top of the bluff and the presence of beach clasts amongst the vegetation along the southern portions of zone B may indicate increased storm activity and/or sea-level rise. The northern end of the

present barrier along zone A was likely part of the island, which has been eroded and breached with rising sea-levels. Diamicton, similar to that exposed along the bluff of zone B, may underlie the surface beach deposits. This possibility is further supported by the increased presence of exposed boulders along the beachface and back here. The clasts, consequently, are found closer to the originating glacial deposits.

Increased sphericity of the rounded clasts in the northern half of zone A may also indicate slight variances in the mode of transportation. Northward transport of sediment largely occurs along the linear ridges within the mid-beachface. As clasts move northward along the ridges they undergo more 'rolling' motions as clasts move northward along the transport corridor (Carter and Orford, 1991). Clast interactions may wear equally on all sides and thus increase sphericity (Dobkins and Folk, 1970). In contrast, the larger clasts to the south may undergo more 'tossing or sliding movement'; thereby favouring the formation and selection of discs (Dobkins and Folk, 1970).

The lack of sorting of sediment by shape or size along the northern end is primarily a response to storm activity. Overwashing was limited between transects BB-9 and BB-12. After storm events large amounts of sand and granules were deposited along the crest and backbeach. Cobbles with seaweed attached were also observed in areas that been overwashed (Plate 33). The seaweed adds buoyancy and cobbles can thus be transported farther up the barrier (Gilbert, 1984).

Subsequent to overwash deposition along the backbarrier between transects BB-9 and BB-12, strong onshore winds and gusts transport sand/granules landward. Eyles (1976) attributes the formation of gravel cones

and depressions to 'wind devils'. This phenomena is thought to cause a circular transport of pebbles around the cones and a circular scour and pebble lag in the depressions.

Plate 33: Cobble with seaweed attached along the barrier crest, zone A.
January 1992.

The features seen at Big Barasway, however, are not as well formed as those described at Holyrood Pond. The beach at Holyrood Pond is considerably wider and contains a larger proportion of sand than does Big Barasway. At Big Barasway the wind devils have less sand into which to scour depressions, and the frequent presence of large clasts interfere with the circular route around the gravel cones. With the limited supply of sand, complete coverage of these features, as described by Eyles, was not observed.

In addition, the southwesterly orientation and steep, high headland bordering both sides of the harbour at Holyrood Pond allow a greater funneling of winds, which results in higher wind speeds at Holyrood Pond than at Big Barasway.

At Holyrood Pond, winds contribute to the presence of sand in the back beach, whereas at Big Barasway sand and granules are mainly deposited by overwashing. Eyles (1976) suggested that wind cones and depressions may be preserved in the geologic record. Sand deposited during more quiescent periods of wind velocity would bury the cones and depressions.

With limited sand supply, this mechanism for preservation is unlikely at Big Barasway. If the intensity of the overwashing is great and erosive overwash channels form, then the features may be destroyed completely. Overwash channels, though, have not developed over the duration of the study. Sedimentary layers formed from storm events along the backbarrier may have nonerosive contacts. The likelihood of nonerosive contacts increases farther from the crest, or source of wave energy. Preservation potential, thus, increases farther from the crest. However, the overwashed sediment filling the depressions and surrounding the cones has a similar texture to that of the cones and depressions and thus it would be difficult to differentiate wind from water-formed deposits. Although as Eyles (1976) concluded, these features may be used to indicate a coastal environment with strong onshore winds, recognition in the sedimentary record in systems as Big Barasway is unlikely.

The limitation of overwash activity between transects BB-9 and BB-12 is a consequence, largely, of the orientation to storm events. This section of

the beach is most exposed to southwesterly storms. Headlands bordering the southern end of the cove provide protection for the southern sections of the beach. Despite the dissipating effects of the platform, storm-induced waves overwash the barrier along that portion. Farther to the north of zone A and zones B, C, and most of zone D, the platform dissipates the wave energies to a greater extent, and overwashing was not observed.

The well-sorted linear ridges formed during the summer months show the main morphological response to wave dynamics along the beachface of the northern half. The higher elevated ridge composed of medium- and large-sized clasts was formed by higher-energy wave action than the lower beach ridges composed of smaller-sized clasts. The northerly merging of the ridges, dominated by smaller-sized clasts, reflects the dissipation of energy caused by the rough-surfaced bouldery platform.

These ridges represent corridors of actively moving sediment directly above the high water mark. Carter and Orford (1991) recognized similar cross-shore zonations along drift-aligned gravel barriers. In their description, the active transport zone is within the upper-beachface, directly below the crest, and above the upper and lower intertidal frames. At Big Barasway, though, the active transport zone is located in the mid-beachface with an upper-beachface extending 1.5 m to the crest.

The organization of cross-shore clast shape and size assemblages along the southern half reveals similarities to Ship Cove. During July 1991, discoid cobbles dominated the beach crest and back, while the mid- and lower-beachface contained larger proportions of pebble-sized equants and rollers.

Clast imbrications on the crest, back-beach and berm crests were not as pronounced as those at Ship Cove.

During the summer months as sediment accumulated, five primary sedimentary zonations occur. The upper- and back-beach were composed of discoid cobbles (zone 1). The mid-beachface contained larger proportions of equant- and roller-shaped pebbles (zone 2), whereas the upper-intertidal frame contained highly-spherical boulders and cobbles with a veneer of pebbles (zone 3). The lower-intertidal frame was marked by more exposure of the bouldery frame (zone 4). Boulders and cobbles dominated the gently-sloping nearshore zone (zone 5). During the higher wave energy months, the sediment from the mid- and lower-beachface is removed, exposing the cobble and boulder framework.

8.2.3 *Fabric Analysis*

The diversity in orientation and plunge of the a-axis clast fabrics of and the imbrication of the a/b planes of the discoid clasts show the complexity of this coastal environment. The dynamics of the waves differ between the northern and southern halves of the system. Of the five a-axis fabrics taken along the southern half, one of the principal normalized eigenvalues was less than 0.600; the northern half, in contrast, had three of five principal normalized eigenvalues lower than 0.600.

The mean of 0.633 and low standard deviation of 0.053 along the southern half is similar to the mean of 0.644 and standard deviation of 0.066 of the fabrics taken along the barrier at Ship Cove. This suggests that they represent similar sedimentary environments, as indicated by the clast shape

and size. Likewise, the strong seaward imbrications of the a/b planes of the discoid clasts in these samples showed deviations that varied to the north and to the south of the transect trends. These deviations result from wave flow through cusps, as discussed in chapter 6.

The clast fabric with the lowest principal eigenvalue (BB-5-2) was influenced by clasts falling from above, which also contributed to the low plunge of 7.5°. This individual clast fabric adds scatter to the overall fabric assemblage. In palaeoenvironmental reconstruction of potential marine environments of coarse clastic deposits, it may thus be advisable to analyze a lateral and vertical collection of fabrics. An unusual fabric, such as BB-5-2, may reflect secondary depositional processes resulting from an erosional surface.

Except for fabric BB-4-1, which was taken on the centre of a cusp horn and has an orientation parallel to the transect trend, the fabrics along the southern end all deviate to the north. At Ship Cove the numbers of north and south deviations were nearly even and reflected the multitude of cusp formations. At Big Barasway, the sample size of the fabrics is smaller (5) versus that at Ship Cove (25). The fabrics at Big Barasway were taken along the southern side of cusped horns (northern side of cusp centres).

The lower mean principal eigenvalue of 0.593 and higher standard deviation of 0.542 along the northern half of Big Barasway corresponds to and is indicative of less-organized sedimentary assemblages. Fabric BB-11-9 was taken directly above high-water mark and was formed during the previous high tide. It had the highest principal eigenvalue (0.746) recorded along zone A. The lower-beachface location makes this sedimentary accumulation a

transitory feature. Depending on the direction and intensity of the waves during the next high tide, the resulting fabric may be totally different.

Preservation of sediments with fabrics with high eigenvalues is possible; however, inconsistency is typically marked by many fabrics with low to moderate orientations surrounding isolated fabrics with strong orientations.

A-axis clast fabrics BB-10-7, BB-11-8, and BB-11-9 all have deviations to the south of the transect trend. Likewise the imbrication of the a/b planes of the discoid clasts deviated to the south of the transect trend by up to 30°. This pattern indicates that longshore drift was more significant. On occasions, poorly defined cusped features form along the northern half. However, cusps are less important in the creation of the sedimentary assemblage here than along the southern half and are much less significant than at Ship Cove. Consequently, swash action is generally from the southwest and not directed and reoriented within cusp centres.

8.2.4 Summary of Sedimentary Assemblages

The proximity of large variations in sedimentary assemblages demonstrates the complexity and variability of this coastal environment. Although the discussion so far has concentrated on describing and generalizing the sediments of zone A into two areas, that is the southern and northern halves, the change between the two halves is gradational.

The sedimentary assemblage of the southern half shows similarities to Ship Cove and correspondingly to Bluck's (1967) model. The crest and backbarrier contain landward-dipping, stratified, open-work bladed- and discoid-cobbles inclined at 8 - 12°. The imbrication, however, is not as strong

as that at Ship Cove. The upper-beachface contains mainly bladed- and discoid-cobbles, dipping seaward at 10 - 15°. As at Ship Cove this area has erosional surfaces, although the vertical height of approximately 0.5 m is less than at Ship Cove (1.5 - 2.5 m). The smaller height results from the lack of large cusate features, such as those that form at Ship Cove. The mid-beachface contains pebbles and cobbles with higher percentages of equants and rollers overlying the framework of larger cobbles and boulders of high sphericity. This section is the most variable with cusate features occasionally forming here, and has a mixture of erosional and depositional surfaces. The lower-beachface dips seaward at 10 - 15° with a veneer of pebbles and sand overlying the cobble and boulder framework. A cobble and boulder-dominated nearshore zone is also present.

The sedimentary assemblage along the northern half is divided into four primary zones. The sediments of the overwash deposits along the beach crest and backbeach show an unsorted mixture of size and shape with a large proportion of sand and granules. The layers are landward-dipping with gentle inclinations of 3 - 5°. Patches of pebbles and cobbles are imbricated in a seaward direction, whereas wind-influenced patches show confused imbrication. Flotsam and organic debris are intermittently found. The principal normalized eigenvalues of fabrics are low (<0.600). The upper-beachface shows a similar mix of unsorted clasts as with the overwash deposits. However, the layers are seaward-dipping, inclined at 7 - 10°, and aeolian features are not present. Clast fabrics are poorly oriented. The mid- and lower-beachface contains inversely graded sorted pebbles overlying a boulder and cobble frame, perhaps underlain by diamicton. The beds dip

seaward at 10 - 12° and show better imbrication than in the other zonations. The lowermost zone is the cobble and boulder dominated platform, extending into the nearshore. Table 17 summarizes the sedimentary assemblages.

	<u>Number</u>	<u>Unit</u>	<u>Zone</u>	<u>Slope</u>	<u>Structure/texture</u>
<u>Southern</u>	1	backbarrier	supratidal	8-12° (landward)	imbricated stratified openwork blades and discs;
	2	upper-beachface	supratidal	10-15° (seaward)	erosional generally; blades and discs
	3	mid-beach	supratidal	varied: 10-20° (seaward) 2-5° (landward)	imbricated pebbles and cobbles with higher percentages of equants and rollers; erosive and depositional cusp development; moderate fabrics
	4	lower-beachface	intertidal	10-15° (seaward)	veneer of pebbles overlying cobble and boulder framework
	5	nearshore	subtidal	3-6° (seaward)	cobbles and boulders
<u>Northern</u>	1	backbarrier	supratidal	3-5° (landward)	poor stratification; unsorted mix of sand-boulders; seaward and confused imbrication; poor fabrics
	2	upper-beachface	supratidal	7-10° (landward)	unsorted clasts; poor fabrics
	3	mid-lower-beachface	intertidal	8-10° (seaward)	landward coarsening imbricated pebbles and sand
	4	nearshore	subtidal to lower-intertidal	1-4° (seaward)	cobbles and boulders

Figure 17: Summary of sedimentary characteristics along zone A, Big Barasway.

8.3 Zones C and D

8.3.1 *Morphology*

Longer term comparisons of the morphology are possible using successive air photos taken in 1948, 1967 and 1980. The small scales of the 1948 (1:40,000) and the 1980 (1:56,000) air photos and the size of the gravel barriers make it difficult to accurately quantify the changes in barrier widths and lengths along the zones, as well as the landward displacement. The 1:17,000 scale of the 1967 air photo shows more detail.

In the 1948 air photo, the stream outlet was narrow and located at the northern end of the lagoon. In contrast, the outlet in the 1967 and 1980 air photos appears wider and more permanent. An oblique photograph taken in August 1954 shows the outlet at the northern location (Plate 29). Evidently, the outlet switched to a more southern location sometime between August 1954 and July 1967. Over the period of the present study the outlet has moved in a southerly direction by approximately 10 m.

The seaward side of the island has eroded approximately 15 - 35 m between 1948 and 1980; likewise, the barrier has moved landward along its entire length. The barrier has decreased in width along the southern half of zone C and the northern half of zone D. This has resulted in the barrier having more of a sinusoidal shape in the 1980 air photo than the seaward convex shape of the 1948 air photo. The lagoon has decreased in area by approximately 1000 - 3000 m².

The progradational ridges shown on the profiles of transects BB-18 and BB-19 within zone C show an accumulation of sediment that most likely occurred after the relocation of the outlet to its present vicinity. With the

outlet south of its present position, the northward transfer of sediment would have been disrupted, causing deposition on the updrift side of the interference created by the stream. Under the present hydrodynamic conditions caused by the boulder platform and the stream outlet, zone C is relatively protected from storm events. Consequently, limited seasonal change or longer term fluctuations were seen along transects BB-15 through BB-19. The longer term trend of landward movement and erosion along the southern half of zone C indicates that this pattern of little seasonal fluctuation will continue for there will be no significant new input of sediment and sea-level will likely continue to rise.

Periods when the outlet was in a southerly position were marked by increased deposition to the north of the outlet (zone D), as this position prevented efficient northward movement of sediment by the dominant southwesterly waves. Sediment has accumulated along zone D largely by the erosive activity of the ocean waves and by the stream flow along the edge of zone C. Gravel material has been and continues to be removed from the stream banks and incorporated into the barrier along zone D. A progradational ridge shown on the profiles of transect BB-26 has formed during the study period and may reflect increased erosion of zone C.

Some sediment along the outlet margin within zone D may originate from the north. The northerly-aligned elongated cusps observed between transects BB-27 and BB-29 and the backwash channels along the beachface between BB-30 and BB-34, however, indicate a dominance of sediment transfer to, not from, the north.

In addition to the evidence for northerly transport of sediment from regions to the south, the barrier front between BB-30 and BB-34 was eroded during the study period. Increased erosion may also have resulted from the southerly relocation of the outlet. By interfering with northward transport, areas downdrift experience sediment depletion and thus increased erosion.

The edge of the boulder platform is located in the vicinity of BB-34. As a result, the orientation of the barrier changes here from a SW-NE trend to a SSW-NNE trend and more closely follows the orientation of the overall coastline. The lack of headlands and the large diamicton bluff bordering the barrier to the north allow occasional transport of sediment from the north to the part of the barrier between transects BB-35 and BB-40. Storms involving N or NW winds erode the toe of the bluff, causing large amounts of sediment to accumulate in the northern part of zone D. Extreme wave heights are not possible under northerly winds, due to the relatively small fetch to the north in Placentia Bay. Consequently, northerly or northwesterly storms are usually constructive, resulting in sediment accumulation. Because of the low wave energies from a limited fetch, the accumulated sediment is largely composed of sand and granules.

The large backbarrier fan along zone D (between transects BB-32 and BB-34) was formed before 1948 and has remained unaltered since then. The comparatively dense vegetation during the summer months supports stability and infrequency of overwashing. No overwashing was observed in this area between 1991 and 1993.

In the 1948 air photo two well-formed overwash fans, oriented N-S, are situated to the south of the large vegetated fan. The 1967 and 1980 photos

show modification of these features. With the change of the outlet location between 1948 and 1967, the margin of the southernmost fan became the edge of zone D along the outlet. The southerly-flowing stream eroded the landward edge of the middle fan (the one adjacent to the large vegetated fan), only leaving remnants in the 1980 air photo. Visual inspection of the barrier showed remains of the middle fan in the vicinity of transect BB-25.

The N-S orientation of the overwash fans visible in the 1948 air photo indicate that incident waves from a northerly direction formed the fans. In order for overwashing to occur from the north, either one or more extreme northerly storms occurred and/or this section of the barrier was lower and contained less sediment. A low crestal height would make this portion of the barrier more susceptible to overwashing.

As the outlet during the last century was located within zone A, the stream would have flowed along the back of the barrier. The modification of the fans by the stream between 1948 and 1967 indicate that the fans were formed after the outlet changed location from zone A to the northern part of zone D. The curved 'fanlike' shape of the overwash fans would not have been visible on the 1948 air photo had the outlet been located to the south at the time after formation.

Also present in the 1967 and 1980, but not in the 1948 air photos, is a small overwash fan to the north of the large vegetated fan. This corresponds to the location of transect BB-35 - BB-36, an area which has undergone overwashing during the study period. The E-W trend of this fan is unlike the other three fans discussed in the 1948 photo, and it was likely formed by

southwesterly storms. Painted clasts placed near BB-30 were deposited on the backbarrier fan along BB-35, and indicate deposition by southwest storms.

As the shore platform generally provides protection from southwest storms, the development of the E-W oriented overwash fan appears somewhat anomalous. A west-southwesterly wave front may have been refracted around the northern edge of the platform resulting in incident waves normal to the shoreline trend. Cuspate features form occasionally along the northern section of zone D and their troughs may facilitate overwashing.

Mr. Edmund O'Keefe, a local resident who has lived at Big Barasway over 60 years, stated that a carriage path in the 1800's traversed Otter Point, the point of land opposite transect BB-27 (Figure 7), and a bridge crossed the point to the north side of the lagoon where the barrier is presently located. In the 1800's the present barrier area was part of the mainland, behind the lagoon. The beach was located considerably seaward, perhaps 30 - 50 m. The carriage path followed the coast northward along what is now the barrier, up the bluff and then landward through the woods. Over the years the beach moved landward and the outlet moved to the north as the barrier extended northward. In his lifetime, Mr. O'Keefe estimates the island, as well as the northern bluff bounding the beach, have eroded approximately 15 metres. The stages shown in the 1954 oblique photo were abandoned and eventually destroyed by storms. Mr. O'Keefe has observed the barrier thin, but remain approximately the same height.

Although the air photos cannot confirm the location of the outlet and the position of the beach in the 1800's, they do confirm Mr. O'Keefe's

observations of landward movement. The present study has not directly observed landward movement, although the island has eroded, as well as the southern part of zone C and the northern part of zone D. The study was of relatively short duration, and may have been conducted during a relatively quiet period. Vegetation growing on the backbarrier suggests stability. During the 1993 - 1994 season more overwashing was observed than during the past few years.

In addition, ice foot development during the study provides some protection from storm events. Mr. O'Keefe has seen an increase in ice foot development (or barricades as he calls them) in the past 5 - 10 years. He remembers ice foot formation similar to that seen in recent years when he was a child. Therefore, roughly between 1945 - 1985, ice foot formation was less common on the beach at Big Barasway.

Mr. O'Keefe also commented that the lagoon has become progressively more shallow during his lifetime. During the 1940's and 1950's, he was able to drive a motor boat within the lagoon, even during low tides. Now, the lagoon nearly empties. Sediment cores have not revealed thick sequences of sediment (chapter 9), thus indicating that deposition has not increased in recent years. Likely, the thinning of the barrier and a resulting larger and more permanent outlet allows a greater exchange of water during tides and, thus, the lagoon level has lowered despite rising sea-levels. Although the outlet at Ship Cove has changed position along the beach, it is unlikely the unstable nature of the outlet has changed over the years. The headlands bordering the sides of the cove hinder removal of sediment from the barrier.

It is unlikely, therefore, the tidal exchange in the lagoon at Ship Cove has changed significantly.

Unlike the pocket beach at Ship Cove, the barrier at Big Barasway is more prone to sediment depletion, particularly along zones C and D. The limited sediment supply along zone B is unlikely to keep pace with the net loss of sediment to the north. Sediment may come from the bluff to the north of zone D but observations have not shown a transfer of sediment to the south of BB-35, where the platform begins. Some sediment from the bluff may travel offshore and eventually be deposited on the barrier to the south in the vicinity of the platform. However, the addition of large amounts of sediment to the southern part of the barrier is improbable, as, after northerly storms, sediment accumulation is confined to the areas north of transect BB-35. To the south, the barrier remains relatively unaffected.

With sediment depletion in conjunction with transgression, the barrier will continue to thin and overwashing frequency will increase. The outlet position may change back to a northerly position perhaps in the vicinity of BB-30 or between BB-35 - BB-37 where the barrier is thinner and erosion is occurring. Without the dampening effect of the stream outlet in its present southerly position, sediment in this area would move northward and landward and the areas around the outlet along zones C and D would move landward at a faster rate.

8.3.2 *Sedimentology*

The angular to subangular cobble and boulder-dominated southern end of zone C indicates its proximity to the originating glacial source along

zone B. As with the northern end of zone A, rising sea-levels would result in erosion of the island of zone B and incorporation of the sediment and the island frame into the barrier complex. The barrier frame towards the southern end of zone C is likely diamicton. Elsewhere along zones C and D the roundness is higher and sphericity is lower.

The beachface along the southern end of zone C contains minor amounts of transportable sediment. The continuation of backwash channels from zone B provide the means of northward sediment transport. Since this area is undergoing net erosion, the more transportable pebble clasts are being moved northward and are leaving the cobble and boulder-dominated frame exposed. Consequently, there is little cross-shore sorting by size here.

With the reduced wave energies reaching the barrier north of BB-17, the sediment texture along the beachface correspondingly becomes dominated by smaller pebbles. The sediment texture of the mid-beachface along BB-18 shows similarities of the mid-beachface textures along BB-26 and BB-32. The ridge dominating the mid-beachface of BB-18 correlates to the mid-beachface along the spit/ridge of BB-26, which continues to the north and terminates near BB-34.

Boulders are likely either relict clasts along the crest and backbarrier from glacial deposits the barrier has incorporated with landward movement, or lag deposits along the lower-beachface. Excluding the contribution of boulders to the textural assemblage, the modal clast size increases up the beach along all transects. However, the clast size range is large, ranging from sand and granules to cobbles within the samples taken along the transects, particularly north of transect BB-26. This differs from

Ship Cove and the southern end of zone A, which show a high degree of sorting by size. The differences in textural sorting are attributable to the amount of wave energy that reach the individual systems on a regular basis and the ability to recycle sediment. The embayed nature at Ship Cove and the deeper nearshore bathymetries and swash alignments at Ship Cove and the southern end of Big Barasway, permit greater sorting by size.

Although the study may have been conducted during a period of relative calmness and extensive ice foot development, the barrier at Big Barasway is still experiencing sediment depletion and landward movement by overwashing. During storm activity, the barrier is overwashed with a wide assortment of sediment sizes transported landward. At Ship Cove the majority of clasts overtopping the barrier are mainly cobbles moved landward from the upper-beachface. In addition, the lack of sand and granules along the mid-, upper and back of the barrier at Ship Cove may in part be a response to the removal of fines to the pit behind the southern end of the beach. During the lower-energy summer season at Big Barasway the best textural sorting along zones C and D is along the mid-beachface ridge, the active transport zone.

Except for transect BB-18, there is a consistent pattern throughout the length of zones C and D of decreasing proportions of the less-suspendable equants and rollers up the beachface. The smallest proportions are found along the crest. Correspondingly, the sedimentary component of the lithology increases from 54% along the lower beach to 90% along the crest, as seen at Ship Cove and zone A at Big Barasway. However, the mid-beachface

of transect BB-18 contained less equants and rollers than the crest and the crest consisted of fewer equants and rollers than the lower-beachface.

The consistency of sorting by shape differs from the southern end of zone A and at Ship Cove, particularly between the lower and mid-beachface areas. The lack of secondary sorting due to cusped features common at Ship Cove, and those occasionally formed along zone A, allows a more consistent sorting based on the varying suspendability and pivotability qualities of the clast shapes. Furthermore, because of the swash alignment at southern zone A and Ship Cove which allows recycling and therefore more attrition and abrasion of the clasts, more discoid clasts prevail throughout the beach at these locations.

The percentage of rollers and equants along transect BB-18 was similar to that found elsewhere along zones C and D. The mid-beachface sample along BB-18 was taken along the top of a seaward ridge. During the study, this ridge marked the vertical limit of storm waves, and consequently, this ridge was the active barrier crest. The same suspendability and pivotability principles hold and are consistent with the rest of the barrier along zones C and D.

8.3.3 *Fabric Analysis*

The a-axis fabrics with the highest plunge values are located on berms. These fabrics have northerly positive deviations that range between 10.2° and 21.2°, with the exception of the insignificant deviation for fabric BB-40-10. The imbrication of the a/b planes of the discoid clasts also showed positive deviations and steeper plunges of 15 - 30° than elsewhere along this zone.

Although located along a linear ridge, fabric BB-29-4 has a low plunge and a large deviation. Clasts from an erosional slope above have fallen from the adjacent beachface, as in clast fabric BB-5-2 along zone A. It also has the lowest S_1 of the fabrics taken along berms. The positive deviations of the a -axes and the a/b planes of the discoid clasts demonstrate the stronger drift component along zones C and D, similar to that of the northern end of zone A. The insignificant deviation of -0.1° for BB-40-10 shows the influence of cusped features, albeit poorly formed here.

The clast fabrics taken along the cobble-dominated step (Zone C-3, BB-22-1, BB-27-2) all have comparatively high orientations ranging between 0.651 and 0.720 and low to moderate plunges. The orientations are similar, 007.0° , 006.5° and 358.7° and are unaffected by changes in barrier orientation. In addition, the clast fabric taken along the lateral bar, primarily pebbles and cobbles, had a trend of 320.1° and moderate plunge of 13.5° .

The fabrics taken on the back of the barrier (BB-27-3, BB-35-6, BB-35-7) all have low plunge values ranging between 7.3 and 10.5° . Their S_1 values, though, range between 0.538 and 0.728 . The clast fabric with the lowest S_1 value was taken on recently formed overwash deposits and shows disorganization. Likewise the imbrications of the a/b planes were not well defined. The high S_1 value was formed in an erosive channel which allowed a focusing of overwash activity into unidirectional flow. Consequently, with overwash deposits, the clast fabrics generally have low S_1 values. Isolated occurrences with seemingly anomalous high S_1 values may occur and are associated with erosive channelization.

8.3.4 *Summary of Sedimentary Assemblages*

Although differences occur along zone C and D, they consist of mostly a single sedimentary assemblage. This assemblage also shows similarities to the northern end of zone A. The sediments along the crest and backbarrier dip landward and incline at 5 - 10° while the texture shows a wide range of clast sizes, but is mainly large pebbles and cobbles. Bladed and discoid shapes prevail. Clast fabrics are generally moderately to poorly oriented, although isolated fabrics with high S_1 values can occur in association with erosive features. Flotsam and organic debris are intermittent. The upper- and mid-beachface areas are grouped and can be either erosive or depositional. The depositional areas are pebble-dominated and may have progradational ridges. These areas are associated with gentler nearshore bathymetry and/or outlet proximity. Beds dip seaward 5 - 10° and occasionally landward at similar or gentler inclinations. The principal eigenvalues of the clast fabrics are generally between 0.57 and 0.63, while plunges are high (> 20°). Erosive areas in the upper- and mid-beachface are composed of larger-sized clasts than the depositional areas, have steeper seaward dips with inclinations of 10 - 15° and no associated landward dips, and have lower principal normalized eigenvalues. The shape assemblage shows greater proportions of rollers and equants. The lowermost zone is the cobble and boulder-dominated platform, extending into the nearshore. Table 18 summarizes the sedimentary assemblage.

<u>Number</u>	<u>Unit</u>	<u>Zone</u>	<u>Slope</u>	<u>Structure/texture</u>
1	backbarrier	supratidal	5-10° (landward)	poor stratification; poor textural sorting with blades and discs dominant; generally poor fabrics
2	mid-upper- beachface	supratidal	varied; 5-10° (seaward); 2-4 (landward)	erosive or depositional; pebbles, higher percentages of rollers and equants; moderate fabrics with frequent steep plunges
3	lower- beachface	intertidal	5-8° (seaward)	sand, granules and pebbles
4	nearshore	subtidal to lower-intertidal	1-4° (seaward)	cobbles and boulders

Table 18: Summary of the sedimentary characteristics along zones C and D, Big Barasway.

Chapter 9

Sediment Cores

9.1 Descriptions

The locations of the four sediment cores taken in the lagoon at Big Barasway are shown in Figure 7. Core #1 was taken along a 305° bearing from the outlet, approximately 50 m from the opposite shore. Core #2 was taken 20 m behind the northern side of zone B, approximately 20 m south of transect BB-15. Core #3 was taken 10 m behind transect BB-7 along the southern side of zone A. Lastly, core #4 was taken 10 m behind the barrier along transect BB-13, towards the northern end of zone A. Figure 84 illustrates the stratigraphic sequences of the four cores.

The depth of water at location #1 is 1.96 m below MHW. The core is 65 cm long and is divided into seven units. Unit 1 measures a minimum of 9 - 10 cm in thickness and consists of disturbed planar laminae spaced 2 mm apart. These laminae incline 5 - 8°, alternate between fine sand and silty sand, and have nonerosional but sharp contacts. The overall texture contains 56% sand and 44% silt. Plant matter aligned at high angles is present throughout the unit, and spruce twigs and a horizontally-aligned angular bladed pebble with a 4 mm long axis are found at the base. The upper contact, marked by spruce twigs, is erosional and undulating .

Unit 2 measures 18.5 - 19.5 cm. The texture contains 70% sand and 30% silt. An asymmetrical ripple of medium sand is located within the basal 2 cm. It measures 1 cm in length, 4 - 5 cm in height and has a 10° stoss angle and

15° lee angle. Above the ripple area the sediment fines upward from fine to medium sand to sandy silt and consists of poorly defined planar laminae inclining 3 - 5°. Minor bioturbation is found in the upper 5 cm. A bladed angular siltstone pebble with 4 mm long axis is aligned vertically, while three granules and a bladed angular shale pebble with 4 mm long axis are aligned horizontally. The upper contact is sharp and horizontal.

Unit 3 measures 9.5 cm and consists of 82% sand and 18% silt. The lower 5.5 cm contains planar laminae alternating between sandy silt and fine to medium sand inclining 2-4°. The laminae of coarser sediment measure 2 mm whereas the finer laminae vary between 0.5 and 1.25 mm thick. Disturbance and laterally discontinuous laminae characterize the upper 4.5 cm. A 2 cm layer of medium-sized pebbles and spruce twigs bound the upper contact and constitutes unit 4.

Unit 5 is 10 cm thick and consists of disturbed horizontal planar laminae of fine to medium sand with lenses of sand towards the base. Deformation is evident under three vertically-aligned well-rounded roller-shaped pebbles with long axes measuring 11 mm, 17 mm and 30 mm. Marine seaweed and bioturbation features are present throughout. The upper contact is sharp and marked by eroded marine shell fragments.

Unit 6 measures 9 cm and consists of normally graded sand to sandy silt. The overall texture contains 80% sand and 15% silt. The upper contact is gradational.

Unit 7 is 6 cm and consists of modern organic muck.

The depth of water at location #2 is 1.82 m below MHW. The core measures 42 cm, and three units are described. Unit 1 is at least 15 cm thick

and contains 65% sand and 30% silt. Marine shell fragments with muscle tissue and a horizontally-aligned bladed siltstone subangular pebble mark the base. The lower 5 cm is bioturbated whereas the upper 10 cm consists of horizontal planar laminae of sandy silt. The laminae are 1 mm thick and have gradational contacts between individual lamina. The upper contact is also gradational.

Unit 2 measures 16 cm and consists of extensively bioturbated sand and silt, with a texture similar to unit 1.

Unit 3 measures 11 cm and consists of modern organic muck.

The depth of water at location #3 is 1.72 m below MHW. The core is 68 cm long and contains 3 units. Unit 1 measures at least 20 cm thick and consists of 57% sand, 42% silt and 1% horizontally-aligned fine pebbles and granules. The unit is bioturbated and has conifer and marine seaweed matter throughout. The upper contact is gradational.

Unit 2 measures 20 cm. It contains 70% sand, 18% silt and 12% clay. This unit is similar to unit 1, although not as extensively bioturbated as disturbed horizontal laminae are visible. The upper contact is erosional.

Unit 3 measures 28 cm. It contains 4% granules, 77% sand and 19% silt. Lenticular bedding forms 1 - 2% of the sediment volume, marked by discontinuous lenses of coarse sand and granules. These are 1 cm long and 3 mm high.

The depth of water at location #4 is 2.06 m below MHW. The core measures a minimum of 40 cm and consists of 1 unit of 51% sand, 31% silt, 18% clay and organics. It is extensively bioturbated and eroded shell fragments lacking muscle tissue are present at the base.

Depth Below MHW
(cm)

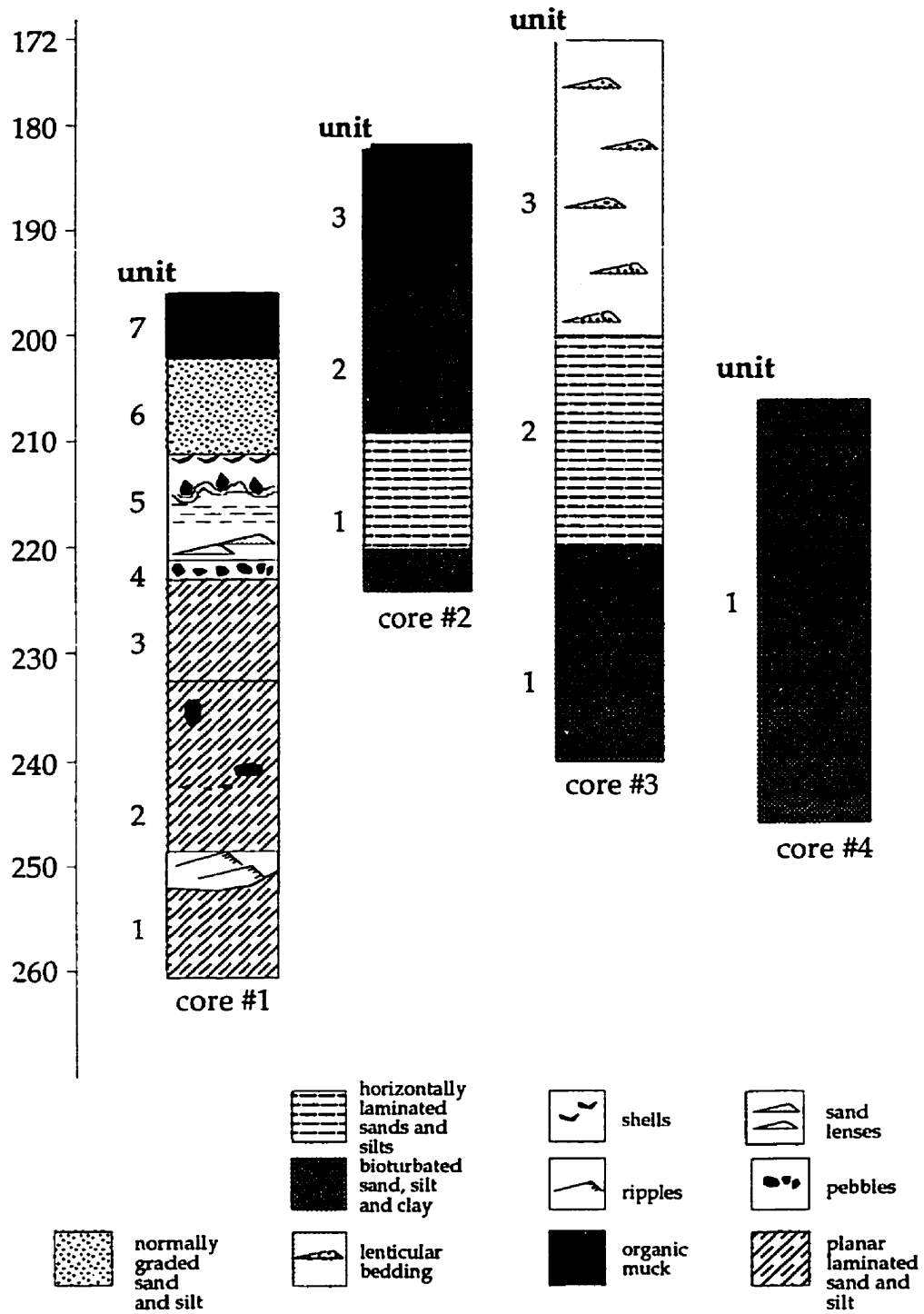


Figure 84: Stratigraphic sequence of cores, Big Barasway.

9.2 Interpretation

The cores were taken in a microtidal to low-mesotidal shallow lagoon environment. Core #1 was located closest to the current outlet whereas the others were removed from direct effects of modern fluvial input. The 800 m by 220 m lagoon limits the fetch, although wind generated waves can be produced and may influence sedimentation. Plate 34 shows the lagoon at low tide. As the lagoonal depths are generally less than 2 m, the entire water column may be moved if the winds are of sufficient strength and duration (Boothroyd *et al.*, 1985). The NE-SW trend of the lagoon and the protection created by the surrounding hills suggest that the winds most likely to generate waves are from the southwest or northwest. The tidal prism (the lagoonal area multiplied by the tidal range) is small, approximately $2.8 \times 10^5 \text{ m}^3$. Tidal activity causes ice blocks to buckle during January and February when the lagoon freezes.

Terrestrial sediment enters the lagoon through runoff and fluvial discharge. Sediment enters the lagoon from the bay by overwashing of the barrier, through the outlet during the tidal cycle, and by surges from storm events. However, the cores did not contain any large clasts characteristic of the barrier. The backbarrier stratigraphy of barrier lagoons in Maine, U.S.A. (Duffy *et al.*, 1989) likewise shows a lack of large clastic storm deposits, despite frequent strong winter storms along that coast. Duffy *et al.* (1989) attribute this characteristic to the behaviour of the reflective barriers during storm events. As individual storms progress, the barrier increases in height. This decreases the occurrence of overwashing (Orford and Carter, 1982b) but eventually causes avalanching of the barrier sediment towards the lagoon,

resulting in a series of gravel lobes in the lagoon-barrier interface. These generally extend less than 2 m from the back of the barrier (Carter and Orford, 1984). Consequently, the barriers protect the lagoons and the lagoons do not indicate the high wave energy associated with the barriers.

The stream is gravel-dominated and the surficial sediment in the area contains minor amounts of fine materials. Although this lagoonal environment could be conducive for the deposition of silt and clay, the availability of these sediments is limited locally. The drainage basin for this stream is small (65.3 km²) and the surficial sediment in the area is largely composed of large-sized clasts, pebble size or greater.

Plate 34: Lagoon at low tide, Big Barasway. August 1991.

Core #1

The presence of spruce twigs and the angular pebble at the base of unit 1 indicates a high-energy event of terrestrial origin, perhaps a spring flood event. The environment subsequently quieted and allowed the accumulation of planar laminae and the growth of aquatic plants. The vertical orientation of the vegetation indicates that the growth was simultaneous with the development of the laminae.

The erosional contact between units 1 and 2 indicates a sharp increase of energy. The preservation of both stoss and lee sides in a ripple indicates that sediment supply was in equilibrium or more significant than flow velocity (Jopling and Walker, 1968; Ashley *et al.*, 1982). As energy waned in unit 2 the laminae became horizontal and the grain size decreased. The vertically-aligned pebble was likely deposited from seasonal ice during spring melt. The absence of deformation underneath the pebbles is attributed to disturbance by bioturbation. The other horizontally-aligned clasts may be attributed to either deposition from seasonal ice or current flow. The latter is unlikely under the low-energy conditions generally associated with this environment.

The alternating strata of fine and coarser sand in unit 3 is similar to epsilon-cross-stratification described by Allen (1963). It is possible, as Allen suggested, that these laminae were deposited on a point bar along a migrating minor tidal channel. The differing grain sizes in the laminae, in this case, are consequences of changes in the strength of tidal currents. Tidal channels are present in the lagoon at Big Barasway and were observed during low tides when the lagoon level is low (Figure 85).

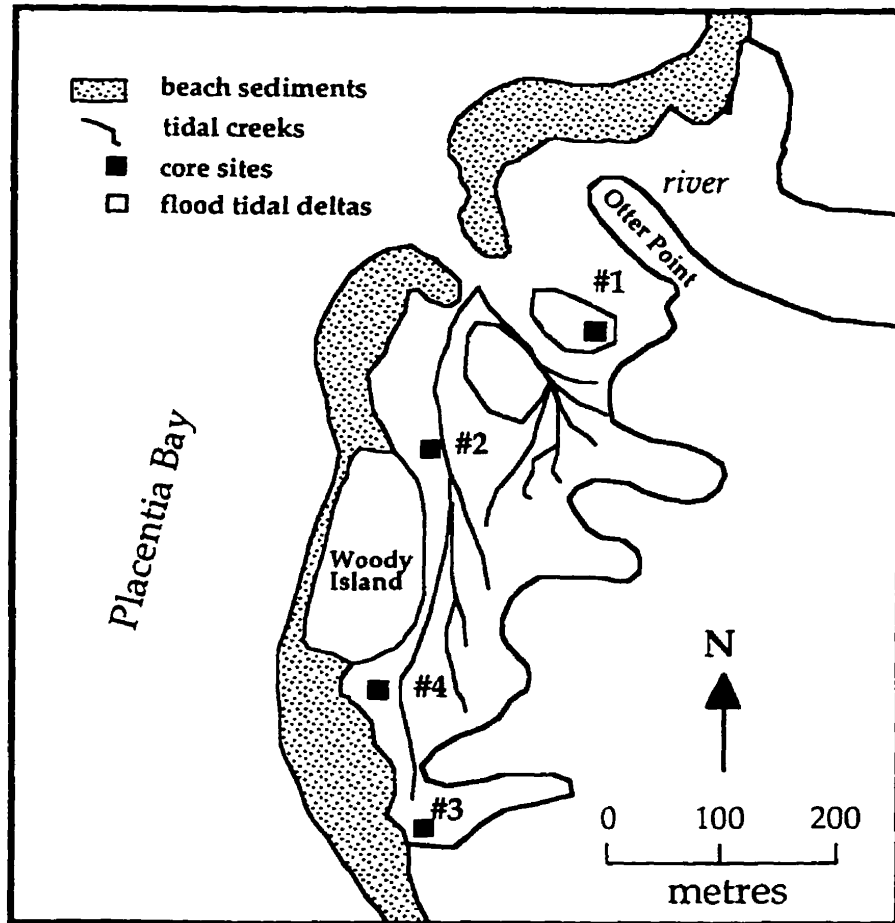


Figure 85: Map of the barrier and lagoon at Big Barasway showing the approximate locations of the tidal features.

The spruce twigs and pebbles of unit 4 indicate an erosive flood event, which brought terrestrial detritus to the tidal lagoon.

Unit 5 shows a similar sequence to unit 2. The lenses of sand toward the base indicate the formation of ripples under higher-flow regimes. The horizontal planar laminae were formed when the energy decreased. The vertically-aligned pebbles with deformation underneath indicate deposition from seasonal ice. The presence of marine plant matter indicates that the increase of energy was more likely the result of a storm event during which sea water entered the lagoon, rather than seasonal runoff.

The presence of marine shell fragments at the contact of units 5 and 6 and the normally graded sand of unit 6 represent another storm event in which large amounts of sediment were in suspension and fell out as energy declined. Israel *et al.* (1987) describe similar sediments for a tidal channel in a microtidal environment along the Texas coast.

The increased marine influx in units 5 and 6 may indicate the change in the location of the outlet in the 1960's from the northern position to the more southerly position near the location of core #1. If this is so, then the upper 20 cm of sediment has accumulated over the past 25 - 30 years, at a rate of 0.6 - 0.8 cm per year. The higher-energy conditions here than in the other core locations suggest that this sedimentation rate is plausible. Boothroyd *et al.* (1985) noted similar rates in sediment limited microtidal lagoons. If sea-level remains relatively constant, the lagoon will be filled in approximately 250 - 300 years.

However, the increased marine input may also be attributed to increased storm activity resulting from a rise in relative sea-level.

Geomorphic and archaeological evidence and radiocarbon dates on wood and peat indicate initial fall followed by a rise in sea-level during the Holocene. The two possible scenarios presented are not mutually exclusive. Sea-level is rising and it is possible that increased marine influx may be due to the change in outlet location. More information is needed to precisely determine current sedimentation rates at Big Barasway.

The general coarsening upward (52% to 80% sand) pattern within the stratigraphy of core #1 and the sedimentary structures are similar to those within the flood tidal deltas described by Boothroyd *et al.* (1985), Hayes (1980), Hayes (1991) and Israel *et al.* (1987). Air photos and visual inspection confirm the presence of flood tidal deltas in the lagoon at Big Barasway. The deltas have remained in relatively the same positions throughout the study (Figure 85). The horizontal segregation of the ebb and flood tidal flows characteristic of these forms would account for the lack of bi-directional laminae in this core.

Core #2

The marine shell with muscle tissue at the base of core #2 was less abraded than those recovered from core #4. Thus, either the shell was deposited near its location while alive, or it was brought to the area by a single storm event and not subjected to continued wave activity. The horizontally-aligned pebble indicates deposition by either storm activity or from seasonal ice. As the pebble is located at the base of the core, it is impossible to discern loading structures associated with dropstones. However, given the juxtaposition of the shell and pebble and the possible means of deposition, it

is likely that both were brought to the lagoon by a single storm event, after which calmer regimes prevailed.

The bioturbated sediment in the lower 5 cm in unit 1 and that of unit 2 is interrupted by horizontally planar laminae of 1 mm thickness with gradational contacts. The texture is the same throughout the two units, suggesting that the depositional environment has not changed significantly. The laminae most likely extended throughout the units before becoming bioturbated. The gradational contacts of the laminae indicate that there were gradual decreases in energy between events.

Core #3

The texture of 57% sand and 43% silt in unit 3 of core #3 and the presence of bioturbation is similar to cores 2 and 4. These suggest similar depositional environments. However, unit 1 of core #3 shows a greater presence of plant matter (conifer and marine) and horizontally-aligned fine pebbles and granules. These indicate a greater influence of terrestrial runoff and of marine storm events. Core #3 was located nearer to the surrounding vegetated embankments of the lagoon than were the other cores. In addition a small brook enters the lagoon on the landward side approximately 100 m from the core site. The horizontal position of the coarser clasts and the disturbance of the sediment from bioturbation make it difficult to discern whether the clasts were deposited by seasonal ice or by storms.

Unit 2 shows a vertical increase of sand content, from 57% to 70%. Although deposited by slightly higher energies than unit 1, the planar horizontal lamination indicates a low-energy environment.

Unit 3 shows a further increase of energy. Lenticular bedding with isolated ripples, similar to that recognized by Reineck and Wunderlich (1968), is usually associated with beds of sand and mud in which a ripple train of sand with a limited supply of sand migrates across a muddy substrate. Isolated ripple forms are preserved within the muddy substrate (Lindholm, 1987). Alternations between quiet and wave or current conditions are necessary for this type of deposition. Reineck and Singh (1973) associated the changes in energy levels with alternating ebb and flood tidal currents. Hawley (1981) discussed the origin of flaser bedding, form sets in which there is a greater proportion of sand to mud than is the case for lenticular bedding. Flume experiments demonstrated that flaser bedding forms when the shear stress necessary to erode mud is greater than that needed to transport sand as bedload. Hawley concluded that flaser bedding is likely associated with either storm events or spring discharge when there are large amounts of sediment in suspension. Thick layers of substrate accumulate during the waning stages of the storm or spring runoff. Between consecutive storm events or seasonal runoffs, the substrate has time to consolidate and withstand erosion during the next high-energy event.

The character of unit 3 shows similarities to the Reineck and Wunderlich (1968) definition, although the substrate is composed of sand and silt instead of mud. As coarser ripples are present throughout the unit, there must have been alternating periods of lower and higher energy. During the periods of higher energy coarse-grained ripples migrated and became isolated, as the sediment supply was limited. The finer sediment in suspension was deposited with decreasing energies, and became somewhat compacted before

the next storm and/or spring runoff event. It is unlikely that the lenticular bedding in core #3 is associated with tidal events, as the tidal energies in the lagoon are comparatively low.

Core #3 shows an increase of energy throughout the vertical succession. Unit 2 has a larger percentage of sand than unit 1. The larger quantities of granules in unit 3 could be attributed either to spring runoff or to overwashing of the barrier during storm events. The latter would indicate that overwashing has increased along this area of the barrier in the recent past. Overwashing has been observed 50 m to the north of the location of core #3 during the course of the study and thus could be the source of granule sediment. Factors that could contribute to increased overwashing are an increase in storm activity, perhaps as a result of sea-level rise; and sediment starvation along the barrier. Both are likely to occur in this system.

Core #4

Core #4, the shortest at 40 cm, was located in the quietest environment. It had the largest fraction of fines of all the cores. Mud formed 49% of the sediment, and bioturbation was extensive. The eroded shells at the base of the core indicate a storm event, after which calmer conditions prevailed. During the last century, the location of this core was near the position of the outlet. Consequently, wave and storm activity may have been stronger here in the past than is presently the case. The shells could mark the period of closure of the outlet at this southern location. If so, the 40 cm of sediment would have accumulated over the past 100 years, a rate of 0.4 cm per year. This rate includes compaction effects, although the sediment texture of the

core and the shallow lagoonal environment and short core suggest negligible influence. Given the modern environment where this core was taken, this sedimentation rate is probable, as Boothroyd *et al.* (1985) described similar rates in quiet lagoonal environments along Rhode Island.

The rate of 0.4 cm per year in core #4 and the possible rate of 0.6 - 0.8 cm per year in core #1 fall within the probable range of recent sea-level rise. Therefore, the accumulation rate may be keeping pace with sea-level rise. Of 21 lagoons studied along the U.S. Atlantic and Gulf coasts, the majority approximate a balance of accretion and sea-level rise (Nichols, 1991).

However, since the surficial sediment in the drainage basin contains large volumes of coarse sediment, these rates may be higher than the actual rate or rates of deposition of fine sediment in the lagoon. Assuming unit 4 of core #1 and the base of core # 4 mark storm events associated with the relocation of the outlet, a portion of the sediment would have been from reworked earlier deposits. Consequently, the sedimentary record of this lagoon environment has been filtered with periods of low depositional rates followed by relatively high rates of reworking (Crowley, 1984).

Figure 86 shows the spatial variability of sedimentation in the lagoon with cores #2 and #4 largely composed of fines, core #1 of sand and silt, and #3 granules, sand and silt. The position of the outlet greatly influences the sedimentary features and largely controls which areas of the lagoon are dominated by muds and others by larger-sized sediment. Repositioning of the outlet results in the deposition of fines over coarser material despite the transgression occurring in this region.

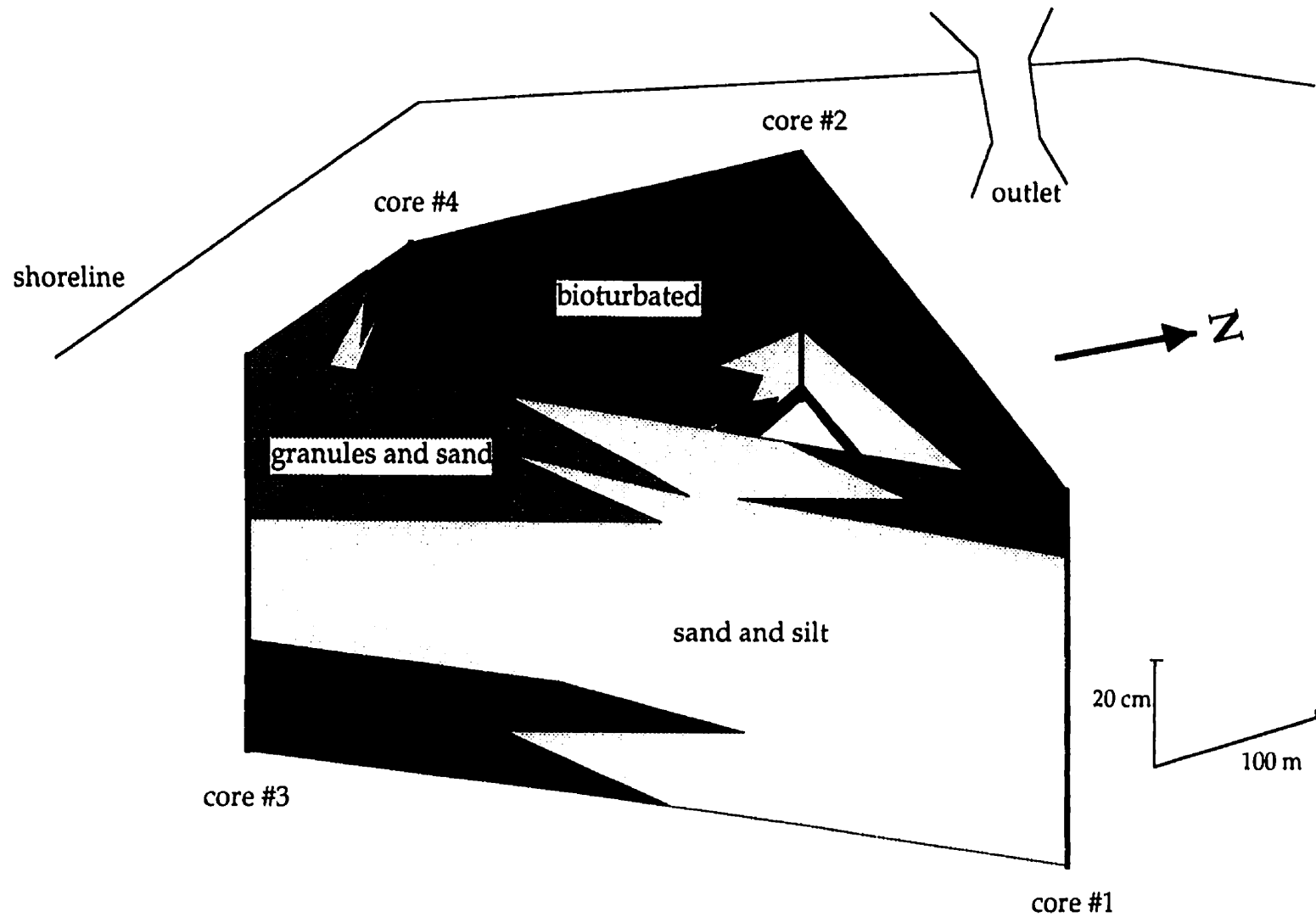


Figure 86: Schematic diagram showing the correlation of the sedimentary units of the cores. Vertical and horizontal axes show approximate scale.

Chapter 10

Conclusions

The barriers at both Ship Cove and Big Barasway are moving landward at similar rates. In part, this is a response to a rise in relative sea-level. Within this general trend, however, the barriers show sedimentological and morphological differences between them, as well as within individual systems. Although the overall sediment textures have slight differences, the barriers at Big Barasway and Ship Cove are pebble and cobble-dominated. Likewise, the clasts at both locations are dominated by sedimentary rock types, although zone D at Big Barasway shows a wider assortment of exotic clasts. Therefore, differences in sediment texture and clast lithology do not contribute to the differences in morphology and sedimentary assemblage.

The barrier at Ship Cove is enclosed by prominent headlands and has a comparatively steep nearshore gradient. Plunging waves break close to the shore. This setting allows swash alignment which, in conjunction with coarse material, creates a steep reflective beach (Wright and Short, 1984). Steeper slopes show better textural sorting, as shown by studies of beaches in New Zealand (McLean and Kirk, 1969). Furthermore, the swash alignment allows the juxtaposition of strong textural differences, such as the sand and granule-dominated area of zone A and the pebble and cobble-dominated area of zone C with a laterally small transitional area along zone B.

The small drainage basin results in an unstable stream outlet and consequently, sediment produced by fluvial action is negligible. Minor

amounts of sediment are added to the beach system from unconsolidated material within adjacent bluffs or veneers overlying the bedrock headlands. The majority of sediment is contained within the cove and undergoes considerable attrition and abrasion, which results in a dominance of rounded, discoid clasts. The greater amount of sand at Ship Cove (at least before anthropogenic removal) and at southern zone A, Big Barasway, than elsewhere along the barriers at Big Barasway, aids in the development of increased clast roundness (Kuenen, 1956; Matthews, 1983). A part of the sediment may be moved to water depths greater than half the incident wavelengths below the wave base and becomes trapped within the boulder-dominated nearshore zone and removed from the beachface. Small rip currents formed by cusp development may be the main agents for seaward sediment removal, particularly during storm events (Gruszczynski *et al.*, 1993). The rough bouldery surface of the nearshore zone is unlikely to support gravel ripples, as described by Forbes and Drapeau (1989). Anthropogenic removal of sediment has resulted in a decrease of fines in the lower-beachface and by removing a potential dissipative element, may have had a profound impact on the beach morphology (Forbes and Taylor, 1987).

The critical factors controlling the morphology and sedimentology of the beach at Ship Cove are its embayed nature, swash alignment, fixed sediment supply, unstable outlet, and steep nearshore bathymetry.

The barriers at Big Barasway show considerable lateral sedimentological and morphological variability and demonstrate the juxtaposition of differing morphodynamic settings. The shallow platform in the nearshore zone and the island along zone B have caused two separate

barriers to form. Zone A has a fixed sediment supply, whereas the location of zones C and D at the mouth of the cove and consequent exposure to the fringing beach to the north allow net removal of sediment. The rapid retreat of the island of zone B causes instability and increased overwashing along the northern half of zone A as the barrier moves landward with its island anchor. Consequently, although the southern half of zone A attempts to maintain a swash alignment, the moving anchor causes the northern half to become drift-aligned. The rapidly eroding front does not allow enough time for the northern half to become swash-aligned. Thus, the sedimentological and morphological organization differs, with the swash alignment of the southern half of zone A resulting in better sorting of the clasts by shape and size than along the northern half.

The net removal of sediment of the barrier to the north of zone B is causing a thinning of the barrier in places. Drift-aligned barriers are inherently weak unless continued sediment supply is maintained (Orford *et al.*, 1991). The shallowest part of the platform, located between transects BB-17 and BB-30, and the present location of the outlet cause an environment conducive for the development of progradational ridges. Consequently, despite an overall removal of sediment from the system under the transgressive regime, isolated areas of sediment accumulation may occur. Preservation of these ridges formed during the Holocene is unlikely and essentially nil for the geologic record before the Holocene. In addition, the ridges at Big Barasway are at nearly the same height above sea-level, unlike the descending ridges in isostatically-falling sea-levels such as Hudson Bay (Hillaire-Marcel, 1980), Labrador (Loken, 1962), Arctic Canada (Andrews, 1970;

Dyke, 1983; 1984), and other places that fall within zone A of Quinlan and Beaumont's (1981) model of Atlantic Canada, or zone 1 in Peltier *et al.* (1978) glacio-isostatic model.

Drift alignment may change to swash alignment, particularly with dwindling sediment supply and/or change in basement control (Orford *et al.*, 1991). A change to swash alignment is occurring to the north of BB-35. This area is generally drift-aligned and subject to northerly wave attacks interspersed within the dominant southwesterly wave regime, thereby causing alternating northward and southward movement of sediment. The barrier is moving landward faster north of BB-35 than between BB-17 and BB-35, causing the northern area to become increasingly protected from direct attack by southwesterly waves. The shallow platform area around the outlet causes refracted southwesterly waves to approach the northern part of the barrier orthogonally and thereby creating a swash alignment. Cuspate features develop when swash alignment occurs under either southwesterly or westerly waves.

The relatively rapid rate of sea-level in this region is similar to the rate occurring in Nova Scotia (Shaw *et al.*, 1993), and there is a limited sediment supply at the barriers at Ship Cove and Big Barasway. As a result, residual gravel scars or gravel patches may be scattered offshore, similar to those found offshore of Chezzetcook Inlet, Nova Scotia (Carter *et al.*, 1991). It is unlikely, though, that drowned barriers would be expected in this environment. The drowned barrier at Story Head, Nova Scotia was formed in the 1950's from a splitting of a pre-existing larger barrier as the barrier

rapidly moved landward (Orford *et al.*, 1991). In contrast, at Big Barasway and Ship Cove, the barriers are moving at slower rates than at Story Head.

The moderate rate of rollover of <1 m/year (Orford *et al.*, 1991) allows the development of stratified units with particle zonation on the beachface at both Big Barasway and Ship Cove. However, because of the swash alignment at Ship Cove and southern Big Barasway, the organization (stratification and particle zonation) is more sharply defined than elsewhere along Big Barasway. This adds complexity to the creation of models which relate the rate of landward movement and the resulting sedimentary assemblages.

Figure 87 outlines the critical factors which differentiate the sedimentology and morphology of the barriers at Ship Cove and Big Barasway under a transgressive regime. Bedrock control creates the pocket barrier beach at Ship Cove. In contrast, an exposed barrier and the relict subaqueous fan at Big Barasway affect the relative amounts of wave energy that reach the barrier. These differences between the two locations also control the lateral variations of energy within the individual beach systems. Based on the geological control and wave climate, either swash or drift alignments result. The morphology and sedimentology of the barriers depends on the relative amounts of energy reaching the barriers and whether the sediment supply is fixed, decreasing, or increasing.

With fixed sediment supply and comparatively high wave energies in a swash alignment, as at Ship Cove and at southern zone A at Big Barasway, high, single ridges characterize the barriers. The sediment is moderately to strongly stratified with moderate to strong particle beachface zonation, although cusp features add complexity to shape and texture zonations.

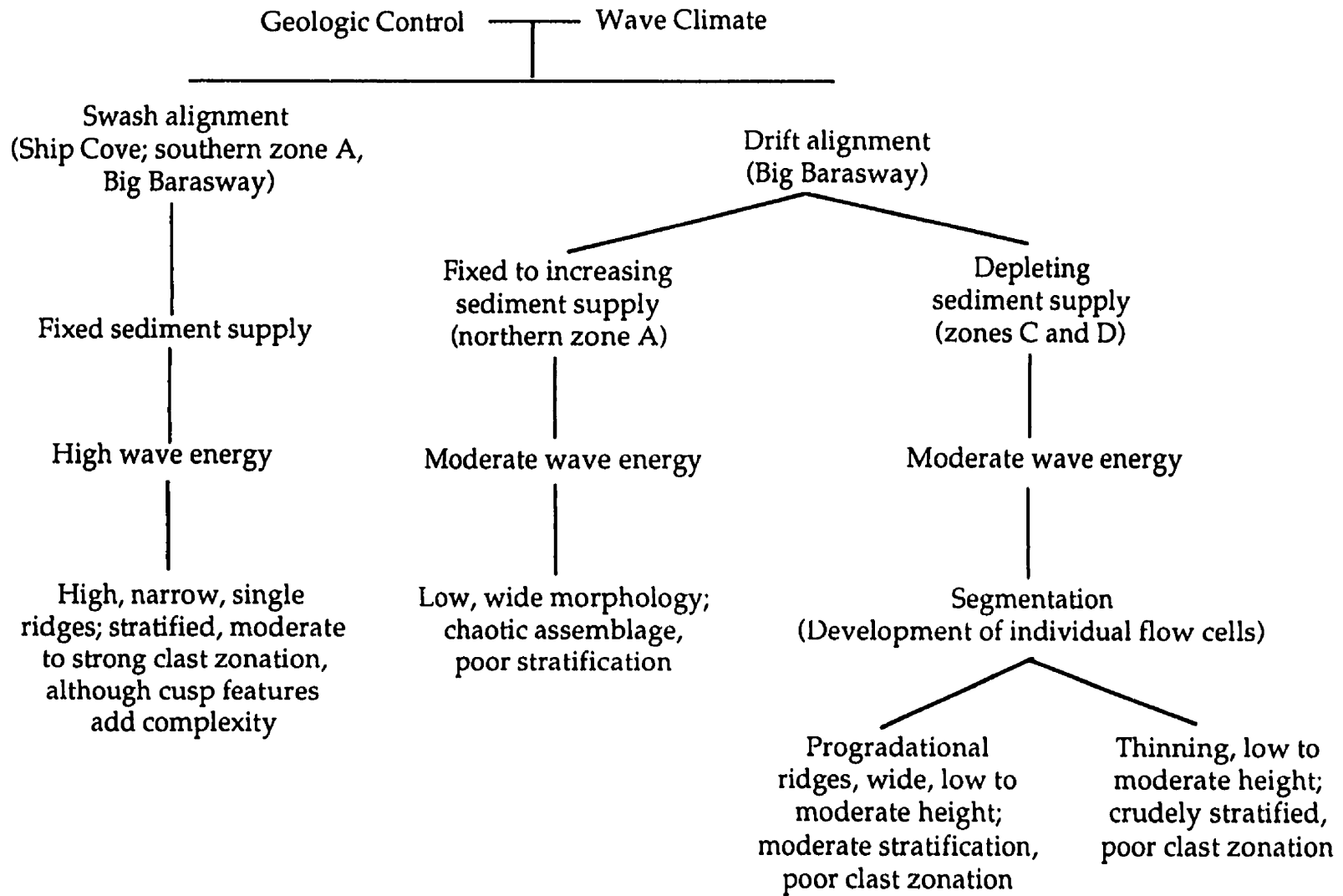


Figure 87: Outline of the critical factors differentiating the sedimentology and morphology of the barriers at Ship Cove and Big Barasway.

With drift alignment and fixed to increasing sediment supply in a downdrift location, as at the northern end of zone A at Big Barasway, the resulting barrier is low and has a wide backbarrier. The sediment shows crude stratification with a chaotic shape and texture.

During barrier breakdown, the development of separate flow cells and even flow sub-cells (cells within cells) may lead into smaller fringing features controlled by the local wave-basement interaction (Orford *et al.*, 1991). With drift alignment, moderate wave energy, and overall depleting sediment supply, as along zones C and D at Big Barasway, the initial stages of barrier breakdown and segmentation of the barrier are occurring with progradational ridges forming in the central shallow area of the barrier and thinning along the other areas. The progradational areas of the barrier at Big Barasway are relatively wide with low to moderate height. The sediment shows moderate stratification with poor particle zonation. The thinning areas have lower elevations, are crudely stratified to chaotic, and have poor particle beachface zonation. Although the northern end of Big Barasway occasionally becomes swash-aligned, it is still largely drift-aligned and characterized by this sedimentary assemblage. In the future, if it becomes more strongly swash-aligned, better particle zonation and stratification will likely occur.

In addition to the factors discussed above, the outlet strongly affects the morphology and sedimentology. The unstable outlet at Ship Cove causes lower barrier elevations in the outlet area when the outlet is closed and weaker particle zonation with larger proportions of higher sphericity equants and rollers than elsewhere on the barrier.

The outlet at Big Barasway has not influenced particle shape assemblages significantly. The overall sphericity at Big Barasway is higher than at Ship Cove because of lower wave energies reaching the barrier in zones C and D and the more recent introduction of diamicton from the erosional front. The outlet at Big Barasway aids in the development of progradational ridges by dampening wave energy. The ridges are composed of well-sorted small- and medium-sized pebbles indicating the size limit of clasts capable of being transported.

This study tested the applicability of using the a-axis fabric method in modern beach environments where large percentages of discoid clasts exist. The similar results in the significance of the orientations and plunges of a-axes and a/b imbrications for sedimentary interpretation demonstrate the usefulness of the a-axis technique in these beach environments. This indicates that the a-axis fabric method may be used in other beach environments where discoid clasts are uncommon.

The potential for the preservation of beach deposits and the transition from terrestrial to brackish to marine environments is considered to be better under rapidly rising sea-levels (Belknap and Kraft, 1981; Belknap and Kraft, 1985; Davis and Clinton, 1987). With the relatively rapid rate of rise occurring along Placentia Bay, the transition between brackish and marine environments should be evident. At Big Barasway, the lagoon is becoming increasingly tide-dominated with a larger and centrally located outlet. Furthermore, it is now more affected by storm events. With continued, and potentially faster landward movement as sediment supply fails, the barrier will overlie lagoon deposits which in turn, overlie subaqueous fan deposits.

The physiography of the valley limits the lagoon to a landward retreat up the stream. At Ship Cove the dynamics of the stream and the small outlet do not allow much deposition of fine sediment. Landward retreat would result in beach deposits directly overlying either fluvial or peat deposits. However, rapid shoreface erosion would truncate the barrier tops and reduce the likelihood of extensive barrier sediment preservation.

Beach ridge deposits are used to indicate former sea-level positions. This study demonstrates, that without detailed analysis, errors associated with determining a former sea-level position can result . There is a difference of four metres between the low and high elevations between Ship Cove and Big Barasway. The morphology and sedimentology of the ridges need to be analyzed to determine the amount of energy reaching beaches, and whether they were drift- or swash-aligned. Single ridge, steep slopes, better size and shape particle zonation indicate high-energy swash-aligned beaches. In addition, a detailed a-axis fabric analysis that shows a wide range of orientations in relations to the trend of the ridge, mainly moderate to steep plunges, and a cluster of moderate to strong principal eigenvalues, indicates cusp formation and further supports swash alignment and high ridge elevations. In contrast, if the fabric analysis yields a general orientation in relation to the trend of the ridge, gentler plunges, and a looser cluster of principal eigenvalues, then a drift-aligned, lower-elevated ridge is indicated.

As demonstrated by the work of Massari and Parea (1988), it is necessary in the geologic interpretation of Quaternary or more ancient potential beach deposits to consider the morphodynamics necessary to create the sedimentary assemblage. However, many works on ancient deposits use comparisons

with Bluck's (1967) model: for example Bourgeois and Leithold (1984) and Postma and Nemec (1990); or work on Chesil Beach (Carr, 1969; Hart and Plint, 1989). However, as Postma and Nemec (1990) conclude, deposits showing similarities to Bluck's model can be formed under either transgressive or regressive regimes. Modern beaches such as at Big Barasway differ from Bluck's model and Chesil Beach and thus it can be inferred that ancient beach deposits do also. Through modern analogues more accurate interpretations of ancient deposits can be made.

Concluding Remarks

This study has shown that gravel barriers can be dynamic and responsive to seasonal change and storm activity. Furthermore, the morphology and sedimentology of these landforms can vary considerably as a result of differences in wave regimes, sediment supplies and types, and alignments. Detailed clast fabric analyses have not been commonly undertaken in modern beach environments, and thus the results in this study may aid in the interpretations of other deposits.

The relatively short duration of this study has limited predictions in changes to the morphologies of the barriers at Ship Cove and Big Barasway. However, continued monitoring of the GSC transects would allow further study of the behaviour of the barriers. The estimates of landward movement made in this study could then be refined.

References

- Allen, J.R.L., 1963: Classification of cross-stratified units, *Sedimentology*, **2**, 93-114.
- Allen, J.R.L., 1983: Gravel overpassing on humpback bars supplied with mixed sediment: examples from the Lower Old Red Sandstone, southern Britain, *Sedimentology*, **30**, 285-294.
- Allen, J.R.L., 1984: *Sedimentary Structures: Their Character and Physical Bases*, Elsevier, Amsterdam, 453-461.
- Andrews, J.T., 1970: A geomorphic study of post-glacial uplift with particular reference to Arctic Canada; Institute of British Geographers, Special Publication 2.
- Antia, E.E., 1989: Studies on swash marks and swash angles on texturally, tidally and morphodynamically distinct beaches, *Geologie en Mijnbouw*, **68**, 297-300.
- Ashley, G.M., Southard, J.B. and Boothroyd, J.C., 1982: Deposition of climbing-ripple beds: a flume simulation, *Sedimentology*, **29**, 67-79.
- Banfield, C.E., 1983 : Climate, *in* Biogeography and Ecology of the Island of Newfoundland, South, G.R.(ed), DrW. Junk Publishers, The Hague, 37-106.
- Barkham, S.H., 1985 : The fishermen's contribution to the early cartography of eastern Canada, a paper presented at the eleventh international conference on the history of cartography, National Map Collection, Public Archives of Canada, Ottawa.
- Barkham, S.H., 1987 : Los vascos y las pesquerias transatlanticas, 1517-1713, *in* Itsasoa Los Vascos en el marco Atlantico Norte. Siglos XVI y XVII, Ayerbe, E. (ed), ETOR, Donostia-San Sebastián: Caupúzcoa), 26-210.
- Barrett, P.J., 1980: The shape of rock particles, a critical review, *Sedimentology*, **27**, 291-303.
- Belknap, D.F. and Kraft, J.C., 1981: Preservation potential of transgressive coastal lithosomes on the U.S. Atlantic shelf, *Marine Geology*, **42**,

- Belknap, D.F. and Kraft, J.C., 1985: Influence of antecedent geology on stratigraphic preservation potential and evolution of Delaware's barrier systems, *Marine Geology*, **65**, 235-262.
- Beschta, R.L. and Jackson, L.J. 1978: The intrusion of fine sediments into a stable gravel bed, *Journal Fisheries Research Board of Canada*, **36**, 204-210.
- Bluck, B.J., 1967: Sedimentation of beach gravels: examples from South Wales, *Journal of Sedimentary Petrology*, **37**, 128-156.
- Boon, J.D. III, 1969: Quantitative analysis of beach sand movement, Virginia Beach, Virginia, *Sedimentology*, **13**, 85-104.
- Boothroyd, J.C., Friedrich, N.E. and McGinn, S.R., 1985: Geology of microtidal coastal lagoons: Rhode Island, *Marine Geology*, **63**, 35-76.
- Bourgeois, J. and Leithold, E.L., 1984 : Wave-worked conglomerates - depositional processes and criteria for recognition, in *Sedimentology of Gravels and Conglomerates*, Canadian Society of Petroleum Geologists, memoir 10, Kowter, D.H., Steel, R.J.(eds), 331-343.
- Brookes, I.A., Scott, D.B. and McAndrews, J.H., 1985: Postglacial relative sea-level change, Port au Port area, west Newfoundland, *Canadian Journal of Earth Sciences*, **22**, 1039-1047.
- Brookes, I.A. and Stevens, R.K., 1985 : Radiocarbon age of rock-boring *Hiatella arctica* (Linne) and postglacial sea-level change at Cow Head, Newfoundland, *Canadian Journal of Earth Sciences*, **22**, 136-140.
- Bryant, E., 1983: Sediment characteristics of some Nova Scotian beaches, *Maritime Sediments*, **19**, 127-142.
- Caldwell, N.E. and Williams, A.T., 1986: Spatial and seasonal pebble beach profile characteristics, *Geological Journal*, **21**, 127-138.
- Canadian Climate Normals: Temperature and Precipitation, Atlantic Provinces, 1951-1980, 1982: Environment Canada, Atmospheric Environment Service.

- Canadian Climate Normals: Temperature and Precipitation, 1951-1980, Atlantic Provinces: Environment Canada, Atmospheric Environment Service.
- Canadian Climate Normals Volume 5 : 1951-1980, 1982 : Environment Canada, Atmospheric Environment Service.
- Canadian Tide and Current Tables 1993, volume 1 Atlantic Coast and Bay of Fundy, Department of Fisheries and Oceans, Ottawa, Canada.
- Carr, A.P., 1969: Size grading along a pebble beach: Chesil Beach, England, *Journal of Sedimentary Petrology*, **39**, 297-311.
- Carr, A.P., Blackley, M.W.L. and King, H.L., 1982: Spatial and seasonal aspects of beach stability, *Earth Surface Processes and Landforms*, **7**, 267-282.
- Carter, R.W.G., 1983: Raised coastal landforms as products of modern process variations, and their relevance in eustatic sea-level studies: examples from eastern Ireland, *Boreas*, **12**, 167-182.
- Carter, R.W.G., Devoy, R.J.N. and Shaw, J., 1989: Late Holocene sea-level changes in Ireland, *Journal of Quaternary Science*, **4**, 7-24.
- Carter, R.W.G., Forbes, D.L., Jennings, S.C., Orford, J.D., Shaw, J. and Taylor, R.B., 1989 : Barrier and lagoon coast evolution under differing relative sea-level regimes: examples from Ireland and Nova Scotia, *Marine Geology*, **88**, 221-242.
- Carter, R.W.G., Johnston, T.W., Orford, C. and Orford, J.D., 1984: Stream outlets through mixed sand and gravel coastal barriers: examples from southeast Ireland, *Zeitschrift für Geomorphologie*, N.F., **28**, 427-442.
- Carter, R.W.G. and Orford, J.D., 1984 : Coarse clastic barrier beaches : a discussion of distinctive dynamic and morphosedimentary characteristics, *Marine Geology*, **60**, 377-389.
- Carter, R.W.G. and Orford, J.D., 1988 : Conceptual model of coarse clastic barrier formation from multiple sediment sources, *Geographical Review*, **78**, 221-239.
- Carter, R.W.G. and Orford, J.D., 1991: The sedimentary organisation and behaviour of drift-aligned gravel barriers, *in* *Proceedings of Coastal Sediments '91*, Kraus, N.C., Gingerich, K.J., Kriebel, D.L. (eds),

proceedings of specialty conference on quantitative approaches to coastal sediment process, American Society of Civil Engineers, New York, 934-948.

Carter, R.W.G., Orford, J.D. and Jennings, S.C., 1990 : The recent transgressive evolution of a paraglacial estuary as a consequence of coastal barrier breakdown : lower Chezzetcook Inlet, Nova Scotia, Canada, *Journal of Coastal Research*, Special Publication no. 9, 564-590.

Carter, R.W.G., Orford, J.D., Forbes, D.L. and Taylor, R.B., 1991: Morphosedimentary development of drumlin-flank barriers with rapidly rising sea-level, Story Head, Nova Scotia, *Sedimentary Geology*, **69**, 117-138.

Carter, R.W.G., Orford, J.D., Jennings, S.C., Shaw, J. and Smith, J.P., 1990: Recent evolution of paraglacial estuary under conditions of rapid sea-level rise: Chezzetcook Inlet, Nova Scotia, *Proceedings of the Geologists' Association*, **103**, 167-185.

Catto, N.R., 1989: *Geology 482 Laboratory Manual*, University of Alberta, Edmonton, Alberta.

Catto, N.R., 1992a : Quaternary geological mapping, southwestern Avalon Peninsula, Current Research, Newfoundland Department of Mines and Energy, Geological Survey Branch, Report 92-1, 23-26.

Catto, N.R., 1992b: *Surficial Geology and Landform Classification of Ship Cove*, NTS 1M/1, Newfoundland Department of Mines and Energy.

Catto, N.R., 1994: Coastal evolution and sea-level variation, Avalon Peninsula, Newfoundland: geomorphic, climatic, and anthropogenic variation, *Coastal Zone Canada*, 1994, Bedford Institute of Oceanography, in press.

Catto, N.R., Anderson, R. and Scruton, D., 1994: *Coastal Classification of the Placentia Bay Shore*, Canada Department of Fisheries and Oceans, Technical Paper, in press.

Catto, N.R. and Hooper, R., 1994: Biological and geomorphological shoreline classification of Placentia Bay, Newfoundland: a preliminary assessment, unpublished report to Department of Fisheries and Oceans.

- Catto, N.R. and Thistle, G., 1993: Geomorphology of Newfoundland, International Geomorphological Congress Guidebook, August 1993, 23-24.
- Chasten, M.A. and Seabergh, W.C., 1993: Beach response and channel dynamics at Little River Inlet, North and South Carolina, U.S.A., *Journal of Coastal Research*, **9**, 973-985.
- Church, M.A., McLean, D.G. and Wolcott, J.F., 1987: River bed gravels: sampling and analysis, *in* *Sediment Transport in Gravel-Bed Rivers*, Thorne, C.R., Bathurst, J.C. and Hey, R.D. (eds), Wiley, Chichester, 43-88.
- Clark, J.A., 1980 : A numerical model of worldwide sea-level changes on a viscoelastic Earth, *in* *Earth Rheology, Isostasy and Eustasy*, Morner, N.-A. (ed), John Wiley and Sons, London, 525-534.
- Clark, J.A. and Lingle, C.S., 1979 : Predicted relative sea-level changes (18,000 years B.P. to present) caused by late-glacial retreat of the Antarctic ice sheet, *Quaternary Research*, **2**, 279-298.
- Cooper, J.A.G., 1990: Ephemeral stream-mouth bars at flood-breach river mouths on a wave-dominated coast: comparison with ebb-tidal deltas at barrier inlets, *Marine Geology*, **95**, 57-70.
- Crowley, K.D., 1984: Filtering of depositional events and the completeness of sedimentary sequences, *Journal of Sedimentary Petrology*, **54**, 127-136.
- Dalrymple, R.A. and Lanan, G.A., 1976: Beach cusps formed by intersecting waves, *Geological Society of American Bulletin*, **87**, 57-60.
- Davies, J.L., 1964: A morphogenic approach to world shorelines, *Zeitschrift für Geomorphologie*, **8**, 127-142.
- Davis, Jr., R.A. and Hayes, M.O., 1984 : What is a wave-dominated coast?, *Marine Geology*, **60**, 313-329.
- Davis, R.A., Jr. and Clinton, H.E., 1987: Sea-level change and the preservation potential of wave-dominated and tide-dominated coastal sequences, *in* *Sea-level Fluctuations and Coastal Evolution*, Nummedal, D., Pilkey, O.H. and Howard, J.D. (eds), Society of Economic Paleontologists and Mineralogists Special Publication, **41**, 167-178.

- Dobkins, Jr., J.E. and Folk, R.L., 1970 : Shape development on Tahiti-Nui, *Journal of Sedimentary Petrology*, **40**, 1167-1203.
- Donoghue, J.F. and Greenfield, M.B., 1991: Radioactivity of heavy mineral sands as an indicator of coastal sand transport processes, *Journal of Coastal Research*, **7**, 189-201.
- Duffy, W., Belknap, D.F. and Kelley, J.T., 1989 : Morphology and stratigraphy of small barrier-lagoon systems in Maine, *Marine Geology*, **88**, 243-262.
- Dyke, A.S., 1983: Quaternary geology of Somerset Island, District of Franklin, Geological Survey of Canada, Memoir 404.
- Dyke, A.S., 1984: Quaternary geology of Boothia Peninsula and northern District of Keewatin, central Arctic Canada, Geological Survey of Canada, Memoir 407.
- Everts, C.H., 1973: Particle overpassing on a flat granular boundary, *Journal of Waterways Harbor Division American Society of Civil Engineers*, **99(WW4)**, 425-438.
- Eyles, N., 1976: Gravel cones and depressions: sedimentary indicators of intense winds, *Maritime Sediments*, **12**, 75-76.
- Flood Information Map: Placentia, 1985: Environment Canada Inland Waters, Newfoundland Department of Environment, Water Resources Division.
- Foley, M.G., 1977 : Gravel-lens formation in antidune-regime flow-quantitative hydrodynamic indicator, *Journal of Sedimentary Petrology*, **47**, 738-746.
- Forbes, D.L., 1984 : Coastal geomorphology and sediments in Newfoundland, in *Current Research, Part B*, Geological Survey of Canada Paper 84-1B, 11-24.
- Forbes, D.L. and Drapeau, G., 1989: Near-bottom currents and sediment transport over the inner Scotian Shelf; sea-floor response to winter storms during CASP, *Atmosphere-Oceans*, **27**, 258-278.
- Forbes, D.L., Shaw, J. and Eddy, B.G., 1993 : Late Quaternary sedimentation and the postglacial sea-level minimum in Port au Port Bay and vicinity, west Newfoundland, *Atlantic Geology*, **29**, 1-26.

- Forbes, D.L. and Taylor, R.B., 1987 : Coarse grained beach sedimentation under paraglacial conditions, Canadian Atlantic coast, *in* *Glaciated Coasts*, Fitzgerald, D., Rosen, P. (eds), Academic Press, San Diego, 52-86.
- Forbes, D.L., Taylor, R.B. and Shaw, J., 1989 : Shorelines and rising sea-levels in Eastern Canada, *Episodes*, **12**, 23-28.
- Forbes, D.L., Taylor, R.B., Shaw, J., Carter, R.W.G. and Orford, J.D., 1990 : Development and stability of barrier beaches on the Atlantic coast of Nova Scotia, *Proceedings of the Canadian Coastal Conference*, Kingston, Ontario, 83-98.
- Forbes, D.L., Taylor R.B., Orford, J.D., Carter, R.W.G. and Shaw, J., 1991 : Gravel-barrier migration and overstepping, *Marine Geology*, **97**, 305-313.
- Frankel, L. and Cowl, G.H., 1961: Drowned forests along the eastern coast of Prince Edward Island, Canada, *Journal of Geology*, **69**, 352-357.
- Fraser, H.J., 1935: Experimental study of the porosity and permeability of clastic sediments, *Journal of Geology*, **43**, 910-1010.
- Frostick, L.E., Reid, I. and Laymann, J.T., 1984: Changing size distribution of suspended sediment in arid-zone flash floods, *in* *Modern and Ancient Fluvial Systems*, Collinson, J.D. and Lenin, J. (eds), Blackwell Scientific; International Association of Sedimentologists, Special Publication 6, 97-106.
- Gale, S. J., 1990: The shape of beach gravels, *Journal of Sedimentary Petrology*, **60**, 787-789
- Gale, S.J. and Hoare, P.G., 1992: Bulk sampling of coarse clastic sediments for particle-size analysis, *Earth Surface Processes and Landforms*, **17**, 729-733.
- Gilbert, R., 1984: The movement of gravel by the alga *Fucus vesiculosus* (L.) on Arctic intertidal flat, *Journal of Sedimentary Petrology*, **54**, 463-468.
- Glossary of Generic Terms in Canada's Geographical Names, Terminology bulletin; 176, Canadian Government Publishing Centre Supply and Services Canada, Ottawa, 1987.

- Gomez, B., 1983: Representative sampling of sandy fluvial gravels, *Sedimentary Geology*, **34**, 301-306.
- Grant, D.R., 1970: Recent coastal submergence of the Maritime Provinces, *Canadian Journal of Earth Sciences*, **7**, 676-689.
- Grant, D.R., 1972 : Postglacial emergence in northern Newfoundland, *in* Report of activities, part B, Geological Survey of Canada, Paper 72-1B, 100-102.
- Grant, D.R., 1989 : Quaternary geology of the Atlantic Appalachian region of Canada, *in* Quaternary Geology of Canada and Greenland, Fulton, R.J. (ed), Geological Survey of Canada, Geology of Canada no 1, 391-440.
- Grant, D.R., 1991: GSC-4670, *in* Geological Survey of Canada Radiocarbon Dates XXIX, Geological Survey of Canada, Paper 89-7, 8-9.
- Gruszczynski, M., Rudowski, S., Semil, J., Slominski, J. and Zrobek, J., 1993: Rip currents as a geologic tool, *Sedimentology*, **40**, 217-236.
- Hansom, J.D., 1983: Ice-formed intertidal boulder pavements in the Sub-Antarctic, *Journal of Sedimentary Petrology*, **53**, 135-145.
- Hansom, J.D., 1986: Intertidal forms produced by floating ice in Vestfiridir, Iceland, *Marine Geology*, **74**, 289-298.
- Hart, B.S. and Plint, A.G., 1989 : Gravelly shoreface deposits: a comparison of modern and ancient facies sequences, *Sedimentology*, **36**, 551-557.
- Hawley, N., 1981: Flume experiments on the origin of flaser bedding, *Sedimentology*, **28**, 699-712.
- Haworth, R.T. and Lefort, J.P., 1979 : Geophysical evidence for the extent of the Avalon Zone in Atlantic Canada, *Canadian Journal of Earth Science*, **16**, 552-567.
- Hayes, M.O., 1980: General morphology and sediment patterns in tidal inlets, *Sedimentary Geology*, **26**, 139-156.
- Hayes, M.O., 1991: Geomorphology and sedimentation patterns of tidal inlets: a review, *in* Coastal Sediments '91, Kraus, N.C., Gingerich, K.J., Kriebel, D.L. (eds), proceedings of specialty conference on quantitative

approaches to coastal sediment process, American Society of Civil Engineers, New York, 1343-1355.

- Henderson, E.P., 1972 : Surficial geology of Avalon Peninsula, Newfoundland, Geological Survey of Canada, Memoir 368.
- Heringa, P.K., 1981a : Soils of the Avalon Peninsula, Newfoundland, Agriculture Canada, Research Branch, Newfoundland Soil Survey, Report no. 3.
- Heringa, P.K., 1981b : Soils of the Avalon Peninsula, Newfoundland, Agriculture Canada, Research Branch, Newfoundland Soil Survey Report no. 47, south sheet map, scale 1:100,000.
- Hillaire-Marcel, C., 1980: Multiple component, post-glacial emergence, Eastern Hudson Bay, Canada, *in* Earth, Rheology, Isostasy and Eustasy, Morner, N.-A. (ed), John Wiley, London, 215-230.
- Hobday, D.K. and Banks, N.L., 1971, A coarse-grained pocket beach complex, Tanafjord (Norway), *Sedimentology*, 16, 125-128.
- House, R., in preparation, MSc. thesis, Department of Geography, Memorial University of Newfoundland, Newfoundland, Canada.
- Howard, J., 1992: An evaluation of shape indices as palaeoenvironmental indicators using quartzite and metavolcanic clasts in Upper Cretaceous to Palaeogene beach, river and submarine fan conglomerates, *Sedimentology*, 39, 471-486.
- Inman, D.L. and Guza, R.T., 1982: The origin of swash cusps on beaches, *Marine Geology*, 49, 133-148.
- Isla, F.I., 1993: Overpassing and armouring phenomena on gravel beaches, *Marine Geology*, 110, 369-376.
- Israel, A.M., Ethridge, F.G and Estes, E.L., 1987: A sedimentological description of a microtidal, flood-tidal delta, San Luis Pass, Texas, *Journal of Sedimentary Petrology*, 57, 288-300.
- Jennings, S. and Smyth, C., 1990: Holocene evolution of the gravel coastline of East Sussex, *Proceedings of the Geologists' Association*, 101, 213-224.

- Johansson, C.E., Structural studies of sedimentary deposits, *Geologiska Föreningens i Stockholm Förhandlingar*, **87**, 3-61.
- Jopling, A.V. and Walker, R.G., 1968 : Morphology and origin of ripple-drift cross-lamination, with examples from the Pleistocene of Massachusetts, *Journal of Sedimentary Petrology*, **38**, 971-984.
- King, A.F., 1988: Geology of the Avalon Peninsula, Newfoundland, Geological Survey Branch, Newfoundland Department of Mines and Energy, map 88-01.
- King, A.F., 1989 : Geological evolution of the Avalon Peninsula, Newfoundland, *in* *Geology of Newfoundland and Labrador*, special issue of the Newfoundland Journal of Geological Education, **10**, Newfoundland Section of the Geological Association of Canada, 17-32.
- Kirk, R.M., 1975; Aspects of surf and run-up processes on mixed sand and gravel beaches, *Geografiska Annaler*, **57A**, 117-133.
- Kirk, R.M., 1980 : Mixed sand and gravel beaches : morphology, processes and sediments, *Progress in Physical Geography*, **4**, 189-210.
- Komar, P.D., 1971: Nearshore cell circulation and the formation of giant cusps, *Geological Society of America Bulletin*, **82**, 2643-2650.
- Komar, P.D., 1987: Selective grain entrainment by a current from a bed of mixed sizes: a re-analysis, *Journal of Sedimentary Petrology*, **57**, 203-211.
- Komar, P.D. and Li, Z., 1986 : Pivoting analyses of the selective entrainment of sediments by shape and size with application to gravel threshold, *Sedimentology*, **33**, 425-436.
- Krumbein, W.C., 1934: Size frequency distribution of sediments, *Journal of Sedimentology Petrology*, **4**, 65-77.
- Krumbein, W.C., 1939: Preferred orientation of pebbles in sedimentary deposits, *Journal of Geology*, **47**, 673-706.
- Krumbein, W.C. and Pettijohn, F., 1938: *Manual of Sedimentary Petrography*, Appleton-Century-Crofts, New York.

- Kuenen, Ph.H., 1956: Experimental abrasion of pebbles 2: rolling by current, *Journal of Geology*, **64**, 336-360.
- Lindholm, R., 1987: *A Practical Approach to Sedimentology*, Allen & Unwin, London, 21-24.
- Liverman, D., in press: ^{14}C dates on marine molluscs, regional geomorphology and relative sea-level history, Newfoundland, Canada, *Boreas*.
- Liverman, D.G.E., Forbes, D.L. and Boger, R.A., 1994: Coastal monitoring on the Avalon Peninsula, *in* Current Research, Newfoundland Department of Mines and Energy, Geological Survey Branch, Report 94-1, 17-27.
- Loken, O.H., 1962: The late glacial and postglacial emergence and deglaciation of northernmost Labrador, *Geographical Bulletin*, **17**, 23-56.
- Longuet-Higgins, M.S. and Parkin, D.W., 1962: Sea waves and beach cusps, *Geographical Journal*, **128**, 194-201.
- Lowry, P. and Carter, R.W.G., 1982: Computer simulation and delimitation of littoral power cells on the barrier coast of southern County Wexford, Ireland, *Journal of Earth Science Royal Dublin Society*, **4**, 121-132.
- MacClintock, P. and Twenhofel, W.H., 1940 : Wisconsin glaciation of Newfoundland, *Bulletin of the Geological Society of America*, **51**, 1729-1756.
- Mannion, J.J., 1974: *Irish Settlements in Eastern Canada: A Study of Cultural Transfer and Adaptation*, University of Toronto Press, Toronto.
- Mark, D.M., 1973: Analysis of axial orientation data, including till fabrics, *Geological Society of America Bulletin*, **84**, 1369-1374.
- Markham, W.E., 1980: *Ice Atlas, Eastern Canada Seaboard*, Toronto, Environment Canada.
- Massari, F. and Parea, G.C., 1988: Progradational gravel beach sequences in a moderate- to high-energy, microtidal marine environment, *Sedimentology*, **35**, 881-913.

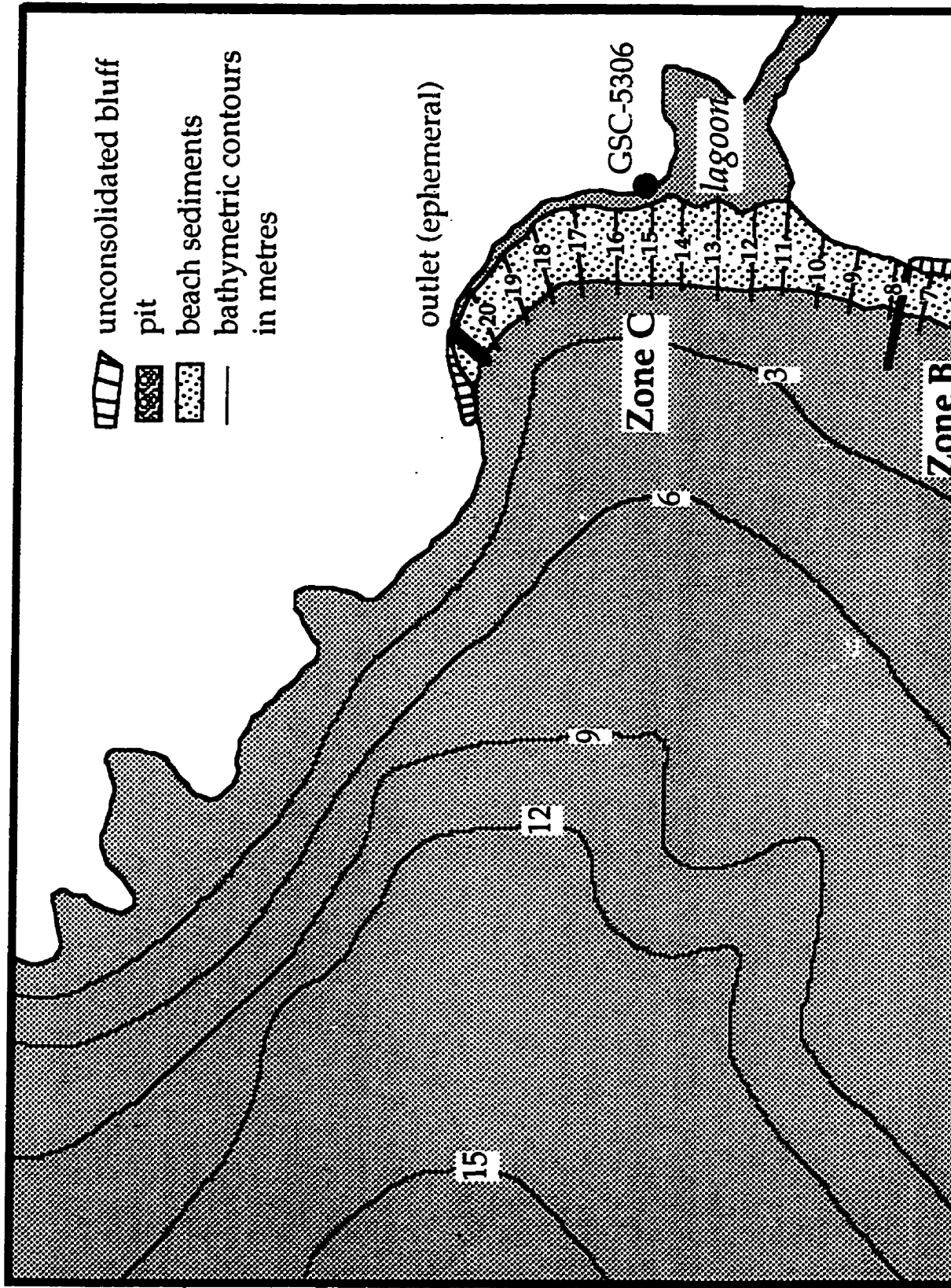
- Matthews, E.R., 1983: Measurements of beach pebble attrition in Palliser Bay, southern North Island, New Zealand, *Sedimentology*, **30**, 787-799.
- McCann, S.B., Dale, J.E. and Hale, P.B., 1981: Subarctic tidal flats in areas of large tidal range, southern Baffin Island, eastern Canada, *Géographie Physique et Quaternaire*, **35**, 183-204.
- McCartney, W.D., 1967 : Whitbourne map-area, Newfoundland, Geological Survey of Canada, Memoir 341.
- McEachran, D.B., 1989: Stereo™, the stereographic projection program for the Macintosh, Distributed by Rockware Inc., Wheat Ridge, Colorado, U.S.A.
- McLean, R.F. and Kirk, R.M., 1969: Relationships between grain size, size-sorting, and foreshore slope on mixed sand-shingle beaches, *New Zealand Journal of Geology and Geophysics*, **12**, 138-155.
- Nichols, M.M., 1991: Response of lagoons to sea-level change, *in* Coastal Sediments '91, Kraus, N.C., Gingerich, K.J., Kriebel, D.L. (eds), proceedings of specialty conference on quantitative approaches to coastal sediment process, American Society of Civil Engineers, New York, 1237-1247.
- Norris, R.M., 1956: Crescentic beach cusps and barchan dunes, *American Association of Petroleum Geologists*, **40**, 1681-1686.
- Norrman, J.O., 1964: Lake Vattern, Investigations on shore and bottom morphology, *GA. XLVI*, 1-238.
- O'Brien, S. and King, A.F., 1982 : The Avalon Zone in Newfoundland, *in* Guidebook for the Avalon Meguma Zones: The Caledonide Orogen, King, A.F. (compiler), International Geological Correlation Project 27, MUN Department of Earth Sciences Report 9, 1-27.
- Orford, J.d., 1975 : Discrimination of particle zonation on a pebble beach, *Sedimentology*, **22**, 441-463.
- Orford, J.D. and Carter, R.W.G., 1982a : Geomorphological changes on the barrier coasts of South Wexford, *Irish Geography*, **15**, 70-84.

- Orford, J.D. and Carter, R.W.G., 1982b : Crestal overtop and washover sedimentation on a fringing sandy gravel barrier coast, Carnsore Point, southeast Ireland, *Journal of Sedimentary Petrology*, **52**, 265-278.
- Orford, J.D. and Carter, R.W.G., 1984 : Mechanisms to account for longshore spacing of overwash throats on a coarse clastic barrier in southeast Ireland, *Marine Geology*, **56**, 207-226.
- Orford, J.D., Carter, R.W.G. and Forbes, D.L., 1991 : Gravel barrier migration and sea-level rise : some observations from Story Head, Nova Scotia, Canada, *Journal of Coastal Research*, **7**, 477-488.
- Orford, J.D., Carter, R.W.G., Forbes, D.L. and Taylor, R.B., 1988 : Overwash occurrence consequent on morphodynamic changes following lagoon outlet closure on a coarse clastic barrier, *Earth Surface Processes and Landforms*, **13**, 27-35.
- Orford, J.D., Carter, R.W.G. and Jennings, S.C., 1991: Coarse clastic barrier environments: evolution and implications for Quaternary sea-level interpretations, *Quaternary International*, **9**, 87-104.
- Otvos, E.G., 1964: Observation of beach cusp and beach ridge formation of the Long Island Sound, *Journal of Sedimentary Petrology*, **34**, 554-560.
- Peltier, W.R., Farrell, W.E. and Clark, J.A., 1978 : Glacial isostasy and relative sea-level: a global finite element model, *Tectonophysics*, **50**, 81-110.
- Pollett, F.C., 1981 : Peatlands of the Avalon Peninsula, *in* Soils of the Avalon Peninsula, Heringa, P.K. (ed), Agriculture Canada, Newfoundland Soil Survey, Report no. 3, 20-22.
- Postma, G. and Nemec, W., 1990: Regressive and transgressive sequences in a raised Holocene gravelly beach, southwestern Crete, *Sedimentology*, **37**, 907-920.
- Powers, M.C., 1953: A new roundness scale for sedimentary particles, *Journal of Sedimentary Petrology*, **23**, 117-119.
- Prentice, N., 1993: The nature and morphodynamics of contemporary coastal sediments at Topsail Beach, Avalon Peninsula, Newfoundland, BA honours thesis, University of Sheffield, England.

- Quinlan, G. and Beaumont, C., 1981 : A comparison of observed and theoretical postglacial relative sea-level in Atlantic Canada, *Canadian Journal of Earth Sciences*, **18**, 1146-1163.
- Quinlan, G. and Beaumont, C., 1982: The deglaciation of Atlantic Canada as reconstructed from the post-glacial relative sea-level record; *Canadian Journal of Earth Sciences*, **19**, 2232-2246.
- Rappol, M., 1985: Clast-fabric strength in tills and debris flows compared for different environments, *Geologie en Mijnbouw*, **64**, 327-332.
- Reineck, H.-E. and Singh, I.B., 1973: *Depositional Sedimentary Environments*, Springer-Verlag, New York, 97-102.
- Reineck, H.-E and Wunderlich, F., 1968: Classification and origin of flaser and lenticular bedding, *Sedimentology*, **11**, 126 and 99-104.
- Russell, R.J. and McIntire, W.G., 1965: Beach cusps, *Geological Society America Bulletin*, **76**, 307-320.
- Sallenger, A.H.Jr., 1979: Beach-cusp formation, *Marine Geology*, **29**, 23-37.
- Sanderson, D.J. and Donovan, R.N., 1974: The vertical packing of shells and stones on some recent beaches, *Journal of Sedimentary Petrology*, **44**, 680-688.
- Shaw, J. and Forbes, D.L, 1990 : Relative sea-level change and coastal response, northeast Newfoundland, *Journal of Coastal Research*, **6**, 641-660.
- Shaw, J. and Forbes, in press: Postglacial relative sea-level changes and coastal evolution, Newfoundland, Canada, *International Coastal Symposium*, Hofu, Iceland.
- Shaw, J., Taylor, R.B. and Forbes, D.L., 1993: Impact of the Holocene transgression on the Atlantic coastline of Nova Scotia, *Géographie Physique et Quaternaire*, **47**, 221-238.
- Shawmont Martec Limited, 1984: Hydrotechnical study of the Placentia flood plain, unpublished contract report to Environment Canada and Newfoundland Department of Environment, St. John's, 132 pages and 5 appendices.

- Shepard, F.P., 1950: Beach Cycles in southern California, U.S. Army Corps of Engineers, Beach Erosion Board Technical Memo No. 20.
- Sherman, D.J., 1991: Gravel beaches, *National Geographic Research & Exploration*, 7, 442-452.
- Sherman, D.J., Bauer, B.O., Nordstrom, K.F., Jagger, K.A. and Allen, J.R., 1989: Sediment transport in the lee of a groin, *Geoöko Plus* 1, 263-264.
- Sherman, D.J., Bauer, B.O., Nordstrom, K.F. and Allen, J.R., 1989: A tracer study of sediment transport in the vicinity of a groin: New York, U.S.A., *Journal of Coastal Research*, 6, 427-438.
- Sherman, D.J., Orford, J.D. and Carter, R.W.G., 1990: Particle sorting on gravel beach cusps, *International Association of Sedimentology, Nottingham, Abstract*, 495.
- Sherman, D.J., Orford, J.D. and Carter, R.W.G., 1993: Development of cusp-related, gravel size and shape facies at Malin Head, Ireland, *Sedimentology*, 40, 1139-1152.
- Shvetsov, M., 1954: Concerning some additional aids in studying sedimentary formations. Academy of Sciences of the USSR, *Koklady Earth Sciences*, 29, 61-66.
- Summers, W.F., 1949 : Physical geography of the Avalon Peninsula of Newfoundland, McGill University, M.Sc. thesis.
- Taylor, R.B., Wittmann, S.L., Milne, M.J. and Kober, S.M., 1985: Beach morphology and coastal changes at selected sites, mainland Nova Scotia, *Geological Survey of Canada, Paper* 85-12.
- Tucker, C.M., Leckie, D.A. and McCann, S.B., 1982: Raised shoreline phenomena and postglacial emergence in south-central Newfoundland, *Géographie Physique et Quaternaire*, 36, 165-174.
- Udden, J., 1898: Mechanical composition of wind deposits, *Augustana Library Publication* 1.
- Waag, C.J. and Ogren, D.E., 1984: Shape evolution and fabric in a boulder beach, Monument Cove, Maine, *Journal of Sedimentary Petrology*, 54, 98-102.

- Wadell, H., 1935: Volume, shape, and roundness of quartz particles, *Journal of Geology*, **43**, 250-280.
- Water Resources Atlas of Newfoundland, 1992 : Water Resource Division, Department of Environment and Lands, Government of Newfoundland and Labrador.
- Wentworth, C.K., 1922: A method of measuring and plotting the shapes of pebbles, *U.S. Geological Survey Bulletin*, 730-C, 91-102.
- Werner, B.T. and Fink, T.M., 1993: Beach cusps as self-organized patterns, *Science*, **260**, 968-971.
- Williams, A.T., 1973: The problem of beach cusp development, *Journal of Sedimentary Petrology*, **43**, 857-866.
- Williams, A.T. and Gulbrandsen, L.F., 1977: The orientation of pebbles on beaches, *Cambria*, **4**, 174-186.
- Williams, A.T., and Caldwell, N.E., 1988 : Particle size and shape in pebble-beach sedimentation, *Marine Geology*, **82**, 199-215.
- Williams, H., 1979 : Appalachian orogen in Canada, *Canadian Journal of Earth Sciences*, **16**, 792-807.
- Woodcock, N.H., 1977: Specification of fabric shapes using an eigenvalue method, *Geological Society of America Bulletin*, **88**, 1231-1236.
- Woodrow, E.F. and Heringa, P.K., 1987 : Pedoclimatic zones of the island of Newfoundland, *Canada Soil Survey, Newfoundland, Report 32*, 12 pages.
- Worrall, G.A., 1969 : Present-day and subfossil beach cusps on the West African coast, *Journal of Geology*, **77**, 484-487.
- Wright, L. and Short, A., 1984: Morphological variability of surf zone and beach: a synthesis, *Marine Geology*, **56**, 93-118.
- Zenkovitch, V.P., 1967: *Processes of Coastal Development*, Oliver & Boyd, London.
- Zingg, T., 1935: Beiträge zur Schotteranalyse, *Schweizerische Mineralogische und Petrographische Mitteilungen*, **15**, 39-140.



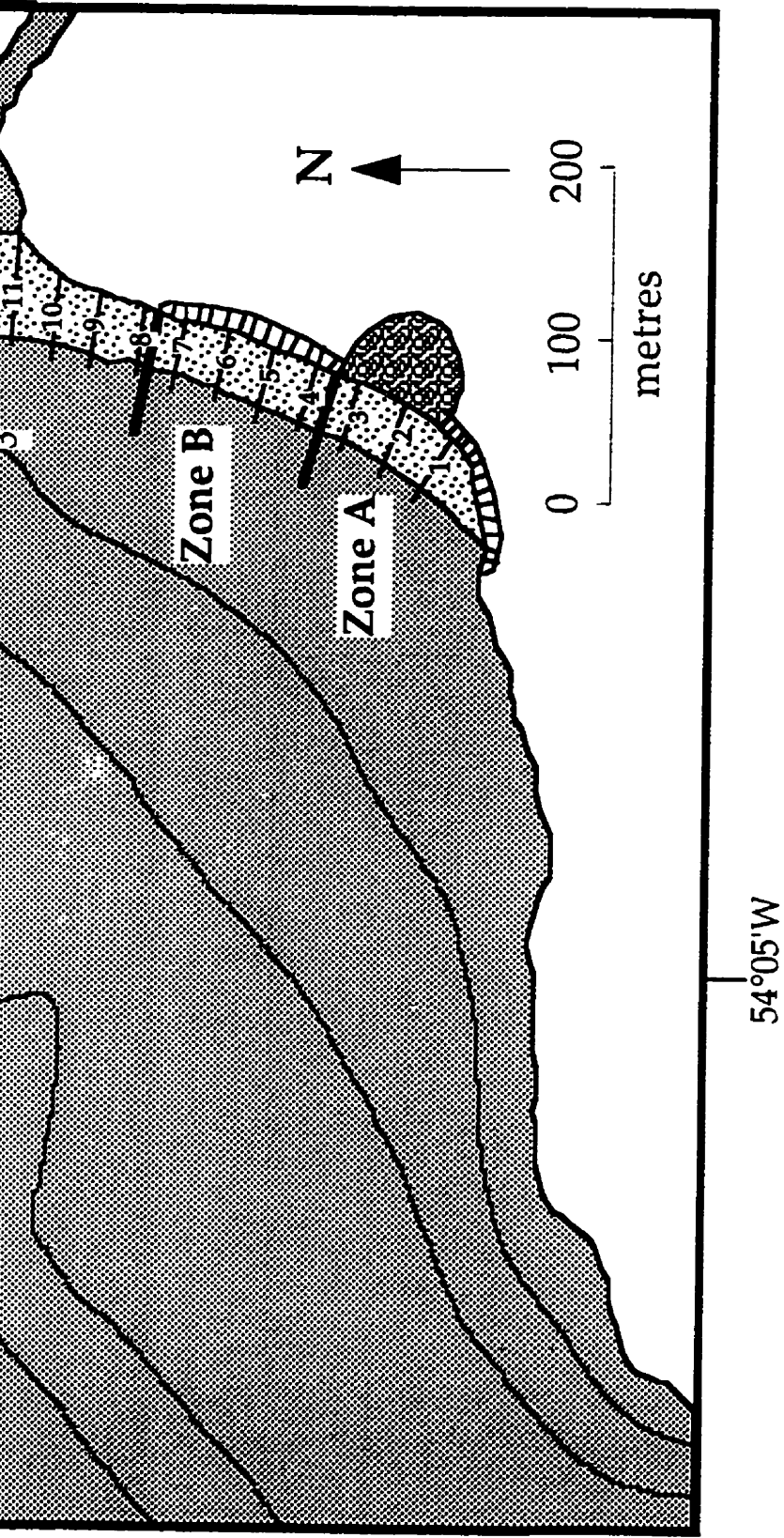
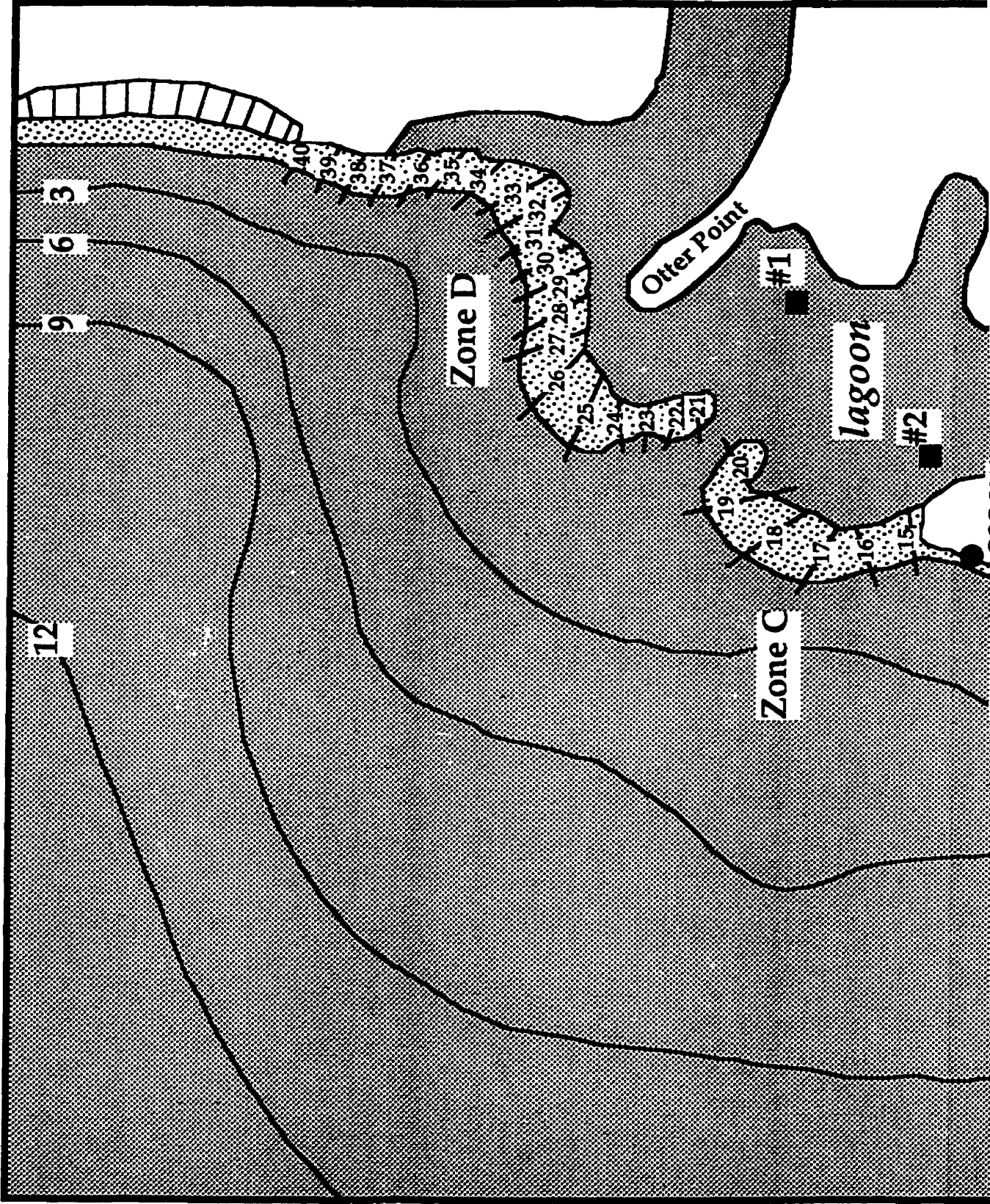


Figure 6: Map of the barrier at Ship Cove.



47°08'N

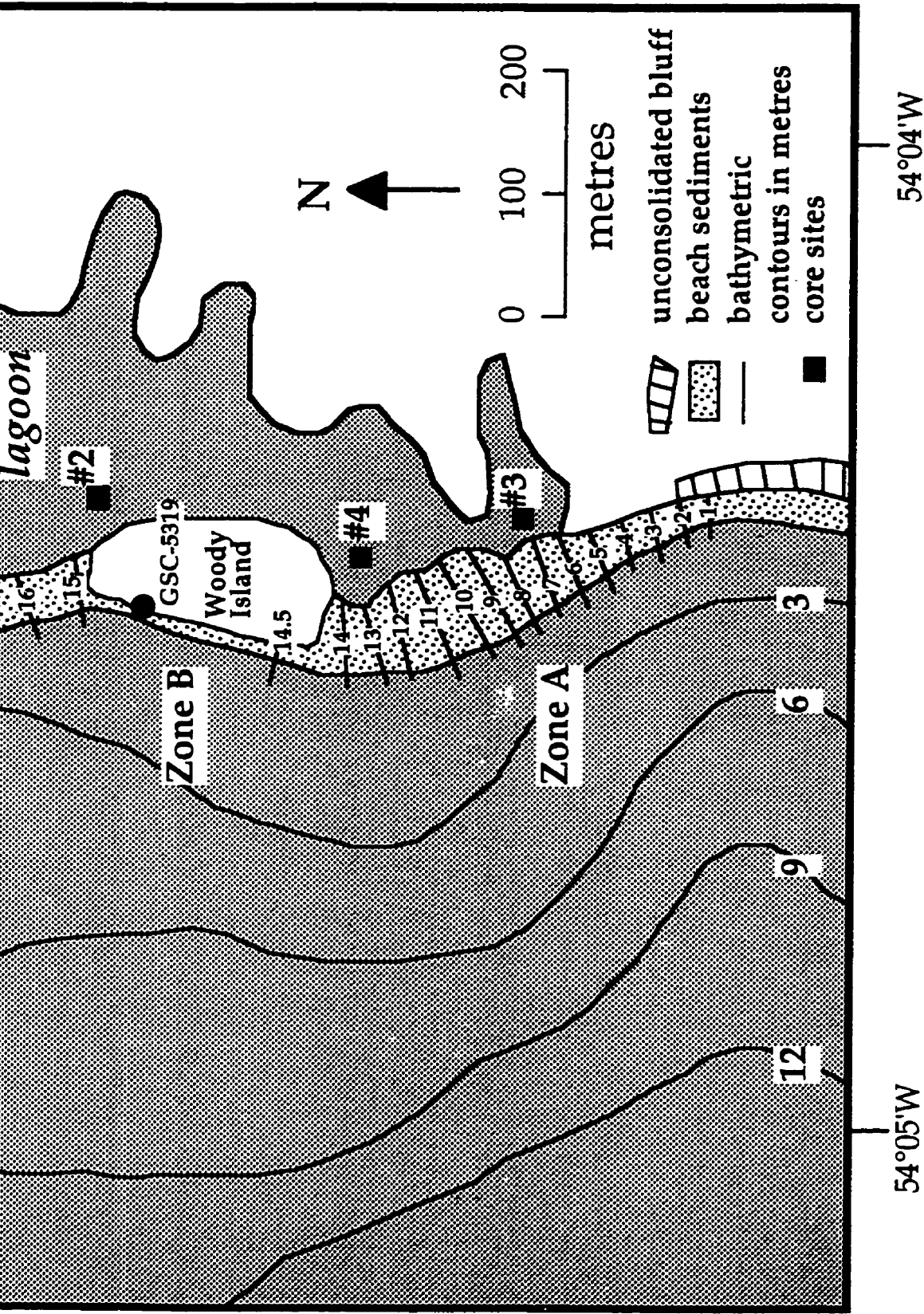


Figure 7: Map of the barrier at Big Barasway.

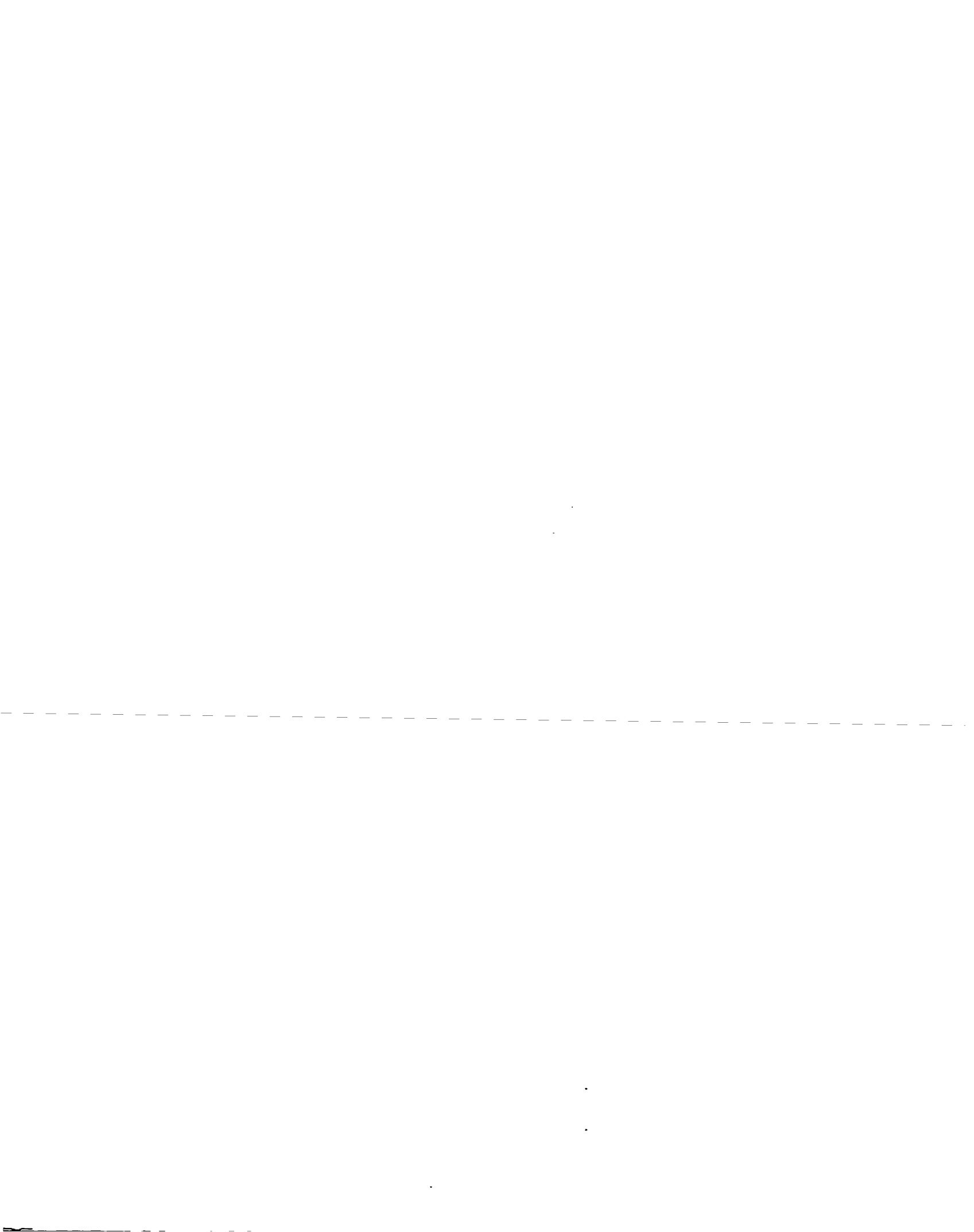
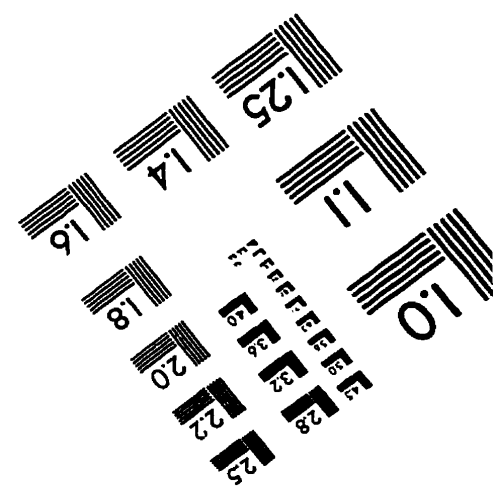
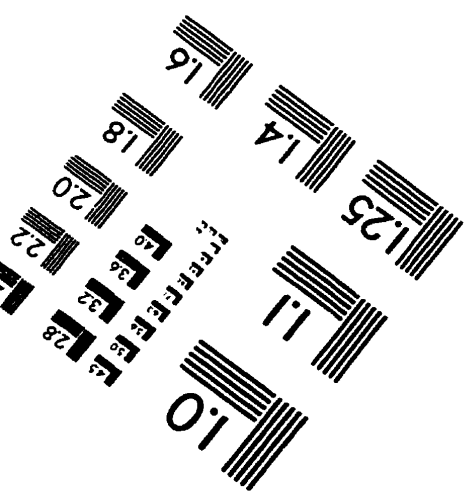
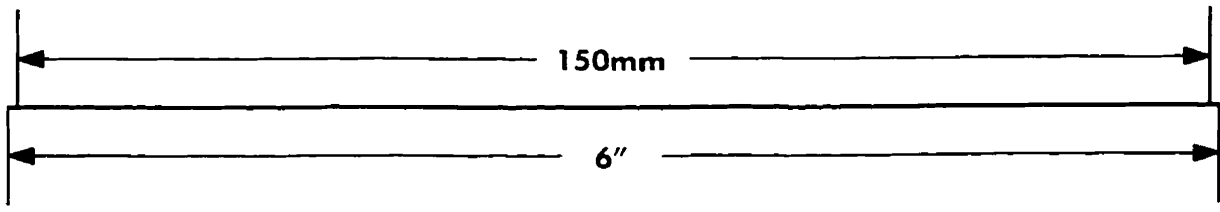
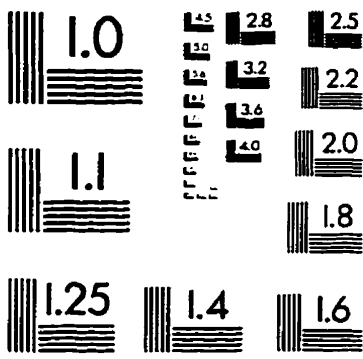
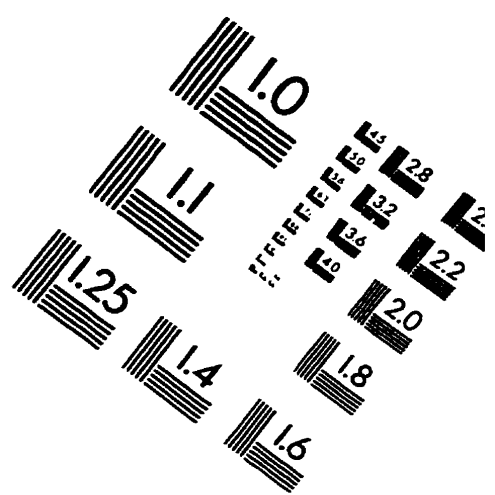
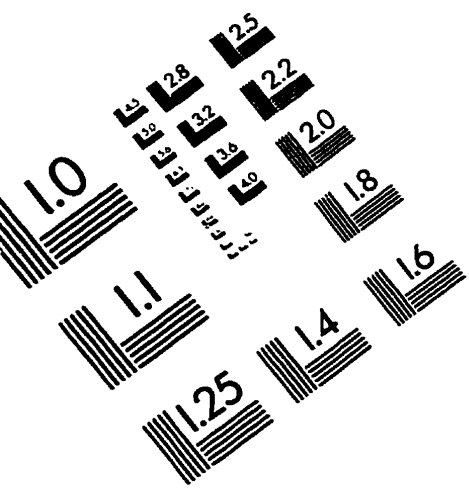


IMAGE EVALUATION TEST TARGET (QA-3)



APPLIED IMAGE, Inc
 1653 East Main Street
 Rochester, NY 14609 USA
 Phone: 716/482-0300
 Fax: 716/288-5989

© 1993, Applied Image, Inc., All Rights Reserved